BIOMATERIALS FOR TISSUE ENGINEERING FOR RHEUMATOID ARTHRITIS BASED ON CONTROLLING DENDRITIC CELL PHENOTYPE

A Dissertation
Presented to
The Academic Faculty

By

Jaehyung Park

In Partial Fulfillment
Of the Requirements for the Degree
Doctor of Philosophy in Bioengineering

Georgia Institute of Technology

August 2009

BIOMATERIALS FOR TISSUE ENGINEERING FOR RHEUMATOID ARTHRITIS BASED ON CONTROLLING DENDRITIC CELL PHENOTYPE

Approved by:

Dr. Julia Babensee, advisor
College of Engineering
Georgia Institute of Technology

Dr. Andrés García
College of Engineering
Georgia Institute of Technology

Dr. Barbara Boyan
College of Engineering
Georgia Institute of Technology

Dr. Robert Guldberg
College of Engineering
Georgia Institute of Technology

Dr. Todd McDevitt
College of Engineering
Georgia Institute of Technology

Date Approved: June 25, 2009

ACKNOWLEDGEMENTS

I especially wish to express my gratitude to my advisor, Dr. Julia Babensee, who from the outset, encouraged me in my research work and provided me with many details and suggestions for the research progress. During my years at Georgia Tech, as ever, I benefited greatly from her vast knowledge, intelligence, and originality of mind. Her sincere guidance and encouragement inspired me to strive during my difficult period. This unforgettable support and trust I have received from her will continue to be indispensable for my future career in whichever place or position I might be. Deepest gratitude is also due to the members of the thesis committee, Dr. Barbara Boyan, Dr. Andrés García, Dr. Robert Guldberg, and Dr. Todd McDevitt, without whose contributions and commitment this thesis study would not have been successful.

There are other kinds of help that make this thesis research possible: I also would like to record my gratitude to Dr. Brani Vidakovic and Dr. Melissa Kemp for their invaluable advice. I am very grateful to the staff at Georgia Tech including Johnafel Crowe, Steve Woodard, and Sha'aqua Asberry for their helpful technical support. I also would like to extend my sincere appreciation to a number of individuals who have given me help and encouragement over the period in which this research work was done. In the successful completion of my doctoral thesis study, the in vitro study using human blood would never have been completed without the help of the staff at the Phlebotomy Laboratory (Georgia Tech Student Health Center): Jack Horner, Erica Waller, LaShonna Stokes, Lisa Carr, and Patricia Dureja. My highest appreciation also goes to all blood donors for their constant support for my research work. The completion of the in vivo rabbit study involved the labor and support of Dr. Laura O'Farrell, Angela Lin, and all staff members at the Physiological Research Laboratory (PRL).

I would like to recognize the creative discussion and helpful input of my remarkable cohorts: Dr. Mutsumi Yoshida, Dr. Stacey Rose, Dr. Sucharita Shankar, Dr. Richard Payne, Dr. Lori Norton, Todd Rogers, Peng Meng Kou, Nathan Hotaling, Inn Inn Chen, Christina Duden, Michael Gerber, Rishi Patel, and Carrie Oliver. I am especially grateful to my undergraduate research assistants, Michael Gerber, Rishi Patel, and Carrie Oliver, for their faith and patient encouragement in this project. I also have greatly appreciated the help and pleasant moments from my friends in school and the Institute of Biosciences and Bioengineering (IBB), especially the Wing 1D.

I would like to take this opportunity to thank my family, my parents, and my sisters. My parents instilled in me the belief that intellectual pursuit is the highest calling, and that ideas do have the power to change people's lives. As always, they have been there, providing all sorts of tangible and intangible support to achieve my academic and personal goals, even from afar. It is a particular pleasure to acknowledge my debt to my lovely daughter, Jasmine (Yunjae), for her patience and understanding. My wife, Yunhee, has patiently supported me in innumerable ways; whatever I might say here cannot do full justice to the extent and the value of her contribution.

This work has been supported by funding from Arthritis Foundation (Arthritis Investigator Grant), National Institutes of Health (NIBIB/NHLBI, 1RO1EB004633-01A1), National Science Foundation (CAREER Award), and Georgia Tech/Emory Center for the Engineering of Living Tissues (GTEC - Critical Animal Model).

TABLE OF CONTENTS

LIST OF TABLES

LIST OF FIGURES

SUMMARY

The host response toward biomaterial component of tissue-engineered devices has been extensively investigated by exploring the potential inflammatory response of the host upon contact with biomaterials. Due to a biomaterial adjuvant effect, questions are raised to understand a role of biomaterials, which has been shown to modulate the host response. Specifically, it has been shown that the adjuvanticity of biomaterials affects the maturation of dendritic cells (DCs), professional antigen presenting cells (APCs) central to controlling immune response (Bennewitz and Babensee, 2005; Yoshida and Babensee, 2004). Dendritic cells have been also recognized as the key regulator of the balance between tolerance and immunity and as determinant for pathogenesis of the autoimmune disease such as rheumatoid arthritis (RA) (Waalen et al., 1986; Pettit and Thomas, 1999).

The objective of this research was to understand the response of DCs to different biomaterials upon contact and identify biomaterials suitable for use in tissue engineering constructs for RA applications. Upon maturation, DCs move to the secondary lymph organs to present the antigenic peptides to T cells so that the adaptive immune response is initiated (Banchereau and Steinman, 1998). Thus, DC maturation is essential to T cell activation which might induce T cell tolerance or T cell immunity (Lanzavecchia and Sallusto, 2001). Based on these facts, phenotype changes of DCs have been extensively investigated with their effects on T cell mediated immunity combined with directing immunogenicity (Schnurr et al., 2001; Hunter et al., 2007) or tolerogenicity (Gao et al., 1999; Mahnke et al., 2003; Banerjee et al., 2006) for immunotherapeutic applications.

It was hypothesized that DCs respond with differential levels of maturation upon contact

with different biomaterials and, further, these DCs treated with different biomaterials induce differential phenotype and polarization of autologous T cells upon co-culture of DCs and T cells, with elucidation of the differential integration effects of biomaterials in the RA knee joint of rabbits, wherein DCs and T cells are seriously involved in its pathophysiology.

Following initial characterization of five different biomaterials including four natural biomaterials [alginate, hyaluronic acid (HA), chitosan, and agarose] and one synthetic biomaterials [Poly(lactic-*co*-glycolic acid) (PLGA, 75:25)], treatment of immature DCs (iDCs) with these different biomaterials was performed to observe the effects of inherently different features of biomaterials on human monocyte-derived DC maturation *in vitro*. Differential levels of functional DC maturation were observed depending on the type of biomaterial in 2-dimensional (2-D) films used to treat iDCs using the variety of immunobiological functional assessment which includes DC morphologies in cytospin, surface marker (MHC class II or co-stimulatory molecules) expression, allostimulatory ability in a mixed lymphocyte reaction, and pro-inflammatory cytokine release. Of the biomaterials tested, PLGA or chitosan films supported higher levels of DC maturation, as compared to iDCs. Alginate films supported moderate levels of DC maturation. Agarose films did not support DC maturation whereas HA films inhibited DC maturation. As another measure of functional impact of different biomaterial films on DC phenotype changes, endocytic ability and CD44 expression of DCs were evaluated upon DC treatment with these different biomaterial films. Only agarose film induced endocytic ability of DC in level similar to iDCs, as expected from the previous observation that agarose did not support DC maturation, while all other biomaterial films did in levels statistically less than iDCs. Unexpectedly, HA film in cross-linked form induced endocytic ability and CD44 expression in levels statistically less than iDCs, even though HA film inhibited DC maturation in the previous examinations and CD44 has been well known as a potent receptor expressed on DCs

to mediate DC cluster, migration, and maturation upon interaction with the hyaluronan components in the extracellular matrix (ECM). To test effects of biomaterial grade such as research or clinical grade, we also examine the clinical grade biomaterials commercially available, compared to the research grade which is mainly studied in the present study. As a result, DC responses to clinical grade biomaterial films were indistinguishable from their responses to the research grade biomaterial films.

In addition to biomaterials in 2-D film form, biomaterial scaffolds in 3-dimensional (3-D) porous form have also been assessed for their effect on changes of DC phenotypes. Extended from the previous result of opposite effects of their 2-D film form on phenotypical changes in DC maturation, PLGA or agarose 3-D scaffold has been used to treat DCs, and effects of DC treatment with these biomaterial scaffolds were assessed with phenotypical changes of DCs. Similarly to the results observed in the previous study using different 2-D biomaterial films, DC phenotypes were differentially modulated by PLGA or agarose scaffolds in porous 3-D form. In the assessments of DC morphologies in confocal microscopy, surface marker (MHC class II or co-stimulatory molecules) expression, and allostimulatory ability in a mixed lymphocyte reaction, PLGA scaffold induced DC maturation in significantly higher levels of phenotypical changes of DCs, as compared to iDCs, while DCs treated with agarose scaffolds had similar phenotypes to iDCs. For twelve different cytokines/chemokines measured in this study, it has been found that both of PLGA and agarose scaffold modulates chemokines, pro-, or anti-inflammatory cytokines in differential levels upon contact of DCs with biomaterial scaffolds; unexpectedly, agarose scaffold induced interleukin (IL)-15 (pro-inflammatory cytokine) and monocyte chemotactic peptide (MCP)-1 (chemokine), while PLGA scaffold induced interleukin (IL)-10 (anti-inflammatory cytokine) in levels higher than the other biomaterial scaffold. Especially, in case of IL-15, MCP-1, interleukin (IL)-1 receptor antagonist, and interleukin (IL)-16, PLGA scaffold

induced in levels significantly lower than negative control of iDCs. Overall, PLGA scaffold trends to induce pro-inflammatory cytokines and chemokines, whereas agarose scaffold does to induce anti-inflammatory cytokines.

Extended from the biomaterial effects on phenotypical changes of DC maturation, DCs treated with different biomaterial films were assessed for their functional impacts in regulating autologous T cell phenotype and polarization. The effect of five different biomaterial films on directing the activation of CD8+ cytotoxic T cells or CD4+ helper T cells (also CD4+CD25+FoxP3+ cells) and the T helper type 1 (Th1) or T helper type 2 (Th2) polarizations was assessed upon *in vitro* interactions between DCs and autologous T cells. When autologous T cells were co-cultured with DCs treated with biomaterial film/antigen (ovalbumin, OVA) combinations, different biomaterial films induced differential levels of T cell marker (CD4, CD8, CD25, CD69) expressions, as well as differential cytokine profiles [interferon (IFN)-γ, interleukin (IL)-12p70, interleukin (IL)-10, interleukin (IL)-4] in the polarization of T helper types. Dendritic cells treated with agarose films induced CD4+CD25+FoxP3+ (T regulatory cells) expression on autologous T cells at level similar to iDCs and interleukin (IL)-10 release at higher levels whereas PLGA film treatment induced release of IFN-γ at higher levels, as compared to DC treatment with other biomaterial films, in the DC-T co-culture system. Interestingly, when DCs were treated with the different biomaterial films, profiles of released cytokines were influenced by the presence of antigen or autologous T cells.

Based on these *in vitro* results, to further understand the influence of RA environment to different biomaterials and to identify biomaterial useful for tissue engineering in the RA situation, integration of inherently different biomaterials (PLGA and agarose) was assessed upon implantation of them into the knee joint of antigen-induced arthritis (AIA) rabbit. Upon RA induction combined with biomaterial implantation or sham operation into the right knee joint, the

knee swelling size and total leukocyte concentration in the right knee remarkably increased, compared to the untreated left knees, and these increased levels in the right knee consistently went through the end point of Day 36. However, total leukocyte concentrations in the peripheral blood or in the joint lavage of the left knees (untreated control) were observed in differential levels depending on the biomaterial implant, possibly due to the systemic circulation of the peripheral blood. Furthermore, cartilage and bone healing progression was differentially observed in the osteochondral defect of the knee joint of RA-induced rabbit, depending on type of biomaterial scaffold implanted into the defect.

Collectively, these results demonstrate the multifunctional impacts of inherently different biomaterials on *in vitro* immunomodulation of phenotype and polarization of DCs and autologous T cells. Furthermore, taken together with these immunomodulatory impacts of biomaterials, *in vivo* effects of different biomaterial scaffolds on RA environment shown in this study can suggest the criteria of selection and design of biomaterials for orthopedic tissue engineering, which may ultimately be best integrated into the diseased cartilage and bone.

CHAPTER 1

INTRODUCTION

Rheumatoid arthritis (RA) is a chronic systemic autoimmune inflammatory disorder that predominantly affects the synovial tissue (ST) of joints, leading to cartilage and bone erosion and subsequent joint destruction (Pettit and Thomas, 1999; Bresnihan, 1999). Damaged cartilage has a limited capacity for self-repair after cartilage failure of arthritis, and joint surface defects that exceed a critical size heal poorly and usually lead to osteoarthritis (O'Driscoll, 1998). Tissue engineering has been recognized as a promising alternative for cartilage reconstruction and regeneration, providing a relatively simple procedure and long-term drug-free remission. Rheumatoid arthritis is believed to be caused by a combination of genetic, environmental, and hormonal factors but the exact mechanism of the autoimmunity initiation is not yet clear. However, among various inflammatory and immune cells involved in RA, dendritic cells (DCs) have been proposed to play a central role in the initiation and perpetuation of RA by presentation of arthritogenic antigen to autoreactive T cells (Waalen et al., 1986; Pettit and Thomas, 1999; Santiago-Schwarz et al., 2001; Radstake et al., 2005). Dendritic cells bridge the innate and adaptive immune response as a professional antigen presenting cell (APC) of the immune system. As such, upon maturation, DCs express high levels of major histocompatibility antigens and co-stimulatory molecules, and interact with T cells for antigen presentation as shown in Figure 1-1. In this way, DCs stimulate T cells in the inflamed RA synovial tissue and are thought to be directly involved in the generation of destructive autoimmune responses (Thomas, 1998; Thomas et al., 1999). Dendritic cells have also been proposed to be matured upon biomaterial contact which then functions as an adjuvant to boost an adaptive immune response (Babensee et al.,

1998; Yoshida and Babensee, 2004; Babensee and Paranjpe, 2005; Matzelle and Babensee, 2004). Accordingly, biomaterials combined in the tissue-engineered constructs for RA is required to be tolerated by the associated intense inflammatory and immune environment.

The objective of this research was to understand DC response towards different biomaterials and further correlate those responses with the integration of different biomaterials implanted into RA joints of rabbit. In particular, DC maturation was assessed upon contact with inherently different biomaterials and the immunomodulation of these biomaterials was tested in biologically induced RA circumstance of rabbit model. **It was hypothesized that DCs respond with different levels of phenotypical changes in their maturation to different biomaterials used to treat immature DCs (iDCs), and the effects of biomaterials on its integration in RA environment is elucidated through biomaterial implantation into the RA knee joint of a rabbit.** Adjuvant effects of biomaterials in different chemistries or different physical forms have been extensively studied (Hunter, 2002; Newman et al., 1998b; Newman et al., 2002; Bennewitz and Babensee, 2005). In addition, these adjuvant effects associated with phenotypical changes in DC maturation have been recently studied (Yoshida and Babensee, 2004; Little et al., 2004). The exact mechanism behind DC maturation by biomaterials, however, is not fully elucidated. Furthermore, from a tissue engineering view point, immunomodulatory effects of biomaterials was not well characterized using *in vivo* model of autoimmune disease wherein DCs are heavily involved. Because control of DC phenotype is central to immunomodulation ability effect of biomaterials, as well as play the critical role in RA pathophysiology as described earlier, DC response towards biomaterials should be well understood and further controlled for the biomaterial selection in the cartilage tissue engineering of RA.

To address the above central hypothesis, three specific aims were pursued.

Specific aim 1: Demonstrate that DC phenotype is differentially induced depending on the type of biomaterials used in orthopedic tissue engineering (*in vitro* study).

The working hypothesis for this aim was that DC maturation is differentially affected depending on different biomaterials in 2-dimensional (2-D) film forms, which include Poly(lactic-co-glycolic acid) (PLGA, 75:25), chitosan, hyaluronic acid (HA), alginate, and agarose, used to treat the DCs. For this aim, iDCs were derived from peripheral human blood mononuclear cells *in vitro*, and treated with these biomaterial films, and resultant DC phenotype assessed by examining DC morphologies, surface marker expression, allostimulatory ability, transcription factor activation, cytokine release, and endocytic ability. Biomaterial film surfaces were characterized using X-ray photoelectron spectroscopy (XPS). To test effects of biomaterial grade such as research or clinical grade, the clinical grade 2-D biomaterial films were also prepared, when the polymer is commercially available, and examined as far as their effect on DC maturation, as compared to the research grade. In addition, to understand DC response towards expanded surface area (larger surface area to volume ratio than 2-D film) in porous scaffold, biomaterial scaffolds in 3-dimensional (3-D) porous form have been examined for their effect on resultant DC phenotypes. Such porous scaffold are also routinely used in tissue engineering. Based on the opposite effects of their 2-D film form on phenotypical changes in DC maturation, PLGA or agarose 3-D scaffold were used to treat DCs, and effects of DC treatment with these biomaterial scaffolds were assessed as far as resultant phenotypical changes of DCs.

Specific aim 2: Demonstrate that phenotype and polarization of autologous T cells are differentially induced by DCs treated with different type of biomaterials (*in vitro* study).

The working hypothesis for this aim was that different biomaterials (2-D) direct phenotype and polarization of autologous T cells upon co-culture of these T cells with DCs pre-treated with biomaterials. To extend biomaterial effects on DCs to an adaptive immunity, autologous T cells were obtained from the identical donor from whom DCs were obtained, and then, co-cultured with DCs treated with five different biomaterial films used in the Specific aim 1. The effect of different biomaterial films on directing the activation of CD8+ cytotoxic T cells or CD4+ helper T cells (also CD4+CD25+FoxP3+ cells) and the T helper type 1 (Th1) or T helper type 2 (Th2) polarization was assessed upon *in vitro* interactions between DCs and autologous T cells, using the measurement of T cell surface marker expressions and cytokine release into supernatant, as well as intracellular marker expression, to provide information of immunomodulatory effects of biomaterials on immunogenicity or tolerogenicity in T cell-mediated immunity.

Specific aim 3: Correlate DC maturation upon treatment with different biomaterials with integration of biomaterials implanted into the RA joint of rabbit (*in vivo* study).

To understand the influence of RA environment to different biomaterials and to identify biomaterial useful for tissue engineering in the RA situation, integration of inherently different biomaterials (PLGA and agarose) based on their effects on DC phenotype, was assessed upon their implantation into the knee joint of rabbit with induced RA. *The working hypothesis was that a selected biomaterial that does not support in vitro DC maturation will demonstrate effective integration and acceptance in the rabbit RA joint.* After rabbits were immunized by subcutaneous injection of antigen (OVA)/adjuvant (CFA) (Day 0) and boosted by subcutaneous injection of antigen (OVA)/adjuvant (IFA) (Day 14), RA was induced in the right knee by intra-articular injection of angiten (OVA) (Day 21) and then, biomaterial scaffolds were implanted into this right knee joint with induced RA (Day 22). The left knee remained untreated as the within-animal control. The host response to implanted biomaterial scaffolds in the rabbit RA joint was assessed by examining joint swelling, total leukocyte concentration in the joint lavage or the peripheral blood, differential leukocyte profiles in the joint lavage, measurement of systemic and joint lavage TNF-α levels, histology of the knee joints, and micro-CT analysis for measurement of cartilage destruction.

Collectively, studies herein are a step forward understanding the effect of inherently different features of biomaterials on DC phenotype to suggest new selection and design criteria for biomaterials to be used in the combination products such as tissue engineering or vaccine delivery where immune responses are of consequence. Results presented here provide novel approaches for identification of multifunctional impacts of biomaterials on immunomodulating DC response and further T cell-mediated adaptive immunity. Especially, because resultant

impacts of biomaterials are central to the modulation of the host response to biomaterials, these studies imply that biomaterials possibly can be utilized in immunotherapy application.

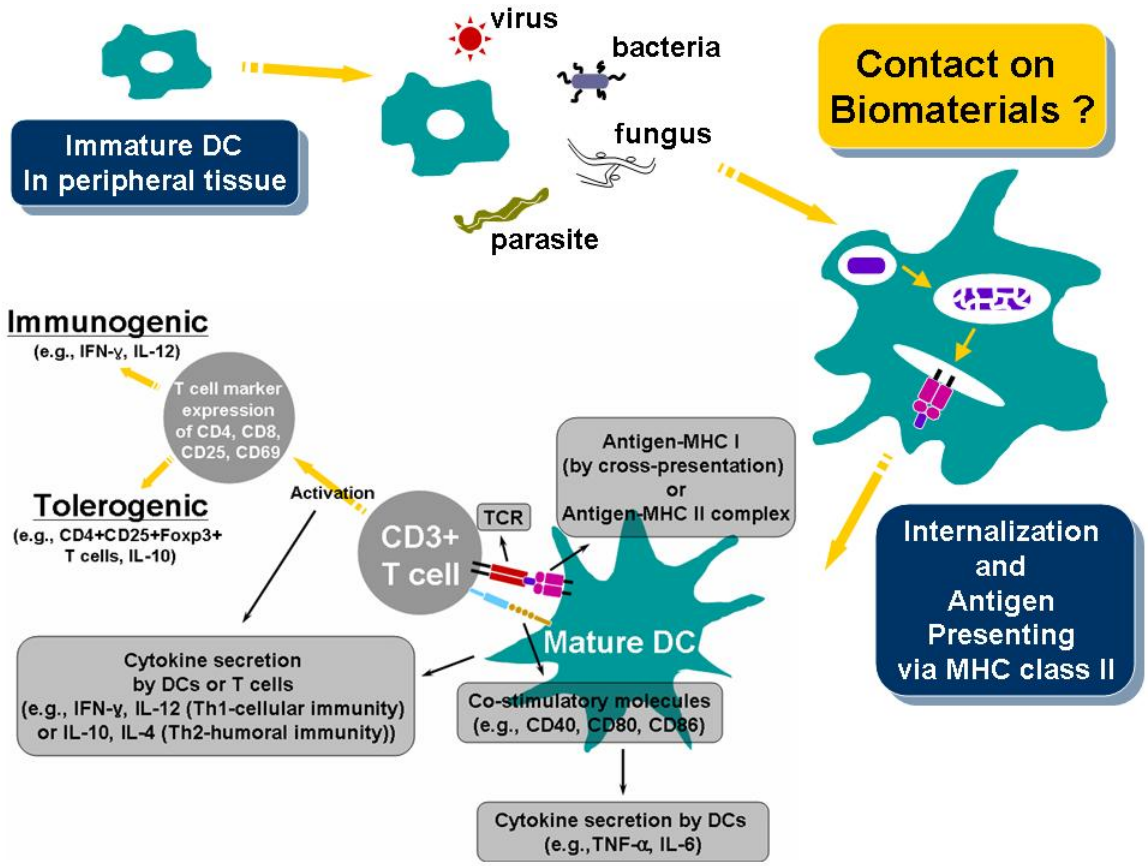

Figure 1-1: Schematic representation of dendritic cell phenotype changes and T cell-mediated adaptive immunity.

It is hypothesized that DC phenotype changes in differential levels upon DC treatment with different biomaterials and these biomaterial treatments of DCs further affect T cell phenotype and polarization upon co-culture of DCs and T cells.

CHAPTER 2

RESEARCH SIGNIFICANCE

Rheumatoid arthritis is a chronic autoimmune disease and it is estimated that more than 1% of the United States population suffers from this disease. Despite of continuous efforts through collaborations of medicine and engineering, the etiology of arthritis still remains unclear (Robbins et al., 2003; Wang and Yu, 2004; Tetik et al., 2004; Tsokos and Tsokos, 2003). Tissue engineering has emerged as a promising method for cartilage reconstruction and regeneration, providing a minimally invasive, and long-term drug-free remissive therapeutic procedure for osteoarthritis patients (Galois et al., 2005; Chang et al., 2006; Jorgensen et al., 2004). Its potential in restoring tissue in rheumatoid arthritic patients remains to be defined. However the host response against the biomaterial component or device is still a major concern on the achievement of tissue restoration (Babensee et al., 1998). Dendritic cells have been proposed to play a central role not only in the initiation and perpetuation of RA (Waalen et al., 1986; Pettit and Thomas, 1999; Santiago-Schwarz et al., 2001; Radstake et al., 2005), but also in host immune response against biomaterials, associated with the adjuvant effects (Babensee et al., 1998). In particular, APCs such as DCs and macrophages are thought to play the central role of the adjuvant effect, which mediate any of the following mechanisms: increasing cellular infiltration, inflammation, and trafficking of APCs to the injection site; upregulating co-stimulatory molecules or MHC expression to induce the activation of APCs; enhancing antigen presentation; or inducing cytokine release for indirect effects (Cox and Coulter, 1997; Singh and O'Hagan, 1999). In addtion, the adjuvant effects of the polymeric biomaterials have been extensively investigated (Singh and O'Hagan, 1999; Hunter, 2002) and further, these effects of polymeric biomaterials suggested as new idea for immunomodulating combination products in tissue engineering or

vaccine delivery (Ertl et al., 1996; Seferian and Martinez, 2000; Jaganathan et al., 2004; Matzelle and Babensee, 2004; Yoshida and Babensee, 2004; Bennewitz and Babensee, 2005; Babensee and Paranjpe, 2005). However, the mechanism behind the immunomodulatory effects of biomaterials on DCs has not been fully elucidated. *The major goal of this research is to identify multifunctional impacts of biomaterials on immunomodulating DC response and further T cell-mediated adaptive immunity to ultimately correlate these in vitro responses of DCs and/or T cells with the biomaterial effect or integration in induced RA animal models*.

The significance of this research is three-fold. First through this work, it fully characterizes the immunological functions imparted to DC through their treatment with biomaterial films or scaffolds, the later which is particularly relevant to tissue engineering. Secondly, it demonstrates the novel concept of non-pharmacological immunomodulatory potential of biomaterials to polarize T-cell mediated adaptive immunity towards immunogenicity or tolerance, as desired for a particular application. The proposed research is further significant as it aims to inform biomaterial design and selection criteria for biomaterials to be used as a platform for tissue engineering approaches for amelioration of orthopedic tissue due to RA by assessing the host response and integration of biomaterial scaffolds implanted into rabbit joints with induced RA. Hence, this research demonstrates the application of an innovative combination of biomaterial implantation into an osteochondral defect in rabbits with induced RA as a clinically relevant model in which to test biomaterials for orthopedic applications in a diseased joint to more closely approximate the actual application.

CHAPTER 3

LITERATURE REVIEW

Immunology of RA and role of dendritic cells

Pathophysiology of RA

Rheumatoid arthritis is generally believed to be caused by a combination of genetic, environmental, and hormonal factors but the exact mechanism of the autoimmunity initiation is not yet clearly understood due to its complicated etiology. Even though tremendous efforts have been extensively made on the immunological mechanisms, which show a massive influx of T cells, B cells, and fibroblast-like synoviocytes, macrophages, and dendritic cells (DCs) in the synovial tissue, the pathophysiological pathways of RA remain unclear, similar to most other autoimmune diseases (Bresnihan and Tak, 1999; Miossec, 1995; Weyand and Goronzy, 1997). As featured on the symptomatic studies, RA is characterized by marked swelling and inflammation. Immune cell infiltration into both the synovial fluid (SF) and synovial tissue (ST) accompanies this inflammation, associated with the proliferation of resident ST cells and angiogenesis. Formation of the destructive tissue front or pannus occurs as the ST extends over cartilage and bone. The majority of the cartilage destruction and bone erosion occurs at the junction with pannus (Bresnihan, 1999; Pettit and Thomas, 1999). For some unknown reasons, the arthritogenic auto-antigens are presented to CD4+ T cells, inducing the auto-reactive CD4+ T cells and auto-reactive B cells which produce auto-antibodies against self (Sheriff et al., 2004). These activated B cells have been proved to play a critical role in disease persistence. In addition to these autoimmune processes, macrophages and neutrophils infiltrating into the ST, accompanied by complicated interactions with lymphocytes, resident osteoclast, and synoviocytes, initiate the cartilage and bone destruction followed by pannus formation and angiogenesis (Pay et

al., 2006; Malemud, 2007; Sweeney and Firestein, 2004). In the course of the disease, associated with the pannus formation and destruction processes, the massive influx of various cells above infiltrates into the ST and accumulates at the junction of the pannus and cartilage. These cells secrete, as the primary source, the pivotal pro-inflammatory cytokines of TNF-α, IL-1β, IL-1, IL-6, IL-17, IL-18, and IL-15. Other than these cytokines, expression of monokine induced by interferon-γ (Mig), growth-related oncogene-α (GRO-α) chemokines, and other angiogenic molecules has been also detected in the synovial resident cells and in inflammatory cells to a level proportional to extent of leukocyte infiltration in RA afflicted joints (Cinelli et al., 2006; Jeong et al., 2004). The pro-inflammatory cytokines subsequently activate signal transduction pathways and transcription factors, which, in turn, control the transcription of cytokines. In addition, TNF-α, IL-1, and IL-6 are also known to induce an osteoclast development and function, cartilage destruction, and synovial hyperplasia. As such, the pro-inflammatory cytokines play a critical role in the perpetuation of RA (Radstake et al., 2005; Zwerina et al., 2005). Toll-like receptor (TLR) -2 and TLR-4 are also involved in the induction of vascular endothelial growth factor (VEGF), IL-6, IL-8, TNF-α, and macrophage migration inhibitory factor (MIF), so that they play a critical role in the amplification or perpetuation of the inflammatory loop of human RA (Popa et al., 2006; Sacre et al., 2007; Cho et al., 2007).

Clinical treatments of RA

For these reasons, unless the symptoms sufficiently is to indicate surgical treatment such as total knee replacement, conventional treatment is anti-cytokine therapies to block cytokines released from the autoimmune environment to relieve the symptoms of RA. For instance, Enbrel (a generic drug name of Etanercept) is one of the most popular drugs for the RA patient, which is a recombinant soluble form of human TNF-α receptor fusion protein. Once the Enbrel

is injected subcutaneously into the RA patient, it would inhibit the signal pathway between TNF-α and TNF-α receptor by blocking TNF-α binding. Another representative drug is Anakinra which is a recombinant non-glycosylated form of human IL-1 receptor antagonist. Anakinra injected into the patient would block IL-1 receptor of the patient, inducing the inhibition of signal pathway between IL-1 and IL-1 receptor. It is still, however, unclear why blocking a certain cytokine is efficacious for some patients whereas not for others who need a multiple treatment (e.g., TNF and IL-1 blockade), even though they have a similar level of RA symptoms. Moreover, this anticytokine therapy should be frequently (e.g., twice weekly) injected into the patients for long time duration and is limited to those with minor RA symptoms. Even though most parts of the pathophysiology system of RA are unclear, it has been clearly identified that the genetic predisposition, which is associated with the MHC class II molecules, is significantly related with RA patients of certain ethnic groups (Winchester, 1981). Together with this, the activation of auto-reactive T and B cells described above indicates that the adaptive immune system is critically involved in the pathophysiology of RA. Recently, although questions still remain to be answered, suppressive mechanisms of T regulatory cells and/or cytokine, IL-10, in the disease course of human RA patients has been partially explained, thereby suggesting potential benefit of therapies based on adaptive immunity in RA patients (Jonuleit et al., 2000; Appel et al., 2004; Valencia et al., 2006).

Dendritic cells in RA pathophysiology

It has been proposed that DCs play a central role in the initiation and perpetuation of RA by presentation of arthritogenic antigen to auto-reactive T cells. Briefly, differentiated DCs have been reported to be enriched in the ST of active RA joints and these differentiated DCs are generally found interdigitating in perivascular lymphoid aggregates, likely being derived from

peripheral blood precursors. Thus DCs are optimally located for the presentation of arthritogenic antigen to T cells and the regulation of B cells in RA ST. For instance, numerous chemokines, such as macrophage inflammatory protein (MIP)-1α, monocyte chemotactic protein (MCP)-1 and regulated on activation normal T cell expressed and secreted (RANTES), have been also observed as strong evidence for the DCs recruited, together with participation of other leukocytes in this inflammatory site, into RA ST (Thomas, 1998; Jeong et al., 2004; Sallusto and Lanzavecchia, 1999; Thomas et al., 1999). Recently, DCs have been demonstrated with their effects on controlling lymphocyte (T and B cell) activation associated with pro-inflammatory cytokine releases in RA pathophysiology using RA patients (Anolik et al., 2008) or *in vivo* RA murine model (Jung et al., 2007).

Rheumatoid Arthritis (RA) and tissue engineering

General facts of rheumatoid arthritis

Arthritis is a general term which describes inflammation in joints. Rheumatoid arthritis is a chronic systemic autoimmune inflammatory disorder that predominantly affects the synovial tissue (ST) of joints, leading to cartilage and bone erosion and subsequent joint destruction. Rheumatoid arthritis occurs in joints on both sides of the body (such as both of hands, wrists or knees). This symmetry of symptoms helps distinguish RA from other types of arthritis. In addition to affecting the joints, RA may occasionally affect the skin, eyes, lungs, heart, blood, nerves, or kidneys too (Cieza and Stucki, 2005). It has been reported that more than 1% of the United States population suffer from RA and it is three times more common in female than male. It usually occurs in people between the ages of 20 to 50 (Cieza and Stucki, 2005; Bansback et al., 2005; Lebwohl et al., 2005). Since the exact pathophysiological pathways unfortunately remain unclear in autoimmune disease such as rheumatoid arthritis (RA), most therapeutic procedures are

currently focused on temporary remission of symptoms in the absence of controlling the origin of problem and preventing recurrence (Tetik et al., 2004; Robbins et al., 2003; Wang and Yu, 2004; Tsokos and Tsokos, 2003). Damaged cartilage has a limited capacity for self-repair after cartilage failure of arthritis and joint surface defects that exceed a critical size heal poorly and usually lead to osteoarthritis. Treating chondral lesions or cartilage defects is still a challenge for orthopedic surgeons and sports medicine physicians (Tetik et al., 2004).

Conventional therapeutic methods employed for RA

Pharmacologic therapies and surgical treatments are currently employed to treat arthritis patients. Conventional pharmacologic therapies for the treatment include non-steroidal anti-inflammatory drugs, immunosuppressive agents, corticosteroids, and disease-modifying drugs (Robbins et al., 2003). These therapies often reduce joint inflammation and provide relief from pain, but are ineffective in preventing the destruction of bone and cartilage or restoring joint function. Moreover, anti-inflammatory drugs and potent immunosuppressive molecules can lead to undesirable side effects (Arend and Dayer, 1995; Brennan et al., 1989; Elliott et al., 1993; Dayer and Fenner, 1992; Wooley et al., 1993). Whilst pharmacologic methods only treat the symptoms, the underlying causes with the retention of inflamed tissue remain and clinical methods of surgical treatments can be utilized to reduce a risk of side effects or recurrences of disease for long-term solutions including modifying or extracting inflamed area out of patient's knee. These surgical treatments being currently applied or considered include representative categories such as total knee replacement, unicompartmental knee replacement, viscosupplementation, autologous chondrocyte implantation, chondral shaving with debridement, abrasion arthroplasty, subchondral drilling, microfracturing of the subchondral plate, transplantation of periosteal, and perichondral or osteochondral autografts (Wang and Yu, 2004;

Chen et al., 1999; Smith et al., 2005). In most cases, surgical methods temporarily relieve symptoms and induce an initial hyaline-like repair, however the repair tissue eventually degenerates to fibrocartilage and the symptoms return. None of the currently available methods can predictably restore a durable articular surface for long term. Moreover some cases such as knee replacements are still associated with harshly complicated procedures, high cost, and limited movements of patients (Buckwalter and Mankin, 1998; Hunziker, 2002).

Tissue engineering as a new therapeutic method

Tissue engineering has been recognized as a promising alternative for cartilage reconstruction and regeneration, providing a relatively simple procedure and long-term drug-free remission. In conjunction with great possibilities of minimally invasive and less complicated procedures for patients, cartilage tissue engineering has been motivated by the need of replace lost or damaged tissue with an already structurally and mechanically functional implant that can be created *in vitro* using chondrocytes or chondroprogenitor cells in combination with biomaterials (Suh and Matthew, 2000; Cancedda et al., 2003; Zhang et al., 2005; Kuo et al., 2006). Including the cartilage tissue engineering, the tissue engineering in regenerative medicine has been generally considered as the newest research field for investigating repair and regeneration of organs and tissues using the natural signaling pathways and components of the organism such as stem cells and growth factors. Cells harvested from donor tissues can be expanded in culture, associated with synthetic or natural biomaterials specifically designed for each tissue. According to this, any tissue can be virtually repaired under properly designed conditions. For application of tissue engineering constructs in humans, skin and epidermis have been widely dealt with for the therapeutic interest but interest is shifting to other pathological situations such as the reconstruction and repair of bone and cartilage (Potten and Booth, 2002; Cancedda et al., 2003).

Studies on development of more efficient methods in cartilage tissue engineering have been recently extended to use of embryonic stem chondrogenic differentiation (Anderson et al., 2004), injectable hydrogel based tissue engineered constructs (Tan et al., 2009), gene therapy for delivery of various biofactors (Venkatesan et al., 2004), signaling molecules (Indrawattana et al., 2004), and dynamic bioreactors (Concaro et al., 2009).

Dendritic cells

Immature dendritic cells and antigen capture

Dendritic cells are generally found in most tissues, solid organs, and blood as immature sentinel cells that are continually sampling the environment for self and non-self antigens. Once they detect and capture the antigens, they would go under processing of internalization such as endocytosis and then, of antigen degradation, followed by antigen presentation to specific lymphocytes for further immune responses. Thus, DCs are usually called professional antigen presenting cells (APCs) which also include macrophages and B cells, bridging between innate and adaptive immune responses (Sallusto et al., 1995; Banchereau and Steinman, 1998). For example, extracellular antigens captured by APCs are processed to be presented by major histocompatibility complex (MHC) of APC to, through T cell receptors (TCRs), the helper T cell (Th) and then, the activated Th secreted cytokines that regulate B cell activation, initiating humoral responses(Banchereau and Steinman, 1998). Dendritic cells recognize pathogens through conserved structures, uniquely characteristic of pathogens, through their cognate binding receptors resulting in their maturation such that they become efficient antigen presenting cells (Janeway and Medzhitov, 1998). To detect pathogens, DCs use a variety of receptors, including pattern recognition receptors (PRRs) such as the Toll-like receptor (TLR) family, which recognize pathogen-associated molecular patterns (PAMPs) such as bacterial Lipopolysaccharide (LPS),

non-methylated oligonucleotides (CpG), and viral double-stranded RNA (Medzhitov, 2000). In addition, PRRs expressed on DCs also include C-type lectin receptors (CLRs) such as mannose receptor (Sallusto et al., 1995), DEC205 (Kato et al., 1998), and dendritic cell-specific intercellular adhesion molecule-3-grabbing nonintegrin (DC-SIGN) that bind to carbohydrate-conjugated molecules (Geijtenbeek et al., 2000), and scavenger receptors that are involved in internalization of polyanionic ligand (Peiser et al., 2002).

Maturation of DCs and migration to secondary lymphoid organs

Immature DCs mature upon encountering pathogens and/or numerous endogenous stimuli including TNF-α, IL-1, CD40L, and heat shock protein (HSP), referred to as 'danger signals'(Matzinger, 1994). Dendritic cells upon maturation migrate via the afferent lymphatics to draining lymph node (LN) to present the previously internalized and processed antigens in context of MHC class molecules for T cells and B cells for their activation (Matzinger, 1994; Banchereau and Steinman, 1998). During this maturation process, DCs show differentiated phenotypes with increased up-regulation of peptide-loaded MHC class I and II molecules for efficient antigen presentation and higher levels of co-stimulatory molecules of CD40, CD80 (B7-1), CD86 (B7-2) to facilitate communications with T cells (Sallusto et al., 1995; Banchereau and Steinman, 1998) as well as DC marker of CD83 (Tsuji et al., 2000), and morphologically showing dendritic processes. These dramatic conformational changes are accompanied by an increased secretion of pro-inflammatory mediators such as cytokines (TNF-α, IL-6, and IL-12) and chemokines and expression of chemokine receptors such as CCR-7 (Bell et al., 1999; Mellman and Steinman, 2001). Translocation (activation) of transcription factor family of NFκB from the cytosol to the nucleus is also a representative intracellular change essential for DC maturation (Rescigno et al., 1998; Yoshimura et al., 2001).

Innate and adaptive immune response

The innate immunity is the front line of the host defense system against various pathogens through a non-specific and rapid response achieved mainly by phagocytes or complement activation. Adaptive immunity is slowly generated following the innate immune response based on specific and memorized response against antigens, owing to the wide repertoire of the clonal T cell receptors (Medzhitov and Janeway, 1997). Upon an invasion of pathogens, tissue-resident phagocytic cells (e.g., macrophages) or heat-labile plasma proteins (e.g., complement) recognize pathogens and lead to an inflammatory response resulting in proteolytic enzyme release, opsonization, and phagocytosis of those pathogens. During this innate immune response, the pathogens are recognized by PRRs expressed on APCs such as DCs or macrophages. Once the pathogens are recognized particularly by iDCs in the innate immunity, DCs mature and then, activate lymphocytes such as naïve T and B cells to initiate the adaptive immune response towards the pathogen – delivered antigen. Upon systematic communication between mature DCs and naïve lymphocytes at lymph nodes, these naïve lymphocytes become differentiated to effector cells such as helper T or cytotoxic T cells and plasma cells (mature B cells) through specifically encoded and clonally expanded receptors such as T cell receptors (TCRs) and immunoglobulin family (Ig) on activated T cells and B cells, respectively. These effector cells subsequently lead the adaptive immunity to eradicate pathogens and some of them become memory T and B cells to facilitate a faster response against identical antigens in future (Medzhitov and Janeway, 1997; Janeway and Medzhitov, 1998; Janeway et al., 2004).

Adjuvant

Adjuvants have been employed to improve the immune response by increasing the

immunogenicity, incorporated with antigens in vaccines, since the early of 1920s (Cox and Coulter, 1997). Aluminum hydroxide, aluminum phosphate, and calcium phosphate are the mineral salt-based adjuvants widely accepted in human and veterinary vaccines since 1930s due to their excellent safety records. Complete freund's adjuvant comprised of oil emulsion and killed bacteria is another representative adjuvant widely used but is limited to animal use due to its toxicity to human. Lastly, the immunostimulatory adjuvants such as cytokines (IL-2 and IL-12) have been also widely recognized in the clinical use for their natural sources (Cox and Coulter, 1997; Singh and O'Hagan, 1999; Hunter, 2002). Since the TLR was discovered in drosophila, studies on TLR and its ligands have been expedited and it has been found that ligands of TLRs include many of the evolutionarily conserved molecules such as LPS, lipoproteins, lipopeptides, flagellin, double-stranded RNA, unmethylated CpG islands as well as various other forms of DNA and RNA released by bacteria and viruses. Moreover, most natural adjuvants employed are lipid-related materials which originate from those bacteria and viruses. For these reasons, TLRs have been considered to essentially act as adjuvant receptors and sustain the molecular basis of adjuvant activity. Further, developments of natural adjuvant have been focused on the identification of specific receptors, such as TLRs, on APCs, which are thought to provide a link between the innate and adaptive immune responses (Medzhitov et al., 1997). Even though the exact mechanisms of adjuvant action are still only poorly understood so that the new design or application of the adjuvants largely depends on the empirical facts, APCs such as DCs and macrophages are thought to play the central role of the adjuvant effect, which mediate any of the following mechanisms: increasing cellular infiltration, inflammation, and trafficking of APCs to the injection site; upregulating co-stimulatory molecules or MHC expression to induce the activation of APCs; enhancing antigen presentation; or inducing cytokine release for indirect effects (Cox and Coulter, 1997; Singh and O'Hagan, 1999).

Based on the typical feature supporting the immunogenicity, the adjuvant effects of the polymeric biomaterials have been extensively investigated. For instance, particulate adjuvants, including polymeric microparticles, are internalized by APCs, thereby activating them, inducing an immune response to associated antigens (Singh and O'Hagan, 1999). Particulate adjuvants also enhance the immune response by creating a depot of antigen at the site of injection to prolong exposure (Hunter, 2002). More recently, nano- or microparticles endocytosed by DCs have been shown with their differential effects on T cell stimulation depending on their different sizes (Koike et al., 2008; Tran and Shen, 2009), as well as on DC or macrophage phenotypes through inflammasome activation depending on their different inherencies (Martinon et al., 2006; Sharp et al., 2009). These effects of polymeric biomaterials suggested as new idea for immunomodulating combination products in tissue engineering or vaccine delivery (Ertl et al., 1996; Seferian and Martinez, 2000; Jaganathan et al., 2004; Matzelle and Babensee, 2004; Yoshida and Babensee, 2004; Bennewitz and Babensee, 2005; Babensee and Paranjpe, 2005).

Biomaterials in tissue engineering and dendritic cells

General facts of biomaterials in tissue engineering

A biomaterial is generally defined as 'a nonviable material used in a medical device, intended to interact with biological systems' (Williams, 1987). To support the functionality of the tissue engineered construct, which facilitates specific proliferation and differentiation of cells in optimized conditions, biomaterials for scaffolds should ideally have following characteristics: porous enough for cell growth and transport of nutrients and metabolic waste; bioresorbable with controllable degradation; proper surface chemistry for cell attachment, proliferation, and differentiation; suitable mechanical properties; reproducible and processable in variety of shapes and sizes as needed; and biocompatible through whole procedure of the tissue regeneration (Kim

et al., 2000; Hutmacher et al., 2001). Due to the processability, high ratio of physical stability to weight, and controllable degradability and resorbability, biomaterials used for the tissue engineering are, in most cases, polymer-based materials and not ceramic or metallic materials (Ratner et al., 2004). According to its origin, they are basically classified as natural polymers or synthetic polymers (Ratner et al., 2004; Li and Tuan, 2005; Hutmacher et al., 2001; Kim et al., 2000). Protein- or polysaccharide-based natural polymers have the potential advantage of biocompatible features due to their origin but difficulties in reproduction and purification from the nature or poor mechanical properties remain as obstacles to their use. Synthetic polymers can be reproduced with well controlled physical properties, such as degradation, resorption, microstructure, and surface chemistry in a large scale. However, synthetic biomaterials are still considered as less biocompatible compared to natural biomaterials because of the absence of the intrinsic biological properties (Kim et al., 2000; Ratner and Bryant, 2004). Collagen and fibrin are representative protein-based polymers while alginate, agarose, hyaluronic acid, and chitosan are most widely investigated polysaccharide-based polymers in tissue engineering. For synthetic biomaterials, poly(lactic-*co*-glycolic acid) (PLGA) and poly(ε-caprolactone) (PCL) are most popular in tissue engineering applications (Hunziker, 2002; Hutmacher et al., 2001; Kim et al., 2000; Ratner and Bryant, 2004). In particular, synthetic biomaterials has been intensively studied with their multifunctional impacts on tissue engineering-based regeneration therapy; biomaterials can modulate microenvironments by delivering biosignaling molecules such as growth factor or gene, as well as fostering the formation of new extracellular matrix and tissue ingrowth (Tabata, 2009).

Dendritic cell response to biomaterials upon contact

However, implantation of a foreign material causes a host response towards the foreign

entity, which is akin to a nonspecific innate immune response. Thus the selection of a foreign material and the associated host response are critical to the successful application of tissue engineering (Anderson, 2001; Ratner and Bryant, 2004). Among biomaterial characteristics necessary for tissue engineered constructs, biocompatibility is of critical importance in a scaffold to endure that the implant and/or its degradation products do not elicit an innate or inflammatory immune response. Based on the role of DCs in RA as described earlier, DCs response towards biomaterials should be well understood and controlled for the biomaterial selection in the cartilage tissue engineering of RA, and for situations with combination products where adaptive immune responses are of consequence.

The adjuvant such as CFA has been shown to induce maturation of DCs by induction of pro-inflammatory cytokine secretion such as IL-12 and upregulation of MHC and co-stimulatory molecules (Tsuji et al., 2000). Extended from similarities to these maturation patterns of DCs, biomaterial-associated adjuvant effects of DCs have been shown in various situations. Copolymers of hydrophilic poly(ethylene glycol) (PEG) and hydrophobic poly(propylene glycol) have shown the adjuvant effects increased in proportion to the fraction of the hydrophobic block in the copolymers (Newman et al., 1998b; Hunter, 2002). For the internalization activity of DCs, particulate forms of PLGA, polystyrene, and latex have been investigated and the phagocytosed PLGA and poly(β-amino ester) microspheres showed an adjuvant effects in DCs to maturation by inducing phenotypical changes such as upregulation of co-stimulatory molecules of CD80, CD86, and CD40 (Newman et al., 2002; Yoshida and Babensee, 2004; Bennewitz and Babensee, 2005; Little et al., 2004). Recently, differential levels of DC maturation upon treatment with different biomaterial films have been observed, showing that PLGA or chitosan films induced the maturation of DCs while agarose, alginate, or hyaluronic acid exhibited moderate or less matured DCs compared to the negative control of iDCs (Yoshida and Babensee, 2004; Babensee and

Paranjpe, 2005; Yoshida and Babensee, 2006). The exact mechanisms involved in this DC maturation by biomaterials, however, is not yet fully elucidated. But it is likely that possible factors are hydrophobicity (or hydrophilicity) of biomaterials and adsorption of complement or other proteins to biomaterials, which are recognized by PRRs of DCs to function in a synergetic manner to control an immune response to associated antigens (Reddy et al., 2006). Recently, adhesive substrates coated with different proteins, on which DCs were cultured, have been shown with their functional impacts on modulation of pro- and anti-inflammatory cytokine releases from DCs, which further showed correlation with allogenic T cell proliferation and polarization (Acharya et al., 2008).

Biomaterials in combination products

As mentioned above, the biomaterial component in the tissue engineered constructs is needed to serve not only as a scaffold but also as a guide for cells to viable functions such as growth, differentiation, tissue regeneration, and vascularization in association with the growth factors. Host immune responses are, therefore, to be minimized and/or controlled for successful tissue regeneration, whereas the biomaterial component in the vaccine systems is required to enhance the host immune response by acting as an adjuvant. Previously, we have shown that differential levels of DC maturation were observed upon DC treatments with different biomaterials used in combination products (Yoshida and Babensee, 2004; 2006; Babensee and Paranjpe, 2005), which suggests that biomaterials can modulate the host immune response based on their inherent physiochemical properties, associated with low or high adjuvant effects. Thus better understanding of the mechanisms involved in these effects of biomaterials would suggest ideal strategies for the future applications of combination products. For instance, it may be possible to control graft rejection by optimal utilization of biomaterial components in tissue

engineered constructs. Furthermore, such understanding can provide strong direction for the improvement of vaccines and adjuvants, and for development of tolerogenic therapeutics for autoimmune diseases, allergy and transplantation (Reddy et al., 2006; Babensee et al., 1998; Singh and O'Hagan, 1999).

Poly(lactic-*co*-glycolic acid)

Poly(lactic-*co*-glycolic acid) (PLGA) is one of most popular synthetic polymers frequently employed for the scaffolds in tissue engineering (Li and Tuan, 2005). As a polyester composed of variable molar ratios of lactic and glycolic acid, PLGA has been recognized for an hydrophobic biomaterial showing good biocompatibility because its degradation products are biocompatible (Ignatius and Claes, 1996). Hydrolysis rate of PLGA can be controlled by its geometric size, molar ratio of lactic to glycolic acid, or polymer molecular weight (Hutchinson and Furr, 1987; Eldridge et al., 1991). However, the immune response supported by PLGA has been used as an adjuvant inducing immunogenicity for the delivery of vaccines (Ertl et al., 1996), often in the form of microparticles, possibly due to the phagocytosis effects of APCs (Ohagan et al., 1993). Cell-mediated immune response has also been elicited using micro- and nanoparticles of PLGA (Newman et al., 1998a). More recently, it has been shown that the adjuvant effects associated with PLGA in the enhancement of the humoral immune response to associated antigen (Matzelle and Babensee, 2004; Bennewitz and Babensee, 2005) can be attributed to a maturation of DCs upon *in vitro* treatment with PLGA microparticles or films (Yoshida and Babensee, 2004; Babensee and Paranjpe, 2005). As a synthetic polymer which is most frequently employed in vaccine delivery or tissue engineering applications, understanding of PLGA effect on host response is essential to the development of biomaterials for use in combination products.

Chitosan

Chitosan is a biomaterial of natural polysaccharides having carbohydrate units which are mainly composed of glucosamine with a high cationic charge density (Chandy and Sharma, 1990; Tangpasuthadol et al., 2003; Li and Tuan, 2005). Chitosan has been previously employed as biomaterials for scaffolds in the tissue engineering (Hutmacher et al., 2001; Hunziker, 2002), but it has also been reported for its adjuvant activities such that it stimulates T and B cells (Seferian and Martinez, 2000) and modulates nitric oxide release by macrophages (Hwang et al., 2000; Peluso et al., 1994). Chitosan consists of N-acetyl-D-glucosamine units (GlcNAc), which can interact with macrophage mannose receptor for mannose- and GlcNAc-glycoproteins (Warr, 1980; Hitchen et al., 1998), inducing brisk inflammatory responses (Hidaka et al., 1999; Feng et al., 2004; Crompton et al., 2006). Moreover, using the murine macrophages, it has been recently reported that chitin or chitosan is directly recognized by the macrophage mannose receptor and this receptor-mediated stimulation induces an expression of MHC class I and II molecules, and macrophage inflammatory protein (MIP)-2 as well as a release of TNF-α and IL-1β (Feng et al., 2004; Mori et al., 2005). The mannose receptor is a representative C-type lectin which is one family of PRRs, expressed on both macrophages and DCs and its specificities of ligand and function are identical for both cell types (Figdor et al., 2002).

Alginate

Alginate is the most frequently employed biomaterials for cell immobilization due to their abundance, easy gelling properties and apparent biocompatibility (de Vos et al., 2006). Alginate molecules are linear block copolymers of mannuronic acids and guluronic acids with a variation in composition and sequential arrangements. Due to its hydrophilic nature, alginate

has been employed as a hydrogel, which is beneficial to minimize the protein adsorption and cell adhesion. Furthermore, the soft and elastic features of the gel reduce the frictional irritation to surrounding tissue (de Vos et al., 2002). However, secretion of IL-1, IL-6, and TNF-α has been induced upon treatment of human monocyte-derived macrophages with the poly-mannuronic acid obtained from alginates (Otterlei et al., 1991) and CD14 expressed on the macrophages has been reported for its critical role in binding to the mannuronic acid and stimulating the macrophages to release those cytokines (Espevik et al., 1993). Furthermore, the alginate with higher content of mannuronic acid has been found to be more immunogenic than that with higher content of guluronic acid, showing more antibodies (to feta porcine islet microencapsulated in alginate) produced when the alginate was transplanted *in vivo* (Kulseng et al., 1999). More recently, the alginate with a high content of mannuronic acid induced TNF-α secretion from murine macrophages (Orive et al., 2005) and TLR-2 and TLR-4 in association with CD14 have been reported for their critical roles in inducing secretions of IL-1α, IL-1β, IL-6, and TNF-α from human macrophages and murine macrophages (Flo et al., 2002; Iwamoto et al., 2005).

Hyaluronic acid

Hyaluronic acid is a negatively charged high molecular weight glycosaminoglycan, which is ubiquitously distributed throughout our body as a physiological component of the cartilage extra cellular matrix (ECM). For instance, high molecular weight HA, exactly in a hydrogel form, plays a critical role as a lubricant in the joints. As such, HA is a polysaccharide composed of repeating glucuronic acid and N-acetylglucosamine showing remarkable hydrophilicity; for example, HA is much more hydrophilic than PLGA (85:15) such that HA showed the water contact angle decreased by around 50% from that of PLGA (Lee and Lee, 2006) and well known for binding huge amount of water by around 1000-fold of its own weight.

Hydrogel form of HA with high molecular weight is an ideal matrix to support articular cartilages (Li and Tuan, 2005). However, soluble fragments of HA have been shown to support DC maturation (Yang et al., 2002a; Termeer et al., 2000), whereas high molecular weight HA fragments (6,000 kDa) induced a decreased level of TNF-α secretion, by specifically inhibiting TLR-2 signaling, from murine macrophages transfected with human TLR-2, as compared to the low molecular weight HA fragments (200 kDa) (Scheibner et al., 2006).

Agarose

Agarose is a polysaccharide containing repeated disaccharides of L- and D-galactose (repeating β-D-galactopyranosyl and 3,6-anhydro-α-L-galactopyranosyl units) derived from natural seaweeds (Hunziker, 2002), showing very hydrophilic nature due to high content of hydroxyl (OH) end groups. A hydrogel of agarose is thermoreversibly formed by hydrogen bonds, facilitated by alignment of the agarobiose molecules (Shoichet et al., 1996). Agarose has been employed as a food ingredient stabilizer and a biomaterial for tissue engineering (Benya and Shaffer, 1982; Sun et al., 1986). Furthermore, its biocompatibility has been well known such that its hydrogel form is frequently employed especially in the cartilage tissue engineering for controlling the chondrogenesis (Fukumoto et al., 2003; Huang et al., 2004) and that it elicited minimal humoral and cellular responses *in vivo* (Starke et al., 1987; Rahfoth et al., 1998). Differently from chitosan and alginate, agarose does not have a specific carbohydrate composition which is recognized by the PRRs expressed on DCs. Possibly due to this reason, minimal DC maturation has been elicited upon DC treatment with agarose microparticles or films (Yoshida and Babensee, 2006; Babensee and Paranjpe, 2005).

Summary

Despite tremendous efforts extensively made on the immunological mechanisms, which show a massive influx of T cells, B cells, and fibroblast-like synoviocytes, macrophages, and dendritic cells (DCs) in the synovial tissue, the pathophysiological pathways of RA remain unclear. Dendritic cells have been recognized to play a central role not only in the initiation and perpetuation of RA, but also in host immune response against biomaterials, associated with the adjuvant effects. Since tissue engineering has been recognized as a promising alternative for cartilage reconstruction and regeneration, cartilage tissue engineering has been motivated by the need of replace lost or damaged tissue with an already structurally and mechanically functional implant in combination with biomaterials. However the host immune response against the biomaterial component or device is still a major concern on the achievement of tissue restoration. Because DCs are thought to play the central role of the adjuvant effect, identification of multifunctional impacts of biomaterials on immunomodulating DC response and further T cell-mediated adaptive immunity is essential to understand the link between these *in vitro* biomaterial effects and *in vivo* effects on integration in induced RA animal models.

CHAPTER 4[†]

DIFFERENTIAL FUNCTIONAL EFFECTS OF BIOMATERIALS ON DENDRITIC CELL MATURATION. PART 1. EFFECTS OF BIOMATERIALS IN 2-DIMENSIONAL FILM FORM

INTRODUCTION:

Identical biomaterials are often used as carriers in combination products where the desired effect on the immune response, due to a biomaterial adjuvant effect, to an associated immunogenic biological component is opposite. In the tissue engineering application, immune responses should be minimized, whereas the vaccine strategy aims to enhance the protective immune response. We have previously shown that PLGA acts as an adjuvant in enhancing humoral response against a co-delivered model antigen (Matzelle and Babensee, 2004; Bennewitz and Babensee, 2005), and that maturation of human peripheral blood-derived DCs (Yoshida and Babensee, 2004) and murine bone marrow-derived DCs (Yoshida et al., 2007) is induced in different extents depending on different forms (film or microparticle) of PLGA. We have also shown that different biomaterials induce different degrees of DC maturation, suggesting the immunomodulating capacities possible by inherently different features of biomaterials (Yoshida and Babensee, 2006; Babensee and Paranjpe, 2005). The exact mechanisms involved in this DC maturation by biomaterials, however, is not yet fully elucidated. Biomaterial properties such as hydrophobicity/hydrophilicity direct protein adsorption to and complement activation on the biomaterial surface with these ligands recognized by pattern recognition receptors (PRRs) of DCs to function in a synergistic manner to control an immune response to associated antigens (Reddy et al., 2006). In this study, the functional immunological DC response to a variety of

[†] A manuscript prepared from this Chapter 4, titled as 'Differential functional eEffects of biomaterials on dendritic cell maturation', is to be submitted to Biomaterials.

biomaterials commonly used in combination products as vaccine delivery vehicles or tissue engineered scaffolds was assessed. The biomaterials used in this study included PLGA as a synthetic polymer and chitosan, alginate, hyaluronic acid (HA), and agarose as natural polysaccharide polymers (Li and Tuan, 2005; Hutmacher et al., 2001; Hunziker, 2002), which have been frequently used as scaffolds or hydrogels for tissue engineering applications (Li and Tuan, 2005; Hutmacher et al., 2001; Hunziker, 2002; Fragonas et al., 2000; Fukumoto et al., 2003; Huang et al., 2004; Mauck et al., 2000). Herein we extend our previous studies to further characterize the effect of different biomaterials on the maturation and functional immunological effects of DC using a variety of immunobiological assays. To test effects of biomaterial grade such as research or clinical grade, we also examine the clinical grade biomaterials commercially available, compared to the research grade which is mainly studied in the present study. In this way, we were able to identify biomaterials which support DC maturation and those biomaterials that did not. These studies are a step forward understanding the effect of inherently different features of biomaterials to suggest new selection and design criteria for biomaterials to be used in the combination products such as tissue engineering or vaccine delivery where immune responses are of consequence.

METHODS:

Preparation of biomaterial films

All biomaterial films were prepared freshly for each experimental procedure. Preparation methods of all biomaterial films were adapted or modified from previously described methods as noted for each biomaterial. As commercially available, films of clinical grade biomaterials were prepared in addition to films of research grade biomaterials. Specifically, for this study, the biomaterial films tested included PLGA (clinical grade), chitosan (research and

clinical grade), alginate (research and clinical grade), HA (research and clinical grade), and agarose (research grade) (sources noted in film preparation methods described forthwith).

Briefly, poly(DL-lactic-*co*-glycolic acid) (PLGA) (clinical grade with ester terminated; molar ratio: 75:25, inherent viscosity: 0.70 dL/g in trichloromethane, 100,000 MW; Birmingham Polymers, Birmingham, AL) was dissolved in 20% w/v in dichloromethane (DCM) overnight at room temperature and poured into the Teflon dish of 50 mm diameter (Cole-Parmer) in the chemical fume hood (Mikos et al., 1994). Upon evaporation of the solvent and drying (36-48 hours), PLGA films were punched of an appropriate size, and washed for 1 hour in ddH_2O changing ddH_2O every 15 min. Chitosan (research grade; high molecular weight: 400,000 MW, degree of deacetylation: ≥ 75%, Fluka, Milwaukee, WI) was dissolved in 1% w/v chitosan in glacial acetic acid (2% v/v in ddH_2O) (Fisher Scientific) for 24 hours at room temperature and then, poured into the Teflon dish of 50 mm diameter in the chemical fume hood. Upon evaporation of the solvent and drying (36-48 hours), chitosan films were then cross-linked by immersion in 20% (v/v) sodium sulfate (Sigma) in ddH_2O (2 hours) and washed by ddH_2O (20 min), followed by immersion in 1 M NaOH (Sigma, 30 min) to neutralize the surface and washed with ddH_2O (20 min).(Lahiji et al., 2000) Chitosan films were punched of an appropriate size, and finally washed for 20 min in ddH_2O. Alginate (research grade; 80,000 MW; mannuronic acid content: ≥ 50%; primarily anhydro-β-D-mannuronic acid residues with 1-4 linkage; Sigma) was dissolved to a concentration of 3% w/v alginate in ddH_2O for 24 hours at 4˚C and then, poured into the Teflon dish of 50 mm diameter in the tissue culture laminar flow hood. Upon drying (36-48 hours), alginate films were cross-linked by immersion in 5% w/v calcium chloride (Sigma) in 40% aqueous ethanol for 48 hours and washed with ddH_2O for 10 min (Papas et al., 1999). Alginate films were punched of an appropriate size, and washed for 30 min in ddH_2O changing water every 10 min. Hyaluronic acid (research grade; 800,000 MW; sodium salt from

Streptococcus equi, BioChemika, Fluka) was dissolved to a concentration of 4% w/v HA in ddH_2O for 24 hours at 4˚C and then, poured into the Teflon dish of 50 mm diameter in the tissue culture laminar flow hood. Upon drying (36-48 hours), HA films were cross-linked by immersion in 50 mM water soluble carbodiimide (Sigma) in 72% aqueous ethanol for 24 hours and washed by ddH_2O for 10 min (Tomihata and Ikada, 1997). Hyaluronic acid films were punched of an appropriate size, and washed for 30 min in ddH_2O changing water every 10 min. Agarose (research grade; type V; high gelling; gel strength of ≥ 800 g/cm^2 at 1.0 %; Sigma; molecular weight is not known) was dissolved in ddH_2O to a concentration of 3% w/v by heating using a microwave until boiling and visible homogeneity was reached (Tun et al., 1996). Agarose films were prepared by dispensing 1 ml of this agarose solution into a well of a 6-well tissue culture plate (Corning), and allowed to solidify at a temperature of 4˚C for at least 30 min, and brought back to room temperature for another 30 min prior to use in treating iDCs. All biomaterial films were UV-sterilized for 30 min per surface in the tissue culture hood prior to use in DC cultures.

Endotoxin contents of biomaterial films were determined using a chromogenic Limulus Amebocyte Lysate assay (QCL-1000 Chromogenic LAL Endpoint Assay, Cambrex, Walkersville, MD). Endotoxin assays were performed on a smaller piece of film (4.5 mm in diameter), which had undergone the same washing and sterilization procedures as films used to treat DCs. The smaller film pieces were suspended in endotoxin-free water and endotoxin assay performed. Standards in tissue culture treated polystyrene wells and sample wells of different biomaterials were treated with endotoxin-free water. Limulus amebocyte lysate was added in the presence of biomaterial and incubated for 10 min at 37˚C. Chromogenic substrate (Ac-Ile-Glu-Ala-Arg-pNA) was added to each well and incubated for 6 min. Glacial acetic acid (25% v/v) (J.T. Baker, Philipsburg, NJ) was added as a stop solution and the mixture was transferred into flat-bottom

microplate and the absorbance was measured at 405 nm. Endotoxin content in the samples was read off standards generated from endotoxin standards, from the manufacturer's kit. Each sample was run in triplicate for quantification. The effective endotoxin content (EU/ml) of 4.5 mm-diameter films of PLGA (clinical grade) was 0.011±0.007, of chitosan (research grade) 0.0007±0.0001, of alginate (research grade) 0.035±0.006, of HA (research grade) 0.004±0.003, and of agarose (research grade) 0.037±0.006. Previous study has shown that minimum E. Coli endotoxin concentration of 100 EU/ml was required for DC maturation (Jotwani et al., 2003).

For the clinical grade biomaterial films, chitosan (clinical grade; Protasan UPB 80/500, 500,000 MW, degree of acetylation: 80-89%, NovaMatrix, FMC Biopolymer, Sandvika, Norway) and HA (clinical grade; 770,000 MW; sodium hyaluronate in European Pharmacopoeia (EP) grade, sodium salt from Streptococcus equi, Genzyme Biosurgery, Cambridge, MA) materials were processed using the identical methods described above for the research grade, whereas alginate (clinical grade; 100,000 MW; mannuronic acid content: ≥ 50%, sodium alginate, Pronova UP LVM, NovaMatrix, FMC Biopolymer, Sandvika, Norway) material were processed using the method described above except that the starting alginate concentration was 3.5% w/v in ddH_2O. The effective endotoxin content (EU/ml) of 4.5 mm-diameter films of chitosan (clinical grade) was 0.0025±0.0024, of HA (clinical grade) 0.0012±0.0002, and of alginate (clinical grade) 0.0997±0.0198. Through the study, except for PLGA which was only available as clinical grade and agarose which was only available as research grade, the material used was research grade unless specified as clinical grade.

X-ray photoelectron spectroscopy (XPS)

To examine the chemistry changes of biomaterial surfaces associated with film processing, low resolution XPS survey scans were obtained for raw polymeric materials, films

before cross-linking and films after cross-linking and atomic percentages determined and compared. Theoretical values were determined based on known chemical structures. A surface Science Laboratories X-100 spectrometer (Surface Science Laboratories, Mountain View, CA) with monochromatized A1 Kα X rays using 1486.6 eV was used at a fixed take-off angle of 55º. The XPS instrument is housed at Georgia Institute of Technology Microelectronic Research Center. Raw polymeric material samples were prepared by placing the material directly on a normal aluminum foils without any adhesive and then, these foils containing samples were placed on the sample stage. Biomaterial films (10 mm × 10 mm) selected from a region of uniform thickness which had been washed using the endotoxin-free water (LAL reagent water, Cambrex) and dried in the tissue culture hood were directly placed on the sample stage for analysis. All samples for XPS were kept in the vacuum desiccator, at least for 24 hours, before analysis. Biomaterial samples were placed under a nickel mesh, and 5 eV flood gun was used to assist with the compensation for differential charging. Atomic percentages of elements were derived from low resolution spectra. High resolution C1s spectra were obtained and resolved using curve fitting routines provided by the manufacturer, and the binding energy scale was adjusted to place the hydrocarbon peak at 284.6 eV.

Dendritic cell culture

Peripheral human blood was collected from donors with informed consent using heparin (333 U/ml blood) (Baxter Healthcare Corporation, Deerfield, IL) as the anticoagulant. This procedure was performed at the Student Health Center Phlebotomy laboratory, in accordance with the protocol (#H05012) of Institutional Review Board (IRB) of Georgia Institute of Technology. Dendritic cells were derived from human peripheral blood mononuclear cells (PBMCs) using a previously described method with some modifications (Romani et al., 1996). Briefly, as shown

in Figure 4-1, after the blood collected from the donor, PBMCs were isolated by differential centrifugation using the lymphocyte separation medium (Cellgro MediaTech). The PBMCs were collected and washed in phosphate buffer saline (PBS), and red blood cells were lysed with buffer [155 mM NH_4Cl, 10 mM $KHCO_3$ (both from Sigma), 0.1 mM EDTA (Gibco)], and remaining cells washed again twice with PBS. Resulting PBMCs were resuspended at a concentration of 5×10^6 cells/ml in the DC media, which was prepared by filter-sterilizing RPMI-1640 containing 25mM HEPES [4-(2-hydroxyethyl)piperazine-1-ethanesulfonic acid)] and L-glutamine (Gibco, Grand Island, NY), supplemented with 10% (v/v) heat inactivated fetal bovine serum (FBS, Cellgro MediaTech) and 100U/mL Penicillin/Streptomycin (Cellgro MediaTech). Cells were plated in a volume of 10ml/plate in a 100 × 20 mm tissue culture plate (Primaria, BD Falcon) and incubated for 2 hours in the incubator with 95% relative humidity and 5% CO_2 at 37˚C to select for adherent monocytes. After the incubation, plates were washed at least three times using warm, fresh DC media to remove non-adherent cells. The adherent cells were supplied with 10 mL of fresh, pre-warmed DC media supplemented with granulocyte macrophage colony-stimulating factor (GM-CSF) (1000 U/mL) and interleukin-4 (IL-4) (800 U/mL) (both from Peprotech, Rocky Hill, NJ) for 5 days. On day 5 of culture, loosely adherent and non-adherent cells containing iDCs were harvested by centrifugation for 10 min at 1100 rpm and plated at 1.5 x 10^6 cells/well in 3 mL/well in DC media supplemented with GM-CSF and IL-4 into 6-well tissue culture plate for various treatments. For DC treatment with biomaterials, biomaterial films were placed into wells of 6-well plate with autoclave-sterilized gaskets (cut from peroxide-cured silicone tubing) (Cole-Parmer) to secure the films and the iDC suspension was applied into each well. Wells for the negative control of iDC remained untreated while wells for the positive control of mature DC (mDC) involved addition of 1 μg/ml of lipopolysaccharide (LPS) (E. coli 055:B5; Sigma). For each experiment, all biomaterials and

controls were included as treatments to allow for comparisons between treatments and to controls. DCs were treated with biomaterial films in an atmosphere of 95% relative humidity and 5% CO_2 at 37˚C for 24 hours (or 5 hours for NF-κB assay) and then, cells or media were analyzed as described below. As a gasket control, DCs were cultured in the presence of gaskets and their phenotype assessed as described below.

To justify that the non-/loosely-adherent DCs are representative for analyses of DC phenotype changes upon DC treatments in this study, numbers of non-/loosely-adherent DCs and adherent DCs have been counted using the Coulter counter (Coulter Multisizer III, Beckman Coulter, Fullerton, CA) and DC maturation marker expressions (CD40, CD80, CD86, CD83, HLA-DQ, and HLA-DR) for each DC fraction above have also been tested with 5,000 events per sample using the flow cytometer (BDLSR, Beckton Dickinson) for DCs obtained from 3 donors. After 24 hours of DC treatment with biomaterial films or controls, non-/loosely-adherent DC fraction was gently collected using a pipette and then, adherent DC fraction was removed from the culture dishes of controls or biomaterial films using the pre-warmed cell dissociation solution (CDS) (Sigma). As a result of cell counting by size, the control of iDC or mDC showed 84 ± 15% or 71 ± 15% of non-/loosely adherent DC population in total DCs (sum of those two fractions) present in the cell culture wells, respectively. The biomaterial treatments with PLGA, chitosan, alginate, HA or agarose resulted in 37 ± 15%, 65 ± 13%, 71 ± 1%, 86 ± 3%, or 86 ± 9% of that, respectively. All maturation marker expressions of the adherent DC fraction of all controls or biomaterial treatments did not show any significantly different values of geometric mean fluorescence intensity (gMFI) compare to those of the non-/loosely-adherent DC fraction, except the HLA-DQ expression of adherent DCs treated with hyaluronic acid film, which exhibited significantly higher gMFI than that of non-/loosely-adherent DCs on the hyaluronic acid film (data not shown). On the other hand, it has been reported that the non-adherent iDCs

can be differentiated to macrophages upon adhesion on the bottom of culture dish wells (Lutz et al., 1999). Moreover, non-/loosely-adherent DCs are generally employed for the immunotherapeutic researches on the migratory blood-resident DCs (Banchereau et al., 2000; Moldenhauer et al., 2003). For all DC treatments, except the treatment with PLGA, non-/loosely-adherent cells make up more than 65% mean value in total DCs present in each well of treatment. Therefore, the non-/loosely-adherent DC fraction was collected and examined in different immunobiological assays throughout this study.

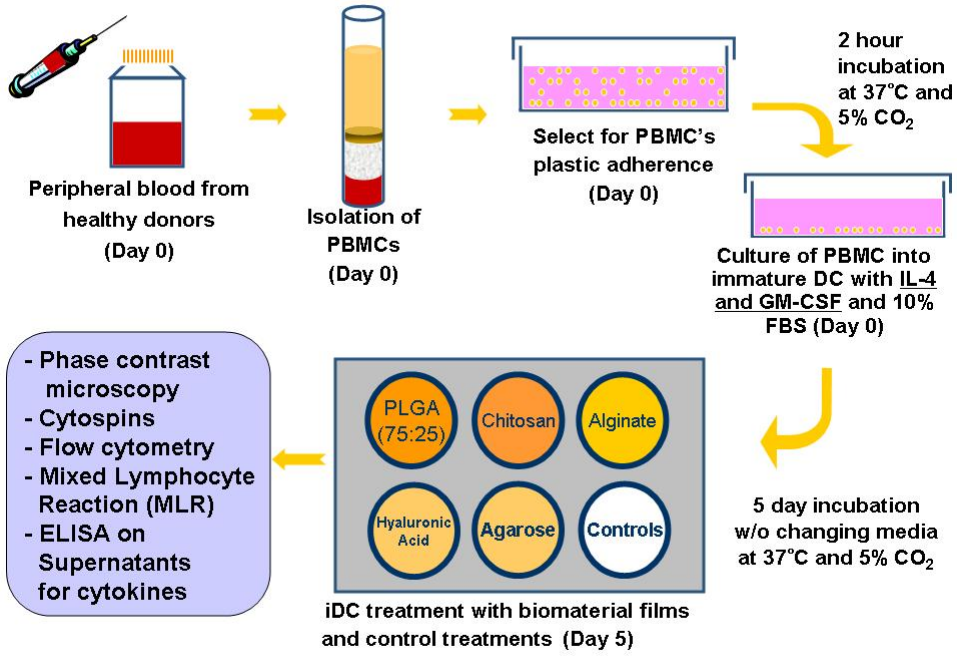

Figure 4-1: Schematic representation of the in vitro experimental procedure of DC culture and treatment with biomaterials.

Cell morphology

Dendritic cell morphology was examined throughout the culture duration by phase contrast microscopy. On day 6, DCs were processed for Cytospin preparations as described previously (Yoshida and Babensee, 2004) (Cytospin Cytocentrifuge, Thermo Shandon, Pittsburgh, PA) and stained with Hematology Stain (Astral Diagnostics, West Deptford, NJ) for light microscopy examination using an Axiovert 135 microscope (Zeiss, Jena, Germany) and imaged using Image-Pro Plus (v.5) software (Media Cybernetics, Inc., Bethesda, MD). A representative image was selected from 6 different Cytospin preparations from 6 separate experiments.

Cell surface marker expression

The levels of surface marker expression were monitored after 24 hours of treatment with biomaterial films, by flow cytometry as per methods described in the literature (Yoshida and Babensee, 2004) and compared to controls. Non-/loosely-adherent cells containing DCs for iDCs, mDCs, or DCs treated with different biomaterial films were collected by centrifugation at 1100 rpm for 10 min and suspended in Hank's HEPES buffer (120 mM NaCl, 10 mM KCl, 10 mM $MgCl_2$, 10 mM glucose, 30 mM HEPES) (all from Sigma) containing 1% (v/v) human serum albumin (HSA) (Calbiochem, Darmstadt, Germany) and 1.5 mM $CaCl_2$ (Sigma). Cells were stained with saturating concentrations of fluorescently conjugated mouse anti-human monoclonal antibodies against CD 40 (clone B-B20; IgG1κ), CD80 (clone BB1; IgMκ), CD86 (clone BU63; IgG1κ) (all from Southern Biotechnology Associates, Birmingham, AL), CD83 (clone HB15a; IgG2b) (IO Test Immunotech, Marseille, France), HLA-DQ (clone TU169; IgG2aκ), HLA-DR (clone TU36; IgG2aκ), CD32 (clone 3D3; IgG1κ), CD206 (clone 19.2; IgG1κ), CD44 (clone 515; IgG1κ), or Annexin V (recombinant purified protein) (all from BD Pharmingen) for 1 hour at 4˚C

in the dark, filtered using 40 μm cell strainer (Becton Dickinson, Franklin Lake, NJ) and then, analyzed immediately with 5,000 events per sample using a BDLSR flow cytometer (Becton Dickinson). Only propidium iodide (PI) (fluorescent vital dye) (BD Pharmingen) was applied into the sample tube less than a minute before scanning in the flow cytometer. Data was obtained together with the negative control of autofluorescence per sample and then, analyzed using WinMDI 2.8 (Scripps Research Institute, La Jolla, CA).

Mixed lymphocyte reaction (MLR)

Allostimulatory capacity of DCs to induce T cell proliferation upon DC treatment with different biomaterials was assessed as per methods in the literature (Yoshida and Babensee, 2004), using an allogeneic mixed lymphocyte reaction (MLR). After 24 hours of DC treatment with biomaterial films, allogenic T cells were isolated from PBMCs by negative selection using Pan T-cell magnetic isolation (Miltenyi Biotech, Auburn, CA) according to the manufacturer's protocols. These cells were used as responder cells. The T cells were resuspended in RPMI-1640 with 25 mM HEPES and L-glutamine (Gibco BRL, Carlsbad, CA) with 100 U/ml penicillin/streptomycin (Cellgro) and heat-inactivated filter-sterilized (0.22 μm) 10% (v/v) human AB serum (Biowhittaker, Walkersville, MD)(complete RPMI-10 media) and plated at a concentration of 10^5 cells/well in a 96-well flat-bottomed plate (Corning) in triplicate per treatment groups or controls. Dendritic cells treated with biomaterial films or controls were resuspended at 1.6×10^5 cells/ml, and treated with 25 μg/ml mitomycin C (Sigma) for 30 min to prevent their proliferation. Upon extensive washing with complete RPMI-10 media, DCs were resuspended in complete RPMI-10 media and added to responder cells in triplicate at graded DC-T cell ratios. Cells were co-cultured for 4 days at 37 °C, with the addition of 10 μM 5-bromo-2-deoxyuridine (BrdU) for the last 24 hours of culture. Dendritic cell-induced T-cell proliferation was measured using BrdU

colorimetric cell proliferation ELISA (Roche Applied Science, Indianapolis, IN) according to the manufacturer's directions.

Pro-inflammatory cytokine release

The amount of pro-inflammatory cytokines, tumor necrosis factor-α or interleukin-6 (TNF-α or IL-6) produced by DCs in the cell culture supernatant after the treatments with biomaterials, normalized to DNA amount, present in the cell culture supernatants were analyzed by ELISAs (R&D systems) according to manufacturer's directions. After 24 hours of DC treatment with biomaterial films or controls, non-/loosely-adherent DC fraction and cell culture supernatants were collected together and then, cleared by centrifugation for 10 minutes at 1,100 rpm. These cleared supernatants were stored at -20˚C until analysis. Non-/loosely-adherent DC fraction was gently collected using a pipette after centrifuge described above and then, adherent DC fraction was removed from the culture dishes of controls or biomaterial films using the pre-warmed cell dissociation solution (CDS) (Sigma). These non-/loosely-adherent DC and adherent DC fractions were combined together per control or treatment and then, DNA quantification was analyzed for whole cell population per each control or treatment group using picoGreen dsDNA quantification kit (Invitrogen) per manufacturer's directions. Amounts of TNF–α or IL-6 were presented normalized against total DNA amounts for each treatment group.

Preparation of DC nuclear extract and measurement of activity of nuclear factor κB (NFκB) family of transcription factors

Nuclear extracts from DCs treated with biomaterial films for 5 or 24 hours were prepared using TransFactor Extraction kit (Becton Dickinson Clontech, Palo Alto, CA) according to manufacturer's directions. In detail, DCs treated with biomaterial films were collected and

washed twice with ice cold PBS (pH 7.5) by centrifugation at 450×g for 5 min at 4˚C. The cell pellet was resuspended in lysis buffer containing protease inhibitors and allowed to incubate for 15 min on ice. After the incubation, the suspension was centrifuged, and the particulate fraction was resuspended in lysis buffer. Cells were disrupted by forcing the suspension through a 27-gauge needle. The resulting suspension was centrifuged at 11,000×g for 20 min at 4˚C. The supernatant and the pellet from this centrifugation were considered as cytosolic and nuclear fractions, respectively. The pellet containing the cell nuclei was resuspended in an extraction buffer, and nuclear membrane disrupted by forcing the suspension through a 27-gauge needle. The suspension was centrifuged at 21,000×g for 5 min at 4˚C, and the supernatant from this centrifugation was considered to be the nuclear extract, transferred to a new chilled tube, and stored at -80˚C until analysis. Activities of the p50 subunit of NF-κB family of nuclear transcription factor were assessed using TransFactor NF-κB Family kit (Becton Dickinson Clontech), an ELISA-based method of detecting transcription factor activities, per manufacturer's protocol. In brief, nuclear extracts were incubated for 60 min in a well pre-coated with consensus binding sequence. Upon washing, the primary antibody corresponding to the p50 subunit of NF-κB family was added, and allowed to incubate for 60 min. The plate was washed and incubated for additional 30 min with the secondary antibody. Binding was detected by the addition of tetramethylbenzidine (TMB) substrate and measured by colorimetric development at 655 nm.

Endocytic ability

Endocytic ability of DCs upon DC treatment with different biomaterials was assessed as per methods in the literature (Piemonti et al., 1999). Briefly, on Day 6, non-/loosely-adherent cells containing DCs for iDCs, mDCs, or DCs treated with different biomaterial films were

collected by centrifugation at 1100 rpm for 10 min and then, resuspended 500 µl of fresh DC media by 2×10^5 cells/ml. Pre-warmed FITC-dextran (dextran labeled with fluorescein isothiocyanate; 40,000 MW; Sigma) solution (0.01 mg/ml in DC media) was added with 50 µl into each 500 µl of DC suspension prepared. After mixed gently by pipetting, each FITC-dextran/DC tube was incubated in the dark at 37°C for 45 minutes and then, cells were washed using PBS (pH 7.2) twice by centrifuging at 300× g for 10 minutes. After washing steps, cells were resuspended in the identical buffer previously used in the flow cytometer for the surface marker expression and then, scanned with 5,000 events per sample in the flow cytometer. Data was obtained together with the negative control of autofluorescence per sample and then, analyzed using WinMDI 2.8 (Scripps Research Institute, La Jolla, CA).

Statistical analysis

For statistical analysis, one sided Student t-test was used to compare mDCs or each sample group to iDCs (negative control) in pairs. To observe significant differences between mDCs and all sample groups in pairs, the general liner model of two-way ANOVA in pairwise was used for a mixed model with repeated measure. For all statistical methods, the Minitab software (Version 14, State College, PA) was used. If not indicated, p-value less than or equal to 0.05 was considered to be significant.

RESULTS:

Characterization of surfaces of biomaterial films

X-ray photoelectron spectroscopy was used to analyze the surface chemistry (30 nm depth from the surface) of the biomaterial films used here. Atomic percentages of C, N, O, Na, Ca, and Cl or chemical (C1s) bond percentages associated with the different biomaterial films

were obtained from scans at low resolution (Table 1) or high resolution (Table 2), respectively. Alginate films showed residual calcium and chloride with 1.9±0.1 and 1.4±0.1 in atomic percentage (%), respectively. The other biomaterial films did not show an elemental composition which deviates from that expected based on raw materials and films before cross-liking procedure. Upon cross-linking or film forming procedure, all biomaterial films showed increased compositions of carbon, showing decreased values of O/C or N/C as shown in Table 1, compared to theoretical or raw material values. Upon cross-linking or final film formation of all biomaterial films, percentages of C-H, C-C, or C-N bonds increased, whereas C-O, O-C-O, or O=C-O bonds decreased, as compared to theoretical or raw material values (Table 2).

Table 1: Low resolution XPS survey scans of biomaterial film surfaces used for DC treatment. More than five measurements for each sample were averaged (mean±SD). Ratios of O/C or N/C were obtained only using mean value of each atomic percentage.

Samples	Atomic percent (%)						Ratios	
	C	N	O	Na	Ca	Cl	O/C	N/C
PLGA (75:25) (theoretical)	55.6		44.4				0.80	
PLGA (raw material)	68.4±1.9		31.6±1.2				0.46	
PLGA (film)	64.3±2.1		35.7±1.1				0.56	
Chitosan (theoretical)	54.5	9.1	36.4				0.67	0.17
Chitosan (raw material)	59.1±1.9	10.4±0.2	30.5±1.1				0.52	0.18
Chitosan (film before X-link)	70.1±2.3	4.1±0.1	25.8±0.3				0.37	0.06
Chitosan (film after X-link)	69.0±1.7	3.9±0.1	27.1±0.2				0.39	0.06
Alginate (theoretical)	44.5		48.1	7.4			1.08	
Alginate (raw material)	47.9±1.5		36.3±0.3	15.8±0.3			0.76	
Alginate (film before X-link)	63.8±1.1		28.9±0.1	7.3±0.1			0.45	
Alginate (film after X-link)	67.5±0.7		29.2±0.1		1.9 ±0.1	1.4 ±0.1	0.43	
HA (theoretical)	51.9	3.7	40.7	3.7			0.78	0.07
HA (raw material)	52.8±0.9	1.9±0.1	37.1±1.3	8.2±0.2			0.70	0.04
HA (film before X-link)	59.2±2.1	3.5±0.2	32.3±0.7	5.0±0.1			0.55	0.06

Table 1 continued

HA (film after X-link)	57.8±0.4	9.8±0.2	29.6±0.5	2.8±0.0	0.51	0.17
Agarose (theoretical)	55.8		44.2		0.79	
Agarose (raw material)	61.3±2.0		38.7±0.9		0.63	
Agarose (film)	64.2±0.7		35.8±0.1		0.56	

Table 2: High resolution XPS scans of biomaterial film surfaces used for DC treatment. More than five measurements for each sample were averaged (mean±SD).

Samples	Chemical (C1s) bond percentage (%)				
	C-H or C-C	C-N	C-O	O-C-O or O=C-O	O=C-OH
PLGA (75:25) (theoretical)	25		37.5	37.5	
PLGA (raw material)	25.6±0.3		37.3±0.3	37.1±1.1	
PLGA (film)	29.0±0.5		35.5±0.9	35.5±0.7	
Chitosan (theoretical)	3.2	23.4	57.8	15.6	
Chitosan (raw material)	7.1±0.1	23.2±0.9	55.1±0.6	14.6±0.2	
Chitosan (film before X-link)	7.7±0.2	29.6±0.4	52.4±0.7	10.3±0.7	
Chitosan (film after X-link)	9.1±0.3	32.6±0.3	46.3±0.6	12.0±0.1	
Alginate (theoretical)	0.0		66.7	25.0	8.3
Alginate (raw material)	11.9±0.4 (adsorbed)		68.6±2.0	11.9±0.1	7.6±0.2
Alginate (film before X-link)	5.2±0.5 (adsorbed)		44.1±0.4	32.8±0.3	17.9±0.5
Alginate (film after X-link)	7.7±0.5 (adsorbed)		46.4±0.5	26.5±0.9	19.4±0.2
HA (theoretical)	7.1	7.1	64.3	21.5	
HA (raw material)	11.6±0.3	7.0±0.2	59.3±1.3	22.1±0.4	
HA (film before X-link)	11.7±0.2	13.3±0.1	61.0±1.1	14.0±0.2	
HA (film after X-link)	13.0±0.2	13.4±0.2	60.6±0.7	13.0±0.7	
Agarose (theoretical)	0.0		83.3	16.7	
Agarose (raw material)	8.6±0.1 (adsorbed)		76.5±1.1	14.9±0.5	
Agarose (film)	10.5±0.2 (adsorbed)		76.1±1.9	13.4±0.2	

Dendritic cells treated with PLGA or chitosan films show morphologies similar to mature DCs

Dendritic cells were treated with different biomaterial films and their morphologies were compared with iDCs and mDCs, in cytospins (Figure 4-2). Dendritic cells were collected after 24 hours of treatment with biomaterial films and stained with Giemsa. As shown, DCs treated with PLGA or chitosan films exhibited dendritic processes similar to mDCs, whereas DCs treated with agarose, alginate or HA films exhibited a morphology similar to iDCs without such processes. Dendritic cells treated with the clinical grade biomaterial films also showed morphologies very similar to DCs treated with the respective research grade films (Figure A4, APPENDIX).

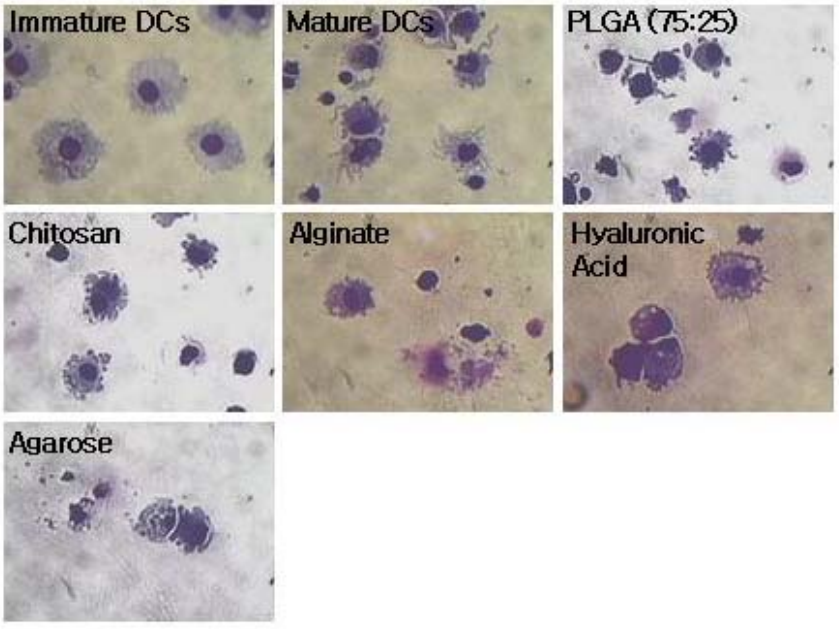

Figure 4-2: Dendritic cell treated with PLGA or chitosan films possess cell morphologies similar to mDC induced with LPS treatment.
DCs derived from peripheral blood monocytes in the presence of GM-CSF and IL-4, treated with PLGA or chitosan films showed similar morphology to that of mDCs, with the presence of dendritic processes. The morphology of DCs treated with agarose, alginate, or hyaluronic acid films was similar to untreated iDCs. Original magnification: 40×.

Dendritic cells treated with PLGA or chitosan film express higher levels of co-stimulatory and MHC class II molecules than iDCs, whereas DCs treated with HA film express lower levels

To measure DC maturation upon 24 hour treatment with different biomaterial films, DCs treated with biomaterial films were analyzed by flow cytometry for their surface expression of co-stimulatory and MHC class II molecules. As shown in the representative flow cytometry histograms (Figure 4-3), focusing on the molecules of CD80, CD86, and HLA-DQ, DCs treated with PLGA or chitosan films also resulted in a higher expression levels, compared to iDCs, similar to mDCs. However, DCs treated with alginate or agarose films resulted in an expression level similar to iDCs. Interestingly, DCs treated with HA film resulted in a shift in the histogram to the left, indicating a lower level of expression of CD80, CD86, HLA-DQ, and HLA-DR molecules. The histograms of surface molecule expressions of DCs treated with the clinical grade films also showed shift patterns very similar to those of DCs treated with research grade films (data not shown).

As shown in Figure 4-4a, geometric mean fluorescent intensities of each treatment for each donor have been normalized by ratios to iDCs to obtain relative values of maturation over the negative control of iDCs. For all surface molecules, DC maturation upon treatment with LPS induced higher levels of expression compared to iDCs. For surface molecules of CD80, CD86, CD83, and HLA-DQ, DCs treated with PLGA or chitosan films resulted in significantly higher levels of molecule expression compared to iDCs. Treatment of DCs with alginate films resulted in significantly higher levels in molecules of CD83, CD86, and HLA-DQ, as compared to iDCs. However, DCs treated with agarose films did not show a significant difference in expression of all surface molecules except for CD83, as compared to iDCs. Interestingly, DCs treated with HA films resulted in significantly lower levels of CD40, CD80, CD86, and HLA-DR

expression as compared to iDCs. As shown with brackets, significantly different gMFIs among biomaterial treatments were observed for CD80, CD86 and HLA-DR. The clinical grade biomaterials induced different extents of specific marker expression on DCs compared to the research grade biomaterials (Figure 4-4b). The clinical grade alginate induced CD80 or CD86 expression on DCs in significantly higher level or similar than iDCs, respectively. Chitosan (CD80), alginate (CD80), or HA (CD80 or CD83) in the clinical grade resulted in significantly lower level than the positive control of mDC previously used in the examination of the research grade biomaterials. The clinical grade chitosan did not exhibit significantly different level of CD86 compared to the clinical grade HA. For HLA-DQ expression, clinical grade chitosan or alginate induced expression level similar to iDCs, whereas clinical grade HA did in level lower than iDCs. However, the overall trends of biomaterial-induced expression of CD40, CD80, CD86, or CD83, normalized to the corresponding iDC controls, are similar for both clinical and research grade biomaterials.

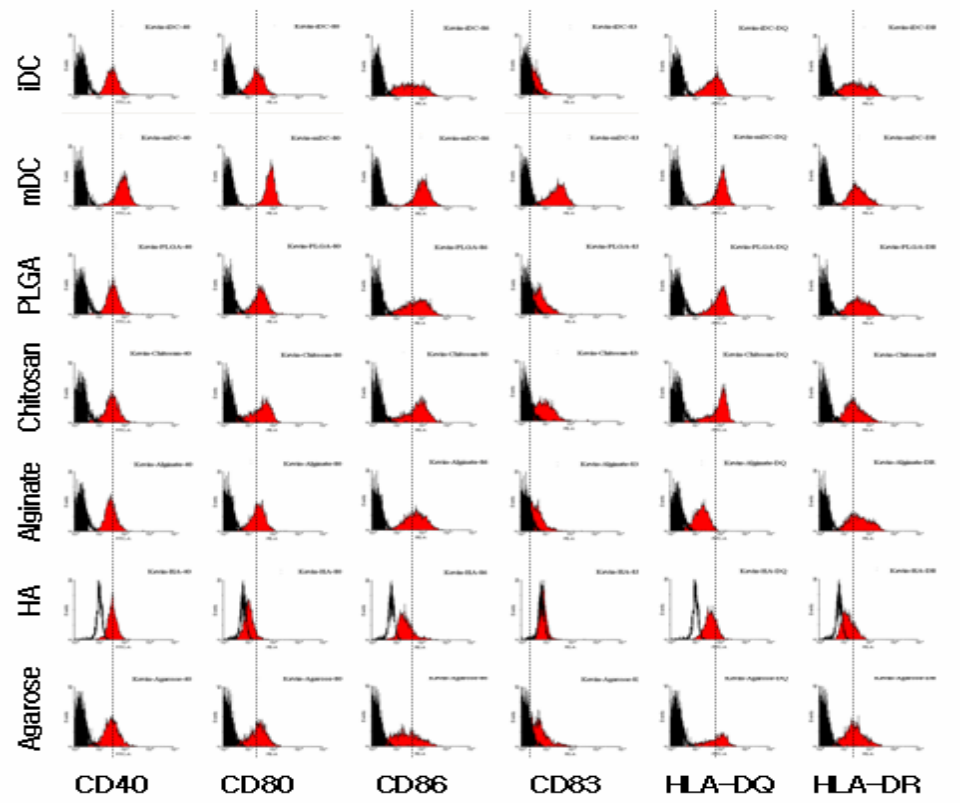

Figure 4-3: Flow cytometry histograms for expression of co-stimulatory molecules, CD40, CD80, CD86, the maturation marker, CD83, and MHC class II molecules, HLA-DQ and HLA-DR in differential levels depending on DCs treated with different biomaterials.

This experiment was performed in 3 replicates from 6 independent experiments with different donors (18 runs in total) and similar results were obtained through all 18 runs. Representative histograms are shown here. Black histograms are unstained samples and red histograms are monoclonal antibodies.

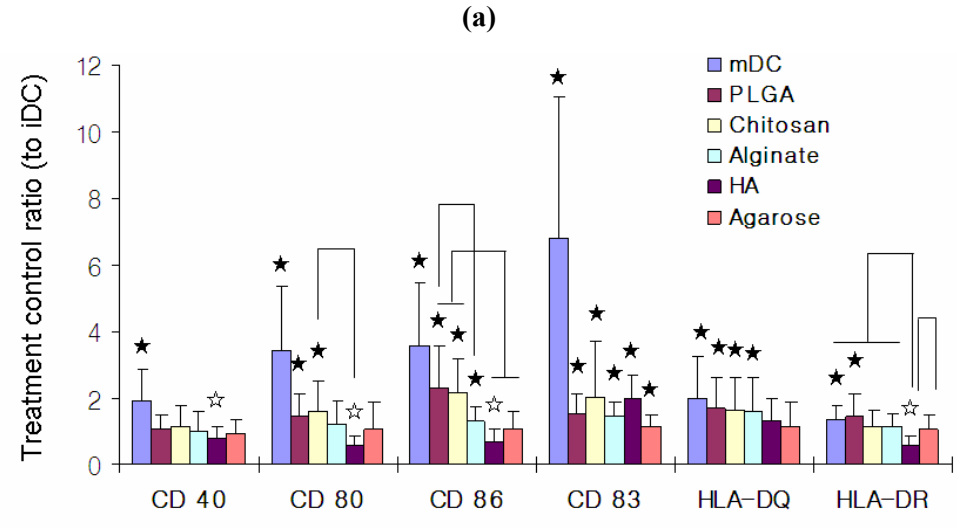

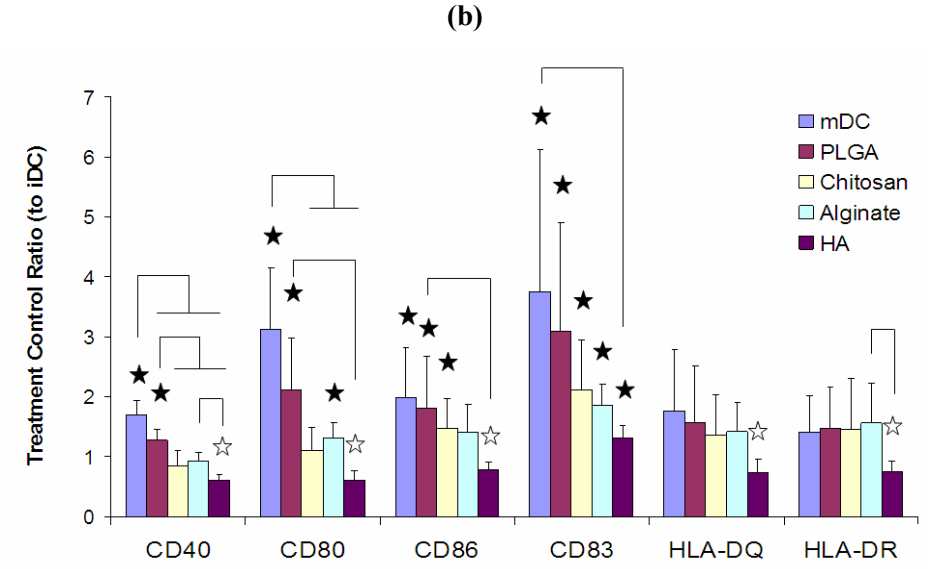

Figure 4-4: Dendritic cells treated with PLGA or chitosan film induced CD 86 expression in levels significantly higher than iDCs or other biomaterial treatments.

Geometric mean fluorescence intensity (gMFI) of flow cytometry analysis on co-stimulatory and MHC class II molecules for DCs treated with research grade biomaterial films (a) and clinical grade biomaterial films (b). Ratios to the iDCs are shown with mean±SD, n=6 donors [3 replicates from 6 independent experiments with different donors (18 runs in total)] (a) and n=6 donors [single run from 6 independent experiments with different donors (6 runs in total)] (b). ★: $p \leq 0.05$, compared to iDCs and higher than iDCs; ☆: $p \leq 0.05$, compared to iDCs and lower than iDC; Brackets: $p \leq 0.05$, statistically different between two biomaterial treatments; '⊥' indicates 'or'.

Dendritic cells treated with PLGA or chitosan films support allostimulatory T cell proliferation while treatment with HA films does not

Allostimulatory capacities of DCs treated with the different biomaterial films were assessed using an MLR as compared to the controls (Figure 4-5). Mature DCs supported a high level of T cell proliferation as compared to iDCs. Dendritic cells treated with PLGA or chitosan films supported T cell proliferation to a higher extent than iDCs, whereas DC treated with HA films, supported lower levels of T cell proliferation than iDCs, actually inhibiting T cell proliferation. In the case of the 1:6.25 DCs : T cells ratio, levels of allostimulatory T cell proliferation showed significant differences among all biomaterial treatments of DCs. For example, DCs treated with PLGA or chitosan films resulted in significantly higher levels of allostimulatory T cell proliferation than DCs treated with alginate, HA, or agarose films. The allostimulatory capacity of DCs treated with the clinical grade films also resulted in patterns very similar to those of DCs treated with the research grade films (Figure A2, APPENDIX).

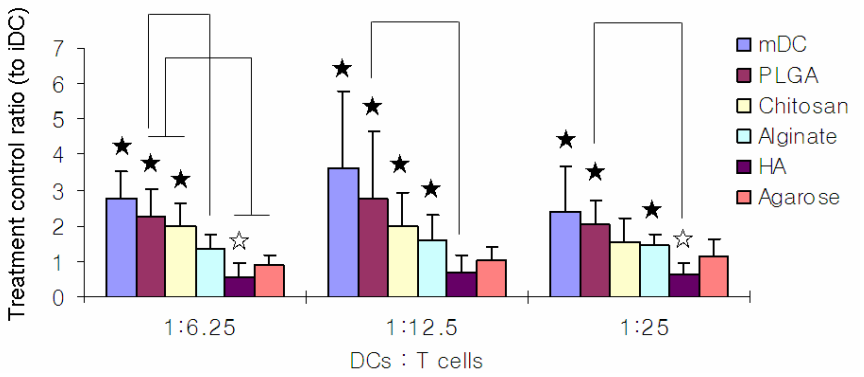

Figure 4-5: Allostimulatory capacities in Mixed Lymphocyte Reaction (MLR) in differential levels depending on DCs treated with different biomaterial films.

Dendritic cells treated with PLGA support allogeneic T cell proliferation much like mDCs, whereas DCs treated with HA actually inhibit. Ratios to the iDCs are shown with mean±SD, n=6 donors (6 independent experiments with different donors). ★: $p \leq 0.05$, compared to iDCs

and higher than iDC; ☆: $p \leq 0.05$, compared to iDCs and lower than iDC; Brackets: $p \leq 0.05$, statistically different between two biomaterial treatments; ' ⊥ ' indicates 'or'.

Dendritic cells treated with PLGA, chitosan, or alginate films secreted significantly higher levels of pro-inflammatory cytokines as compared to iDCs, whereas DCs treated with HA films secreted significantly lower levels

Pro-inflammatory cytokine (TNF-α and IL-6) release into the supernatant was measured using ELISA to assess phenotypical changes in DC maturation upon DC treatment with biomaterial films. Mature DCs secreted high levels of the autocrine maturation stimulus, TNF-α, as compared to iDCs (Figure 4-6a). Similarly, DCs treated with PLGA, chitosan or alginate films secreted significantly higher levels of TNF-α as compared to iDCs. Dendritic cells treated with chitosan films released the highest average of levels of TNF-α and also showed significantly higher levels as compared to all other biomaterial treatments. However, DCs treated with agarose films did not secrete levels of TNF-α that were significantly different from iDCs, whereas DCs treated with HA films released significantly lower levels of TNF-α as compared to iDCs. Similar to the results of for TNF-α release, DCs treated with PLGA, chitosan or alginate films also secreted in significantly higher levels of IL-6 release as compared to iDCs. However, DCs treated with agarose films did not secrete levels of IL-6 that were significantly different from iDCs. Again, DCs treated with HA films released significantly lower levels of IL-6 as compared to iDCs. No significant difference was observed among all biomaterial treatments for IL-6 release (Figure 4-6b).

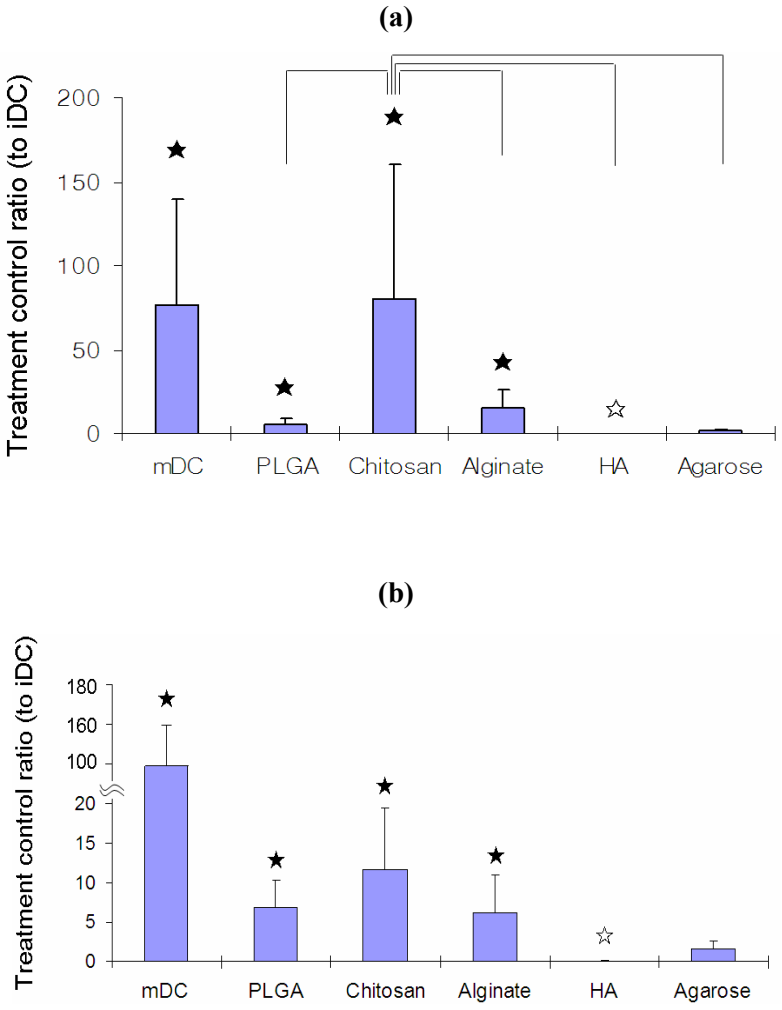

Figure 4-6: Differential levels of tumor necrosis factor (TNF) – α (a) and Interleukin -6 (IL-6) (b) in differential levels upon DC treatment with biomaterial films.

Dendritic cells treated with PLGA, chitosan, or alginate release pro-inflammatory cytokines in levels significantly higher than iDCs, whereas DCs treated with HA did in levels significantly less than iDCs. Only agarose induced both cytokines in level similar to iDCs. TNF-α or IL-6 released from each treatment group for each donor was normalized to total DNA amount and then, ratios to the iDCs are shown with mean±SD, n=6 donors (6 independent experiments with different donors). ★: $p \leq 0.05$, compared to iDCs and higher than iDC; ☆: $p \leq 0.05$, compared to iDCs and lower than iDC; Brackets: $p \leq 0.05$, statistically different between two biomaterial treatments.

Activation of NF-κB transcription factor, subunit of p50, do not show significantly different levels among DCs treated with PLGA, chitosan, alginate, or agarose films

To measure activation of NF-κB transcription factor subunit p50, upon DC treatment with different biomaterial films, nuclear extracts were prepared for DCs treated with different biomaterial films for 5 or 24 hours and levels of p50, were determined as compared to the controls (Figure 4-7). The p50 subunit of NF-κB was selected for analysis of DC responses to biomaterials since it was expressed at a high level and most responsive to treatments as determined previously (Yoshida and Babensee, 2006). Mature DCs exhibited significantly higher activation levels of p50 subunit of NF-κB at both 5 and 24 hours of time points, compared to iDCs. In addition, DCs treated with alginate films for 5 hours or DCs treated with agarose films for 24 hours showed significantly lower or higher levels of activated p50 compared to iDCs, respectively. However, no significant difference in levels of activated p50 was observed for the DCs treated with the other biomaterial films as compared to iDCs. Activation of subunit p50 also was not induced in significantly differential levels among DCs treated with PLGA, chitosan, alginate, or agarose films. The levels of p50 were undetectable from DCs treated with HA films. Assessing the effect of time, the levels of p50 increased from 5 to 24 hours for mDCs or DCs treated with alginate films.

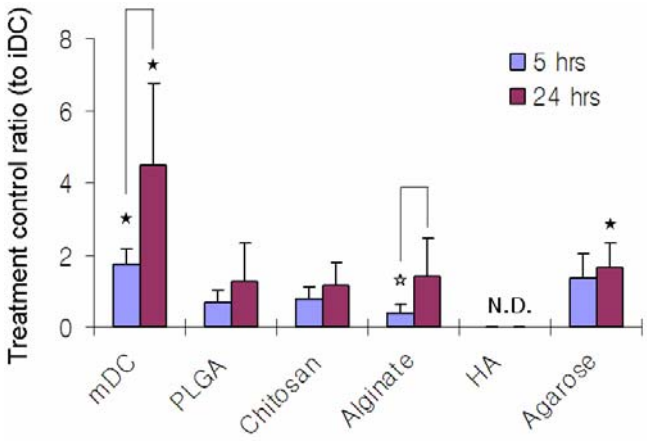

Figure 4-7: Activation of NF-κB (subunit of p50) upon DC treatment with biomaterials as a function of time (5 and 24 hours).

For both time points, all biomaterial treatments do not show significant difference each other. While no significantly different level was observed between treatments, agarose induced significantly higher level than iDCs after 24 hours and alginate induced significantly higher level after 24 hours compared to that after 5 hours. Dendritic cells treated with HA exhibited in levels that are not detectable for both time points. Ratios to the iDCs are shown with mean±SD, n=6 donors (6 independent experiments with different donors). ★: $p \leq 0.05$, compared to iDCs and higher than iDC; ☆: $p \leq 0.05$, compared to iDCs and lower than iDC. For statistical comparisons between 5 and 24 hours within a same treatment, one-sided Student t-test was also used. Brackets: $p \leq 0.05$, statistically different between 5 and 24 hours of biomaterial treatments for a same treatment; N.D.: not detectable.

DCs treated with PLGA, chitosan, alginate, or HA films underwent apoptosis at a level significantly higher than iDCs, whereas DCs treated with agarose films were similar to iDCs

Apoptosis or necrosis of DCs upon 24 hour treatment with different biomaterial films was measured using flow cytometry analysis of DCs stained with Annexin V (apoptosis) and propidium iodide (PI) (necrosis). Mature DCs and DCs treated with PLGA films showed significantly higher staining levels of Annexin V, whereas DCs treated with agarose films does not show significantly different level, as compared to iDCs (Figure 4-8). Unexpectedly, DC treatment with HA films induced significantly higher levels of apoptosis compared to iDCs and DC treatment with chitosan, alginate, or HA films induced significantly higher levels of apoptosis than mDCs or DCs treated with agarose films. Only alginate films induced DC necrosis in levels significantly higher than iDCs while mDCs or other biomaterial treatments did not induce significantly different levels of necrosis in DCs as compared to iDCs. The staining levels of Annexin V and PI of DCs treated with clinical grade biomaterial films also showed very similar results as for DCs treated with research grade films (Figure A3, APPENDIX).

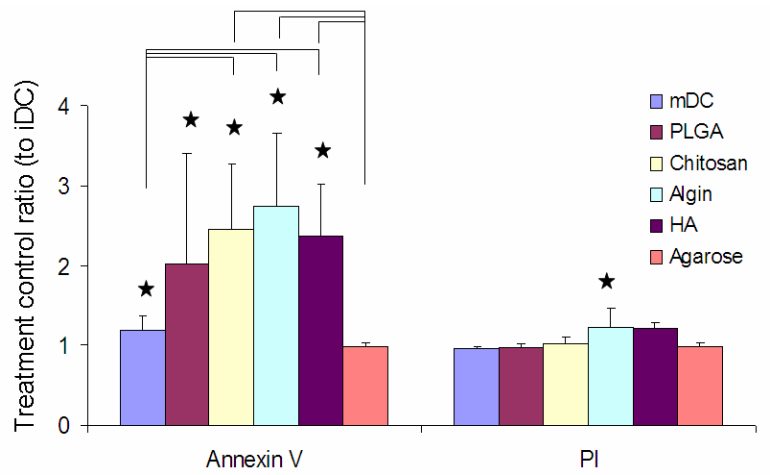

Figure 4-8: Geometric mean fluorescence intensity (gMFI) of flow cytometry analysis of Annexin V and propidium iodide (PI) expression in differential levels upon DCs treated with different biomaterial films.

Dendritic cells treated with PLGA, chitosan, or alginate exhibited Annexin V expressions in higher levels than iDC. However, DCs treated with HA unexpectedly exhibited Annexin V expression in higher level than iDCs. Only agarose induced levels similar to iDCs for both Annexin V and PI. Ratios to the iDCs are shown with mean±SD, n=9 donors (9 independent experiments with different donors). ★: $p \leq 0.05$, compared to iDCs and higher than iDC; ☆: $p \leq 0.05$, compared to iDCs and lower than iDC; Brackets: $p \leq 0.05$, statistically different between two biomaterial treatments.

Dendritic cells treated with agarose films showed endocytic ability in level similar to that of iDCs while all other biomaterial films induced levels significantly less than iDCs

To measure the endocytic ability of DCs upon treatment with different biomaterial films, DCs treated with biomaterial films were co-incubated with FITC-conjugated dextran and then, the intensity of FITC uptaken by DCs was measured using flow cytometry. In accordance with the documented result that lower levels of endocytic activity are associated with DC maturation (Schnurr et al., 2001), the studies here showed that mDC, or DCs treated with PLGA or chitosan films induced significantly lower levels of endocytic ability while the endocytic activity of DCs

treated with was not significantly affected, as compared to iDCs (Figure 4-9). Treatment of DCs with agarose films actually induced a higher level of endocytic ability than observed for mDCs and DCs treated with all other biomaterials films except for alginate. Similarly, treatment of DCs with alginate films induced a higher level of endocytic ability than observed for mDCs and DCs treated with all other biomaterials films except for agarose. However, DC treatment with HA films unexpectedly induced endocytic ability that was at a significantly lower level than for iDCs, or DCs treated with alginate or agarose films.

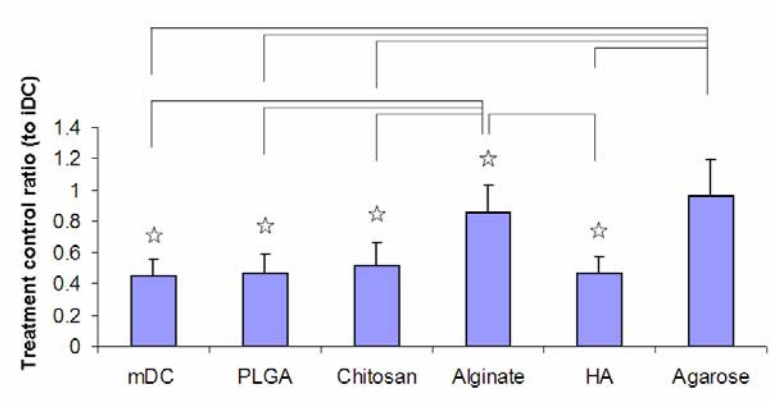

Figure 4-9: Geometric mean fluorescence intensity (gMFI) of flow cytometry analysis of FITC-dextran uptake by DCs in differential levels upon DCs treated with different biomaterial films.

Dendritic cells treated with PLGA, chitosan, or alginate which induced DC maturation significantly higher than iDCs exhibited endocytic ability significantly less than iDCs. Unexpectedly, HA induced the endocytic ability significantly less than iDC. Only agarose induced the endocytic ability similar to iDCs. Ratios to the iDCs are shown with mean±SD, n=6 donors (6 independent experiments with different donors). ★: $p \leq 0.05$, compared to iDCs and higher than iDCs; ☆: $p \leq 0.05$, compared to iDCs and lower than iDCs; Brackets: $p \leq 0.05$, statistically different between two biomaterial treatments.

Dendritic cells treated with HA films induced lower levels of expression of endocytic and migration receptors

To provide explanation of the functional changes in DC phenotype upon treatment with different biomaterial films, expression levels of endocytic receptors, CD32 (Fcγ Type II) and CD206 (mannose receptor) and migration receptors, CD44, were examined by flow cytometry (Figure 4-10). Both CD32 and CD206 expression on DCs upon treatment with different biomaterial films showed patterns in accordance with those of the endocytic ability shown in Figure 4-9. Even though the CD44 is well known for receptor specific to the hyaluronan component in the extracellular matrix (ECM) for migration of DCs, the HA films in this study induced significantly lower level of expression than iDCs or DCs treated with other biomaterial films. For instance, mDCs or DCs treated with PLGA films expressed CD44 in significantly higher levels than DCs treated with alginate, HA, or agarose films while DCs treated with chitosan films expressed significantly higher levels only compared to DCs treated with HA films.

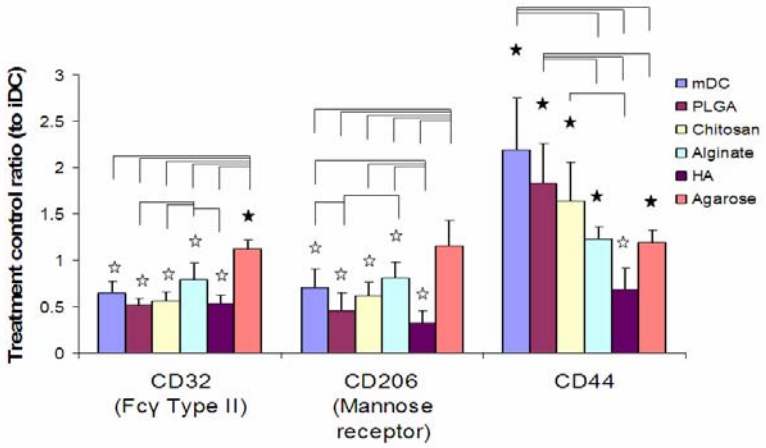

Figure 4-10: Geometric mean fluorescence intensity (gMFI) of flow cytometry analysis of CD32, CD206, and CD44 expression in differential levels upon DCs treated with different biomaterial films.

As expected from the measurement of endocytic ability, only agarose induced CD32 or CD206 expression levels higher than or similar to iDCs, whereas other all biomaterial treatments induced those lower than iDCs. Unexpectedly, DCs treated with HA exhibited CD 44 expression level significantly lower than iDCs even though CD44 is specific to hyaluronan component in ECM. Ratios to the iDCs are shown with mean±SD, n=6 donors (6 independent experiments with

different donors). ★: $p \leq 0.05$, compared to iDCs and higher than iDC; ☆: $p \leq 0.05$, compared to iDCs and lower than iDC; Brackets: $p \leq 0.05$, statistically different between two biomaterial treatments.

DISCUSSION:

The purpose of this research was to assess the differential effects on DC maturation of different biomaterials used in combination products, particularly focusing on immunobiological functional assessment of differentially treated DCs. Results indicate that PLGA or chitosan films supported higher levels of DC maturation as compared to iDCs as shown in Figure 4-11. Agarose or alginate film supported moderate levels of DC maturation while DC maturation was inhibited by HA film which is cross-linked and insolublized. Unexpectedly, PLGA or chitosan, while supporting DC maturation, did not induce significantly higher levels of the transcription factor, NF-κB (subunit of p50) activation as compared to iDCs. Hyaluronic acid (HA) film (cross-linked and insolublized form) interestingly induced lower expression of CD44, higher apoptosis level, and lower endocytic ability of DCs, as compared to iDCs.

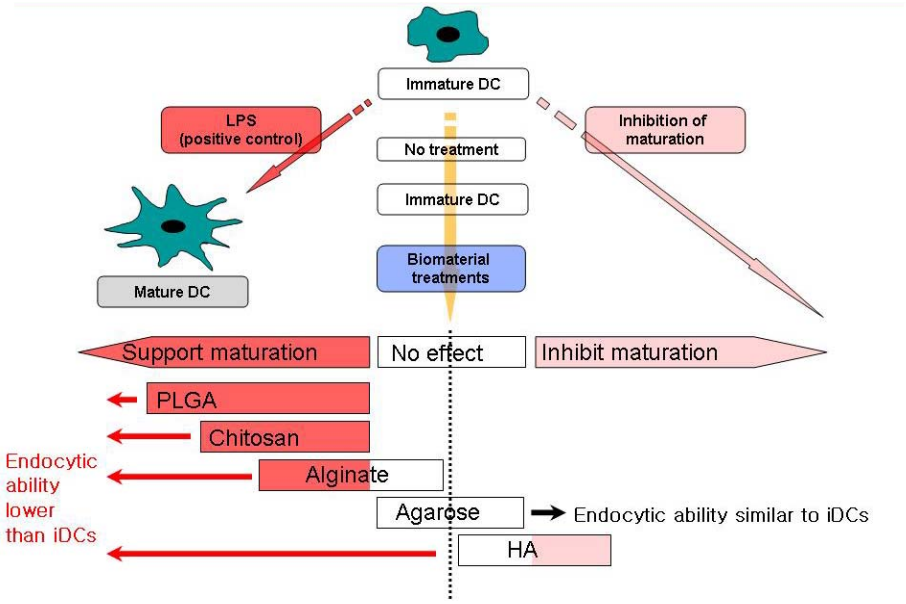

Figure 4-11: Schematic representation of effects of biomaterials in 2-dimensional film forms on human monocyte-derived DCs. Agarose or alginate film supported moderate levels of DC

maturation while DC maturation was inhibited by HA film which is cross-linked and insolublized.

Since the surface chemistry of a biomaterial can be a strong director of cellular interactions and the expected chemistry can be modulated due to biomaterial processing conditions, the chemical compositions of all biomaterial film surfaces were determined by XPS. The film processing induced a change in surface chemistry of the biomaterials as indicated by increasing amounts of carbon upon film formation and cross-linking procedure while those of oxygen decreased, compared to the theoretical values (Table 1 and 2). It is estimated that unknown contaminants were introduced (e.g. hydrocarbons) or gas (e.g., CO_2) were adsorbed from the environment during the film forming process (Tam et al., 2005). It is also estimated that the hydrophilic sites of biomaterial molecules were rearranged towards the inside of biomaterial films due to the gradient of evaporation rate of distilled water or solvents during the film formation (Bu et al., 2002). After the cross-linking procedure, only alginate films showed introduction of chlorine (1.4±0.1%) presumably due to residual $CaCl_2$ cross-linking reagent on the film surface. However, XPS low resolution spectra for all other biomaterial films did not indicated presence of residual cross-linking agents on their surface.

Dendritic cell follows a similar linage (derived from the monocyte) as macrophage and both cell types have been known to up-regulate similar sets of genes in response to pathogens, as such they share similarity on more than 96% of basal gene expression (Foti et al., 2006). Macrophages easily interact with proteins adsorbed on the hydrophobic surface of biomaterials such that many studies on effects of macrophages on immune responses have been performed on macrophages adherent to surfaces of biomaterials (Collier and Anderson, 2002; Shen and Horbett, 2001; Shen et al., 2004; Nathan, 1987).

The adhesion stability of protein adsorbed on different surface chemistries with different

hydrophobicities has been shown with the highest level on the hydrophobic surface followed by the next highest one on the cationic surface (e.g., hydrophobic surface > cationic surface > neutral surface > anionic surface) under the physiological pH (Fraaye et al., 1986; Brash, 1983; Young et al., 1988). Among all biomaterials examined in this study, PLGA has been recognized for an hydrophobic biomaterial showing good biocompatibility because its degradation products are biocompatible (Ignatius and Claes, 1996). However, PLGA has also been used as an adjuvant inducing immunogenicity for the delivery of vaccines (Ertl et al., 1996), often in the form of microparticles, due to the phagocytosis effects (Ohagan et al., 1993). In addition, chitosan is another hydrophobic biomaterial of natural polysaccharides having carbohydrate units which are mainly composed of glucosamine with a high cationic charge density (Chandy and Sharma, 1990; Tangpasuthadol et al., 2003; Li and Tuan, 2005). After 24 hour-treatment of DCs with biomaterial films, non-/loosely-adherent DC portion collected from PLGA film was observed with the least amount of 37±15% among all biomaterial films used in this study, followed by the next least one of 65±13% obtained from chitosan film as mentioned earlier in the method section. Furthermore, CD44, a functional marker expressed on DCs for migration also was induced by PLGA or chitosan films in significantly higher levels than iDCs. These indicate that, during 24 hour-treatment of DCs with these films, protein adsorption on these biomaterial films and consequent adhesion of cells to those protein adsorbed might be induced in higher levels compared to other biomaterial films or iDC control.

Overall, these two biomaterial films induced DC phenotypical changes in DC maturation in significantly higher levels compared to the negative control of iDCs for most assessments. Moreover, PLGA was found, in the absence of carbohydrate unit recognizable by PRRs on DCs, as the most potent stimulus (among all biomaterial examined herein) induced DC maturation in levels similar to the positive control of mDCs in the most examinations performed in this study.

Taken together, even though non-/loosely-adherent DCs were mainly examined herein, hydrophobicity or cationic charges of PLGA or chitosan film employed here might be involved in induction of DC maturation, at least, in various assessments performed in this study.

Dendritic cells showed upregulation in CD86 expression only when treated directly with biomaterials (Yoshida and Babensee, 2004). This indicates that DC maturation or allostimulatory capacity of DC can be partially caused by certain interactions between DCs and proteins adsorbed on biomaterial surfaces even though DCs are loosely adherent to protein-coated biomaterial surfaces. Dendritic cells recognize pathogens through conserved structures, uniquely characteristic of microbial pathogens, through their cognate binding receptors resulting in their maturation such that they become efficient antigen presenting cells (Janeway and Medzhitov, 1998). Considering these critical roles of the receptors in DC response against foreign bodies, PRRs of DC might play a key role in the interaction between DCs and biomaterials.

Chitosan consists of N-acetyl-D-glucosamine units (GlcNAc), which can interact with macrophage mannose receptor for mannose- and GlcNAc-glycoproteins (Warr, 1980; Hitchen et al., 1998), inducing brisk inflammatory responses (Hidaka et al., 1999; Feng et al., 2004; Crompton et al., 2006). Chitin (acetylated chitosan) also induced accumulation of innate immune cells such as eosinophils and basophils and mediated alternative macrophage activation, independently with tissue specificity of mice (Reese et al., 2007).

Moreover, using the murine macrophages, it has been recently reported that chitin or chitosan is directly recognized by the macrophage mannose receptor and this receptor-mediated stimulation induces an expression of MHC class I and II molecules, and macrophage inflammatory protein (MIP)-2 as well as a release of TNF-α and IL-1β (Feng et al., 2004; Mori et al., 2005). The mannose receptor is a representative C-type lectin which is one family of PRRs,

expressed on both macrophages and DCs and its specificities of ligand and function are identical for both cell types (Figdor et al., 2002). The chitosan film tested in this study supported DC maturation especially in terms of pro-inflammatory cytokine (TNF-α and IL-6) secretion wherein it showed the highest average values amongst the biomaterials. Thus, it is conceivable that DC maturation may be controlled by hydrophobicity of biomaterial surfaces and/or inherent chemistries of biomaterials, which can be recognized by specific receptors such as PRRs expressed on DCs.

Alginate molecules are linear block copolymers of mannuronic acids and guluronic acids with a variation in composition and sequential arrangements. Due to its hydrophilic nature, alginate has been employed as a hydrogel, which is beneficial to minimize the protein adsorption and cell adhesion (de Vos et al., 2002). Also, microencapsulation technique using alginate has been proposed for immunoisolation of transplanted islet from the host immune responses (Weber et al., 1999; Black et al., 2006). However, secretion of IL-1, IL-6, and TNF-α has been induced upon treatment of human monocyte-derived macrophages with the poly-mannuronic acid obtained from alginates (Otterlei et al., 1991) and CD14 expressed on the macrophages has been reported for its critical role in binding to the mannuronic acid and stimulating the macrophages to release those cytokines (Espevik et al., 1993). More recently, TLR-2 and TLR-4 in association with CD14 have been reported for their critical roles in inducing secretion of IL-1α, IL-1β, IL-6, and TNF-α from human macrophages or murine macrophages in contact with mannuronic acid polymers or alginates (Flo et al., 2002; Iwamoto et al., 2005; Orive et al., 2005). In accordance with these, in the present study herein, alginate with a high content of mannuronic acid induced a secretion of TNF-α and IL-6 by DCs in levels significantly higher than iDCs. Thus, it is also conceivable that the alginate with a high content of mannuronic acid may interact with the TLRs, associated with CD14, expressed on human DCs, to modulate their function.

In contrast to chitosan and alginate, agarose does not have a specific carbohydrate composition which is recognized by the PRRs expressed on DCs and elicited minimal DC maturation in the system used here. Due to its non-inflammatory feature, agarose has been employed in the agarose gel immunodiffusion (AGID) assay for the serological infection diagnosis (Kustritz, 2000) or used as a plate in assessment of chemokinetic behavior of inflammatory lung macrophages (Newtonnash et al., 1990). For most assessments of DC maturation in this study, agarose films induced DC maturation in levels statistically similar to iDCs. However, for measurement of activation of transcription factor NF-κB, subunit of p50, DC treatment with agarose films induced significantly higher levels compared to iDCs after 24 hours' treatment of iDCs with agarose films. As suggested by our previous studies (Yoshida and Babensee, 2006), twenty four hours of treatment may be too long to observe NF-κB activation of DCs treated with hydrophobic PLGA because it may possibly have already peaked and declined. However, as shown in Figure 4-7, DC treatment with PLGA or agarose films induced lower levels of activation of the subunit of p50 at the time point of 5 hours and higher levels at the time point of 24 hours, thereby showing a same trend of increasing levels overtime. Furthermore, DC treated with PLGA films did not induced significantly higher levels of p50 than DC treatment with agarose films at both time points.

Agarose is composed of repeating β-D-galactopyranosyl and 3,6-anhydro-α-L-galactopyranosyl units that show very hydrophilic nature due to high content of hydroxyl (OH) end groups. The content of water is estimated as 97% (3% of agarose) after the film formation, assuming the water content at dissolving the agarose retained but exact determinations are not possible (Yoshida and Babensee, 2006). Consistently, the lack of maturation effect observed for DCs treated with agarose films was not surprising, given its hydrophilicity and presumably low protein adsorption and/or the absence of the carbohydrate component recognizable by DC PRRs

that result in an consistent but opposite basis for explaining the mechanism of DC response as compared to treatment with PLGA or chitosan films as discussed above.

Interestingly, DC treatment with HA films induced significantly lower levels of DC maturation than iDCs, actually suppressing the DC maturation for all assessments in the present study herein. Hyaluronic acid is a negatively charged high molecular weight glycosaminoglycan, which is ubiquitously distributed throughout our body. For instance, high molecular weight HA, exactly in a hydrogel form, plays a critical role as a lubricant in the joints. As such, HA is very hydrophilic taking up water to 1000-fold of its own weight. In the present study, HA film was cross-linked for treatment of DCs. After cross-linked, compared to other biomaterial films used here, HA film showed the highest ratio of swelling with water, expanding by 2~3 fold of the size of its dried film, and had very slippery surfaces after swelled with water. Actually, soluble fragments of HA have been reported to support DC maturation (Termeer et al., 2000; Yang et al., 2002a). However, high molecular weight HA fragments (6,000 kDa) induced a decreased level of TNF-α secretion, by specifically inhibiting TLR-2 signaling, from murine macrophages transfected with human TLR-2, as compared to the low molecular weight HA fragments (200 kDa) (Scheibner et al., 2006). It has also been reported that hydrophilic and anionic surfaces of biomaterials promote an increased anti-inflammatory response and decreased pro-inflammatory response by dictating selective cytokine production by human monocytes and macrophages (Brodbeck et al., 2002) or mouse macrophages (Ademovic et al., 2006). Surface chemistries of biomaterials can determine properties such as conformation of adsorbed proteins on biomaterials and dictate activation of macrophage and neutrophils, associated with cytokines secreted depending on biomaterials. In accordance with this, treatment of DCs with the negatively charged and hydrophilic surfaces of cross-linked HA films in the present study actually inhibited human DC maturation for all assessments performed here, contrary to DC treatment with

positively-charged chitosan films. However, except for non-detectable levels of the activation of p50 for DCs treated with HA films were not significantly different among all biomaterial treatments for each time course of 5 or 24 hours as shown in Figure 4-7.

Currently in our laboratory, efforts are being made to assess NF-κB activation in TLR4-expressing HEK293 cells upon treatments with PLGA or agarose films for 5 or 24 hours. And, in TLR4-expressing HEK293s, PLGA or agarose film treatments do not activate NF-κB at 5 or 24 hours while LPS treatment activates NF-κB at both time points (T.H. Rogers and J.E. Babensee, unpublished observations). These results collectively support independency of NF-κB activation from DC maturation mechanisms as suggested previously (Ouaaz et al., 2002; Zeyda et al., 2005). These also indicate, to further understand DC maturation upon treatment with different biomaterials, that it might be needed to assess other signal pathways such as transcription factor AP-1 for additional mechanisms behind the induced DC maturation and the time courses of the activation of these transcription factors in response to biomaterials.

Apoptosis of DCs was unexpectedly induced in higher levels, as compared to iDCs, by treatment with HA films in this study while most of all other measurements revealed, upon DC treatment with HA films, DC maturation levels were even lower than iDCs. Endocytic ability of DCs treated with HA films also unexpectedly resulted in levels that were lower than for iDCs. Antigen presentation by DCs to antigen-specific T cells is a successive step to antigen uptake and migration of DCs. CD32 (Fcγ Type II) or CD206 (mannose receptor) are well known for their important roles of mediating endocytosis by DCs and it has been reported that these receptors on iDCs or dexamethasone-treated DCs were necessary for higher efficiency in antigen uptake, which is up-regulated more than for mDCs or DCs treated with ultraviolet B radiation (Piemonti et al., 1999; Sallusto et al., 1995; Mizuno et al., 2004). CD44 has been well known as a potent receptor expressed on DCs to mediate DC cluster, migration, and maturation upon interaction

with the hyaluronan components in the ECM (Weiss et al., 1997; Termeer et al., 2001). This receptor has been extensively studied *in vitro* or *in vivo* with interactions of soluble fragments of low molecular weight HA (≤ 200,000 Da) that enhanced DC clustering, migration and/or maturation (Weiss et al., 1997; Termeer et al., 2000; Termeer et al., 2001; Do et al., 2004). Particularly, interaction of CD44 with intermediate-sized HA (MW ~ 200,000 Da) has been reported to induce apoptosis of DCs through nitric oxide (NO) production by DCs when tumor cells were involved (Yang et al., 2002b). Also, it has been suggested that endocytosis by Langerhans cell-like DCs were deeply related with an increased migration activity of these DCs (Mizuno et al., 2004).

However, in the present study, DCs treated with HA films expressed lower levels of CD44, higher apoptosis level, and lower endocytic ability than iDCs and were associated with levels of DC maturation which were less than iDCs. It is conceivable that insolublized (cross-linked) film forms processed with high molecular weight (≥ 800,000 MW) HA in this study might induce these peculiar effects on DCs as seen in CD44 expression, endocytic ability, and apoptosis that would direct DC behaviors in immune responses. Interestingly, patterns of CD44 expression were very similar to those of co-stimulatory molecule expression (Figure 4-4) or MLR (Figure 4-5) results as far as differential DC maturation upon DC treatment with different biomaterial films. Thus, these features induced by HA films in this study are expected to provide a therapeutic tool of HA film-mediated immunosuppression, associated with apoptosis of immune cells, in disease situations (Pope, 2002; You et al., 2008) which will require *in vivo* validation.

The extents of marker expression were different between the research grade and clinical grade biomaterials as shown in Figure 4-4. Upon DC activation and TCR engagement by peptide-MHC class II molecules such as HLA-DQ or HLA-DR, co-stimulatory surface molecules

on DCs increase in their expression levels to effectively stimulate T cells. For instance, B7 family molecules of CD80 and CD86 are expressed on DCs and interact with CD28 expressed on T cells while CD40 expressed on DCs does with CD40 ligand (CD40L) on T cells. At the same time, CD83, specific marker for DC maturation, is also expressed on DCs depending on maturation extent. So, it is conceivable that difference between the research and clinical grades (e.g., purification in the biomaterial processing) might affect differential expression of specific markers on DCs with differential maturation extents in the context of biomaterial treatment. However, in consideration of overall results of DC treatment with the clinical grade biomaterials as shown in Appendix (examination of cytospin, MLR, or annexin V/PI staining upon DC treatment with the clinical grade biomaterials) as well as surface marker expressions, DC responses to the clinical grade biomaterials were indistinguishable from their responses to the research grade biomaterials. Five different biomaterials commonly used and relevant to combination products such as tissue engineered constructs or vaccine delivery systems were used to fully characterize DC immunological phenotype upon treatment with these biomaterials. Different biomaterials had differential effects on DC maturation wherein PLGA or chitosan films induced DC maturation, alginate or agarose films did not and HA films inhibited DC maturation. The biomaterial films used herein have different chemistries and properties among them but it was not possible to elucidate the specific key biomaterial property(ies) that have resulted in these observed differential effects on DC maturation. More controlled systems for varying biomaterial properties in a controlled manner are more amenable to elucidating critical biomaterial properties for controlling DC response with the view to directing immune responses (Yang et al., 2008; Kohn et al., 2007).

The strength of the study described herein is the assessment and comparison of DC responses to biomaterials so widely and commonly used in combination products. An

understanding of DC maturation as predictive of a biomaterial adjuvant effect can suggest selection or design criteria for biomaterials in applications of tissue engineering or vaccine/drug delivery with associated immune responses. For example, *ex vivo* culture and adoptive transfer regimes in which DCs would be treated with PLGA films or HA films would be useful potentially inducing cancer immunity or tolerance, respectively.

CHAPTER 5[†]

DIFFERENTIAL FUNCTIONAL EFFECTS OF BIOMATERIALS ON DENDRITIC CELL MATURATION. PART 2. EFFECTS OF BIOMATERIALS IN 3-DIMENSIONAL SCAFFOLD FORM

INTRODUCTION:

Since tissue engineering has been recognized as a promising alternative for restoring damaged or diseased tissues (Freed et al., 1999; Freed et al., 1993; Temenoff and Mikos, 2000; Timmins et al., 2007), 3-D scaffolds in porous form have been extensively developed for requirement in tissue engineering to support cellular adherence and delivery as well as to facilitate the transport of nutrients and metabolic wastes, thereby fostering the formation of new extracellular matrix and tissue ingrowth (Agrawal and Ray, 2001; Hu et al., 2002; Wang et al., 2008). When biomaterials are selected or designed for use in tissue engineered combination products as scaffolds/carriers, consideration of the biomaterial-adjuvant effect should be taken into account to minimize any enhancement of an adaptive immune response to the associated biological component (Bennewitz and Babensee, 2005; Ertl et al., 1996; Li and Tuan, 2005). Clearly from a tissue engineering point of view, immune responses are to be minimized or all together avoided while DNA or protein-based vaccines seek to initiate and enhance a protective immune response.

Adjuvants function in enhancing an immune response by interacting with antigen presenting cells, most notably, DCs during an innate immune response, to induce their maturation such that they become efficient at presenting antigen for effective stimulation of T cells for an adaptive immune response (Cox and Coulter, 1997; Singh and O'Hagan, 1999).

[†] A manuscript prepared from this Chapter 5, titled as 'In vitro control of dendritic cell phenotypes in 3-dimensional scaffolds for tissue engineering', is to be submitted to Biomaterials.

Functional changes associated with DC maturation include acquiring enhanced expression of major histocompatibility (MHC) class I and II molecules and co-stimulatory molecules, with the effect of increased stimulation of T cell proliferation in an allostimulatory mixed lymphocyte reaction (MLR), DC morphologies and release of immunomodulatory cytokines (Banchereau and Steinman, 1998; Matzinger, 1994; Sallusto et al., 1995; Tsuji et al., 2000; Mellman and Steinman, 2001). Dendritic cells have also been proposed to be modulated in their maturation levels upon contact with different biomaterials in 2-dimensional film form (Yoshida and Babensee, 2004; Babensee and Paranjpe, 2005; Park and Babensee, 2009). Upon interaction between DCs and T cells, the resultant immunity can be polarized toward either T helper (Th) type 1 or T helper (Th) type 2 depending on the various cytokines released from DCs or T cells (Moser and Murphy, 2000; Kapsenberg, 2003). In this way, the adaptive immunity can be modulated into immunogenicity or tolerogenicity (Lanzavecchia and Sallusto, 2001; Sakaguchi, 2005).

Three-dimensional scaffold form has been frequently employed in the studies of tissue engineering or drug delivery due to their exceptional properties of supporting tissue regeneration combined with controllable degradation by physical and/or chemical treatment. Furthermore, efforts have been recently made to develop a strategy for localization or migration of immune cells using biomaterial scaffolds, to control adaptive immunity more effectively (Stachowiak and Irvine, 2008; Suematsu and Watanabe, 2004; Okamoto et al., 2007). However, effects of different biomaterials in 3-D scaffold form on human monocyte-derived DCs have not been fully understood yet, which should be of great worth as preliminary examinations that are believed to provide valuable information correlated with immunomodulatory effects of 3-D porous scaffolds of these biomaterials in future *in vivo* applications.

Herein, using 3-D scaffolds processed from two inherently different biomaterials (PLGA or agarose) that showed opposite effects of their film form on DC maturation or autologous T cell

phenotype and polarization (in the Chapter 6), we extend our previous studies (in the Chapter 4) to characterize the effect of contact with 3-D porous scaffolds on the maturation of human monocyte-derived DC using a variety of assays. We also examined the release of cytokines and chemokines that have been recognized as their important roles in host response of the general pathology upon *in vitro* contact of DCs with biomaterial scaffolds. Dendritic cells treated with PLGA scaffolds support high levels of DC maturation in phenotypical changes while treatment with agarose scaffolds results in a DC phenotype similar to the negative control of iDCs. Interestingly, *in vitro* releases of various cytokines and chemokines important for general pathology were observed in levels modulated upon DC treatment with different biomaterial scaffolds. An understanding of the mechanism behind effects of the 3-D biomaterial scaffolds on DC phenotypical changes is expected to suggest new selection and design criteria for biomaterial scaffolds to be used in immunotherapy and tissue engineering.

METHODS:

Preparation of biomaterial 3-D porous scaffolds

The biomaterials used for scaffolds include poly(DL-lactic-*co*-glycolic acid) (PLGA) and agarose. All biomaterial scaffolds were prepared freshly for every experimental procedure. Preparation methods of all biomaterial scaffolds were adapted or modified from the previously described methods; PLGA scaffolds were prepared by salt-polymer casting particulate-leaching technique with NaCl at the leachable component (Mikos et al., 1994) and agarose scaffolds prepared by inverted colloidal crystal templating method using polystyrene beads as leachable component (Lee et al., 2006). Briefly, poly(DL-lactic-*co*-glycolic acid) (PLGA) (ester terminated; molar ratio: 75:25, inherent viscosity: 0.70 dL/g in trichloromethane, 100,000 MW; Birmingham Polymers, Birmingham, AL) was dissolved with 8.3% w/v in dichloromethane

(DCM) overnight at room temperature. Then, this PLGA/DCM solution was poured over 4.5 g NaCl (90-125 μm) in a Teflon dish of 50 mm diameter (Cole-Parmer) in the chemical fume hood. After complete mixing PLGA/DCM solution and salts using paper clip, evaporation of the solvent (DCM) and drying were performed in the chemical fume hood for 36-48 hours followed by leaching salts in ddH_2O using shaker for 2 days changing water 3 times. After leaching salts, scaffolds were dried in the tissue culture hood for 24 hours, and freeze-dried overnight. For agarose scaffolds, polystyrene beads with 100 (±1.5%)μm (particle counter size standards, Duke Scientific, Palo Alto, CA) were washed 3 times using isopropanol (Sigma), and sonicated in isopropanol for 20 minutes followed by evaporation of isopropanol in the oven at 60ºC overnight. Then, polystyrene beads in Teflon beaker were sintered in the oven at 120ºC for 4 hours, and the crystal templates were prepared. Agarose (type V; high gelling; gel strength of ≥ 800 g/cm^2 at 1.0%; Sigma; molecular weight is not known) was dissolved in ddH_2O to a concentration of 3% w/v by heating using a microwave until boiling and visible homogeneity was reached. Agarose solution was applied into the Teflon beaker having polystyrene bead template, and the beaker spun at 2,000 rpm for 3 minutes. After solidification of agarose hydrogel at room temperature, polystyrene beads were leached in tetrahydrofuran (THF) (Sigma) using shaker for 2 days changing THF 3 times in the chemical fume hood, followed by rinsing agarose scaffolds in ddH_2O for 30 minutes (3 times) using shaker in the chemical fume hood. Prepared scaffolds of PLGA and agarose were moved into the tissue culture hood, and punched of an appropriate size, immersed into 70% EtOH for 30 minutes, and washed for 1 hour in endotoxin free water (LAL reagent water, Lonza, Walkersville, MD) changing water every 15 min. All scaffolds were UV-sterilized for 30 min per surface of top and bottom in the tissue culture hood prior to use in DC cultures. Endotoxin contents of biomaterial scaffolds were determined using a chromogenic Limulus Amebocyte Lysate assay (QCL-1000 Chromogenic LAL Endpoint Assay, Cambrex,

Walkersville, MD). Endotoxin assays were performed on a smaller piece of scaffold (1.5 mm in thickness and 4.5 mm in diameter), which had undergone the same washing and sterilization procedures as scaffolds used to treat DCs. The scaffold pieces were suspended in endotoxin-free water and endotoxin assay performed. Standards in tissue culture treated polystyrene wells and sample wells of different biomaterials were treated with endotoxin-free water. Limulus amebocyte lysate was added in the presence of biomaterial and incubated for 10 min at 37˚C. Chromogenic substrate (Ac-Ile-Glu-Ala-Arg-pNA) was added to each well and incubated for 6 min. Glacial acetic acid (25% v/v) (J.T. Baker) was added as a stop solution and the mixture was transferred into flat-bottom microplate and the absorbance was measured at 405 nm. Endotoxin content in the samples was read off standards generated from endotoxin standards, from the manufacturer's kit. Each sample was run in triplicate for quantification. The effective endotoxin content (EU/ml) of 1.5 mm-thickness and 4.5 mm-diameter scaffold of PLGA was 0.036±0.015 and of agarose was 0.134±0.019. Previous study has shown that minimum E. Coli endotoxin concentration of 100 EU/ml was required for DC maturation (Jotwani et al., 2003).

Dendritic cell culture

Peripheral human blood was collected from donors with informed consent using heparin (333 U/ml blood) (Baxter Healthcare Corporation, Deerfield, IL) as the anticoagulant. This procedure was performed at the Student Health Center Phlebotomy laboratory, in accordance with the protocol (#H05012) of Institutional Review Board (IRB) of Georgia Institute of Technology. Dendritic cells were derived from human peripheral blood mononuclear cells (PBMCs) using a previously described method with some modifications (Romani et al., 1996). Briefly, after the blood collected from the donor, PBMCs were isolated by differential centrifugation using the lymphocyte separation medium (Cellgro). The PBMCs were collected

and washed in phosphate buffer saline (PBS), and red blood cells were lysed with buffer [155 mM NH_4Cl, 10 mM $KHCO_3$ (both from Sigma), 0.1 mM EDTA (Gibco)], and remaining cells washed again twice with PBS. Resulting PBMCs were resuspended at a concentration of 5 × 10^6 cells/ml in the DC media, which was prepared by filter-sterilizing RPMI-1640 containing 25mM HEPES [4-(2-hydroxyethyl)piperazine-1-ethanesulfonic acid)] and L-glutamine (Gibco, Grand Island, NY), supplemented with 10% (v/v) heat inactivated fetal bovine serum (FBS, Cellgro MediaTech) and 100U/mL Penicillin/Streptomycin (Cellgro MediaTech). Cells were plated in a volume of 10ml/plate in a 100 × 20 mm tissue culture plate (Primaria, Falcon) and incubated for 2 hours in the incubator with 95% relative humidity and 5% CO_2 at 37˚C to select for adherent monocytes. After the incubation, plates were washed at least three times using warm, fresh DC media to remove non-adherent cells. The adherent cells were supplied with 10 mL of fresh, pre-warmed DC media supplemented with granulocyte macrophage colony-stimulating factor (GM-CSF) (1000 U/ mL) and interleukin-4 (IL-4) (800 U/ mL) (both from Peprotech, Rocky Hill, NJ) for 5 days. On day 5 of culture, loosely adherent and non-adherent cells containing iDCs were harvested by centrifugation for 10 min at 1100 rpm and plated at 1.5 x 10^6 cells/well in 3 mL/well in DC media supplemented with GM-CSF and IL-4 into 6-well tissue culture plate for various treatments. For DC treatment with biomaterial scaffolds, PLGA or agarose scaffolds were placed into wells of 6-well plate with sterilized gaskets (Cole-Parmer) to secure the scaffolds and the iDC suspension was applied into each well. Wells for the negative control of iDC remained untreated while wells for the positive control of mature DC (mDC) involved addition of 1 μg/ml of lipopolysaccharide (LPS) (E. coli 055:B5; Sigma). For each experiment, all scaffolds and controls were included as treatments to allow for comparisons between treatments and controls. DCs were treated with biomaterial scaffolds in an atmosphere of 95% relative humidity and 5% CO_2 at 37˚C for 24 hours and then, cells or media were

analyzed as described below. Based on the justification made in the Chapter 4, all assessments of cells in this study, except morphologies by confocal microscopy, have been performed using non-/loosely-adherent cells for DCs for iDCs, mDCs, or DCs treated with different biomaterial scaffolds.

After 24 hours of DC culture on biomaterial scaffolds or controls, non-/loosely-adherent DC fraction was gently collected using a pipette and then, adherent DC fraction was removed from the culture dishes of controls or biomaterial scaffolds using the pre-warmed cell dissociation solution (CDS) (Sigma). As a result of cell counting by size, the control of iDC or mDC showed 80 ± 12% or 72 ± 12% of non-/loosely adherent DC population in total DCs (sum of those two fractions) present in the cell culture wells, respectively. The treatments with PLGA or agarose scaffold resulted in 29 ± 13% or 65 ± 11% of that, respectively.

Cell surface marker expression

The levels of surface marker expression were monitored after 24 hours of treatment with biomaterial scaffolds, by flow cytometry as per methods described in the literature (Yoshida and Babensee, 2004) and compared to controls. Non-/loosely-adherent cells containing DCs for iDCs, mDCs, or DCs treated with different biomaterial scaffolds were collected by centrifugation at 1100 rpm for 10 min and suspended in Hank's HEPES buffer (120 mM NaCl, 10 mM KCl, 10 mM $MgCl_2$, 10 mM glucose, 30 mM HEPES) (all from Sigma) containing 1% (v/v) human serum albumin (HSA) (Calbiochem, Darmstadt, Germany) and 1.5 mM $CaCl_2$ (Sigma). Cells were stained with saturating concentrations of fluorescently conjugated mouse anti-human monocloncal antibodies against CD 40 (clone B-B20; IgG1κ), CD80 (clone BB1; IgMκ), CD86 (clone BU63; IgG1κ) (all from Southern Biotechnology Associates, Birmingham, AL), CD83 (clone HB15a; IgG2b) (IO Test Immunotech, Marseille, France), HLA-DQ (clone TU169;

IgG2aκ), HLA-DR (clone TU36; IgG2aκ), CD44 (clone 515; IgG1κ), or Annexin V (recombinant purified protein) (all from BD Pharmingen) for 1 hour at 4˚C in the dark, filtered using 40 μm cell strainer (Becton Dickinson, Franklin Lake, NJ) and then, analyzed immediately with 5,000 events per sample using a BDLSR flow cytometer (Becton Dickinson). Only propidium iodide (PI) (fluorescent vital dye) (BD Pharmingen) was applied into the sample tube less than a minute before scanning in the flow cytometer. Data was obtained together with the negative control of autofluorescence per sample and then, analyzed using FLOWJO version 7.2.5 (Tree Star, Inc. Ashland, OR).

Mixed lymphocyte reaction (MLR)

Allostimulatory capacity of DCs to induce T cell proliferation upon DC treatment with different biomaterial scaffolds was assessed as per methods in the literature (Yoshida and Babensee, 2004), using an allogeneic mixed lymphocyte reaction (MLR). After 24 hours of DC treatment with biomaterial films, allogenic T cells were isolated from PBMCs by negative selection using Pan T-cell magnetic isolation (Miltenyi Biotech, Auburn, CA) according to the manufacturer's protocols. These cells were used as responder cells. The T cells were resuspended in RPMI-1640 with 25 mM HEPES and L-glutamine (Gibco BRL, Carlsbad, CA) with 100 U/ml penicillin/streptomycin (Cellgro) and heat-inactivated filter-sterilized (0.22 μm) 10% (v/v) human AB serum (Biowhittaker, Walkersville, MD)(complete RPMI-10 media) and plated at a concentration of 10^5 cells/well in a 96-well flat-bottomed plate (Corning) in triplicate per treatment groups or controls. Dendritic cells treated with biomaterial scaffolds or controls were resuspended at 1.6×10^5 cells/ml, and treated with 25 μg/ml mitomycin C (Sigma) for 30 min to prevent their proliferation. Upon extensive washing with complete RPMI-10 media, DCs were resuspended in complete RPMI-10 media and added to responder cells in triplicate at graded

DC:T cell ratios. Cells were co-cultured for 4 days at 37 °C, with the addition of 10 μM 5-bromo-2-deoxyuridine (BrdU) for the last 24 hours of culture. Dendritic cell-induced T-cell proliferation was measured using BrdU colorimetric cell proliferation ELISA (Roche Applied Science, Indianapolis, IN) according to the manufacturer's directions.

Cytokine and chemokine release

The amount of pro-inflammatory cytokine, interleukin-6 (IL-6) produced by DCs in the cell culture supernatant after the treatments with biomaterial scaffolds, normalized to DNA amount present in the cell culture supernatants were analyzed by ELISAs (R&D systems) according to manufacturer's directions. In addition, the amount of pro-inflammatory cytokines [tumor necrosis factor-α (TNF-α), IL-1β, IL-15, IL-18], chemokines [growth-regulated oncogene-α (GRO-α), macrophage inflammatory protein-1α (MIP-1α), monocyte chemotactic protein-1 (MCP-1), IL-8], and anti-inflammatory cytokines [IL-1 receptor antagonist (IL-1ra), IL-10, IL-16] produced by DCs in the cell culture supernatant after the treatments with biomaterial scaffolds, normalized to DNA amount present in the cell culture supernatants were analyzed by Bio-Plex sets for human cytokine assays (Bio-Rad, Hercules, CA) according to manufacturer's directions.

After 24 hours of DC treatment with biomaterial scaffolds or controls, non-/loosely-adherent DC fraction and cell culture supernatants were collected together and then, cleared by centrifugation for 10 minutes at 1,100 rpm. These cleared supernatants were stored at -20˚C until analysis. Non-/loosely-adherent DC fraction was gently collected using a pipette after centrifuge described above and then, adherent DC fraction was removed from the culture dishes of controls or biomaterial scaffolds using the pre-warmed cell dissociation solution (CDS) (Sigma). These non-/loosely-adherent DC and adherent DC fractions were combined together

per control or treatment and then, DNA quantification was analyzed for whole cell population per each control or treatment group using picoGreen dsDNA quantification kit (Invitrogen) per manufacturer's directions. Amounts of cytokines or chemokines were presented normalized against total DNA amounts for each treatment group.

Morphologies of cell or scaffold by confocal microscope or scanning electron microscope (SEM)

Dendritic cell morphology and distribution into the porous structures of scaffolds were examined using Zeiss LSM/NLO 510 Confocal/Multi-Photon Microscope (Zeiss) after cells were stained with Calcein AM (Sigma). On day 6, after 24 hour-treatment with biomaterial scaffolds, cell culture media in the well of treatment with scaffolds were aspirated without disturbing cells contacting with scaffolds and then, cells were stained with Calcein AM (1 μM) added into wells having cells/scaffolds for 1 hour at room temperature in the dark. To obtain morphologies of control DCs, non-/loosely-adherent fraction of iDCs or mDCs resuspended in PBS were also stained with Calcein AM. Upon 1 hour-incubation at room temperature for staining, 6-well plates having control cells or cells/scaffolds immersed in Calcein AM solution were examined using confocal microscopy wherein cell morphologies at horizontal layers along depth of scaffolds or distribution in a cross-sectional view were examined after samples were placed on a circular slide glass with a holder. For imaging the porous structure of scaffolds without cells, agarose scaffold was cut using a razor and then, the cross-section was observed by auto-fluorescence of agarose hydrogel using the same confocal microscope above, whereas, after frozen in liquid nitrogen, PLGA scaffold was fractured and then, the gold-sputtered cross-section was observed using SEM (S-800, Hitachi, Japan) at 10 kV electron beam radiation.

Statistical analysis

For statistical analysis, one sided Student t-test was used to compare mDCs or each sample group to iDCs (negative control) in pairs. To observe significant differences between mDCs and all sample groups in pairs, the general liner model of two-way ANOVA in pairwise was used for a mixed model with repeated measure. For all statistical methods, the Minitab software (Version 14, State College, PA) was used. If not indicated, p-value less than or equal to 0.05 was considered to be significant.

RESULTS:

Porous structure of agarose scaffold was well patterned while that of PLGA was irregular.

Morphology of scaffolds used in the study was examined using confocal microscope for agarose or SEM for PLGA scaffold (Figure 5-1). Agarose scaffolds showed well-patterned pores combined with interconnected pores that are seen as small black circles inside each of bigger pores consistent with the benefits of the crystal templating technique (Figure 5-1b). As expected, the bigger pores of agarose scaffold have approximately 100 μm of diameter almost same as the size of leachable component (polystyrene beads). However, PLGA scaffold showed an irregular and non-homogeneous pore structure (Figure 5-1a). Also, pore sizes of PLGA scaffold vary as much as leachable component (NaCl) sizes range from 90 to 125 μm.

(a) **(b)**

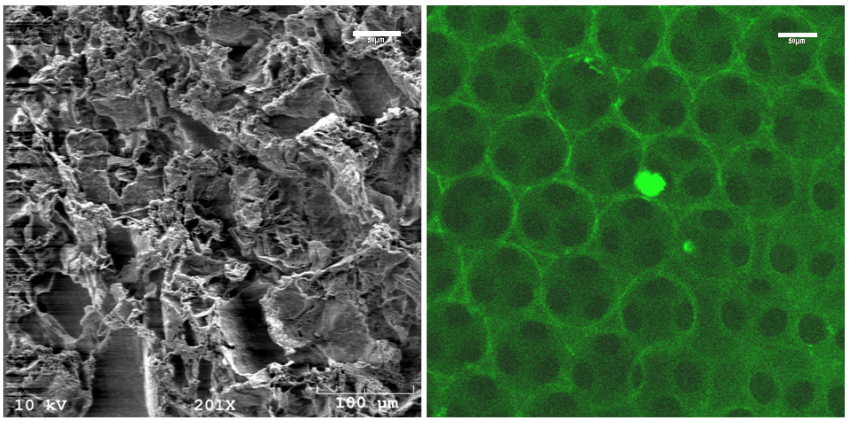

Figure 5-1: PLGA and agarose scaffolds exhibited different morphologies of cross-section. While PLGA showed irregular and non-homogeneous pore structure (a), agarose scaffold showed well-patterned pores combined with interconnected pores that are seen as small black circles inside each of bigger pores (b). All pictures show the cross-section of scaffolds used in this study and the PLGA scaffold was observed using SEM (a) while the agarose scaffold was observed using a multiphoton confocal microscope (autofluorescence) (b). White scale bars in all images indicate 50 μm.

DC treatment with PLGA scaffolds induced activated DC morphologies on the surface or in the porous structure of scaffold however, better distribution of DCs into the 3-D porous structure was obtained for the agarose scaffold.

Dendritic cells were treated with different biomaterial scaffolds in 3-D porous form and their morphologies were compared with iDCs and mDCs as visualized by the cytoplasmic cell viability stain, Calcein (upon intracellular enzymatic cleavage of Calcein AM) and confocal microscopy (Figure 5-2). The DC/scaffold construct was incubated with Calcein AM solution after aspirating DC media in each well of the well plate without disturbing the DC/scaffold construct. Both scaffolds showed most concentrated live cell population at the top surface, on which cells were cultured for one day, and density of live cells decreased along the depth toward the bottom of scaffold (Figure 5-2a and 5-2b). However, DCs were unexpectedly not distributed very well into PLGA scaffold along the depth, whereas DCs were well distributed into the depth of agarose scaffolds. Morphologies of live cells in contact with scaffolds were also examined for cells on the top surface or at the depth of 100±10 μm from the top surface of scaffolds (Figure 5-2e, 5-2f, 5-2g, 5-2h). For each biomaterial scaffold, cells exhibited very similar morphologies both on the top surface and at 100±10 μm depth. DC treatment with PLGA scaffolds induced activated DC morphologies with extensive dendritic processes (Figure 5-2e and 5-2g) similar to mDCs (Figure 5-2d), whereas DC treatment with agarose scaffolds resulted in

rounded morphologies (Figure 5-2f and 5-2h) similar to iDCs (Figure 5-2c).

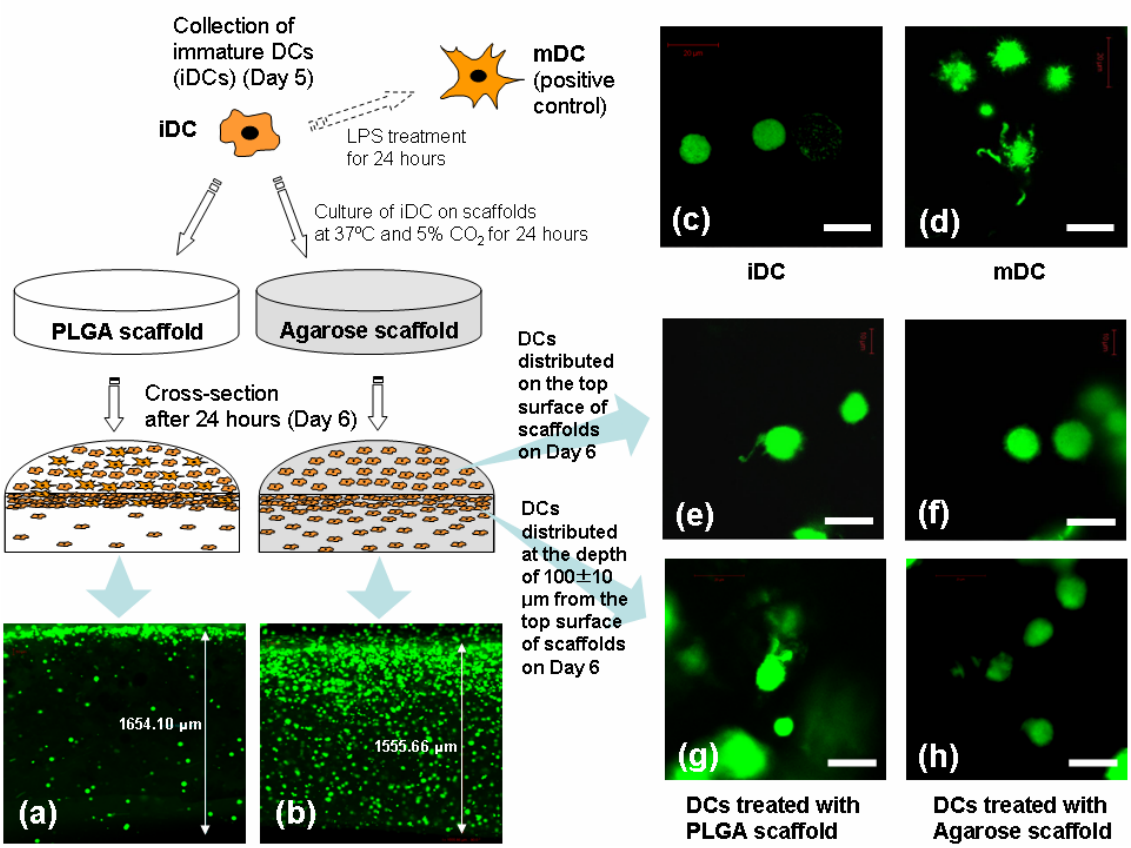

Figure 5-2: Schematic representations (view of top surface and cross-section of scaffolds) of cell distributions into 3-D porous scaffolds and cell morphologies of control DCs or upon DC treatment with scaffolds.

Morphologies of live cells contacting on the top surface or at the depth of 100±10 μm from the top surface of scaffolds exhibited differential morphologies upon DCs treated with different biomaterial 3-D scaffolds. Similarly to the results obtained from DCs treated with 2-D biomaterial films in the Chapter 4, DCs treated with PLGA scaffolds induced activated DC morphology with extensive dendritic processes, whereas DC treatment with agarose scaffolds resulted in rounded morphology similar to iDCs. Unexpectedly, DCs were not distributed very well into PLGA scaffold along the depth, whereas DCs were well distributed into the depth of agarose scaffold. All confocal images were obtained on Day 6 (after 24 hour-treatment of DCs with biomaterial scaffolds). (a) & (b) depth distribution of cells (cross-sectional view of scaffolds) in PLGA & agarose scaffolds, respectively; double-sided arrow indicates an entire thickness of each scaffold observed in cross-section (5x). (c) iDCs & (d) mDCs suspended in PBS on glass slides (100x; white scale bars indicate 20 μm). (e) & (f) DCs distributed on the top

surface of PLGA & agarose scaffolds, respectively (100x; white scale bars indicate 20 μm). (g) & (h) DCs distributed at the depth of 100±10 μm from the top surface of PLGA & agarose scaffolds, respectively (100x; white scale bars indicate 20 μm).

Dendritic cells treated with PLGA scaffold express higher levels of co-stimulatory, MHC class II molecules, and CD44 than iDCs, whereas DCs treated with agarose scaffold express similar level with iDCs

To measure DC maturation upon 24 hour-treatment with different biomaterial scaffolds, DCs treated with scaffolds were analyzed by flow cytometry for their surface expression of co-stimulatory and MHC class II molecules. As shown in Figure 5-3, DCs treated with PLGA scaffold resulted in higher expression levels of CD40, CD80, and CD86, compared to iDCs, similar to mDCs. In addition, only DC treatment with PGLA scaffolds induced HLA-DR expression at higher levels compare to iDCs while mDCs or DCs treated with agarose scaffolds expressed this surface molecule at levels similar to iDCs. Dendritic cells treated with agarose scaffolds expressed all surface molecules examined in levels similar to iDCs except for CD40 which resulted in significantly lower levels of expression than iDCs. Interestingly, these patterns of molecule expressions on DCs treated with PLGA or agarose scaffolds are very similar to those of DCs treated with PLGA or agarose films, respectively, in the Chapter 4.

In addition, to further examine functional DC phenotype changes upon DC treatment with different biomaterial scaffolds, expression of the DC receptor, CD44, which is associated with migration of DCs, was measured using the flow cytometry. Dendritic cells treated with PLGA scaffold expressed CD44 at significantly higher levels compared to iDCs, similar to the levels for mDCs. However, differently from the significantly higher levels of CD44 expression on DCs treated with agarose in the film form as compared to iDCs shown in the Chapter 4, DCs treated with agarose here in the scaffold form, expressed CD44 levels that is not significantly

different from iDCs.

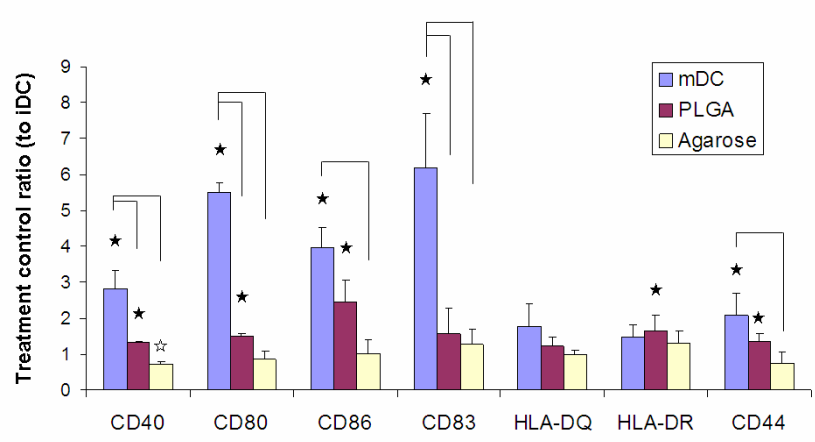

Figure 5-3: Geometric mean fluorescence intensity (gMFI) of flow cytometry analysis on co-stimulatory, MHC class II, and other functional (DC migration) molecules of CD44 on DCs treated with biomaterial scaffolds (PLGA or agarose).
Similarly to the results obtained from DCs treated with 2-D biomaterial films in the Chapter 4, PLGA scaffold induced significantly higher levels of maturation marker or CD44 expression compared to iDCs, whereas agarose scaffold induced expression levels of these markers at levels similar to iDCs. Ratios to the iDCs are shown with mean±SD, n=6 donors (6 independent experiments with different donors). ★: $p \leq 0.05$, compared to iDCs and higher than iDC; ☆: $p \leq 0.05$, compared to iDCs and lower than iDC; Brackets: $p \leq 0.05$, statistically different between two biomaterial treatments.

Dendritic cells treated with PLGA scaffold support the allostimulatory T cell proliferation

Allostimulatory capacities of DCs treated with the different biomaterial scaffolds were assessed using an MLR as compared to the controls (Figure 5-4). Mature DCs supported a high level of T cell proliferation as compared to iDCs. For all ratios of DCs:T cells, DCs treated with PLGA scaffolds supported allostimulatory T cell proliferation to a significantly higher extent than iDCs, similar to mDCs, whereas DC treated with agarose scaffolds supported T cell proliferation in levels similar to iDCs. The DC:T cell ratios of 1:6.25 or 1:12.5 induced significant difference

between DCs treated with agarose scaffold and mDCs or DCs treated with PLGA scaffold while more T cells (1:25) did not. Interestingly, the allostimulatory capacity of DCs treated with PLGA or agarose scaffolds also resulted in patterns very similar to those of DCs treated with PLGA or agarose films for different DC:T cell ratios in the Chapter 4.

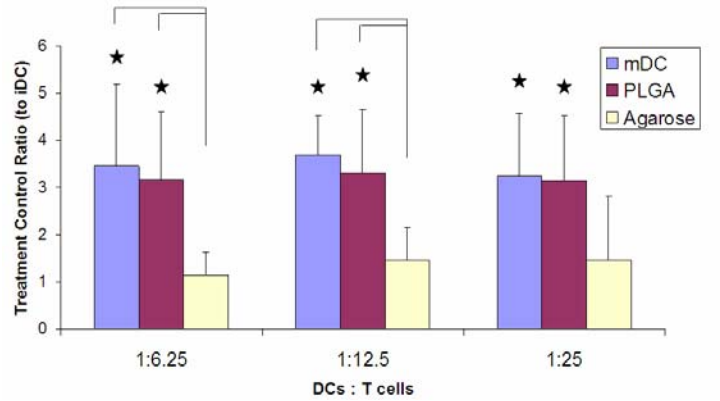

Figure 5-4: Allostimulatory capacities in Mixed Lymphocyte Reaction (MLR) in differential levels upon DCs treated with biomaterial scaffolds (PLGA or agarose).
Similarly to the results obtained from DCs treated with 2-D biomaterial films in the Chapter 4, DC treatment with PLGA scaffolds supported allogeneic T cell proliferation at levels significantly higher than iDCs, whereas treatment with agarose scaffolds resulted T cell proliferation levels similar to iDCs. Ratios to the iDCs are shown with mean±SD, n=6 donors (6 independent experiments with different donors). ★: $p \leq 0.05$, compared to iDCs and higher than iDC; ☆: $p \leq 0.05$, compared to iDCs and lower than iDC; Brackets: $p \leq 0.05$, statistically different between two biomaterial treatments.

Level of pro-inflammatory or anti-inflammatory cytokines and chemokines were modulated depending on different biomaterial scaffolds used to treat DC in vitro.

Pro-inflammatory cytokines (TNF-α, IL-1β, IL-6, IL-15, IL-18), chemokines (GRO-α, MIP-1α, MCP-1, IL-8), and anti-inflammatory cytokines (IL-1ra, IL-10, IL-16) release into the supernatant were measured using ELISA or Bio-Plex to assess *in vitro* effect of biomaterial 3-D porous scaffolds on DC phenotype. Most pro-inflammatory cytokines (TNF-α, IL-1β, IL-6, IL-

18) were released in significantly higher levels by DCs treated with PLGA scaffolds compared to treatment with agarose scaffolds (Figure 5-5a). However, one anomaly was the release of the pro-inflammatory cytokine, IL-15, which was released at significantly higher levels for DCs treated with agarose scaffolds as compared to treatment with PLGA scaffolds. Dendritic cells treated with PLGA scaffold secreted chemokines of GRO-α, MIP-1α, and IL-8 at levels significantly higher than for DCs treated with agarose scaffolds (Figure 5-5b). Again, there was one anomaly wherein MCP-1 was released at significantly higher levels for DCs treated with agarose scaffolds as compared to treatment with PLGA scaffolds. As far as release of anti-inflammatory cytokines, DCs treated with agarose scaffolds secreted significantly higher levels of IL-1ra and IL-16 as compared to mDC or DCs treated with PLGA scaffolds (Figure 5-5c). However for the release of the anti-inflammatory cytokine, IL-10, its release was greater for mDCs or DCs treated PLGA scaffolds as compared to the levels for DCs treated with agarose scaffolds (Figure 5-5c).

(a)

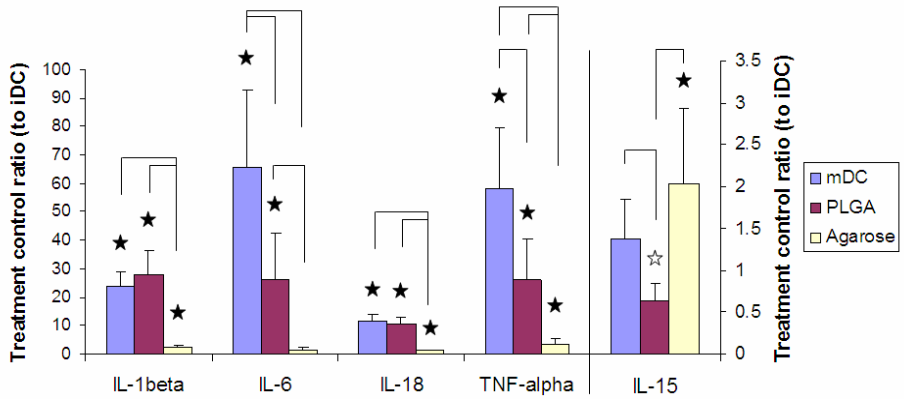

(b)

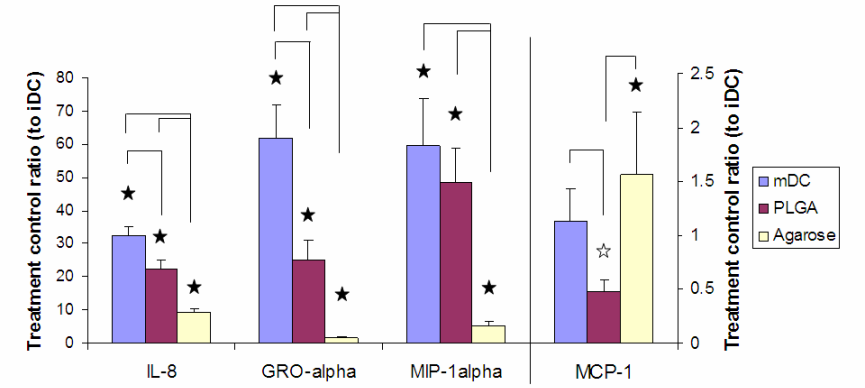

(c)

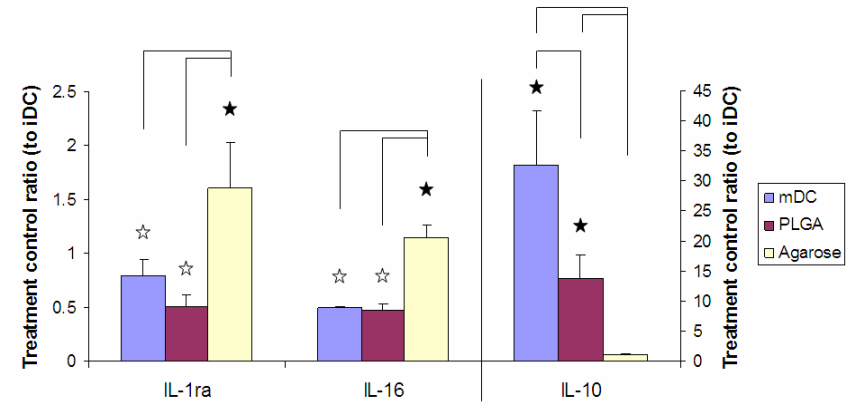

Figure 5-5: Differential levels of pro-inflammatory cytokine (a), chemokine (b), & anti-inflammatory cytokine (c) release upon DC treatment with biomaterial scaffolds (PLGA or agarose).

Release of cytokines or chemokines tested in this study was differentially modulated depending on the type of scaffold used to treat DCs. Most pro-inflammatory cytokines (TNF-α, IL-1β, IL-6, IL-18) were released at significantly higher levels by DCs treated with PLGA scaffold as compared to DCs treated with agarose scaffolds. Most anti-inflammatory cytokines (IL-1ra, IL-16) were released at significantly higher levels by DCs treated with agarose scaffolds as compared to DCs treated with PLGA scaffolds. There were a couple of anomalies however. Cytokines or chemokines from each treatment group for each donor was normalized to DNA amount and then, ratios to the iDCs are shown with mean±SD, n=6 donors (6 independent experiments with different donors). ★: $p \leq 0.05$, compared to iDCs and higher than iDC; ☆: $p \leq$

0.05, compared to iDCs and lower than iDC; Brackets: $p \leq 0.05$, statistically different between two biomaterial treatments.

DISCUSSION:

The purpose of this research was to assess the differential effects of DC treatment with 3-D porous biomaterial scaffolds prepared from different biomaterials on resultant DC phenotype. Similar to the results observed in the Chapter 4 using different 2-D biomaterial films, DC phenotypes were differentially modulated by treatment with PLGA or agarose scaffolds in porous 3-D form as shown in Figure 5-6. For instance, PLGA scaffold induced DC maturation at significantly higher levels of phenotypical changes of DCs in most assessments, as compared to iDCs, while DCs treated with agarose scaffolds demonstrated similar phenotypes to iDCs as shown in Figure 5-2, 5-3, and 5-4.

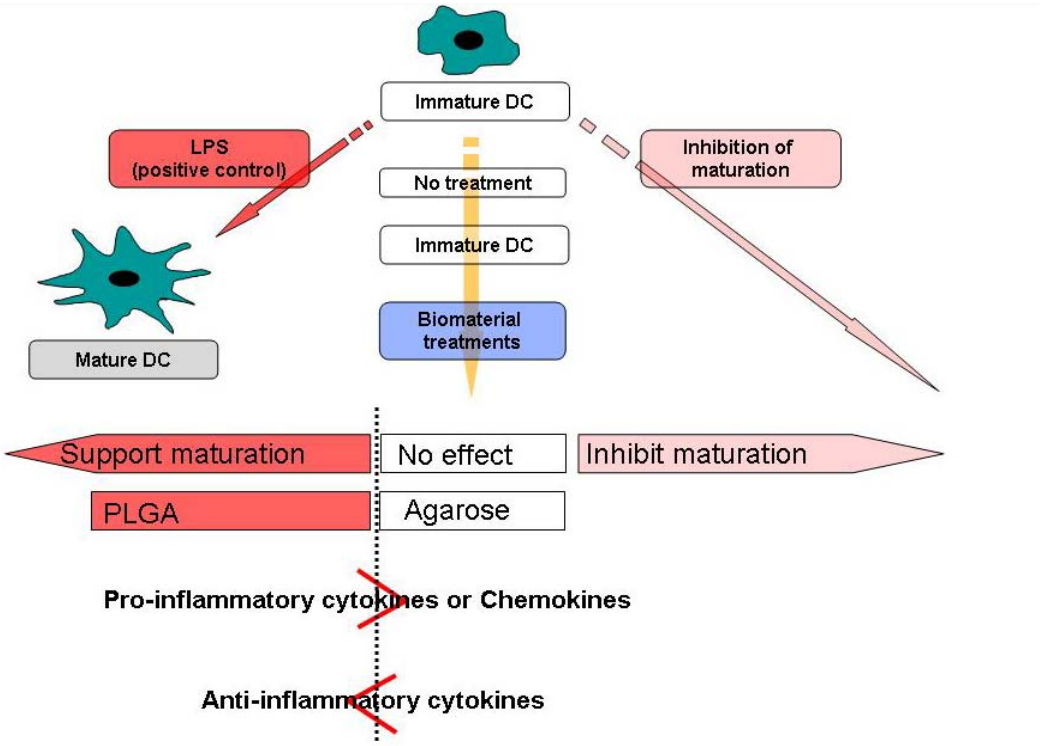

Figure 5-6: Schematic representation of effects of biomaterials in 3-dimensional scaffold forms on human monocyte-derived DCs.

Morphologies of live cells contacting with biomaterial scaffolds have been examined along the depth from the top surface using multiphoton confocal microscope as shown in Figure 5-2. Due to transparency of agarose scaffolds, live cells could be observed within these scaffolds to a depth of approximately 700 μm from the top surface (data not shown for depth deeper than 100 μm from the top surface), whereas opaque PLGA scaffolds resulted in 100±10 μm depth as the deepest level possible for imaging live cells from the top surface. At various depths at which observations were made (at increments of 100 μm-depth) even to a depth of approximately 700 μm from the top surface of agarose scaffolds, DCs exhibited a morphology similar to iDCs suspended in PBS, as observed using confocal imaging (Figure 5-2c, 5-2f, and 5-2h). DCs on the top surface or within depths of 100±10 μm within PLGA scaffolds exhibited a morphology similar to mDCs with dendritic processes (Figure 5-2d, 5-2e, and 5-2g).

CD44 has been well known as a potent receptor expressed on DCs to mediate DC clustering, migration, and maturation upon interaction with the hyaluronan components in the ECM (Weiss et al., 1997; Termeer et al., 2001). In accordance with the previous result of CD44 expression on DCs treated with PLGA or agarose films in the Chapter 4, DC treatment with PLGA scaffolds induced significantly higher expression of CD44 as compared to iDCs, whereas treatment of DCs with agarose scaffolds resulted in expression levels similar to iDCs (Figure 5-3). These results indicate that, during 24 hour-treatment of DCs with these scaffolds, protein adsorption on these biomaterial scaffolds and consequent adhesion of cells to those adsorbed protein may be induced in higher levels for PLGA scaffolds (hydrophobic surface) compared to agarose scaffolds (hydrophilic surface) or the negative control of iDC. However, PLGA scaffold unexpectedly exhibited poor distribution of live cells at the cross-section along the depth as shown in Figure 5-2a; most cells observed in the cross-section of PLGA scaffold were concentrated at the top surface, where they were placed for treatment on Day 5. As seen in

Figure 5-1, condition of porous structures likely plays a significant role in the resultant cell distribution into the scaffolds. PLGA scaffolds used in this study were prepared using the conventional method of salt-polymer casting particular-leaching technique with NaCl at the leachable component (Mikos et al., 1994). This method has been widely accepted for its very straightforward and simple technique but, due to discontinuous porogen particles irregular or non-homogeneous pore structure has been observed necessitating development of modifications to the method to improve pore interconnectivity (Thomson et al., 1995; Hou et al., 2003; Murphy et al., 2002; Lee et al., 2004; Reignier and Huneault, 2006). Even though, more effective migration of DCs would have been expected into PLGA scaffolds based on their respective higher expression of CD44 (Figure 5-3), this was not observed, likely due to the non-homogeneity and poor interconnectivity of pores in these scaffolds as well as a role for CD44 of supporting cell-cell interaction during cell clustering. In contrast, DCs were able to penetrate deep within the porous agarose scaffolds (Figure 5-2b) likely due to the well-patterned, -interconnected pores of these scaffolds (Stachowiak and Irvine, 2008; Lee et al., 2006). Auto-fluorescence image of agarose scaffold showed very consistent diameter size (20 ~ 30 μm) of interconnected channels between pores. Taking into account that size of DCs in this study ranged 10~20 μm (by the coulter counter), the size of interconnected channels in agarose scaffolds should be big enough for DC's moving through it without hindrance. Hence, DC penetration into these agarose scaffolds was effective in spite of a low level of expression of an important migration receptor, CD44, on these DCs. Another factor which appears to have influenced DC migration into the scaffolds is the hydrophilic nature of agarose increasing internal wettability of the scaffold, facilitating cell migration in response to chemoattractants (Stachowiak and Irvine, 2008) and cell viability due to preferential cell-cell interactions rather than cell-scaffold interactions (Glicklis et al., 2000). In addition, it should be further examined how these distribution of live cells correlate with

apoptosis or necrosis of cells, upon treatment with different biomaterial scaffold.

As same as the study in the Chapter 4, wherein 2-D biomaterial films were used to treat DCs, non-/loosely-adherent cell fraction from each well of DC treatment with biomaterial scaffold was used for examination of phenotypical changes. As mentioned earlier in the method section, DC treatment with biomaterial scaffold of PLGA or agarose showed 29 ± 13% or 65 ± 11% of non-/loosely adherent DC population in the total DCs (including adherent cells) present in the cell culture wells, respectively. Compared to this fraction from 2-D biomaterial films, which showed 37 ± 15% or 86 ± 9% for PLGA or agarose film, respectively, in the Chapter 4, the percentage of non-/loosely adherent DCs was lower for cells recovered from scaffolds, likely, due to the inability to recover those cells which had penetrated into the porous scaffolds. However, even though agarose scaffold showed better distribution of cells into 3-D porous structure compared to PLGA scaffold, more than 60% of the cells in the culture well were non-/loosely-adherent. Moreover, as shown in Figure 5-2, 5-3, and 5-4, this non-/loosely-adherent fraction for PLGA or agarose scaffold also showed phenotypical changes very similar to those obtained for DCs treated with PLGA or agarose in 2-D film form in the Chapter 4. This result suggests that porous agarose scaffolds would induce less of a host response even for situations of high surface area of a porous scaffold.

Cytokines and chemokines examined herein include pro-inflammatory cytokines, chemokines, and anti-inflammatory cytokines as shown in Figure 5-5, which have been extensively studied for their roles in directing immune responses (Asquith and McInnes, 2007; Klimiuk et al., 1999; Cho et al., 2008; McInnes and Liew, 2005; Thomas et al., 1999; Lebre et al., 2008; Rudolph and Woods, 2005; Baslund et al., 2005).

In the Chapter 4, DCs treated with PLGA film resulted in higher levels of TNF-α and IL-6 releases compared to iDCs while DCs treated with agarose films did so at levels similar to iDCs.

Hence, it would be expected that treatment of DCs with PLGA scaffolds would induce release of pro-inflammatory cytokines at levels higher than for iDCs. Furthermore, it would be expected that treatment of DCs with agarose scaffolds would induce release of pro-inflammatory cytokines at levels similar to iDCs or induce release of anti-inflammatory cytokines at higher or similar levels compared to iDCs. In general, this was the situation observed except for a few anomalies such as the high level of pro-inflammatory IL-15 and MCP-1 released upon agarose scaffold treatment of DCs and high level of the anti-inflammatory IL-10 release upon PLGA scaffold treatment of DCs.

Interestingly, results of IL-15 and IL-10 are possibly correlated with the results obtained from the study in the Chapter 6 wherein autologous T cells were co-cultured with DCs treated with different biomaterial films in the absence or presence of a model antigen, ovalbumin (OVA), and then, T cell marker expressions and cytokine releases were assessed. As will be seen in Chapter 6, the T helper type I (Th1) cytokine, IL-12p70, was released from DCs at levels higher than iDCs when DCs were treated with PLGA film in the absence of OVA antigen, whereas this cytokine was released at levels similar to iDCs when DCs were treated with agarose film in the absence of OVA antigen. However, when DCs were treated with biomaterial films and (in the presence of) OVA antigen, PLGA film induced this cytokine at levels similar to iDCs, whereas agarose film treatment induced levels of release higher than iDCs. In addition, when these DCs were treated with agarose and OVA antigen and then, co-cultured with autologous T cells, this cytokine was released from DC-T co-culture wells at levels higher than most other biomaterial films including PLGA film. Avice et al. have found that IL-15 activates monocytes to release IL-12 and induces T cell activation by synergizing with IL-12 (Avice et al., 1998). This proposed co-dependence between IL-12 and IL-15 may explain, at least in part, why DC treatment with agarose scaffolds induced expression of only IL-15, of pro-inflammatory cytokine

group, at levels higher than for iDCs, or DCs treated with PLGA scaffolds.

Again, in the Chapter 6 for co-culture of autologous T cells with DCs treated with different biomaterial films, the positive control of mDCs or DCs treated with chitosan film (independently from the presence of antigen OVA) released T helper type II (Th2) cytokine of IL-10 in levels higher than iDCs, whereas DCs treated with agarose film and OVA antigen did at levels lower than or similar to those for iDCs. However, once these DCs, treated with agarose film (independent of the presence of OVA antigen) were co-cultured with autologous T cells, this cytokine was released from DC-T co-culture wells at levels higher than for most other biomaterial film treatments of DCs including PLGA film treatment. In the study presented herein, there was no model antigen or T cells involved and IL-10 was released from mDCs or DCs treated with PLGA scaffold at levels higher than for iDCs, whereas DCs treated with agarose scaffold released this cytokine at levels similar to that of iDCs. However, the actual circumstance of disease such as RA has antigens and autologous T cells together with antigen presenting cells (APCs) such as DCs. Thus, it may be expected that agarose scaffold would induce IL-10 release in the disease circumstance wherein a certain antigen is involved. This indicates, considering additional anti-inflammatory cytokines of IL-1ra and IL-16 induced by agarose scaffold (Fig. 5-5c), that effects of agarose scaffold on suppression of inflammatory or immune response might be maximized in an actual disease circumstance.

Dendritic cell follows a similar linage (derived from the monocyte) as macrophage and both cell types have been known to up-regulate similar sets of genes in response to pathogens since they share similarity of more than 96% of their basal gene expression (Foti et al., 2006). Different chemistries (e.g., hydrophilicity/hydrophobicity or charge) of biomaterial surfaces have been extensively studied *in vitro* or *in vivo* to understand how they affect cytokine or chemokine release from monocytes/macrophages adherent on biomaterial surfaces (Jones et al., 2007; Chang

et al., 2008; Schutte et al., 2009a; Schutte et al., 2009b). They found that different surface chemistries dictate different cytokine or chemokine release from monocyte/macrophage, possibly associated with differential conditions of protein adsorbed on biomaterials that do not have any carbohydrate composition recognizable by the pattern recognition receptors (PRRs) expressed on DCs. Both PLGA and agarose scaffold used herein also do not have carbohydrates recognizable by the PRRs on DCs but they induced DC phenotypes differentially between them. Thus, all results observed in this study should be related with, at least, the apparent differences between these biomaterials; PLGA scaffold is hydrophobic/degradable while agarose scaffold is hydrophilic/non-degradable. However, further studies are certainly needed to fully understand interactions between PLGA or agarose scaffold and immune cells including DCs, particularly focusing on use of these biomaterial scaffolds for multifunctional tools for specific immunotherapy or tissue engineering.

Acute immune response has been reported to positively affect vascularization (Kyriakides et al., 1999), thereby suggesting that controlling immune response such as pro-inflammatory cytokine release might be beneficial to tissue remodeling (Chan and Mooney, 2008; Tsiridis et al., 2007; Mountziaris and Mikos, 2008). For instance, agarose scaffold induced a marked release of MCP-1 (chemokine) at level higher than iDCs or DCs treated with PLGA scaffold in this study (Fig. 5-5b). This chemokine is well known for its critical role in angiogenesis in a certain disease or in wound healing associated with angiogenesis, resulting in enhancing the disease progress (Rudolph and Woods, 2005). In this way, controlling cytokine or chemokine release by properties of different biomaterial scaffolds may play a further role in fostering the formation of new extracellular matrix and tissue growth. In addition, from another viewpoint of immunotherapy for inducing secondary immune responses using artificial lymphoid organ, efforts have been made to develop a strategy for localization or migration of immune cells (lymphocytes

and DCs) using biocompatible scaffolds implanted closely to a target site, thereby directing adaptive immunity more effectively than remote strategies of vaccination or injection of soluble protein such as cytokines (Suematsu and Watanabe, 2004; Okamoto et al., 2007; Stachowiak and Irvine, 2008). Therefore, elucidating multifunctional effects of different biomaterial scaffolds *in vitro* or *in vivo* on changes of DC phenotypes are expected to provide a guidance to design biomaterial scaffolds in applications of immunotherapy, various tissue engineering, or a combination of immunotherapy and tissue engineering.

CHAPTER 6[†]

PHENOTYPE AND POLARIZATION OF AUTOLOGOUS T CELLS BY BIOMATERIAL-TREATED DENDRITIC CELLS

INTRODUCTION:

Biomaterials are used as scaffolds and carriers of biologics in combination products. As such, due to the innate immune response towards the biomaterial component, they have the potential to modulate the adaptive immune response towards the biological component due to a biomaterial adjuvant effect (Zhao and Leong, 1996). In the tissue engineering applications, those immune responses should be minimized or all together avoided, whereas the strategy for DNA- or protein-based vaccines aims to enhance the protective immune responses. The question arises whether biomaterials can be used to modulate, either inhibiting (inducing tolerance) or enhancing adaptive immune responses towards a biological component, by affecting T cell responses.

Dendritic cells (DCs) are the most effective professional antigen-presenting cells (APCs) that have a potential role in initiating T-cell mediated immunity (Banchereau and Steinman, 1998). Pathogenic motifs, "pathogen associated molecular patterns" (PAMPs), are recognized by DCs using the cognate binding receptors of pattern recognition receptors (PRRs) such as toll-like receptors (TLRs) on DCs (Aderem and Ulevitch, 2000). The most significant consequence of TLR ligation is an intracellular signaling cascade leading to activation of the transcription factor, nuclear factor-κB (NF-κB), which regulates genes involved in pro-inflammatory responses and maturation of DCs (Zhang and Ghosh, 2001; Medzhitov et al., 1997). Upon their maturation, DCs bridge the innate immune response with the adaptive immune response by

[†] A manuscript prepared from this Chapter 6, titles as 'Phenotype and polarization of autologous T cells by biomaterial-treated dendritic cells', is to be submitted to Journal of Immunotherapy.

stimulating T lymphocytes. In this way, the biomaterial component in a combination product can act as an adjuvant in intensifying the host immune response to an immunogenic biological component, associated with the stimulation of APCs through induction of an innate immune response, recruiting antigen presenting cells, and inducing their activation (Babensee et al., 1998; Singh and O'Hagan, 1999).

To test these hypotheses, *in vivo* adjuvant effects of the polymeric biomaterials have been extensively investigated. For instance, particulate adjuvants, including polymeric microparticles, induced or enhanced an immune response in association with APCs and antigens, creating the depot effects that prolonged an exposure of antigens (Singh and O'Hagan, 1999; Hunter, 2002; Matzelle and Babensee, 2004; Yoshida and Babensee, 2004; Bennewitz and Babensee, 2005). *In vitro* effects of biomaterials on DC maturation have also been studied using inherently different biomaterials or biomaterials in different forms and differential levels of DC maturation were observed with phenotypical changes of DCs depending on the type of biomaterials used to treat the iDCs (Chapter 4) (Yoshida and Babensee, 2004; 2006; Babensee and Paranjpe, 2005)

Upon maturation, DCs move to the secondary lymph organs to present the antigenic peptides to T cells so that the adaptive immune response is initiated (Banchereau and Steinman, 1998). Thus DC maturation is essential to T cell activation which might induce to T cell tolerance or T cell immunity (Lanzavecchia and Sallusto, 2001). Dendritic cells can control the adaptive immune response by processing and consequently presenting the exogenously introduced antigens in the context of major histocompatibility complex (MHC) molecules for activation of naïve T cells; the antigenic peptide-MHC class II compartments elicit CD4+ T cell responses while the antigenic peptide-MHC class I compartments induced by the cross-presentation elicit CD8+ T cell responses (Kalinski et al., 1999; Lanzavecchia and Sallusto, 2001). In addition, upon interaction between DCs and T cells, the resultant immunity can be polarized

toward either T helper (Th) type 1 (cellular response) or T helper (Th) type 2 (humoral response) depending on the cytokines such as interferon (IFN)-γ/interleukin (IL)-12 or IL-10/IL-4, respectively, released from DCs or T cells (Moser and Murphy, 2000; Kapsenberg, 2003). In this way, the adaptive immunity can be modulated into immunogenicity by IL-12 or IFN-γ, or tolerogenicity by IL-10 or CD4+CD25+ T cells combined with forkhead box P3+ (FoxP3+) expression, which is a transcriptional regulator and specific marker of natural T regulatory cells (Sakaguchi, 2005; Lanzavecchia and Sallusto, 2001).

Based on these facts, DCs have been extensively investigated with their effects on T cell mediated immunity for immunotherapeutic applications. Dendritic cells generated in CD40-deficiency *in vitro* released IL-10 (immunosuppressive and regulatory Th2 cytokine), but not IL-12 (Th1 cytokine) and prevented allograft rejection in the murine model (Gao et al., 1999). In an *in vitro* model, T cells specific for pancreatic carcinoma cells were generated by lysate-pulsed DCs and, upon co-culture of these DCs and T cells, the lysate-pulsed DCs induced IL-12 and IFN-γ indicating a Th1 immune response (Schnurr et al., 2001). In another instance, CD40-stimulated human DCs displayed a mature phenotypes and released IL-12 in high levels, consequently promoting a specific anti-tumor T cell response (Hunter et al., 2007). Autoantigen-pulsed DCs induced CD4+CD25+ regulatory T cells (Mahnke et al., 2003), and cytokine-treated DCs induced expansion of $FoxP3^{high}$ T regulatory cells (Banerjee et al., 2006), suggesting that immunosuppressive effects might be induced. These studies suggest impressive directions to possibly utilize the cytokine profiles and the resultant immune response elicited via T cells, combined with Th1/Th2 polarizations and CD4+, CD8+, CD25+, and/or FoxP3+ T cell responses, so that these regulated T cell responses may provide means of immunity for cancer therapy, immunosuppression in autoimmunity, or tolerance of tissue engineered grafts.

Biomaterial effects on T cell immunity through associated adjuvant effects, have been

demonstrated wherein poly(lactic-*co*-glycolic acid) (PLGA) scaffolds or microparticles, upon incorporation of a model antigen, OVA, acted as adjuvant in enhancing a predominately Th2-dependent humoral immune response (Matzelle and Babensee, 2004; Bennewitz and Babensee, 2005). We have also previously shown that PLGA microparticles with adsorbed OVA were able to elicit a delayed type hypersensitivity (DTH) reaction in mice, which is a Th1-dependent response (Yoshida and Babensee, 2004). However, in these *in vivo* studies performed, only a single type of biomaterial was tested and the disparity between inducing Th1 or Th2 polarization was not addressed due to limited number of cytokine examined to determine the nature of the Th response (polarization), as well as different forms of antigen or modes of antigen co-delivery used in the studies.

To understand the *in vitro* effects of inherently different biomaterials on DC-directed autologous T cell phenotype and polarization, DCs were treated with different biomaterial films in the presence or absence of a model antigen, OVA, and co-cultured with autologous T cells. Resultant T cell phenotype and polarization were determined by assessing T cell surface marker expression and profile of cytokines released. The biomaterials used in this study included PLGA, chitosan, alginate, hyaluronic acid (HA), and agarose that were used in the previous study (Chapter 4) for on their effects on DC maturation. In this study, differential autologous T cell phenotypes and polarization were observed as directed by differentially biomaterial-treated DCs (with associated OVA). Briefly, mature DCs (mDCs) or DCs treated with PLGA, or chitosan induced polarization to a Th1 phenotype of autologous T cells while DCs treated with alginate or agarose induced both of Th1 (IL-12p70) and Th2 (IL-10) polarizations, simultaneously. Upon DC treatment with antigen, CD4 expression levels of co-cultured T cells were modulated by biomaterial films used to treat DC, whereas CD8 expressions were not changed for all biomaterial films as compared to the untreated CD3+ T cells. Agarose film induced CD4+CD25+FoxP3+ T

cells upon DC treatment with antigen (at level similar to iDCs) as compared to the untreated CD3+ T cells, whereas the other biomaterial films induced only CD25 or CD69 expression. Therefore, we could demonstrate multifunctional effects of DCs treated with different biomaterial films on autologous T cell mediated immunity, thereby elucidating the potential T cell activation or polarization in the adaptive immune response, which can be expected when those biomaterials are introduced *in vivo* in combination products.

METHODS:

Preparation of biomaterial films

All biomaterial films were freshly prepared for each experimental procedure. Preparation methods of all biomaterial films were adapted or modified from the previously described methods. Briefly, poly(DL-lactic-*co*-glycolic acid) (PLGA) (ester terminated; molar ratio: 75:25, inherent viscosity: 0.70 dL/g in trichloromethane, 100,000 MW; Birmingham Polymers, Birmingham, AL) was dissolved in 20% w/v in dichloromethane (DCM) overnight at room temperature and poured into the Teflon dish of 50 mm diameter (Cole-Parmer) in the chemical fume hood (Mikos et al., 1994). Upon evaporation of the solvent and drying (36-48 hours), PLGA films were punched of an appropriate size, and washed for 1 hour in ddH_2O changing ddH_2O every 15 min. Chitosan (high molecular weight: 400,000 MW, degree of deacetylation: ≥ 75%, Fluka, Milwaukee, WI) was dissolved with 1% w/v chitosan in glacial acetic acid (2% v/v in ddH_2O) (Fisher Scientific) for 24 hours at room temperature and then, poured into the Teflon dish of 50 mm diameter in the chemical fume hood. Upon evaporation of the solvent and drying (36-48 hours), chitosan films were then cross-linked by immersion in 20% (v/v) sodium sulfate (Sigma) in ddH_2O (2 hours) and washed by ddH_2O (20 min), followed by immersion in 1 M NaOH (Sigma, 30 min) to neutralize the surface and washed with ddH_2O (20

min).(Lahiji et al., 2000) Chitosan films were punched of an appropriate size, and finally washed for 20 min in ddH_2O. Alginate (80,000 MW; mannuronic acid content: ≥ 50%; primarily anhydro-β-D-mannuronic acid residues with 1-4 linkage; Sigma) was dissolved to a concentration of 3% w/v alginate in ddH_2O for 24 hours at 4˚C and then, poured into the Teflon dish of 50 mm diameter in the tissue culture laminar flow hood. Upon drying (36-48 hours), alginate films were cross-linked by immersion in 5% w/v calcium chloride (Sigma) in 40% aqueous ethanol for 48 hours and washed with ddH_2O for 10 min.(Papas et al., 1999) Alginate films were punched of an appropriate size, and washed for 30 min in ddH_2O changing water every 10 min. Hyaluronic acid (800,000 MW; sodium salt from Streptococcus equi, BioChemika, Fluka) was dissolved to a concentration of 4% w/v HA in ddH_2O for 24 hours at 4˚C and then, poured into the Teflon dish of 50 mm diameter in the tissue culture laminar flow hood. Upon drying (36-48 hours), HA films were cross-linked by immersion in 50 mM water soluble carbodiimide (Sigma) in 72% aqueous ethanol for 24 hours and washed by ddH_2O for 10 min (Tomihata and Ikada, 1997). Hyaluronic acid films were punched of an appropriate size, and washed for 30 min in ddH_2O changing water every 10 min. Agarose (type V; high gelling; gel strength of ≥ 800 g/cm^2 at 1.0 %; Sigma; molecular weight is not known) was dissolved in ddH_2O to a concentration of 3% w/v by heating using a microwave until boiling and visible homogeneity was reached (Tun et al., 1996). Agarose films were prepared by dispensing 1 ml of this agarose solution into a well of a 6-well tissue culture plate (Corning), and allowed to solidify at a temperature of 4˚C for at least 30 min, and brought back to room temperature for another 30 min prior to culture with iDCs. All biomaterial films were UV-sterilized for 30 min per surface in the tissue culture hood prior to use in DC cultures. Endotoxin contents of biomaterial films were determined using a chromogenic Limulus Amebocyte Lysate assay (QCL-1000 Chromogenic LAL Endpoint Assay, Cambrex, Walkersville, MD). Endotoxin assays were

performed on a smaller piece of film (4.5 mm in diameter), which had undergone the same washing and sterilization procedures as films used to treat DCs. The smaller film pieces were suspended in endotoxin-free water and endotoxin assay performed. Standards in tissue culture treated polystyrene wells and sample wells of different biomaterials were treated with endotoxin-free water. Limulus amebocyte lysate was added in the presence of biomaterial and incubated for 10 min at 37˚C. Chromogenic substrate (Ac-Ile-Glu-Ala-Arg-pNA) was added to each well and incubated for 6 min. Glacial acetic acid (25% v/v) (J.T. Baker) was added as a stop solution and the mixture was transferred into flat-bottom microplate and the absorbance was measured at 405 nm. Endotoxin content in the samples was read off standards generated from endotoxin standards, from the manufacturer's kit. Each sample was run in triplicate for quantification. The effective endotoxin content (EU/ml) of 4.5 mm-diameter films of PLGA was 0.011±0.007, of chitosan 0.0007±0.0001, of alginate 0.035±0.006, of HA 0.004±0.003, and of agarose 0.037±0.006. Previous study has shown that minimum E. Coli endotoxin concentration of 100 EU/ml was required for DC maturation (Jotwani et al., 2003).

Dendritic cell culture

Peripheral human blood was collected from donors with informed consent using heparin (333 U/ml blood) (Baxter Healthcare Corporation, Deerfield, IL) as the anticoagulant. This procedure was performed at the Student Health Center Phlebotomy laboratory, in accordance with the protocol (#H05012) of Institutional Review Board (IRB) of Georgia Institute of Technology. Dendritic cells were derived from human peripheral blood mononuclear cells (PBMCs) using a previously described method with some modifications (Romani et al., 1996). Briefly, after the blood collected from the donor, PBMCs were isolated by differential centrifugation using the lymphocyte separation medium (Cellgro MediaTech). The PBMCs

were collected and washed in phosphate buffer saline (PBS), and red blood cells were lysed with buffer [155 mM NH_4Cl, 10 mM $KHCO_3$ (both from Sigma), 0.1 mM EDTA (Invitrogen, Carlsbad, CA)], and remaining cells washed again twice with PBS. Resulting PBMCs were resuspended at a concentration of 5×10^6 cells/ml in the DC media, which was prepared by filter-sterilizing RPMI-1640 containing 25mM HEPES [4-(2-hydroxyethyl)piperazine-1-ethanesulfonic acid)] and L-glutamine (Invitrogen), supplemented with 10% (v/v) heat inactivated fetal bovine serum (FBS, Cellgro MediaTech) and 100U/mL Penicillin/Streptomycin (Cellgro MediaTech). Cells were plated in a volume of 10ml/plate in a 100 × 20 mm tissue culture plate (Primaria, BD Falcon) and incubated for 2 hours in the incubator with 95% relative humidity and 5% CO_2 at 37˚C to select for adherent monocytes. After the incubation, plates were washed at least three times using warm, fresh DC media to remove non-adherent cells. The adherent cells were supplied with 10 mL of fresh, pre-warmed DC media supplemented with granulocyte macrophage colony-stimulating factor (GM-CSF) (1000 U/ mL) and interleukin-4 (IL-4) (800 U/ mL) (both from Peprotech, Rocky Hill, NJ) for 5 days. On Day 5 of culture, loosely adherent and non-adherent cells containing iDCs were harvested by centrifugation for 10 min at 1100 rpm and plated at 1.5 x 10^6 cells/well in 3 mL/well in DC media supplemented with GM-CSF and IL-4 into 6-well tissue culture plate for DC treatment with different biomaterial films. During this Day 5 procedure, biomaterial films were placed into wells of 6-well plate with sterilized gaskets (cut from peroxidized silicone tubing) (Cole-Parmer) to secure the films and the iDC suspension was applied into each well. Wells for the negative control of iDC remained untreated while wells for the positive control of mDC involved addition of 1 μg/ml of lipopolysaccharide (LPS) (E. coli 055:B5; Sigma). For each experiment, all biomaterial films and controls were included as treatments to allow for comparisons between treatments and to controls.

In some experiments, DCs were treated with biomaterial films as described above except

that the model antigen, ovalbumin (OVA) (Grade VII, Sigma), was added to DC media at a concentration of 150 μg/mL. Immature DCs and mDCs were also suspended in DC media containing OVA as appropriate controls. Dendritic cells were treated with biomaterial films in the presence or absence of OVA in an atmosphere of 95% relative humidity and 5% CO_2 at 37˚C for 24 hours and then, on Day 6, DCs or supernatants were collected for the co-culture with autologous T cells or cytokine analysis, respectively.

For whole duration through Day 14, on which day T cells were collected or supernatants were saved for analysis of T cell markers or cytokines, respectively, the DC treatment with different biomaterial films for 24 hours were achieved twice at different time points on Day 6 and Day 12 for 1st co-culture with T cells (initiation of co-culture) and 2nd co-culture (additional stimulation toward the identical T cells), respectively (Fig. 6-1a and 6-1b). Following the justifications described in the Chapter 4, the non-/loosely-adherent DC populations were also used for the co-culture with T cells in this study.

(a)

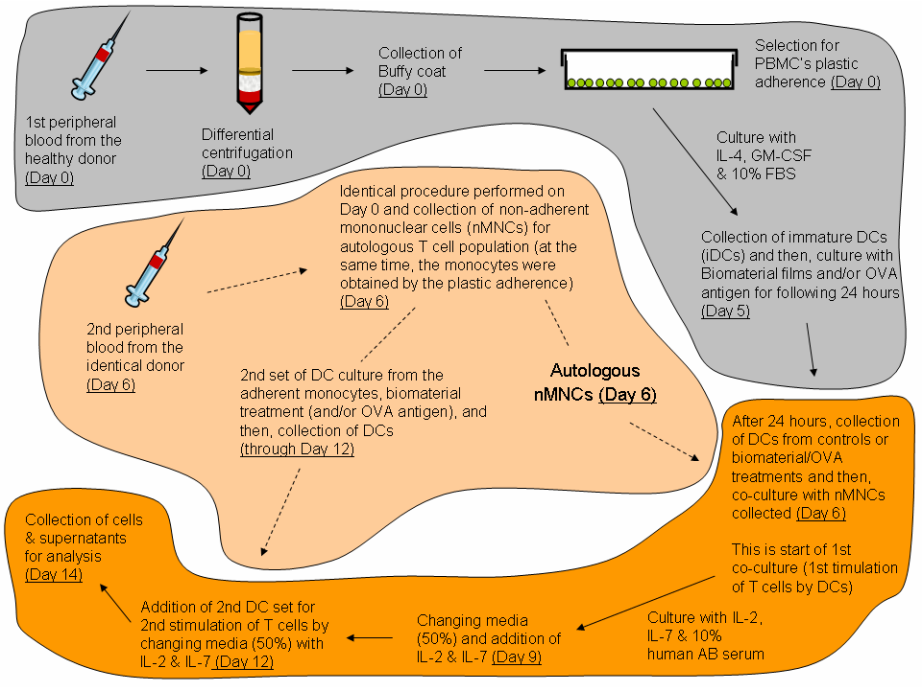

(b)

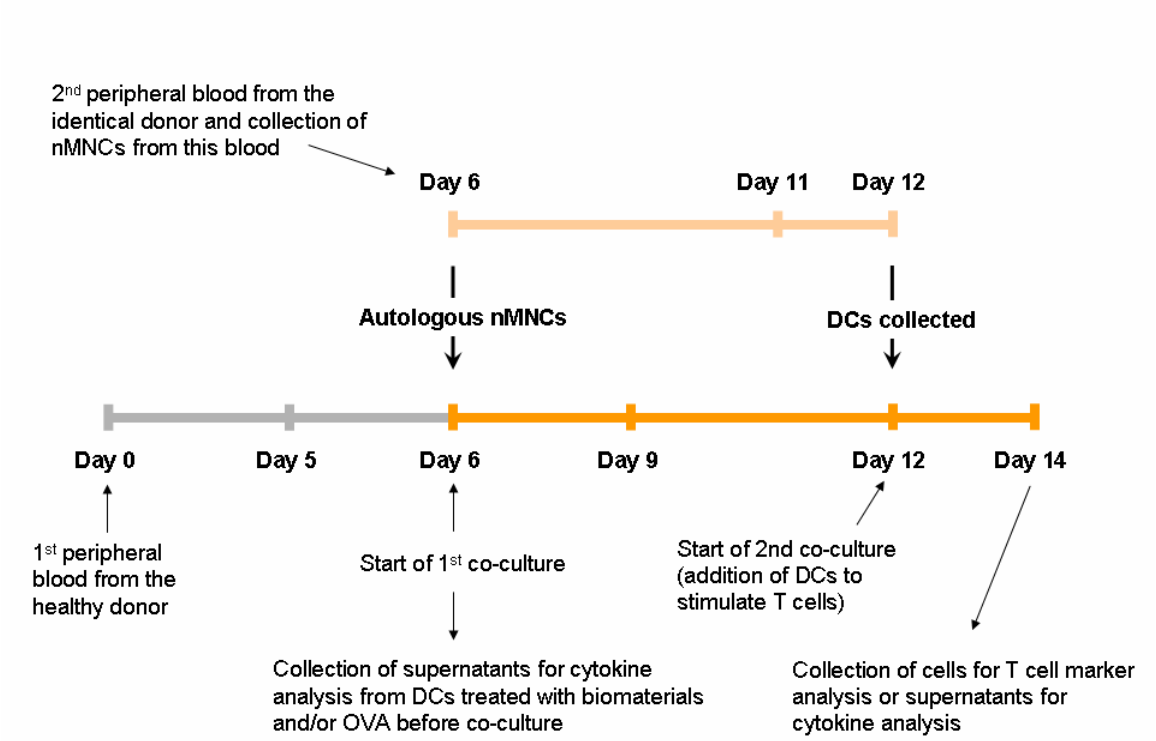

Figure 6-1: Schematic representation of the study procedure (Fig. 6-1a) & time line (Fig. 6-1b). During 14 days, the study has been performed based on three main procedures as shown by color-coded blocks.

: 1st blood collection and DC treatment with biomaterial films (with or without OVA)

: 2nd blood collection and collection of non-adherent mononuclear cells (nMNC) and DC treatment with biomaterial films (with or without OVA)

: Co-culture (DC & T) procedure

Autologous T cell preparation

A preparation method of autologous T cells was adapted with some modifications, from the previously described methods (Schnurr et al., 2001; Pockaj et al., 2004; Shilyansky et al., 2007). On the day of blood collection from the donors, PBMCs were incubated for 2 hours for selecting the adherent mononuclear cells as described above. After this 2 hour-incubation for

the plastic adherence, the adherent cells on the culture dish were used for generation of DCs as described above. At the same time, non-adherent mononuclear cells (nMNCs) collected and used for the autologous T cell population after straining nMNCs using a cell strainer with 40 μm pore size (Becton Dickinson, San Jose, CA). Purity of these strained nMNCs was confirmed by staining for CD3 using a fluorescently conjugated mouse anti-human monoclonal antibodies against CD3 (clone HIT3a; IgG2aκ) (BD Pharmingen) with 10,000 events per donor on a BDLSR flow cytometer (Becton Dickinson). For the nMNCs, the percentage of CD3+ T cells was 75±5% (n=6 different donors).

Co-culture of DCs and autologous T cells

A whole procedure of the co-culture of DCs and autologous T cells was adapted or modified from the previously described methods (Schnurr et al., 2001; Pockaj et al., 2004; Shilyansky et al., 2007). Briefly, from an identical donor, blood was collected twice at two different time points for two separate DC treatments with the different biomaterial films and a single collection of nMNCs (autologous T cell population) as shown in Figure 6-1a and 6-1b. On Day 0, the first blood collection was made from a donor and the adherent mononuclear cells have been cultured for 5 days to generate iDCs as described above, followed by DC treatment with different biomaterial films for 24 hours for Day 5 procedure. On Day 6, the second blood collection was made from the identical donor and then, processed for generation of 2nd set of DCs to be treated with biomaterial films as described above. At the same time, the nMNCs were also collected for the autologous T cell population for co-culture with the 1st DC culture. On the same day (Day 6), these autologous nMNCs and the first set of DCs treated with biomaterial film/OVA or only with biomaterial films for 24 hours were co-cultured after non-/loosely-adherent DCs were collected from treatment with biomaterial films and washed twice

using PBS (pH 7.2) by centrifugation at 1100 rpm for 10 min. The ratio of DCs and nMNCs (1:6.25) in the co-culture was adapted from that of the mixed lymphocyte reaction (MLR) in the previous study (Chapter 4) (Yoshida and Babensee, 2004; Park and Babensee, 2009) because the ratio showed most explicit results among different biomaterial films. Using this ratio, DCs and T cells were resuspended at concentration of 5×10^4 cells/ml and 3.125×10^5 cells/ml, respectively, together in the complete RPMI-10 media (the co-culture media), which was prepared RPMI-1640 with 25 mM HEPES and L-glutamine (Gibco BRL, Carlsbad, CA) with 100 U/ml penicillin/streptomycin (Cellgro) and heat-inactivated filter-sterilized (0.22 μm) 10% (v/v) human AB serum (Biowhittaker, Walkersville, MD). These suspension of DCs and nMNCs were plated into the 96-well flat-bottomed plate (Corning) (200 μl/well) with the addition of the cytokines of IL-2 (10 units/ml) and IL-7 (5ng/ml) (both from Peprotech). For the negative control of the co-culture system, only nMNCs were cultured using the same concentration of the nMNCs in the co-culture wells. At the same time, this negative control (only nMNCs) was partially treated with transforming growth factor (TGF)-β (5ng/ml) (Peprotech) to induce FoxP3 expression as a positive control for FoxP3 measurement upon DCs-T cell co-culture (Tran et al., 2007).

After 3 days (on Day 9), the complete RPMI-10 media was changed with fresh media by 50% (100 μl) per well of the 96-well plate and the cytokines of IL-2 (25 units/ml), IL-7 (10 ng/ml) and TGF-β (5ng/ml) (the later only for the control wells of FoxP3 measurement) were added into each well of the co-culture.

On Day 11, the 2nd set of DCs generated from the second blood collection on Day 6 as described above were treated with freshly prepared biomaterial films and then, after 24 hours (on Day 12), non-/loosely-adherent DCs were collected and washed twice as above. On the same day (Day 12), the complete RPMI-10 media was changed with fresh media by 50% (100 μl) one

more time and the cytokines of IL-2 (25 units/ml) and IL-7 (10 ng/ml) were added together with those collected 2nd DC set above at a concentration of 5×10^4 cells/ml (5×10^3 cells/well of 96-well plate). This addition of DCs was for the 2nd stimulation of T cells. As before, TGF-β (5ng/ml) was also added into the control wells (only nMNCs) of FoxP3 measurement. After 2 days (on Day 14), the whole procedure was finalized by collecting all cells for examination of T cell marker or FoxP3 expression and supernatant collected for analysis of cytokine profiles.

Due to the limited cell numbers obtained from each donor, this 14 day-procedure of DC-T cell co-culture for FoxP3 measurement was separately performed using another 6 donors different from the 6 donors used for the 14 day-procedure of DC-T cell co-culture for T cell marker expressions and cytokine release.

Samples and controls

The present study herein has different controls depending on the time points or treatments with biomaterial films or OVA as shown in Table 3. Briefly, before mixed with nMNCs, DCs were treated with biomaterial film/OVA or only with biomaterial films for 24 hours and collected on Day 6 for the 1st DC set and on Day 12 for the 2nd DC set. From Day 6 to Day 14, in the 96-well plate for the co-culture system, 4 different groups were used; Group 1 was for the co-culture of T cells and DCs treated with biomaterial film/OVA, Group 2 for the co-culture of T cells and DCs treated with biomaterial films (without OVA), Group 3 only DCs treated with biomaterial film/OVA, and Group 4 only DCs treated with biomaterial films (without OVA). The Group 3 and 4 had only DCs collected after treated with biomaterial films with or without OVA in the DC media followed by resuspending in the complete RPMI-10 media and then, these wells for only DCs were cultured with the identical cell concentration of DCs, addition of cytokines, changing media, and the additional DC for 2nd stimulation on Day 12 as same as done

for the co-culture wells. Each of the groups had iDC, mDC, and DCs treated with different biomaterial films.

Table 3: Samples and controls in 4 different groups used in the Chapter 6.

Immature DCs were treated with biomaterial/OVA or only biomaterial for 24 hours and then, only DCs collected from the culture wells including biomaterials and/or OVA. These isolated DCs were then used for co-culture with autologous T cells from Day 6. On Day 12, another DCs (2nd DC set from 2nd blood collection) were added into culture wells for each DC in all 4 groups to stimulate autologous T cells. In addition to 4 groups above, only T cells (control) were cultured from Day 6 to Day 14. Arrow indicates that DCs were isolated and then, transferred to 96-well plates including T cell culture media.

From Day 6 to Day 14		iDC treatment with biomaterial/OVA or only biomaterial for 24 hours (1^{st} DC set for Day 5 to Day 6 or 2^{nd} DC set for Day 11 to Day 12)		From Day 6 to Day 14
Group 1 (each DC + T cells)	←	iDC treatment with OVA	→	Group 3 (each DC only)
	←	iDC treatment with LPS/OVA	→	
	←	iDC treatment with PLGA/OVA	→	
	←	iDC treatment with Chitosan/OVA	→	
	←	iDC treatment with Alginate/OVA	→	
	←	iDC treatment with HA/OVA	→	
	←	iDC treatment with Agarose/OVA	→	
Group 2 (each DC + T cells)	←	iDC untreated	→	Group 4 (each DC only)
	←	iDC treatment with only LPS	→	
	←	iDC treatment with only PLGA	→	
	←	iDC treatment with only Chitosan	→	
	←	iDC treatment with only Alginate	→	
	←	iDC treatment with only HA	→	
	←	iDC treatment with only Agarose	→	

T cell surface marker expressions

The levels of T cell surface marker expression was determined for T cells following co-culture with differentially treated DCs since Day 6, by flow cytometry, as previously described (Yoshida and Babensee, 2004) and compared to controls. Whole cell population from the each co-culture well was collected by centrifugation at 300 ×g for 10 min and suspended in Hank's HEPES buffer (120 mM NaCl, 10 mM KCl, 10 mM $MgCl_2$, 10 mM glucose, 30 mM HEPES) (all from Sigma) containing 1% (v/v) human serum albumin (HSA) (Calbiochem, Darmstadt, Germany) and 1.5 mM $CaCl_2$ (Sigma). Cells were stained with saturating concentrations of fluorescently conjugated mouse anti-human monoclonal antibodies against CD3 (clone HIT3a; IgG2aκ), CD4 (clone L200; IgG1κ), CD8 (clone RPA-T8; IgG1κ), CD25 (clone M-A251; IgG1κ), CD69 (clone FN50; IgG1κ) (all from BD Pharmingen) for 1 hour at 4˚C in the dark, filtered using 40 μm cell strainer (Becton Dickinson, Franklin Lake, NJ) and then, analyzed immediately with 10,000 events per sample using a BDLSR flow cytometer (Becton Dickinson). Data was obtained together with the negative control of autofluorescence per sample and then, analyzed using FLOWJO version 7.2.5 (Tree Star, Inc. Ashland, OR).

FoxP3 expression

From the overall observations in the Chapter 4, 5 and this Chapter, PLGA induced immunogenic response of DC maturation or IFN-γ release from co-culture of T cells and DCs treated with PLGA, whereas agarose induced tolerogenic response of no effect on DC maturation much like iDCs or CD4+CD25+ T cell induction from co-culture of T cells and DCs treated with agarose. For this reason, measurement of FoxP3 expressions on T cells upon co-culture with DCs treated with biomaterial films with these most distinct effects was followed up for a confirmatory marker of regulatory T cells, FoxP3 expression. The levels of FoxP3 expression

was determined for T cells following co-culture with DCs treated with PLGA or agarose since Day 6, by flow cytometry, using the FITC anti-human FoxP3 Staining Kit (eBioscience, San Diego, CA). Rat IgG2aκ FITC (eBioscience) was used as isotype control. Whole cell population from the each co-culture well was collected by centrifugation at 300 ×g for 10 min and then, cells were fixed and permeabilized using a fixation/permeabilization kit according to the manufacturer's protocol. Cells were stained with FoxP3 (clone PCH101; IgG2aκ) or the Isotype control together with CD3, CD4, and CD25 (same as above) to gate CD4+CD25+ T cells from CD3+ population. After staining procedure, cells were filtered using 40 μm cell strainer (Becton Dickinson) and then, analyzed immediately with 10,000 events per sample using a BDLSR flow cytometer (Becton Dickinson). Data was obtained together with the negative control of autofluorescence per sample and then, analyzed using FLOWJO version 7.2.5 (Tree Star).

Cytokine release

The amount of cytokines, IFN-γ, IL-12p70, IL-10, and IL-4 produced by DCs or T cells in the treatment of DCs (with biomaterial films with and without OVA) or in the co-culture of differentially-treated DCs and T cells were analyzed by Cytometric Bead Array (CBA) Human Inflammation Kit (BD Pharmingen) according to manufacturer's directions. Cell culture supernatants were cleared by centrifugation for 10 minutes at 400 ×g and stored at -20˚C until analysis. Each cytokine amount was normalized to the respective total DNA quantified using a picoGreen dsDNA quantification kit (Invitrogen) per manufacturer's directions. The CBA analysis was performed using the flow cytometry and then, data analyzed using FLOWJO version 7.2.5.

Statistical analysis

For statistical analysis, one sided Student t-test was used to compare sample group to appropriate control group in pairs. To observe significant differences between all sample groups in pairs, the general liner model of two-way ANOVA in pairwise was used for a mixed model with repeated measure. For all statistical methods, the Minitab software (Version 14, State College, PA) was used. If not indicated, p-value less than or equal to 0.05 was considered to be significant.

RESULTS:

T cell marker and FoxP3 expression

To measure differential effects of different biomaterial films treated with DCs on autologous T cell-mediated immunity, expression levels of T cell markers (CD4, CD8, CD25, CD69) were examined after autologous T cells were co-cultured with DCs treated with different biomaterial films (with and without OVA).

Upon DCs treatment with different biomaterial films in the presence of the model antigen, OVA, autologous CD3+ T cells co-cultured with these DCs exhibited differential expression of T cell markers depending on the type of biomaterial films used to treat the DCs as shown in Figure - 6-2, 6-3, and 6-4. However, no significant difference was observed in autologous T cell marker expression upon co-culture with DCs treated with biomaterial films in the absence of exogenous OVA (Figure A5, APPENDIX).

When DCs were treated with biomaterial films in the presence of OVA, CD4 expression levels showed significant differences between T cells co-cultured with DCs treated with different biomaterial films. T cells co-cultured with DCs treated with agarose films in the presence of OVA, exhibited significantly higher levels of CD4 expression compared to other all biomaterial films as shown in Figure 6-2. Interestingly, DC treated with HA films in the presence of OVA

induced significantly lower levels of CD4 expression on T cells compared to the negative control of untreated CD3+ T cells, actually inhibiting CD4+ T cell response. However, CD8 expression levels of T cells for DC treated with all biomaterial films in the presence of OVA did not show any significant differences compared to the negative control of untreated CD3+ T cells or other biomaterial films.

Dendritic cells treated with PLGA, chitosan, alginate, or agarose films in the presence of OVA antigen, induced significantly higher levels of CD25 expressions compared to the negative control of untreated CD3+ T cells. Dendritic cell treated with agarose films in the presence of OVA induced significantly higher levels of CD25 expression compared to DC treated with PLGA films or HA films in the presence of OVA while DC treated with alginate films in the presence of OVA did only when compared to DCs treated with HA films in the presence of OVA. Except for iDC treated with OVA, DC treated with any of the biomaterial films in the presence of OVA induced significantly higher levels of CD69 expressions on the T cells compare to the negative control but no significant difference between biomaterial film treatments was observed.

To assess effects of DC treatment with biomaterial films in the presence of OVA on the double positive staining for T cell marker expressions, the representative quadrant dot plots from one donor (out of total 6 donors) and the percentage numbers of the double positive quadrant were averaged for all 6 donors and shown in Figure 6-3 and 6-4, respectively. As shown, CD4+ quadrant percentages for T cells changed depending on different biomaterial films/OVA while CD8+ quadrant percentages did not change appreciably shown in the column of CD4 and CD8 dot plots (Fig. 6-3). However, DC treatment with alginate film/OVA or agarose film/OVA induced significantly higher levels of the double positive of CD4+CD8+, similar to iDC (no OVA), mDC (no OVA), iDC/OVA, or mDC/OVA, as compared to the negative control of untreated CD3+ T cells, whereas treatment with the other biomaterial films (PLGA, chitosan, or

HA film)/OVA induced levels similar to the negative control of untreated CD3+ T cells (Fig. 6-4). Treatment of DCs with agarose film/OVA induced significantly higher levels of CD4+CD25+ expression in T cells compared to mDC/OVA, or DC treatment with PLGA film/OVA, chitosan film/OVA, or HA film/OVA. Whereas co-culture of T cells with iDC (no OVA), mDC (no OVA), iDC/OVA, or DCs treated with alginate film/OVA induced significantly higher levels of CD4+CD25+ expression in T cells only compared to the negative control of untreated CD3+ T cells (Fig. 6-4). Interestingly, even though DC treatment with PLGA film/OVA or chitosan film/OVA induced significantly higher levels of single CD25+ or CD69+ expression in co-cultured T cells compared to the negative control of untreated CD3+ T cells (Fig. 6-2), they did not induce significant differences in the CD4+CD25+ double positive expression levels in T cells compared to the negative control however, significant differences were observed for CD4+CD69+ double positive expression levels (Fig. 6-4).

When DCs were treated with PLGA/OVA or agarose/OVA, autologous T cells co-cultured with these DCs showed differential levels of FoxP3 expressions (Fig. 6-5). Confirming results of CD4+CD25+ quadrant in dot plots differentially induced depending on DC treatment with PLGA or agarose as shown in Figure 6-3, iDCs or agarose-treated DCs induced higher percentages of CD4+CD25+ population upon co-culture with autologous T cells, compared to mDCs or PLGA-treated DCs (Fig. 6-5a). Histograms gated only within the CD4+CD25+ population in each of these quadrant dot plots in Figure 6-5a exhibited differential shifts of isotype or FoxP3 expressions. Immature DCs or DCs treated with agarose resulted in a shift in the histogram to the right for FoxP3 and to the left for the isotope, compared to mDCs or PLGA (Fig. 6-5b). For statistical comparisons of this FoxP3 expression, gMFI of isotype staining was subtracted from that of FoxP3 staining for T cells co-cultured with each of iDCs, mDCs, or DC treated with PLGA or agarose and then, the final values (gMFI difference) was normalized by

untreated CD3+ MNCs. As a result, T cells co-cultured with iDCs or agarose-treated DCs exhibited significantly higher levels of FoxP3 expression than untreated CD3+ T cells and T cells co-cultured with mDCs or PLGA-treated DCs, while T cells treated with TGF-β [a specific inducer of FoxP3 expression (Tran et al., 2007)] exhibited the value significantly higher only compared to untreated CD3+ T cells (Fig. 6-5c) (quadrant dot plot and histogram of MNCs treated with TGF-β are not shown here). However, T cells co-cultured with mDCs or PLGA-treated DCs did not exhibit levels significantly different from untreated CD3+ T cells for FoxP3 expression.

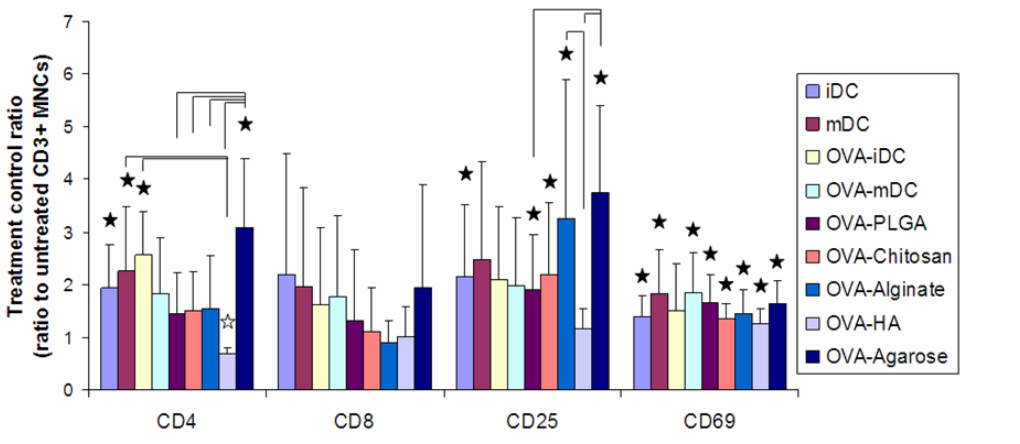

Figure 6-2: Geometric mean fluorescence intensity (gMFI) of CD4, CD8, CD25, & CD69 expression for autologous CD3+ T cells in differential levels upon co-culture with DCs treated with different biomaterial films and OVA antigen.

Agarose induced CD4 or CD25 expression in higher levels than other biomaterial treatments, whereas HA induced suppression of CD4 expression compared to untreated CD3+ T cells. Ratios to the untreated CD3+ MNCs are shown with mean±SD, n=6 donors (6 independent experiments with different donors). ★: $p \leq 0.05$, compared to control and higher than control; ☆: $p \leq 0.05$, compared to control and lower than control; Brackets: $p \leq 0.05$, statistically different between two T cells for DC treatment with different biomaterial films.

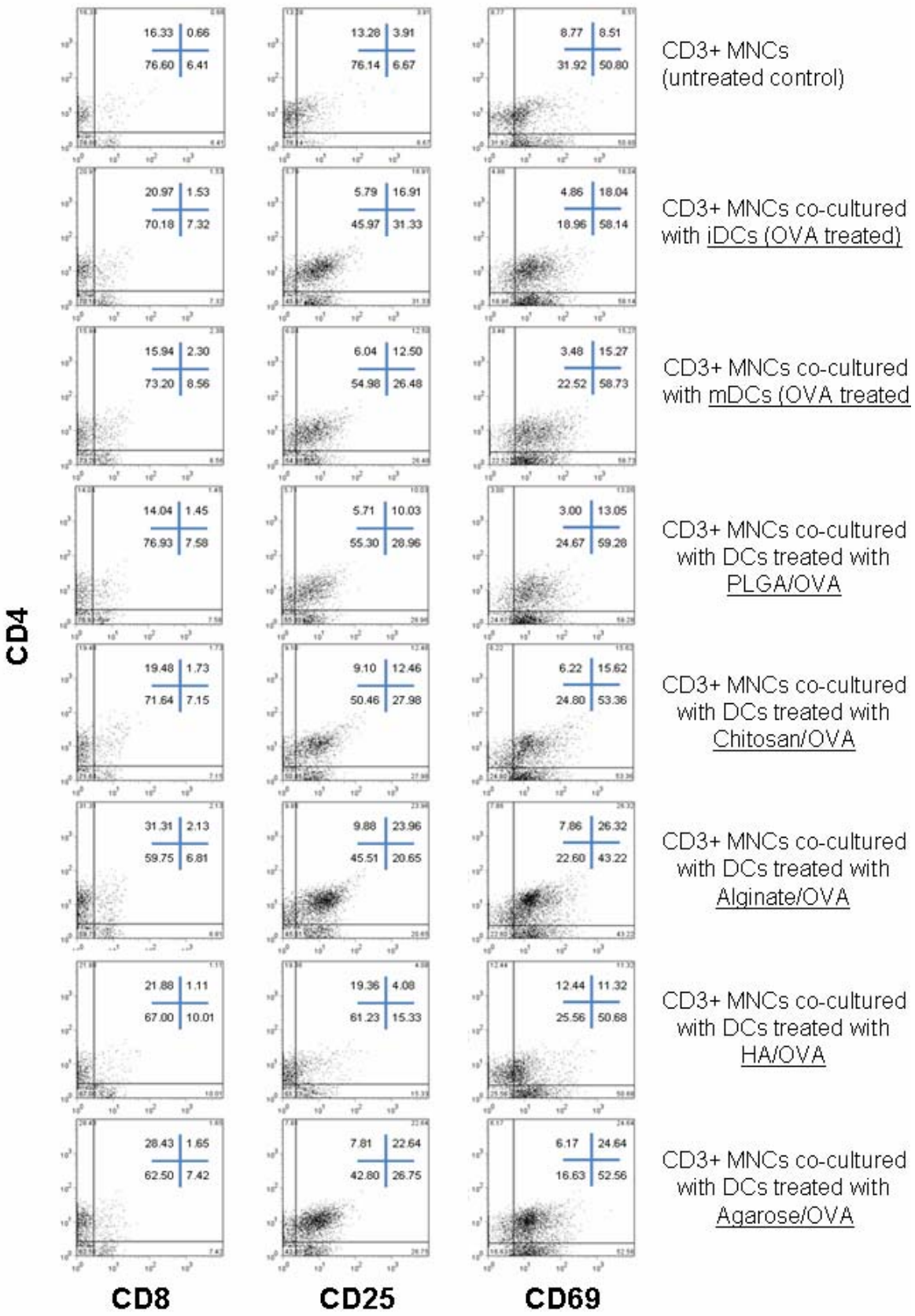

Figure 6-3: Representative quadrant dot plots for autologous T (CD3+) cell markers after co-culture with DCs treated with different biomaterial films and OVA antigen.

Representative plots for one donor were selected from all 6 donors. Different biomaterials directed various T cell markers expressions in differential levels upon co-culture of T cells and DCs treated with biomaterials. In particular, agarose and alginate induced higher quadrant percentages in double positive of CD4+CD25+ or CD4+CD69+ compared to other biomaterial treatments. Y-axis for all plots indicates CD4 expression while X-axis for all plots in each column indicates CD8, CD25, or CD69 expressions as shown. Numbers shown together with the cross in each plot indicate the percentage of dots for each quadrant.

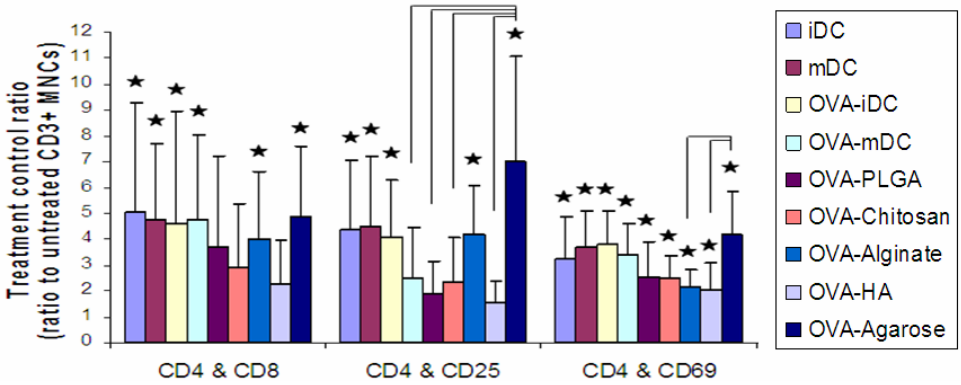

Figure 6-4: Percentage numbers in double positive quadrant dot plots of CD4 & CD8, CD4 & CD25, CD4 & CD69 expression on autologous CD3+ T cells upon co-culture with DCs treated with different biomaterial films and OVA antigen. Different biomaterials induced differential levels of CD4+CD25 or CD4+CD69+ expression on T cells upon co-culture with DCs treated with biomaterials.

As seen in the quadrant dot plots in Figure 6-3, T cells co-cultured with DCs treated with agarose exhibited CD4+CD25+ or CD4+CD69+ in statistically higher levels than other biomaterials, whereas T cells co-cultured with DCs treated with alginate did not exhibit statistically difference compared to other biomaterials. Ratios to the untreated CD3+ MNCs are shown with mean±SD, n=6 donors (6 independent experiments with different donors). ★: $p \leq 0.05$, compared to control and higher than control; ☆: $p \leq 0.05$, compared to control and lower than control; Brackets: $p \leq 0.05$, statistically different between two T cells for DCs treated with different biomaterial films.

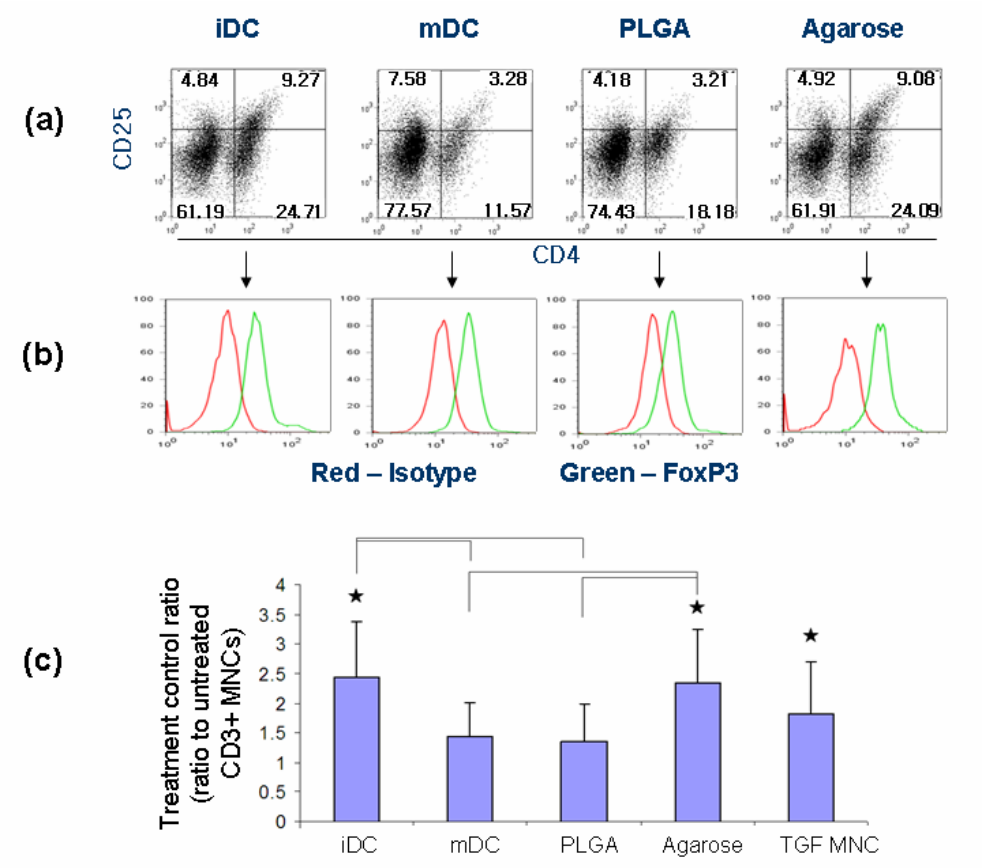

Figure 6-5: Foxp3 expressions on autologous CD3+ T cells upon co-culture with DCs treated with different biomaterial films (PLGA or agarose) and OVA antigen.

Representative plots for one donor were selected from all 6 donors. PLGA or agarose directed FoxP3 expressions in differential levels upon co-culture of T cells and DCs treated with biomaterials. Agarose treatment of DCs maintained FoxP3 expression on co-cultured T cells gated from CD4+CD25+ population at level similar to iDCs whereas a decrease in expression was induced by PLGA-treated DCs or mDCs. Y-axis for all plots indicates CD25 expression while X-axis for all plots indicates CD4 expression as shown (Fig. 6-5a). Numbers shown in each quadrant indicate the percentage of events for each quadrant. Representative histograms (from all 6 donors) for Foxp3 expressions on CD4+CD25+ T cells gated from the quadrant dot plots above (Fig. 6-5b). Geometric mean fluorescence intensity (gMFI) of Foxp3 expressions on CD4+CD25+ T cells gated above (Fig. 6-5c). TGF MNC indicates MNCs treated with TGF-β to induce Foxp3+ from CD4+ T cells. gMFIs of the isotype were subtracted from gMFIs of FoxP3 per control or treatment and then, ratios to the untreated CD3+ MNCs are shown with mean±SD, n=6 donors (6 independent experiments with different donors). ★: $p \leq 0.05$, statistically higher than control (=1); ☆: $p \leq 0.05$, statistically lower than control (=1); Bracket: $p \leq 0.05$, statistically different between two T cells for DC treatments with different biomaterial films.

Cytokine releases in Th1/Th2 polarization

As another measurement of differential effects of different biomaterial film treatments of DCs on autologous T cell-mediated immunity, cytokine release profiles for Th1/Th2 polarization were determined in the supernatants of DCs treated with biomaterial films (with and without OVA antigen) without co-cultured autologous T cells or co-culture of these differentially treated DCs with autologous T cells.

Dendritic cells treated with different biomaterial films in the presence or absence of OVA resulted in differential cytokine profiles depending on the biomaterials used to treat the DCs (Figure 6-6). In addition, co-culture of these differentially-treated DCs with autologous T cells resulted in differential levels of cytokine release into the supernatant collected on Day 14, independent of whether OVA antigen was added to DCs treatment with biomaterials (Fig. 6-7). This was contrary to the results for induced T cell marker expression that only showed significantly different levels depending on biomaterial used to treat the DCs if OVA was present.

As shown in Figure 6-6, before co-culture with autologous T cells, DCs treated with different biomaterial films in the presence or absence of OVA released significantly different levels of some cytokines depending on the type of biomaterial used. For IFN-γ or IL-4 release, mDCs or DCs treated with most biomaterial films did not exhibit significantly different levels of release from iDCs. However, DCs treated with agarose films (in the absence of OVA) induced significantly lower levels of IFN-γ release compared to iDCs (Fig. 6-6a). Dendritic cells treated with agarose films [in the presence (Fig. 6-6b) or absence of OVA (Fig. 6-6a)] resulted in levels of IL-4 release that were significantly lower than iDCs. Mature DCs or DCs treated with PLGA, or chitosan films released IL-12p70 in significantly higher levels compared to iDCs while only mDCs induced significantly higher levels of IL-10 compared to iDCs, when DCs were treated

with biomaterial films only, in the absence of OVA (Fig. 6-6a). Interestingly, the profiles of release for IL-12p70 and IL-10, depending on the biomaterial treatment of the DCs, were different when DCs were treated with biomaterial films in the presence of OVA antigen as shown in Figure 6-5b. For DC treatment with biomaterial films in the presence of OVA, only DCs treated with agarose films induced significantly higher levels of IL-12p70 release, whereas mDCs or DCs treated with PLGA or chitosan films did not show any significant difference in levels of IL-12p70 release, as compared to iDCs (Fig. 6-6b). For IL-10, mDCs or DCs treated with chitosan films (in the presence of OVA) released significantly higher levels than iDCs while DCs treated with agarose films (in the presence of OVA) induced significantly lower levels, as compared to iDCs (Fig. 6-6b).

As mentioned earlier in the Materials and Methods section, for the negative controls of the co-culture procedures from Day 6 to Day 14, a half of DCs from treatments with each biomaterial film, which were collected on Day 6 (supernatants from these DCs were discussed above for cytokine profiles as shown in Figure 6-6), were washed twice and then, kept cultured without T cells through Day 14 in the same condition as with the DC-T co-culture system while the other half was used for the co-culture with autologous T cells. Interestingly, for the control culture of DCs without added autologous T cells, the cytokine profiles were the same at day 14 (Figure A6, APPENDIX) as they were at Day 6 (Fig. 6-6) in the presence or absence of OVA antigen.

For cytokine profiles in the co-culture supernatant saved on Day 14, to compare DC treated with different biomaterial films obtained from different donors, data were normalized by cytokine levels of only DCs (negative control) for DCs treated with each biomaterial film after subtracting those of only T cells (negative control) from those of the actual co-culture of DCs and T cells (Fig. 6-7). As shown in Figure 6-7, once T cells were co-cultured with DCs treated

different biomaterials in the presence or absence of OVA (Fig. 6-7), the profiles of released cytokines changed significantly from those of DCs treated with biomaterial films (Fig. 6-6) or only DCs culture (negative control) (Figure A6, APPENDIX). Upon co-culture with T cells, mDCs or DCs treated with PLGA films [with (Fig. 6-7b) and without (Fig. 6-7a) OVA] induced IFN-γ release at a significantly higher level compared to iDCs or DCs treated with the other biomaterial films.

In the absence of OVA antigen during DC treatment with biomaterial films, only the alginate film treatment of the DCs, then co-cultured with the T cells, induced IL-12p70 release in significantly higher levels as compared to co-cultures with DCs treated with most other biomaterial films (Fig. 6-7a), whereas mDCs or DCs treated with PLGA or chitosan film released IL-12p70 at significantly higher levels compared to iDCs before the co-culture with T cells (Fig. 6-6a). However, in the presence of OVA antigen during DC treatment with biomaterial films, only DCs treated with agarose films, then co-cultured with the T cells, induced significantly higher levels of IL-12p70 release as compared to co-cultures with iDCs or DCs treated with most other biomaterial films from Day 6 (Fig. 6-6b) through Day 14 (Fig. 6-7b).

Dendritic cells treated with alginate or agarose films (in the absence of OVA) co-cultured with T cells resulted in significantly higher levels of IL-10 release as compared to co-cultures with DCs treated with most of the other biomaterials (Fig. 6-7a), whereas only mDCs released IL-10 in significantly higher levels than iDCs on Day 6 before co-cultured with T cells (Fig. 6-6a). Interestingly, DCs treated with agarose films in the presence of OVA secreted IL-10 at significantly lower levels than iDCs on Day 6 before co-cultured with T cells (Fig. 6-6b) but, upon co-culture with T cells, significantly higher levels of IL-10 release were observed as compared to co-cultures with DCs treated with most of the other biomaterial films (Fig. 6-7b).

Treatment of DCs with any of the biomaterial films did not induce IL-4 release in the co-

cultures with T cells that were significantly different between treatment groups in the presence or absence of OVA (Fig. 6-7). This was in spite of the fact that DCs treated with agarose films alone induced significantly lower levels of IL-4 release as compared to iDCs on Day 6 before co-culture with T cells (Fig. 6-6).

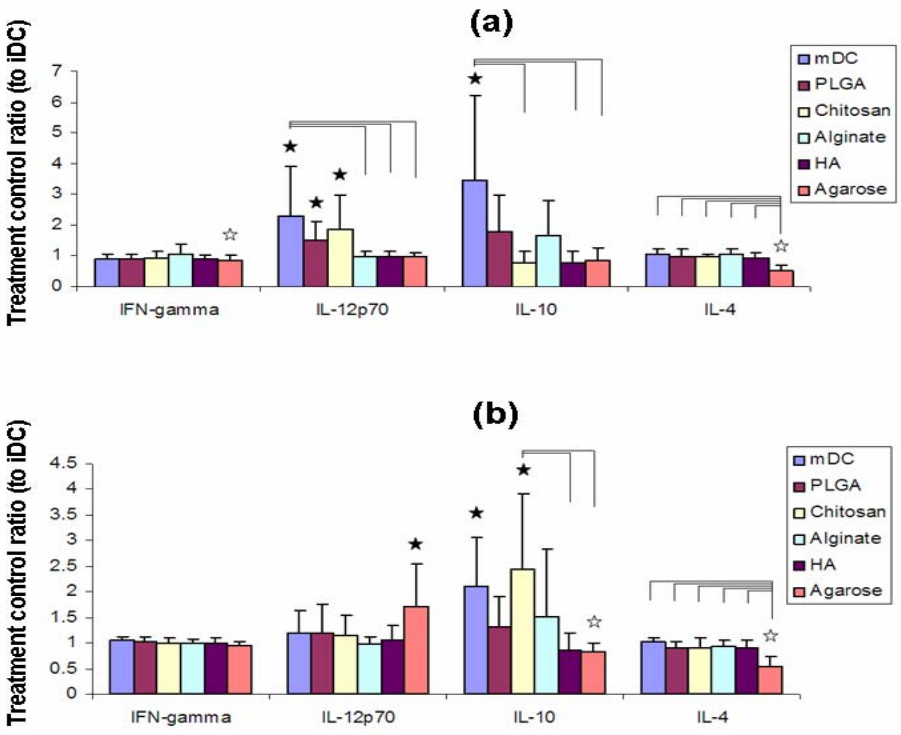

Figure 6-6: Geometric mean fluorescence intensity (gMFI) of cytometric bead array (CBA) for interferon (IFN)-gamma, IL-12p70, IL-10, IL-4 release for DCs treated with different biomaterial films without (Fig. 6-6a) or with (Fig. 6-6b) OVA antigen after 24 hour-treatment of DCs with biomaterial films with or without antigen.

Cytokines were measured using the supernatant saved on Day 6 (after 24 hour-treatment of DCs with biomaterial films with or without antigen). Th1 or Th2 cytokines were modulated in differential levels upon DC treatment with different biomaterials and/or model antigen, OVA. IL-12p70 was released in higher levels upon DC treatment with LPS, PLGA or chitosan in the absence of OVA, whereas IL-12p70 was released in higher levels upon DC treatment with agarose in the presence of OVA, as compared to iDCs. Ratios to the iDCs are shown with mean±SD, n=6 donors (6 independent experiments with different donors). ★: $p \leq 0.05$,

compared to iDCs and higher than iDC; ☆: $p \leq 0.05$, compared to iDCs and lower than iDC; Brackets: $p \leq 0.05$, statistically different between two T cells for DCs treated with different biomaterial films.

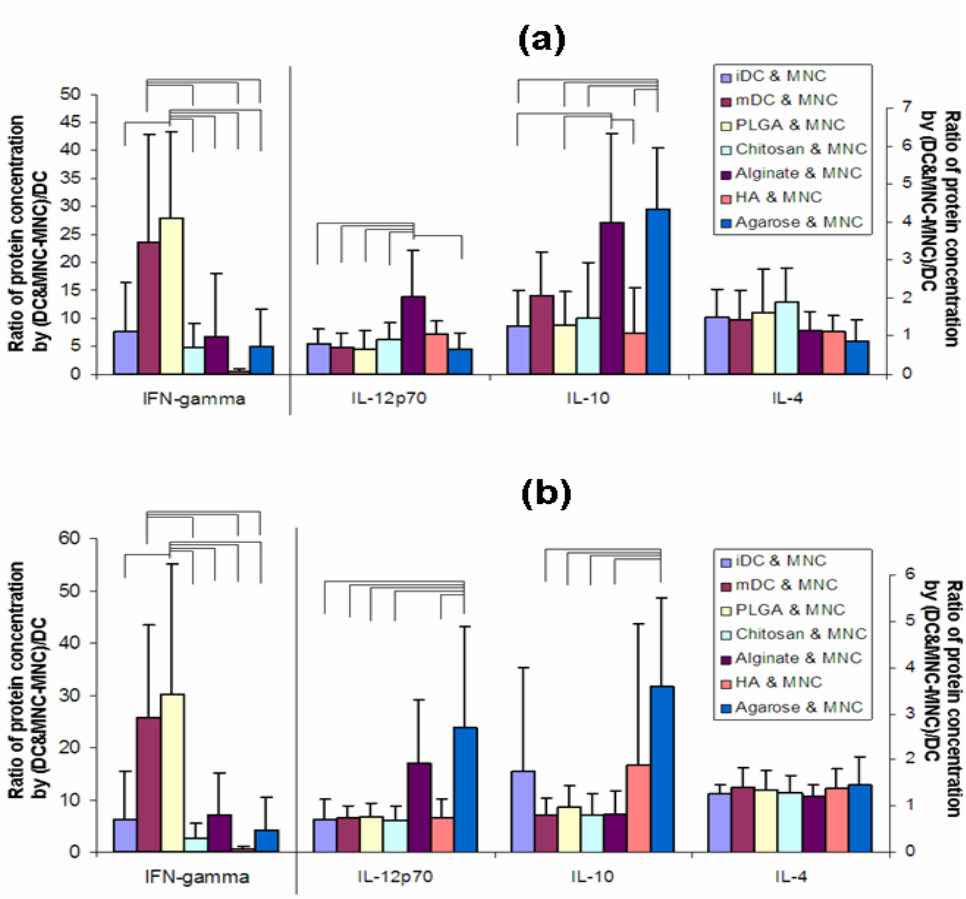

Figure 6-7: Geometric mean fluorescence intensity (gMFI) of cytometric bead array (CBA) for interferon (IFN)-gamma, IL-12p70, IL-10, IL-4 releases upon co-culture of auto T cells and DCs treated with different biomaterial films without (Fig. 6-7a) or with (Fig. 6-7b) OVA antigen after 8 days of DC-T co-culture.

Cytokines were measured using the supernatant saved on Day 14 (after 8 days of DC-T co-culture). Th1 or Th2 cytokines were modulated in differential levels upon co-culture of autologous T cells and DCs treated with different biomaterials and/or model antigen, OVA. PLGA or agarose induced IFN-γ or IL-10 release, respectively, in higher levels compared to other biomaterials independently from the presence of antigen, OVA. However, focusing on DC treatment with alginate, IL-12p70 or IL-10 release was modulated in differential levels depending on treatment with antigen, OVA, compared to other biomaterial treatments. To compare DC treatments with different biomaterial films obtained from different donors, data were normalized

by each negative control (only DC treated with each biomaterial film) after subtracting only MNCs control from the actual co-culture of DCs and MNCs. Normalized ratios are shown with mean±SD, n=6 donors (6 independent experiments with different donors). Brackets: $p \leq 0.05$, statistically different between two DCs treated with different biomaterial films.

DISCUSSION:

The purpose of this research was to assess the indirect effects of different biomaterials in differential levels of autologous T cell mediated immunity, through direct effects of the different biomaterials on DC phenotype. In this way, we are assessing the ability of differentially biomaterial-treated DCs to non-pharmacologically drive T cell responses. Clearly the results show that the phenotype of autologous T cells can be differentially modulated in co-cultures with DC treated with different biomaterials. Furthermore, Th1/Th2 polarization of the cytokine profiles was possible through biomaterial-treated DCs using the model antigen (OVA) and/or the co-culture of those biomaterial-treated DCs and autologous T cells as shown in Figure 6-8.

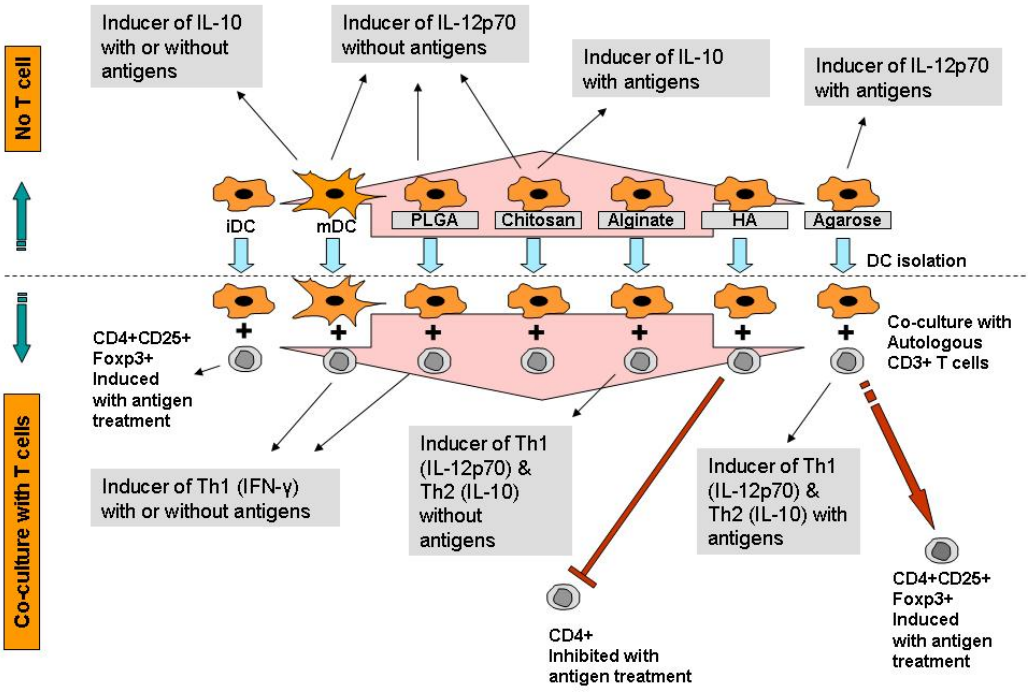

Figure 6-8: Schematic representation of autologous T cell phenotype and polarization directed by DCs treated with different biomaterials.

In the Chapter 4, the efforts of a large variety of immunobiological assays have been used to understand the mechanism behind DC phenotypical changes when DCs are treated with different biomaterial films. As results, differential levels of DC maturation have been observed depending on the type of biomaterial films used to treat the DCs, possibly associated with the inherently different chemistries of those biomaterials that are used. Based on these facts together with the previous results (Yoshida and Babensee, 2006; Babensee and Paranjpe, 2005; Park and Babensee, 2009), showing the DC phenotypical changes in differential levels depending on the type biomaterial used to treat the DCs, it was hypothesized that different biomaterial films would indirectly affect autologous T cell activations and polarizations through direct effects on DCs.

When DCs were treated with biomaterial films in the presence of the antigen (OVA), autologous T cells co-cultured with these DCs showed significantly differential levels of expression, at least, for CD4 and CD25 among DC treatments with biomaterial films as shown in Figure 6-2, whereas expressions for each of all T cell markers (CD4, CD8, CD25, CD69) among DC treatments with biomaterial films were not induced at differential levels when DCs were treated with biomaterial films in the absence of OVA (Figure A5, APPENDIX). These indicate that DCs treated only with biomaterial films, in the absence of co-delivered antigen, might be not sufficiently activated to induce differential T cell marker expression. Similar results have also been reported showing that DC exposure to an actual pathogen component is necessary to promote T helper responses (Sporri and Sousa, 2005). With the addition of OVA to DC treatment with biomaterial films, the CD4+ T cell response were affected by DCs treated with different biomaterial films, whereas the CD8+ T cell response was not affected as shown in Figure 6-2. It is conceivable that the system of DC treatment with biomaterial films and

subsequent co-culture with autologous T cells more effectively promotes CD4+ T cell responses than CD8+ T cell responses, the later of which would depend on cross-presentation of extracellular antigen component (Lanzavecchia and Sallusto, 2001).

Expression of CD4 or CD25 on co-cultured autologous T cells were modulated by biomaterial films used to treat the DCs as compared to controls of iDCs, mDCs, or a control of untreated CD3+ T cells. This indicates that biomaterial films might play an important role in controlling T cell responses in the presence of the antigen, possibly extended from the differential levels of endocytic ability of DCs treated with different biomaterial films. Enhanced endocytic ability of DCs in treatment with LPS is transient so that, after around 1 hour of LPS treatment, the endocytic ability kept down over time (West et al., 2004). However, in the Chapter 4, after 24 hours of DC treatment with biomaterial films, DCs isolated from treatment with agarose films maintained an endocytic capacity similar to the level for iDCs which was reduced with maturation of DCs or DC treatment with the other biomaterial films such as PLGA. In this study, DCs were treated with biomaterial films in the presence of OVA antigen for 24 hours, and then, DCs were isolated from biomaterial films and OVA antigen prior to co-culture with T cells. Possibly related with those previous findings, differential endocytic abilities during the 24 hours of DC treatment with biomaterial films in the presence of OVA may partially explain why iDCs or DCs treated with agarose film induced significantly different levels of CD4 expression of autologous T cells compared to mDCs or other DCs, given the well-known role of peptide-MHC class II complexes derived from the antigen (OVA) in promoting CD4+ T cell responses.

The α chain of IL-2 receptor, CD25, has been widely accepted for an activation marker of T cells whose expression level of T cells (along with another T cell activation marker, CD69) is up-regulated by mature or activated DCs (Stegel et al., 2006; Chan et al., 2007). In addition, CD80 and CD86 expressed on DCs were shown to have a critical role in providing important

signals for CD25 expression on CD4+ T cells (Coyle and Gutierrez-Ramos, 2001). As seen in Figure 6-2, except for T cells co-cultured with DCs treated with HA film, T cell expression of CD25 in co-cultures with DCs treated with the other biomaterials were significantly higher as compared to the control of untreated CD3+ T cells. In the previous studies, up-regulations of co-stimulatory molecules, DC maturation marker, and MHC class II molecules (CD40, CD80, CD86, CD83, HLA-DQ, or HLA-DR) on DCs in differential levels were induced by DC treatment with different biomaterial films (Chpater 4) (Yoshida and Babensee, 2006; Babensee and Paranjpe, 2005; Park and Babensee, 2009). These findings emphasize that surface molecules up-regulated when DCs were treated with biomaterial films possibly affected CD25+ T cell responses in the co-cultures presented herein. As shown in Figures 6-3 and 6-4, expression of double positive of CD4+CD25 T cells were induced in significantly higher levels for T cells co-cultured with control DCs (iDC, mDC, or iDCs treated with OVA) and DCs treated with alginate or agarose films; most notably for agarose treatment (Fig. 6-4). It has been reported that repetitive stimulation of naïve T cells with iDCs or *in vivo* targeting of iDCs with specific antibody-antigen complexes induced CD4+CD25+ T cell activation (Jonuleit et al., 2000; Mahnke et al., 2003) and iDCs pulsed with alloantigen efficiently enhanced the number of CD4+CD25+FoxP3+ T regulatory cells (Marguti et al., 2009). Moreover, human volunteers vaccinated with iDCs exhibited induction of IL-10-producing T cells (Dhodapkar and Steinman, 2002). Interestingly, the CD25+ T cell population was found to suppress IL-2 production and CD4+ T cell responses (Mahnke et al., 2003). Despite higher expression levels of CD25 on T cells in co-cultures with DCs treated with agarose films (compared to untreated CD3+ T cells or DCs treated with the other biomaterial films), DCs treated with agarose films were also associated with higher levels of CD4+ T cell responses (Fig. 6-2) and CD4+CD25+FoxP3+ T cell responses (Figs. 6-3, 6-4, and 6-5). Thus, taken together with endocytic abilities and surface

molecule up-regulation as demonstrated in the Chapter 4, DC treatment with agarose films is a strong inducer of CD4+CD25+FoxP3+ T cell responses to a greater extent than iDCs.

Interestingly, expression of double positive of CD4+CD69+ by T cells in co-culture with DCs treated with agarose films was higher that for T cells co-cultured with DCs treated with alginate or HA films (Fig. 6-4), similar to the results of CD4+CD25+ expressions as shown in Figure 6-3 and 6-4. However, it has been found that co-stimulatory molecule of CD80 or CD86 up-regulated on DCs was not required for stimulation of CD69+ T cell response (Rothoeft et al., 2006). This indicates that, even though CD25 and CD69 are considered together as activation markers on T cells, phenotypical changes (e.g., co-stimulatory molecule expressions) when DCs were treated with different biomaterial films may affect T cell responses through different/independent mechanisms affecting CD25 and CD69 expression.

Dendritic cells treated with HA films induced significantly lower levels of CD4 expression on co-cultured T cells as compared to the negative control of untreated CD3+ T cells as well as significantly lower levels of CD25 expression compared to T cells in co-culture with DC treated with alginate or agarose films (Fig. 6-2). When CD44 surface molecules on DCs were blocked with anti-CD44 antibodies, proliferation of CD4+ T cells co-cultured with those DCs was inhibited (Termeer et al., 2003). Thus this result may be correlated with the previous results from phenotypical changes of DCs treated with HA film, which exhibited significantly lower levels of CD44 expression as compared to iDCs, even though the CD44 marker is specific to hyaluronan component, possibly due to the high molecular weight HA in cross-linked and insolublized forms in the Chapter 4 and present study.

It was only possible to observe differential levels of T cell marker expression in co-cultures with biomaterial treated DCs if OVA was added to the treatments. However, DCs treated with different biomaterial films in the presence or absence of OVA resulted in differential

cytokine profiles depending on the biomaterials used to treat the DCs for DC alone (Fig. 6-6) or upon co-culture with T cells (Fig. 6-7). These indicate that DCs treated with biomaterial films might indirectly affect differential levels of cytokine releases in the co-culture of T cells and DCs more intensively than T cell marker expressions. In the absence of the antigen, DCs treated with PLGA or chitosan film secreted IL-12p70 at significantly higher levels than iDCs while mDCs released IL-12p70 and IL-10 at significantly higher levels than iDCs or DC treated with some other biomaterial films as shown in Figure 6-6a. IL-12p70, a heterodimeric and bioactive form of IL-12, is well known for immunogenic Th1 cytokine, along with IFN-γ (Gautier et al., 2005). In some *in vitro* studies, DCs treated together with antigens (tumor lysates or OVA) and an immunogenic protein [keyhole limpet hemocyanin (KLH) or a CD40 ligand] secreted IL-12 or IL-12p70 at significant higher levels than the negative control DCs, associated with upregulation of CD80, CD86, CD83, or MHC class II molecules (Schnurr et al., 2001; Hunter et al., 2007). IL-10 is well known as a regulatory and immunosuppressive cytokine in Th2 response and DCs treated with dexamethasone or CD40-deficient DCs have been reported to release IL-10 associated with upregulation of CD80, CD86, CD83, or MHC class II molecules or endocytic ability at levels similar to the negative control DCs (Gao et al., 1999; Xia et al., 2005). However, as shown in Figure 6-6b, if DCs were treated with biomaterial films in the presence of OVA, cytokine profiles changed showing that only DCs treated with agarose films in the presence of OVA released IL-12p70 at significantly higher levels than iDCs while, together with mDCs, DCs treated with chitosan films released IL-10 at significantly higher levels than iDCs. Considering that only DCs treated with agarose films showed endocytic ability at high levels similar to iDCs in the Chapter 4, these results may indicate that IL-12p70 secretion from the DCs examined here was more potently affected by antigen-processing through formation of peptide-MHC complexes than other phenotypical changes such as co-stimulatory molecule expression on DCs. In

addition, DCs treated with chitosan films can modulate their intracellular pathway to secret IL-10 in the presence of co-delivered antigen. Interestingly, DC maturation with LPS induced significantly higher levels of IL-12p70 release (in the absence OVA) and IL-10 (independently of the presence of OVA) than iDCs, as shown in Figure 6-6. In accordance with these results, LPS-treated DCs have been found to release significantly higher levels of IL-12p70 and IL-10, compared to the negative control DCs (Chan et al., 2007; Stax et al., 2008), even though this DC maturation induced by LPS is usually accompanied with phenotypical changes such as upregulation of co-stimulatory molecules to high levels of expression. Thus it is conceivable that LPS is a strong inducer of IL-10 release by DCs independently of antigen presence, possibly associated with TLR-4 pathway rather than other co-stimulatory molecules on DCs.

For the control culture of DCs without added autologous T cells, the cytokine profiles were the same at day 14 (Figure A6, APPENDIX) as they were at Day 6 (Figure 6-6) in the presence or presence of OVA antigen. These results indicate that, even though DCs were isolated from biomaterial films and extracellular OVA antigen after the 24 hour-culture, they continued to secrete the same cytokines at almost the same levels under the wholly changed culture conditions for 8 days.

As seen in Figure 6-7, once autologous T cells were co-cultured with biomaterial-treated DCs in the presence of OVA, the cytokine profiles were changed from those of the control cultures of DCs without T cells shown in Figure 6-6. First of all, the co-culture of T cells and mDCs or DCs treated with PLGA films induced significantly higher levels of IFN-γ compared to iDCs or DCs treated with other biomaterial films, in both absence and presence of the antigen. These indicate that the resultant patterns of IFN-γ including statistical differences between DC treatments with biomaterial films were independent with the introduction of OVA antigen to DCs. IFN-γ is also known as immunogenic cytokines representative for Th1 response and has been

recently accepted for immunotherapeutic tool targeting tumors (Whiteside and Odoux, 2004). It has been reported that autogeneic or allogeneic T cells stimulated by DCs treated with CD40 ligand, adjuvant such as aluminum hydroxide, LPS, or KLH induced significantly high levels of IFN-γ production, combined with DC maturation phenotypes such as increased upregulation of co-stimulatory molecules or decreased endocytic ability (Schnurr et al., 2001; Stax et al., 2008; Hunter et al., 2007; Sokolovska et al., 2007). In the Chapter 4, mDCs or DCs treated with PLGA films also showed phenotypical changes with increased up-regulation of co-stimulatory molecules and DC maturation markers, and decreased endocytic ability. However, as shown in Figure 6-7, mDCs or DCs treated with PLGA films did not induced IL-12p70 in co-cultures with T cells at significantly different levels compared to the negative control of iDCs. Production of IFN-γ in co-cultures of T cells with mDCs or DCs treated with PLGA films appeared to suppress IL-12p70 production in the absence of the antigen as shown in Figure 6-6 and 6-7. These results are different from what is typically seen in that IFN-γ and IL-12 (p40 or p70) are supportive each other in the inducing the immunogenicity of DCs and T cells (Gautier et al., 2005; Fujii et al., 2005; Grauer et al., 2007). However, it has also been reported that, if inflammatory mediators induced DC maturation by showing peptide-MHC complex expressions and upregulation of co-stimulatory molecules without IL-12 release, these DCs did not induce CD4+ T cell differentiation (Sporri and Sousa, 2005). This might partially explain why mDC and DCs treated with PLGA, chitosan, or alginate film did not induce differential levels of CD4+ expression in co-cultured T cells (Fig. 6-2), associated with IL-12p70 release from DCs treated with these biomaterial films (Fig. 6-6b) or associated with co-cultures of T cells and DCs treated with these biomaterial films (Fig. 6-7b) without differential levels in the presence of the antigen.

Unexpectedly, co-cultures of T cells with DCs treated with alginate or agarose films induced significantly increased levels of IL-12p70 and IL-10 release at the same time as shown in

Figure 6-7; alginate film induced significantly higher levels of IL-12p70 and IL-10 release at the same time compared to some other biomaterial films in the absence of the antigen, whereas agarose film did the same in the presence of the antigen. Treatment of DCs with agarose films resulted in higher levels of IL-10 release in co-cultures with T cells as compared to the other biomaterial films both in the absence and presence of OVA. This suggests that DC treatment with agarose films is a strong inducer of IL-10 in co-cultures with autologous T cells. Presicce et al.(Presicce et al., 2008) recently found that mannose receptors (MR) on surface of human monocyte-derived DCs partially mediated stimulatory activity of KLH on DC phenotype changes. In their study, both IL-12 and IL-10 were secreted from DCs treated with KLH in significantly higher levels than the negative control DCs, combined with upregulation of CD40, CD80, CD86, CD83, or HLA-DR. However, once MRs were blocked by monoclonal antibodies, DCs treated with KLH released IL-12 and IL-10 at significantly decreased levels and the capacity of these DCs for allogeneic T cell proliferation also decreased in association with decreased upregulation of CD40, CD80, CD86, CD83, or HLA-DR, compared to DCs treated with KLH without monoclonal anti-MR antibody treatment. In the Chapter 4, DC treatment with alginate films resulted in lower levels of endocytic ability and expression of CD32 (Fcγ Type II) and CD206 (MR) as compared to iDCs while agarose had the opposite effect. Thus receptors related with endocytosis of DCs or peptide-MHC complexes expressed on the surface of DCs might, at least, partially dictate release of both IL-12p70 and IL-10 upon DC-T cell contact through the immunological synapse.

As a major factor in driving the Th2 subset, IL-4 is known to be produced by Th2 lymphocytes, mast cells, or eosinophils (Nelms et al., 1999). Actually, recombinant human IL-4 has been employed in the present study during DC culture to suppress macrophage activation but other specific effects of IL-4 on DC culture remain unclear (Yao et al., 2005). Interestingly, as

shown in Figure 6-6, only DCs treated with agarose films exhibited significantly lower levels of IL-4 release than iDCs and DCs treated with the other biomaterial films. However, after co-culture of agarose-treated DCs with T cells levels of IL-4 release were similar to the negative control and all other biomaterials treatments with and without OVA (Fig. 6-7). This indicates that DC treatment with agarose films induced IL-4 release in a certain amount more than DC treatment with other biomaterial films upon DC-T cell contact. Similarly, DCs treated with LF 15-0195, an immunosuppressive reagent which induced decreased upregulations of CD40, CD86, and MHC II, resulted in increasing levels of IL-4 release along with increasing amount of LF 15-0195 for DC treatment in the co-culture with allogeneic T cells (Popov et al., 2006).

It has been generally accepted that, in the procedure of T cell mediated immunity, if DCs present the signal 1 (peptide-MHC complexes) without the signal 2 (co-stimulatory molecule up-regulations), this leads to anergy which is a critical pathway to tolerogenic response (Cunningham and Lafferty, 1977; Lenschow et al., 1996). Thus, given that DC treatment with agarose films induced endocytic ability or co-stimulatory molecule expressions in levels very similar to those of the negative control, iDCs as shown in the Chapter 4, it might not be a surprising observation that DCs treated with agarose films induced T cell CD4+CD25+FoxP3+ expression in levels very similar to iDCs (Fig. 6-5). However, upon DC treatment with agarose film in the presence of OVA antigen as well as in co-culture with T cells as shown in Figures 6-6 and 6-7, IL-12p70 or IL-10 release was modulated in significantly higher levels than iDCs and/or DCs treated with other biomaterial films. This indicates that agarose might be a potential inducer of tolerogenicity to a greater extent than iDCs. In addition to the possible involvement of LPS treatment of DCs and TLR-4 signaling pathway in IL-12p70 and IL-10 induction as mentioned earlier, Ghosh et al.(Ghosh et al., 2006) recently reported the demographic picture of individual TLR (TLRs 2–9)-driven profiles of various cytokines and chemokines using human PBMCs

(cells including DCs, B cells, and T cells were cultured together with agonist for T cell receptor (TCR) or each of all TLRs and then, cytokines and chemokines in the supernatant were examined). Using this autologous system, they found that TLR8 or TLR7/8 seemed to induce maximal Th1 (IL-12 and IFN-γ) or Th2 (IL-4) cytokines, respectively, among all TLRs examined, whereas almost all TLRs were simultaneously involved in IL-10 (Th2 cytokine) induction. Interestingly, TCR activated by agonists including anti-CD28 (ligand for CD80 or CD86 on DCs) induce most potent impact only on IFN-γ induction, compared to all other agonists for all TLRs. These all suggest that, to understand more detailed mechanisms behind indirect effects of biomaterial films on autologous T cell mediated immunity through phenotypical changes of DCs, future works might need to be performed focused on signaling pathways or engagements of PRRs (such as TLRs) or TCRs on DCs or T cells, respectively, depending on different biomaterial films or antigen presentation through peptide-MHC complexes during DC-T cell contact through immunological synapse.

Overall, the experiments presented herein support the premise that different DC phenotypes directed by different biomaterial films and/or the model antigen (OVA) control helper T- helper cell polarizations. First of all, T cell markers and cytokine profiles in Th1/Th2 polarizations were, at least, partially modulated depending on DC treatment with different biomaterial films and/or antigen, or co-culture with autologous T cells. The representative Th1 cytokine, IFN-γ was induced by mDCs or DCs treated with PLGA films at significantly higher levels compared to negative control and DCs treated with other biomaterial films when co-cultured with T cells. Treatment with agarose films was the only biomaterial which induced the release of IL-10 upon co-culture of DCs and T cells in association with induction of regulatory, CD4+CD25+FoxP3+ T cell activation. This is strong evidence indicating agarose is an inducer of immunosuppressive effects in the T cell mediated immunity. Taken together, DC

phenotypical changes, such as increased up-regulations of CD40, CD80, CD86, CD83, and HLA-DQ and low endocytic ability of mDCs or DCs treated with PLGA films as shown in the previous study, appeared to induce a Th1 response, whilst expression levels of these molecules and high endocytic ability similar to iDCs obtained for DCs treated with agarose films appeared to induce an immunosuppressive Th2 response.

In this study, we have demonstrated multifunctional effects of DCs treated with different biomaterial films on autologous T cell mediated immunity, thereby elucidating the potential T cell activation or polarization in the adaptive immune response, which can be expected when those biomaterials are introduced *in vivo* in combination products. This understanding of T cell activation or polarization associated with DC maturation when DCs are treated with biomaterial films is expected to provide key information on selection of biomaterials in the combination products for tissue engineering or vaccine delivery, further expanding the application into the immunotherapeutic tools. For instance, PLGA might be useful for anti-cancer (immunogenic) therapy through the Th1 polarization induced, whereas agarose might be beneficial to obtain an immunosuppressive (tolerogenic) effect on autoimmune disease such as rheumatoid arthritis through the Th2 polarization and CD4+CD25+FoxP3+ autologous T regulatory cell induction.

CHAPTER 7[†]

DIFFERENTAIL INTEGRATION OF BIOMATERIALS IMPLANTED INTO THE KNEE JOINT OF RHEUMATOID ARTHRITIS-INDUCED RABBIT

INTRODUCTION:

Rheumatoid arthritis (RA) is generally believed to be caused by a combination of genetic, environmental, and hormonal factors but the exact mechanism of the autoimmunity initiation is not yet clearly answered due to its complicated etiology. Even though tremendous efforts have been made on the immunological mechanisms, which show a massive influx of T cells, B cells, and fibroblast-like synoviocytes, macrophages, and dendritic cells (DCs) in the synovial tissue, the pathophysiological pathways of RA remain unclear, like as most of the other autoimmune diseases (Bresnihan and Tak, 1999; Miossec, 1995; Weyand and Goronzy, 1997). In the course of the disease, associated with the pannus formation and destruction processes, the massive influx of various cells above infiltrates into the synovial tissue (ST) and accumulates at the junction of the pannus and cartilage. The pro-inflammatory cytokines such as tumor necrosis factor (TNF)-α, interleukin (IL)-1, and IL-6 subsequently activate signal transduction pathways and transcription factors, which, in turn, control the transcription of cytokines.

To treat arthritis patients. various anti-inflammatory drugs have been employed for pharmacologic therapies (Robbins et al., 2003). However, these drugs should be frequently injected into the patients for long time duration and is limited to treatment of those with minor RA symptoms. Moreover, these drugs are not only ineffective at preventing the destruction of bone and cartilage or restoring joint function, but also can lead to undesirable side effects (Arend and Dayer, 1995; Brennan et al., 1989; Elliott et al., 1993; Dayer and Fenner, 1992; Wooley et al., 1993).

[†] A manuscript will be prepared from this Chapter 7 upon completion of data analysis.

As another clinical method for RA patients, surgical treatments have also utilized to reduce a risk of side effects by extracting inflamed area out of patient's knee. However, such surgical treatments still have problems of limited restoration of a durable articular surface for long term. Moreover such surgical procedures for the knee are associated with harshly complicated procedures, high cost, and limited movements of patients (Buckwalter and Mankin, 1998; Hunziker, 2002).

Tissue engineering has been recognized as a promising alternative for cartilage reconstruction and regeneration, providing a relatively simple procedure and long-term drug-free remission. In conjunction with great possibilities of minimally invasive and less complicated procedures for patients, cartilage tissue engineering has been motivated by the need of replace lost or damaged tissue with an already structurally and mechanically functional implant that can be created *in vitro* using chondrocytes or chondroprogenitor cells in combination with biomaterials (Suh and Matthew, 2000; Cancedda et al., 2003; Zhang et al., 2005; Kuo et al., 2006). However the host immune response against the biomaterial component or device is still a major concern on the achievement of tissue restoration (Babensee et al., 1998).

Dendritic cells have been proposed to play a central role not only in the initiation and perpetuation of RA (Waalen et al., 1986; Pettit and Thomas, 1999; Santiago-Schwarz et al., 2001; Radstake et al., 2005), but also in host immune response against biomaterials, associated with the adjuvant effects (Babensee et al., 1998). Adjuvant effects associated with biomaterials *in vivo* (Matzelle and Babensee, 2004; Babensee and Paranjpe, 2005; Yoshida and Babensee, 2004; Bennewitz and Babensee, 2005) and human monocyte-derived DC maturation upon treatment with biomaterials *in vitro* (Babensee and Paranjpe, 2005; Yoshida and Babensee, 2004; 2006; Yoshida et al., 2007) have been previously demonstrated. Following these basic studies to understand biomaterial effect on phenotypical changes in DC maturation, five inherently different

biomaterials in 2-dimensional (2-D) form were used to treat DCs and these different biomaterials induced differential levels of phenotypical changes in DC maturation as shown in the Chapter 4. Furthermore, when DC treated with these different biomaterials in 2-D form were co-cultured with autologous T cells, phenotype and polarization of co-cultured T cells were differentially induced depending on different biomaterials as shown in the Chapter 6. Interestingly, among different biomaterials tested, PLGA and agarose exhibited opposite results: PLGA induced phenotypical changes of DC maturation in higher levels much like the positive control of LPS-treated DCs, whereas agarose treatment of DCs resulted in a phenotype very similar to the negative control of iDCs. Also, PLGA treated DCs induced a T helper type-1 (Th1) phenotype of co-cultured autologous T cells for immunogenicity while DCs treated with agarose induced a T helper type-2 (Th2) phenotype of co-cultured autologous T cells for tolerogenicity. Recently, as shown in the Chapter 5, these PLGA and agarose in 3-dimensional (3-D) scaffold in porous form have been used to treat DCs and induced DC maturation with phenotype changes in levels very similar to those obtained from DC treatment with those in 2-D film form above.

To understand the influence of RA environment to different biomaterials and to identify biomaterial useful for tissue engineering in the RA situation, integration of inherently different biomaterials (PLGA and agarose) based on their effects on DC phenotype, was assessed upon their implantation into the knee joint of rabbit with induced RA. Upon RA induction and biomaterial implantation, the knee swelling size and total leukocyte concentration of the right knee joints remarkably increased, compared to the untreated left knees. However, total leukocyte concentration in the peripheral blood or in the joint lavage of the left knees (untreated control) were observed in differential levels depending on the biomaterial implants. Furthermore, the profile of leukocytes in the knee with induced RA (right knee) was predominately granulocytes (eosinophils and neutrophils) while the contralateral untreated left

knee shown a distinctly different profile of leukocytes wherein a more balanced proportion of granulocytes and monocytes was observed.

METHODS:

Preparation of biomaterial scaffolds in porous form

The biomaterials used for scaffolds include poly(DL-lactic-*co*-glycolic acid) (PLGA) and agarose. All biomaterial scaffolds were prepared freshly for implanting procedure. Preparation methods of all biomaterial scaffolds were adapted or modified from the previously described methods (Chapter 5); PLGA scaffolds were prepared by salt-polymer casting particulate-leaching technique with NaCl at the leachable component (Mikos et al., 1994) and agarose scaffolds prepared by inverted colloidal crystal templating method using polystyrene beads as leachable component (Lee et al., 2006). Briefly, poly(DL-lactic-*co*-glycolic acid) (PLGA) (ester terminated; molar ratio: 75:25, inherent viscosity: 0.70 dL/g in trichloromethane; 100,000 MW; Birmingham Polymers, Birmingham, AL) was dissolved with 8.3% w/v in dichloromethane (DCM) overnight at room temperature. Then, this PLGA/DCM solution was poured over 16 g NaCl (90-125 μm) in a Teflon dish of 50 mm diameter and 24 mm depth (BrandTech, Essex, CT) in the chemical fume hood. After complete mixing PLGA/DCM solution and salt using paper clip, the Teflon dish was gently shaken on the vortex for 20 ~ 30 minutes in the chemical fume hood, to facilitate homogeneous distribution of salts and expedite initial evaporation of solvent (DCM). Then, final evaporation of the DCM and drying were performed without shaking in the chemical fume hood for 36-48 hours followed by leaching salt in ddH_2O using a shaker for 2 days changing water 3 times. Scaffolds were then air-dried in the tissue culture hood for 24 hours, and freeze-dried overnight. For agarose scaffolds, polystyrene beads with 100 (±1.5%) μm (particle counter size standards, Duke Scientific, Palo Alto, CA)

were washed 3 times using isopropanol (Sigma), and sonicated in isopropanol for 20 minutes followed by evaporation of isopropanol in the oven at 60ºC overnight. Then, polystyrene beads in Teflon beaker were sintered in the oven at 120ºC for 4 hours, and the crystal templates were prepared. Agarose (type V; high gelling; gel strength of ≥ 800 g/cm^2 at 1.0 %; Sigma; molecular weight is not known) was dissolved in ddH_2O to a concentration of 10% w/v by heating using a microwave until boiling and visible homogeneity was reached. Agarose solution was applied into the Teflon beaker having polystyrene bead template, and the beaker spun at 2,000 rpm for 3 minutes. After solidification of agarose hydrogel at room temperature, polystyrene beads were leached in tetrahydrofuran (THF) (Sigma) using shaker for 2 days changing THF 3 times in the chemical fume hood, followed by rinsing agarose scaffolds in ddH_2O for 30 minutes (3 times) using shaker in the chemical fume hood. Prepared scaffolds of PLGA and agarose were moved into the tissue culture hood, and punched of an size of 3.5 mm diameter and 4 mm length (cylindrical form), immersed into 70% EtOH for 30 minutes, and washed for 1 hour in endotoxin free water (LAL reagent water, Lonza, Walkersville, MD) changing water every 15 min. All scaffolds were UV-sterilized for 30 min per surface of top, bottom, and side in the tissue culture hood prior to use in implantation. Endotoxin content of biomaterial scaffolds was determined using a chromogenic Limulus Amebocyte Lysate assay (QCL-1000 Chromogenic LAL Endpoint Assay, Cambrex, Walkersville, MD). Endotoxin assays were performed on a smaller piece of scaffold (1.5 mm in thickness and 4.5 mm in diameter), which had undergone the same washing and sterilization procedures as scaffolds used for implantation. The scaffold pieces were suspended in endotoxin-free water and endotoxin assay performed. Standards in tissue culture treated polystyrene wells and sample wells of different biomaterials were treated with endotoxin-free water. Limulus amebocyte lysate was added in the presence of biomaterial and incubated for 10 min at 37˚C. Chromogenic substrate (Ac-Ile-Glu-Ala-Arg-pNA) was added to each well

and incubated for 6 min. Glacial acetic acid (25% v/v) (J.T. Baker) was added as a stop solution and the mixture was transferred into flat-bottom microplate and the absorbance was measured at 405 nm. Endotoxin content in the samples was read off standards generated from endotoxin standards, from the manufacturer's kit. Each sample was run in triplicate for quantification. The effective endotoxin content (EU/ml) of 1.5 mm-thickness and 4.5 mm-diameter scaffold of PLGA was 0.036±0.015 and agarose 0.134±0.019. Previous study has shown that minimum E. Coli endotoxin concentration of 100 EU/ml was required for DC maturation (Jotwani et al., 2003).

Establishment of antigen-induced arthritis (AIA)

Arthritis (AIA) was induced in rabbits as previously described (Storgard et al., 1999) and approved by Georgia Institute of Technology Institutional Animal Care and Use Committee (no. A08053). Briefly, as shown in Figure 7-1, 7-2a & 7-2b, male New Zealand White rabbits (3 kg; Myrtle's Rabbitry, Thomson Station, TN) were immunized on Day 0 in multiple subcutaneous sites with a total of 1 ml OVA (Sigma, 20 mg/ml) in 1:1 dilution of PBS and Freund's complete adjuvant (CFA, Sigma), and boosted 2 weeks later in multiple subcutaneous sites (Day 14) with 0.6 ml OVA (Sigma, 20 mg/ml) in 1:1 dilution of PBS and Freund's incomplete adjuvant (IFA, Sigma). Arthritis was induced 1 week later (Day 21) by intra-articular injection of 0.5 ml OVA/PBS (20 mg/ml) into the knee joint of anesthetized rabbits.

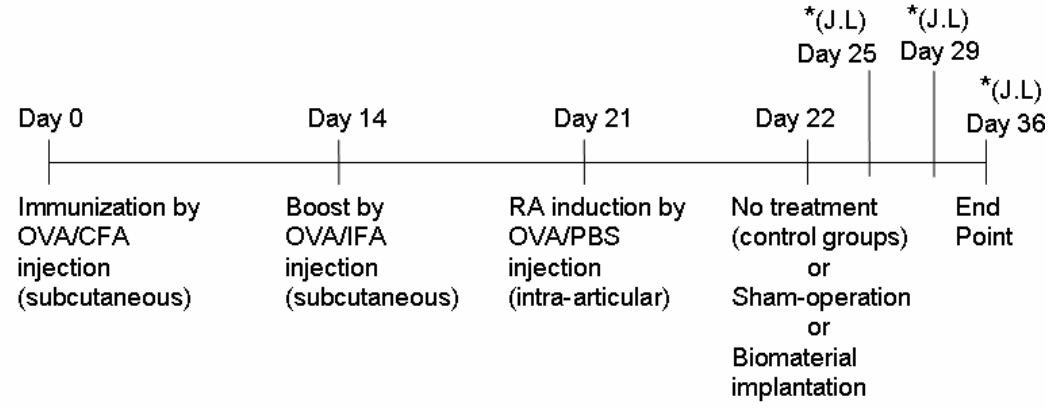

Figure 7-1: Time line of the rabbit study presented herein. This time line shows the procedure for the model combined together with RA induction and biomaterial implantation.

Survival anesthetizations were performed on Day 22, 25, 29, and 36 (the end point) for surgery or procedures. *(J.L) indicates the joint lavage procedure on scheduled time points of Day 25, 29, and 36.

Biomaterial scaffold implantation into rabbit knee joints

After 24 hours (Day 22) of arthritis induction above (Figure 7-1), aseptic survival surgery was performed on the knee joint of rabbits for implantation of biomaterial scaffold (Figure 7-2d & 7-2e). Under general anesthesia using 2% isoflurane, the lateral parapatellar incision was made and the patellar was dislocated. After the articular surface of the distal femur was exposed, a single osteochondral defect (3.2 mm diameter and 4 mm depth) was created in the trochlea groove using nitrogen-powered hand drill (Hall Powerpro, Conmed, Utica, NY). Then, PLGA or agarose scaffold was fitted into the defect, producing a fit flush with the articular surface. The patellar was relocated so that the patella glides over that fit flush to secure biomaterial scaffold in the defect (Kang et al., 1991) and then, the joint capsule and skin were closed by interrupted intradermal suturing using absorbable 5-0 suture and subcuticular suturing using absorbable 3-0 suture, respectively (both from Ethicon, Somerville, NJ). For the negative control of biomaterial implantation, one group was sham-operated without biomaterial implantation.

Treatment and control of rabbits

This *in vivo* research presented herein is composed of two different studies as shown in Table 4. Because this rabbit model combined together AIA induction and biomaterial implantation into the knee joint which has not been performed previously by us or others, to learn

techniques for rabbit handling and surgery as well as feasibility for this model, a pilot study was performed first and then, a full (experimental) study was performed incorporating points learned during the pilot study. Arthritis was induced for all rabbits, except the group of only PLGA implantation in the pilot study, by intra-articular injection of OVA/PBS as described above only into the knee joint of right hind limb per rabbit and biomaterial implantation or sham operation was also performed only into the same knee joint, whereas the left knee joint per rabbit was left untreated for the within-animal control. Only the control group of RA was not performed with surgical procedure as shown in Table 4.

Table 4. Rabbit groups and treatments

Study	Group identification code	Treatment	Rabbit number
Pilot study	RA	RA induction only	2
	RAPL	RA induction and PLGA implantation	2
	PL	PLGA implantation only	2
Full study	RA	RA induction only	3
	RAAG	RA induction and agarose implantation	3
	RAPL	RA induction and PLGA implantation	3
	RASH	RA induction and sham operation	3

Measurement of joint swelling

Joint swelling was measured using an electronic digital caliper (Control Company, Friendswood, TX) on Days 21, 22, 25, 29, and 36 (endpoint). The degree of joint swelling was calculated as swelling ratio, determined as joint size of the AIA and/or biomaterial implanted right knee divided by that of the contralateral untreated left knee.

Joint lavage and peripheral blood collection

On Days 25, 29, and 36 (endpoint), joint fluid from knee joints of both hind limbs per rabbit was lavaged by injection of 1 ml Gey's balanced salt solution (GBSS, Sigma) containing 5 U/ml heparin (Heparin Sodium Injection, 10,000 USP unit/ml, Abraxis, Schaumburg, IL) through

the patellar tendon. After manipulation of the joint to allow for ample mixing of joint fluid, using the same needle but another syringe pre-loaded with 50 µl of heparin, 250 ~ 300 µl joint fluid was aspirated per knee joint and then, kept on ice until cell analysis. At the same time of joint lavage, peripheral blood was also collected by piercing the central artery of rabbit ear using needle (BD vacutainer, Franklin Lakes, NJ). A single collection of blood was made per rabbit for each time of collection; 2 ml of blood was collected into a sampling tube pre-inserted with 500 µl of heparin for future cell analysis, whereas 1 ml of blood was collected into an empty tube for serum preparation for cytokine content analysis. Blood sample for cell analysis (2 ml with heparin) was gently shaken on a hemotology mixer, for a minimum of 2 hours to prevent blood clotting and then, kept on ice until cell analysis. The other blood sample (1 ml without heparin) for serum preparation was left at room temperature, for at least 3 hours to induce appropriate clotting until spinning for serum collection. After blood was clotted, the tube containing this blood for serum was spun at 12,000 rpm for 5 minutes and then, clear part at the top of sample was collected and saved at -20ºC until protein analysis.

Assessment of joint lavage sample

After collecting the joint fluid, the original sample was shaken by vortex and then, 200 µl was taken per knee joint sample and transferred into another tube. This 200 µl was spun at 1,100 rpm for 10 minutes to save supernatant for future TNF-α analysis and the supernatant was kept at -20 ºC until analysis. The cell pellet was resuspended in 1000 µl PBS for the right knee or 250 µl PBS for the left knee, and 10 µl of this cell suspension per sample was taken for total leukocyte concentration using the coulter cell counter (Multisizer 2, Beckman Coulter, Fullerton, CA) and then, cells with 7 ~ 20 µm size were counted as leukocytes according to the literature.(Manning et al., 1994) At the same time, 200 µl of this cell suspension in PBS was

taken and processed for Cytospin preparations as described previously (Yoshida and Babensee, 2004) (Cytospin Cytocentrifuge, Thermo Shandon, Pittsburgh, PA) and stained with Hematology Stain (Astral Diagnostics, West Deptford, NJ). Using this cytospin slide prepared, differential leukocyte counting was performed using light microscopy examination with an Axiovert 135 microscope (Zeiss, Jena, Germany). Due to unexpected difficulty of visual differentiation between neutrophil and eosinophil in rabbit blood, leukocytes were differentially counted as granulocytes (neutrophil + eosinophil), lymphocyte, and monocyte by percentages in total 100 ~ 300 cells per cytospin slide. For this differential leukocyte profiles, one cytospin slide was prepared per leg so that one rabbit had two slides for each of the right and left knee. In addition, a representative cell morphology using cytospin slide was selected from 3 rabbits per group using Image-Pro Plus (v.5) software (Media Cybernetics, Inc., Bethesda, MD).

Assessment of peripheral blood sample

For blood samples, 2 ml of blood mixed with heparin was shaken by vortex and then, 10 µl of this blood was added into a tube having 990 µl of red blood cell lysis buffer for total leukocyte concentration, whereas 100 µl was added into a tube having 900 µl of red blood cell lysis buffer for differential leukocyte counting using cytospin. These blood samples mixed with lysis buffer were incubated at 37 ºC for 20 minutes and then, processed with total leukocyte concentration and differential leukocyte profile as same as above. After blood was clotted, 1 ml of blood collected for serum collection was spun at 12,000 rpm for 5 minutes and then, clear portion at the top was collected and kept at -20 ºC until future TNF-α analysis.

Histology and micro-CT analysis on rabbit knee joints

At Day 36 of the end point, intact knee joints (both hind limbs per rabbit) were harvested

by cutting at the femoral and tibial diaphyses from all rabbits. One rabbit out of three rabbits per group was used for the histology analysis while two rabbits were used for the micro-CT analysis. For histology procedure, whole intact knee joints were fixed in 10% formalin and decalcified in 10% formic acid for 21 days in each of formalin and formic acid changing formalin or formic acid 3 times. The decalcified joints were embedded in paraffin and sections were prepared in 5 μm thickness. Sections were stained for cellularity with hematoxylin and eosin (H&E) and for proteoglycan content with safranin-O (fast green used as a counterstain). Focusing on the position of the osteochondral defect for the biomaterial implant or sham operation, one sagittal section of this defect per knee joint was selected (a sagittal plane at 500±50 μm away from the center of biomaterial/defect for all rabbits), and then, samples from all rabbits were compared for morphologies of cells and tissues including cartilage or synovial tissues from femur, tibia, and joint cavity adjacent to the defect position. A section for the RA-induced rabbit without the defect was prepared by sectioning the sagittal plane with a position corresponding to that of other knee joints with biomaterial/defect.

For micro-CT procedure, the distal femur of each knee joint was exposed by removing all skin and tissues except cartilage, bone and biomaterial implant, and these samples were fixed in 10% formalin for 3 days (Figure 7-2e). Then, these samples were incubated for 18 hours with 40% Hexabrix (contrast agent)/60% PBS at 37ºC. Femora of all samples were consistently secured such that the exposed surface of the defect was as close to perpendicular to the vertical axis of the micro-CT scanning tube (30 mm diameter). However, perfect alignment was not possible due to defect placement, femoral length, and tube diameter, therefore the z-axis of the defect was not equivalent to the z-axis of scanning. The scanning tube, containing PBS at the bottom, was sealed with parafilm to prevent dehydration during scanning. All scanning was performed in air using a μCT 40 (Scanco Medical, Bruttisellen, Switzerland) at a voxel size of 30

μm, E = 45 kVp, I = 177 μA, 200 ms integration time, and approximately 45 min acquisition time. Approximately 360 slices (4.3 mm) of each distal femur were scanned. After scanning, the reconstructed 2D axial slices were resectioned coronally for easier identification of the tissue formed around and on top of the defect or biomaterial implant. For defect femora, a volume of interest (VOI) was defined to include approximately 1mm (wherever possible) of surrounding cartilage on all sides of the defect as well as the superficial region of the defect to a depth that was level with the subchondral bone. For femora with no defects, a similar VOI was defined using relative bony and cartilaginous landmarks. Similar to the histology analysis, the defect and surrounding tissues including cartilage and bone were selected for images in the coronal and sagittal view. Additionally, to quantify average thickness and average attenuation changes, these parameters were calculated for the defect VOIs and normalized by contralateral control VOIs then compared between groups.

Statistical analysis

For statistical analysis, a two-way pairwise ANOVA utilizing a mixed model with repeated measure was used to determine statistical significance. For all statistical methods, the GraphPad (Version 5, La Jolla, CA) was used. If not indicated, p-value less than or equal to 0.05 was considered to be significant.

RESULTS:

RA induction, biomaterial implantation, and the knee joint swelling

On Day 22 (24 hours after the intra-articular injection of OVA), remarkable swelling of the right knee joint was observed compared to the untreated left knee joint as shown in Figure 7-2c and the swelling ratios of the right knee joint to the untreated left knee were shown in Figure

7-3 and 7-6. When the knee joint was opened for surgical procedure for biomaterial implantation on Day 22, inflamed tissues were observed (red color tissues) from the right knee joint as shown in Figure 7-2d and biomaterial implantation was performed fitting the implant flush with the joint.

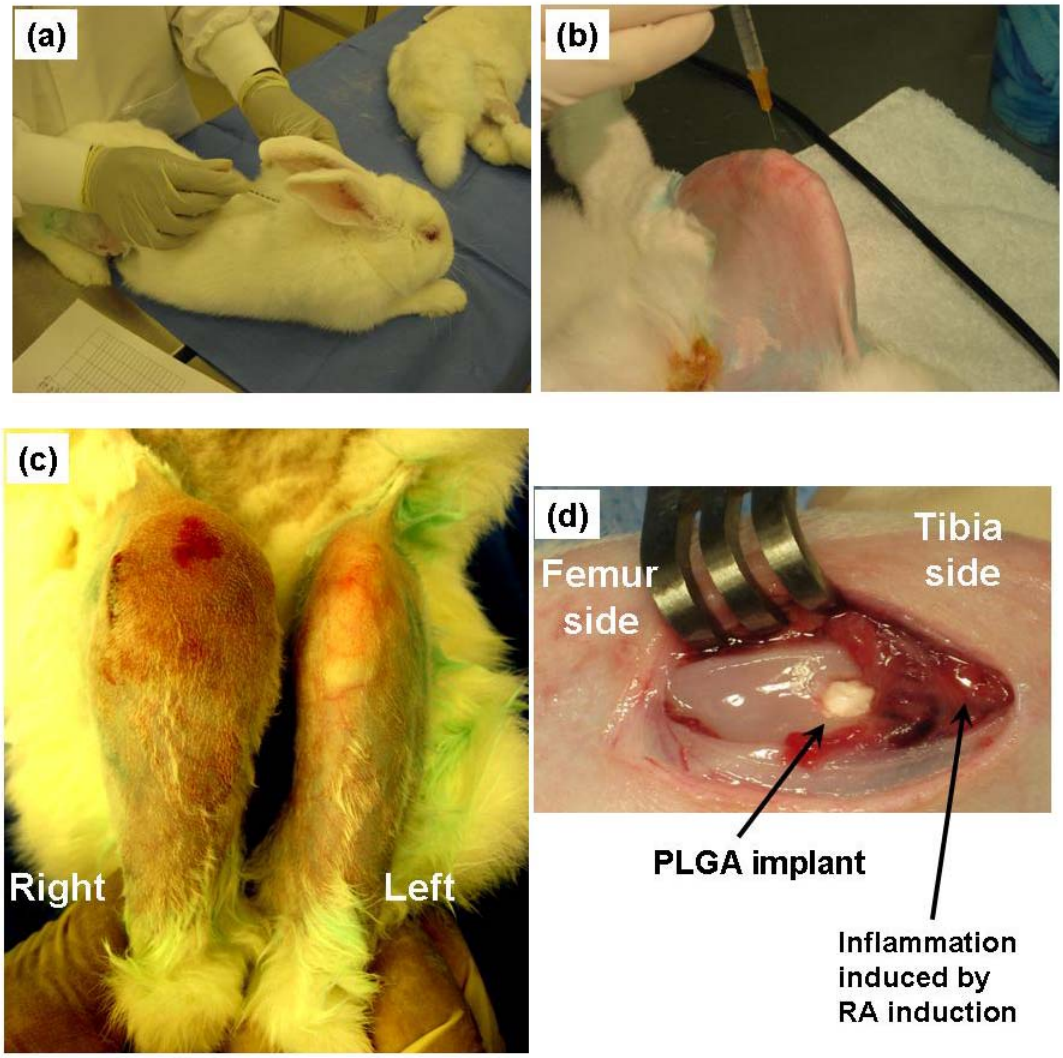

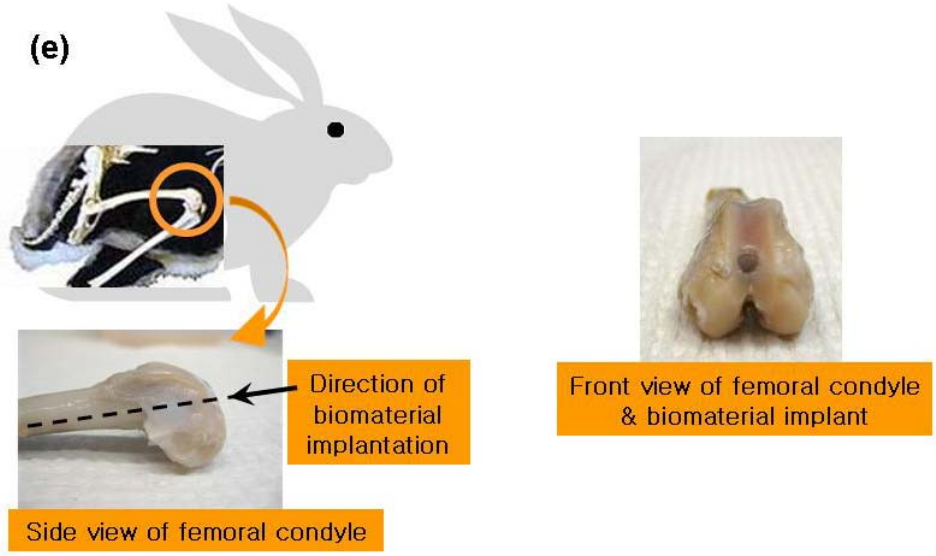

Figure 7-2: Representative pictures for the experimental procedure of the in vivo rabbit study.

(a) Subcutaneous injection for immunization (Day 0) or boost (Day 14). (b) Intra-articular injection of OVA/PBS for RA induction into the right knee after shaving hair (Day 21). (c) After 24 hours, intra-articular injection of OVA/PBS into the right knee induced remarkable swelling compared to the untreated left knee. (d) PLGA implantation was performed into the trochlea groove and inflamed tissue. (e) The femoral condyles dissected at the end point (Day 36) and biomaterial implanted position.

Results of the pilot study – joint swelling

As a result of the pilot study, wherein two rabbit were examined for each group of RA induction (RA), RA induction combined with PLGA implantation (RAPL), and PLGA implantation without RA induction (PL), upon RA induction, the right knees induced remarkable swelling as shown in Figure 7-2c above and the swelling ratio of the right knee to the untreated left knee peaked on Day 22 (Figure 7-3). However, the ratio decreased over time and did not show specific difference compared to only PLGA implantation especially on Day 29 and 36.

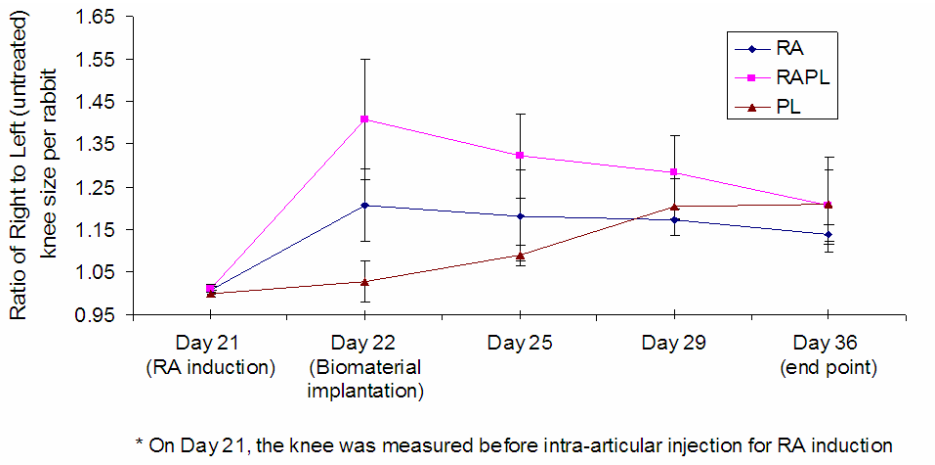

Figure 7-3: Joint swelling ratio of the right knee to the untreated left knee per rabbit in the pilot study.

The swelling ratios of rabbit with RA induction exhibited remarkable increase on Day 22 (24 hours after the RA induction by intra-articular injection). However, ratios from all rabbits did not show specific difference each other especially on Day 29 and 36. Ratios are shown as mean±SEM, n=2 rabbits.

Results of the pilot study – total leukocyte concentration in the joint lavage

Upon RA induction and/or PLGA implantation into the right knee, total leukocyte concentration increased in level much higher than the left knee and these patterns were maintained through the study (Figure 7-4). The total leukocyte concentrations in the lavage of joints with PLGA implantation without induced RA were lowest as compared to the other treatment groups with induced RA. However, the number of leukocytes for all treatments decreased over time.

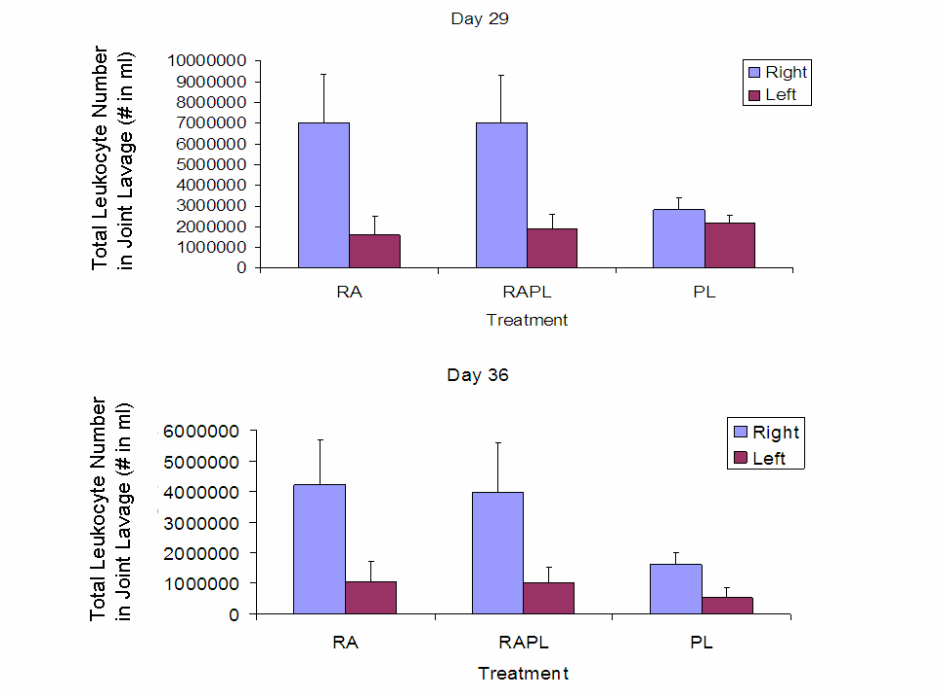

Figure 7-4: Total leukocyte concentration in the joint lavage fluid harvested from right or left knees in the pilot study.

Upon RA induction with or without PLGA scaffold implantation into the right knee, total leukocyte concentrations increased in harvested joint lavage fluids at a level much higher than in the left knee and these patterns were maintained through the study. However, the number of leukocytes for all treatments decreased over time. Due to unexpected problem with the coulter counting machine, it was impossible to obtain data on Day 25. Leukocyte numbers are shown as mean±SEM, n=2 rabbits.

Results of the pilot study – differential leukocyte profiles in the joint lavage fluid

Upon RA induction with or without PLGA scaffold implantation into the right knee, granulocyte percentages were present at a higher level than lymphocytes or monocytes in the right knees (Figure 7-5). For the contralateral left knee control the proportions of granulocytes and monocytes were more equal. In most cases, the percentages of lymphocytes were the lowest of the leukocyte types for all knee joints. Interestingly, on Day 36, both knees of rabbits having implanted PLGA scaffolds exhibited higher levels of monocytes compared granulocytes or

lymphocytes.

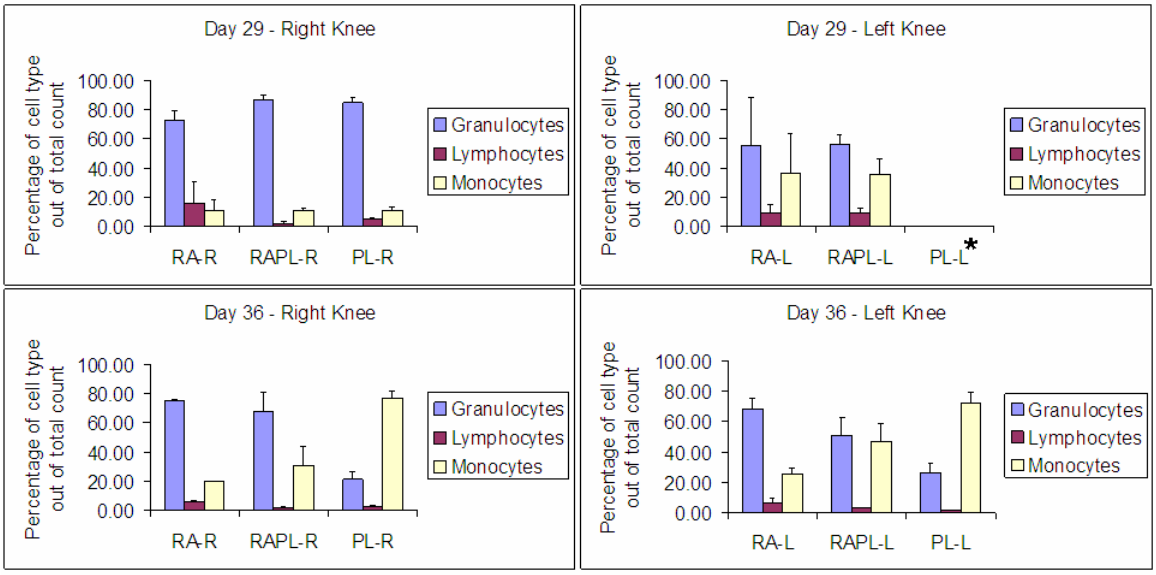

Figure 7-5: Differential leukocyte profiles in joint lavage fluid harvested from right or left knees in the pilot study.

Upon RA induction with or without PLGA scaffold implantation into the right knee, granulocyte percentages were present at level higher than lymphocytes or monocytes in the right knees, whereas the proportions of granulocytes and monocytes were more equal for the contralateral left knee control. Interestingly, on Day 36, both knees of rabbits having implanted PLGA scaffolds exhibited higher levels of monocytes compared granulocytes or lymphocytes. The differential leukocyte profile for Day 25 for all treatments and for the left knee of rabbit with only PLGA implant (PL-L*) on Day 29 was not obtained due to unexpected clotting problem of the lavage samples. Percentages of cell types per knee joint are shown as mean±SEM, n=2 rabbits.

From this pilot study, information valuable for next full study was obtained. First of all, feasibility of this rabbit model was confirmed by showing remarkable swelling of knee joints upon RA induction. In addition, various techniques useful for experimental procedures were acquired. For instance, rabbit handling, subcutaneous injection under physical restraint of rabbit, anesthetization of rabbit, and surgery techniques for appropriate implantation of biomaterials

were learned. For procedure of sample collections during the study, techniques for joint lavage and optimum dilution of this joint lavage for cell counting and cytospin were also learned. These all acquired techniques were subsequently applied to the full study.

Results of the full study – joint swelling

Similarly to the results of the pilot study, after 24 hours of RA induction, the joint swelling ratios of the right knee to the untreated left knee for all rabbits were remarkably increased on Day 22 and were maintained over time throughout the study duration without significant differences with other treatments, except for the groups of agarose scaffold implantation or sham operation on Day 29 (Figure 7-6). Agarose scaffold implantation into the RA joint induced average values of swelling ratio levels which were lower than joints with PLGA scaffold implantation or sham operation. Especially on Day 29, joints with implanted agarose scaffolds exhibited significantly lower swelling rations as compared to the sham operated joints. In addition, separate statistical analysis on joint swelling in the right and the left knee without ratio of the right to the left knee showed that only the left knee size of agarose-implanted rabbit was significantly different from that of sham-operated rabbit on Day 29 (these separate graphs are not shown here). This might affect the significant difference in the normalized data (ratio of the right to the left knee) on Day 29 as shown in Figure 7-6.

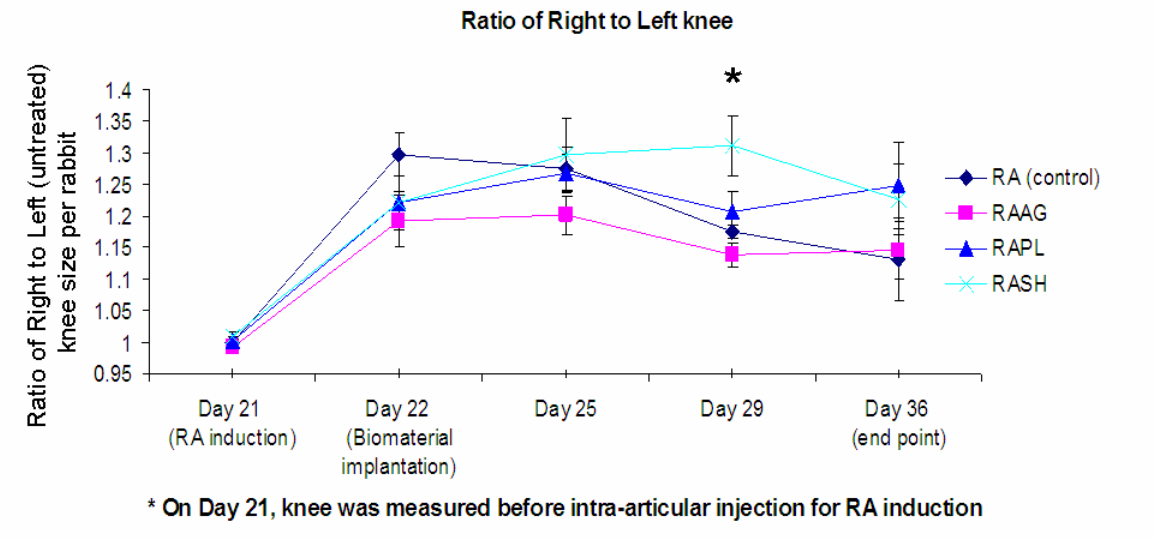

Figure 7-6: In the full study, the joint swelling ratios of the right knee to the untreated left knee per rabbit were remarkably increased on Day 22 and were maintained throughout the study duration without significant differences with other treatments, except for the groups of agarose scaffold implantation or sham operation on Day 29.

Agarose scaffold implantation into the RA joint induced average values of swelling ratio levels which were lower than joints with PLGA scaffold implantation or sham operation. Especially on Day 29, joints with implanted agarose scaffolds exhibited significantly lower swelling rations as compared to the sham operated joints. Ratios are shown as mean±SEM, n=3 rabbits. *: $p \leq 0.05$, compared pairwise among all treatments and statistically different between two treatments.

Results of the full study – total leukocyte concentration in the joint lavage

After RA induction and biomaterial scaffold implantation in the full study, the total leukocyte concentrations in the right knee joint were consistently higher than the untreated left knee for all treatment groups for the duration of the study (Figure 7-7). While the right knees of all treatments or control did not show any statistically different total leukocyte concentration amongst each other, at early time points, PLGA scaffold implantation into RA joints showed a trend of higher total leukocyte concentration. This observation was associated with the statistically higher number of total leukocytes in the left knee of rabbits with implanted PLGA scaffolds with induced RA as compared to all other treatments or control at all time points. All

treatments and control rabbit maintained the trends through the study duration, but the numbers of total leukocytes decreased over time.

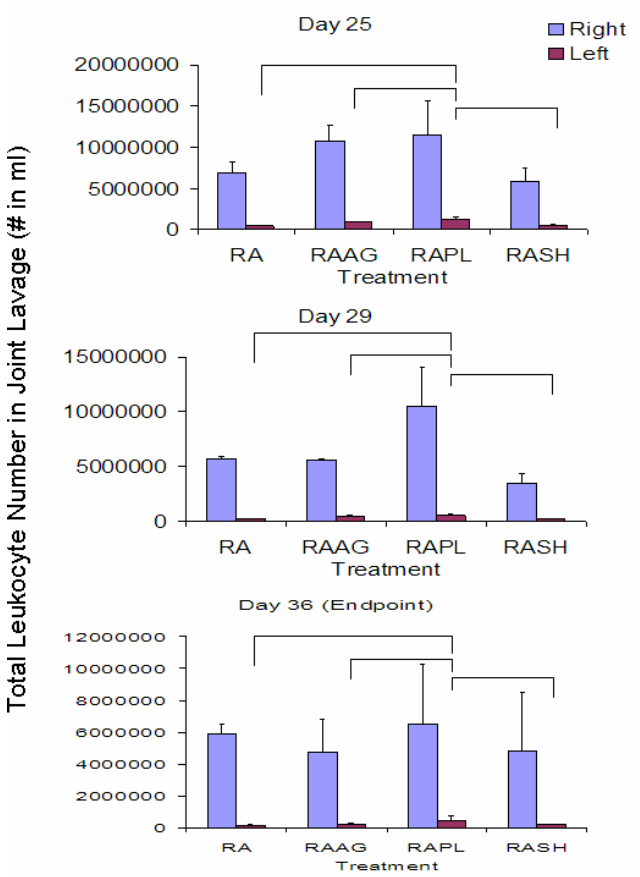

Figure 7-7: In the full study, the total leukocyte concentrations in the joint lavage fluid harvested from right or left knees.

After RA induction and biomaterial scaffold implantation in the full study, the total leukocyte concentrations in the right knee joint were consistently higher than the untreated left knee for all treatment groups for the duration of the study. While all treatments and control rabbit maintained the trends through the study duration, the numbers of total leukocytes decreased over time. Interestingly, at all time points, statistically higher number of total leukocytes in the left knee of rabbits with implanted PLGA scaffolds with induced RA was observed as compared to all other treatments or control. Leukocyte numbers are shown as mean±SEM, n=3 rabbits. Brackets: $p \leq 0.05$, compared pairwise among all treatments and statistically different between two treatments.

Results of the full study – differential leukocyte profiles in the joint lavage fluid

Upon RA induction and implantation of biomaterial scaffolds in the full study, granulocyte percentages were present at a higher level than lymphocytes or monocytes in the right knees for the duration of the study (Figure 7-8). For the right knee, on Day 25, sham-operated rabbits exhibited granulocyte percentages at levels significantly higher than for other treatments or control, whereas monocyte percentages of sham-operated rabbits were observed at levels significantly lower than for other treatments or control. Percentages of granulocytes or monocytes in the untreated left knees of all rabbits were very similar amongst each other on Day 25. However, from Day 29 onwards, there was a change towards higher percentages of monocytes compared to granulocytes for RA-induced rabbits with implanted PLGA scaffolds or sham operations. Finally, joint lavages of the left knee of RA-induced rabbits with implanted agarose scaffolds demonstrated percentages of monocytes that were significantly higher than granulocytes, on Day 36.

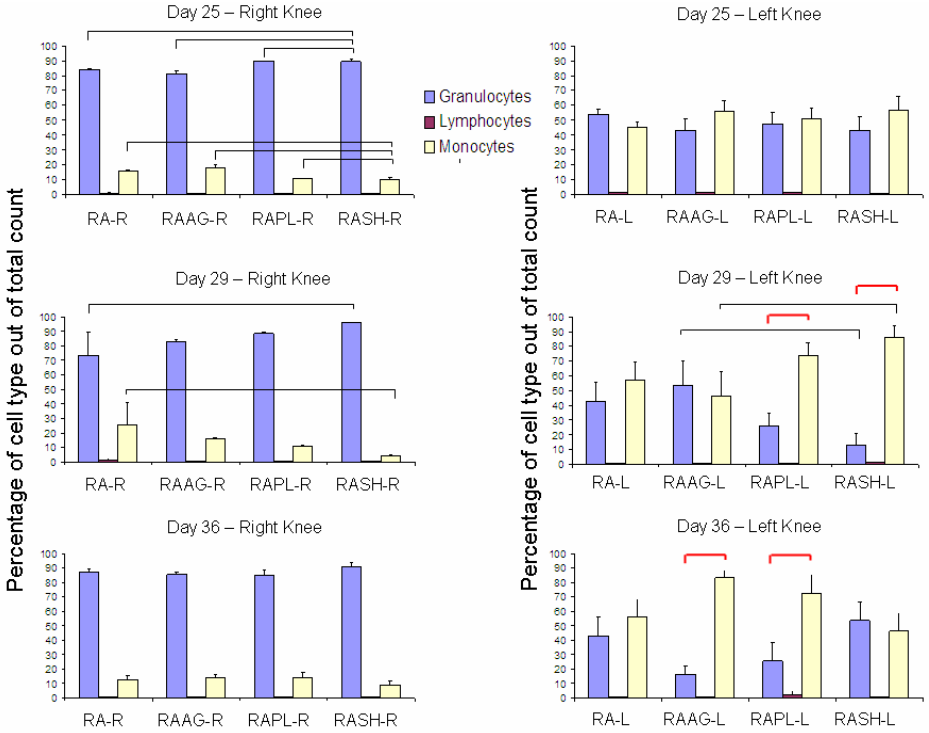

Figure 7-8: In the full study, upon RA induction and implantation of biomaterial scaffolds, granulocyte percentages were present at a higher level than lymphocytes or monocytes in the right knees for the duration of the study.

Percentages of granulocytes or monocytes in the untreated left knees of all rabbits were very similar amongst each other on Day 25.. However, from Day 29 onwards, there was a change towards higher percentages of monocytes compared to granulocytes for RA-induced rabbits with implanted PLGA scaffolds or sham operations.. Percentages of cell types per knee joint are shown as mean±SEM, n=3 rabbits. Black brackets: $p \leq 0.05$, compared pairwise among all treatments and statistically different between two treatments; Red brackets: $p \leq 0.05$, compared pairwise among all cell types within a single treatment or control, and statistically different between two cell types. For both knees of all rabbits at all time points, difference between lymphocytes and granulocytes or monocytes is significant, and only for the right knees of all rabbits at all time points, difference between granulocytes and monocytes is significant. Brackets for these differences are not shown.

Results of the full study – total leukocyte concentration in the peripheral blood

Upon RA induction, total leukocyte concentrations in the peripheral blood were measured at the same time point as collection of the joint lavage. The total leukocyte concentrations in the peripheral blood were observed at differential levels depending on biomaterial scaffold implantation in the RA knee joint (Figure 7-9). On Day 25 and 36, total leukocyte concentrations in rabbit peripheral blood were not significantly different each other for all rabbit groups. However, on Day 29, RA-induced rabbits with implanted PLGA scaffolds showed significantly higher total peripheral blood leukocyte concentrations, similar to the RA-only rabbits, as compared to RA-induced rabbits with implanted agarose scaffolds or sham-operated rabbits.

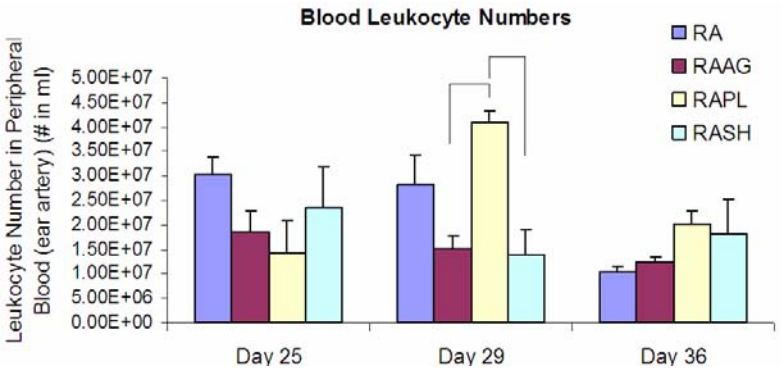

Figure 7-9: The total leukocyte concentrations in the peripheral blood were observed at differential levels depending on biomaterial implantation in the RA knee joint.

After RA induction, total leukocyte concentrations in the peripheral blood were measured at the same time point as collection of the joint lavage. On Day 25 and 36, total leukocyte concentrations in rabbit peripheral blood were not significantly different each other for all rabbit groups. However, on Day 29, RA-induced rabbits with implanted PLGA scaffolds showed significantly higher total peripheral blood leukocyte concentrations, similar to the RA-only rabbits, as compared to RA-induced rabbits with implanted agarose scaffolds or sham-operated rabbits. Leukocyte numbers are shown as mean±SEM, n=3 rabbits. Brackets: $p \leq 0.05$, compared pairwise among all treatments and statistically different between two treatments.

Results of the full study – histology and micro-CT analysis

To investigate morphological changes of cartilage or bone tissue and degradation of cartilage upon biomaterial implantation into the RA-induced knee joints, histology and micro-CT analysis were performed on the right and left knee joints of all rabbits. First of all, as seen in the attenuation numbers in Table 5, the control group of RA-induced rabbits exhibited higher value of x-ray attenuation in the right knee compared to the left knee. This indicates that the RA induction in the right knee might have proteoglycan content less than the untreated left knee, possibly correlated with thinner cartilage weakly stained with safranin-O (red) in the right knee as compared to the untreated left knee for only RA-induced rabbit as shown in the histology (Figure 7-11). Similar to this control group of RA-induced rabbits, biomaterial implanted rabbits or sham-operated rabbits also showed x-ray attenuation at higher levels in the right knee than the

untreated left knee. However, x-ray attenuations for both right and left knees and normalized cartilage thickness (Figure 7-10) obtained from biomaterial implanted rabbits or sham-operated rabbits were observed at levels similar amongst them. In line with these attenuation numbers and cartilage thickness (a top layer in green color per each image) shown in the micro-CT images (Figure 7-10), safranin-O staining in the histological analysis (Figure 7-11) showed that cartilage thicknesses of the biomaterial implanted or sham operated (right) knee have cartilage thicknesses thinner than those of the untreated left knees. Histological images showed that RA induction into the right knee induced lots of inflammatory cell infiltration (especially into the synovial tissue) and biomaterials are well integrated into the osteochondral defect. Interestingly, agarose-implanted rabbit exhibited cartilage layer healed over the defect while PLGA-implanted rabbit or sham-operated rabbit did not. In addition, sham-operated or agarose-implanted rabbit showed healing procedure of bone tissue into the osteochondral defect to higher extent than PLGA-implanted rabbit.

Table 5. X-ray attenuation values obtained from the micro-CT analysis on rabbit groups.
Two different rabbits per treatment or control group were examined on both hind limbs. Higher value indicates less content of proteoglycan in the cartilage layer examined using the micro-CT scanning (Palmer et al., 2006). Right or left indicates the right knee joint or the left knee joint, respectively. R/L is a ratio of x-ray attenuation value of the right knee joint to that of the left knee joint.

	RA			**RAAG**			**RAPL**			**RASH**		
	Right	Left	R/L	Right	Left	R/L	Right	Left	R/L	Right	Left	R/L
Rabbit 1	2.50	1.98	1.26	2.39	2.09	1.14	2.65	2.20	1.20	2.71	1.92	1.41
Rabbit 2	2.17	1.95	1.11	2.39	1.97	1.21	2.58	1.96	1.32	2.32	1.97	1.18

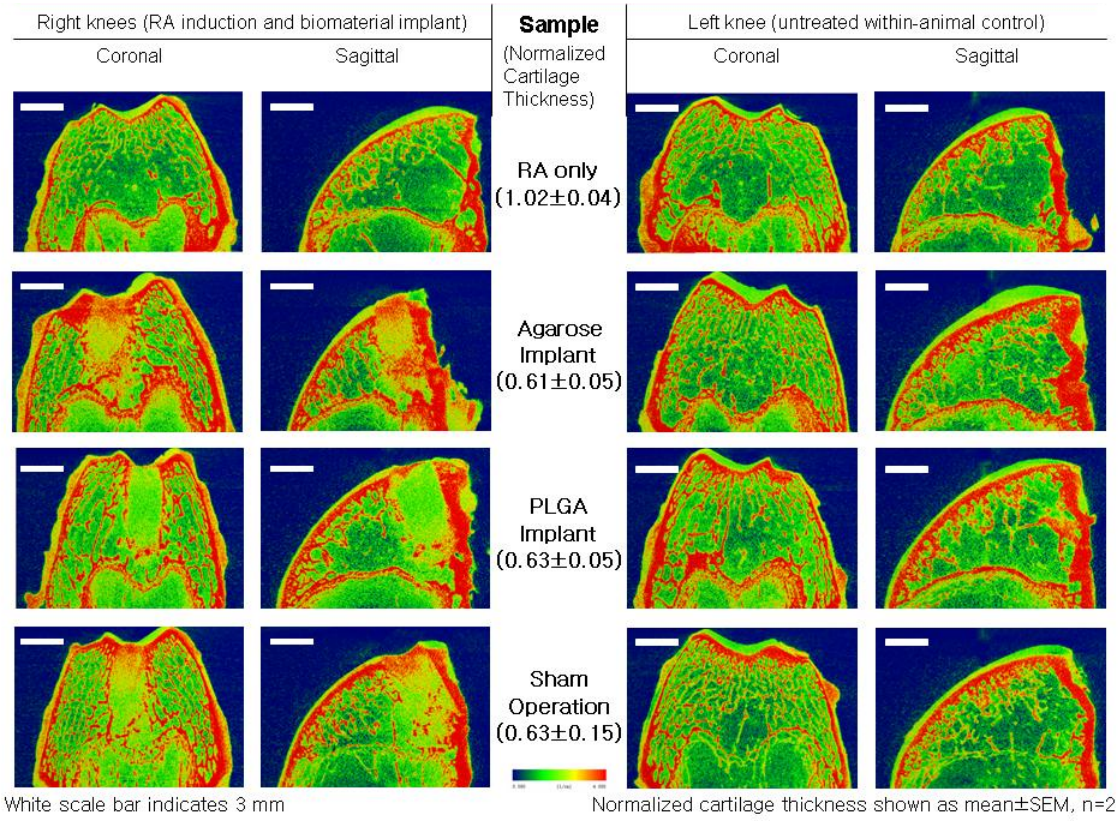

Figure 7-10: Representative micro-CT images of rabbit knee joints in treatment or control group.

After incubation of femoral condyle samples with the contrast agent (Hexabrix), samples were scanned using the micro-CT and then, the coronal or sagittal image was obtained per knee joint in differential colors depending on the contrast agent distribution into each sample. Red color indicates higher x-ray attenuation combined with higher contrast agent content (lower proteoglycan content) while green color does lower x-ray attenuation combined with lower contrast agent content (higher proteoglycan content). Images are shown by coronal or sagittal view in column and by treatment or control group in row. For instance, the coronal images of the right knee of biomaterial-implanted or sham-operated rabbit show the biomaterial scaffold or osteochondral defect in the middle. The cartilage thickness per knee joint was obtained as described in the Method section and the ratio (normalized cartilage thickness) of the thickness of the right knee joint to that of the left knee joint was averaged for two different rabbits per group.

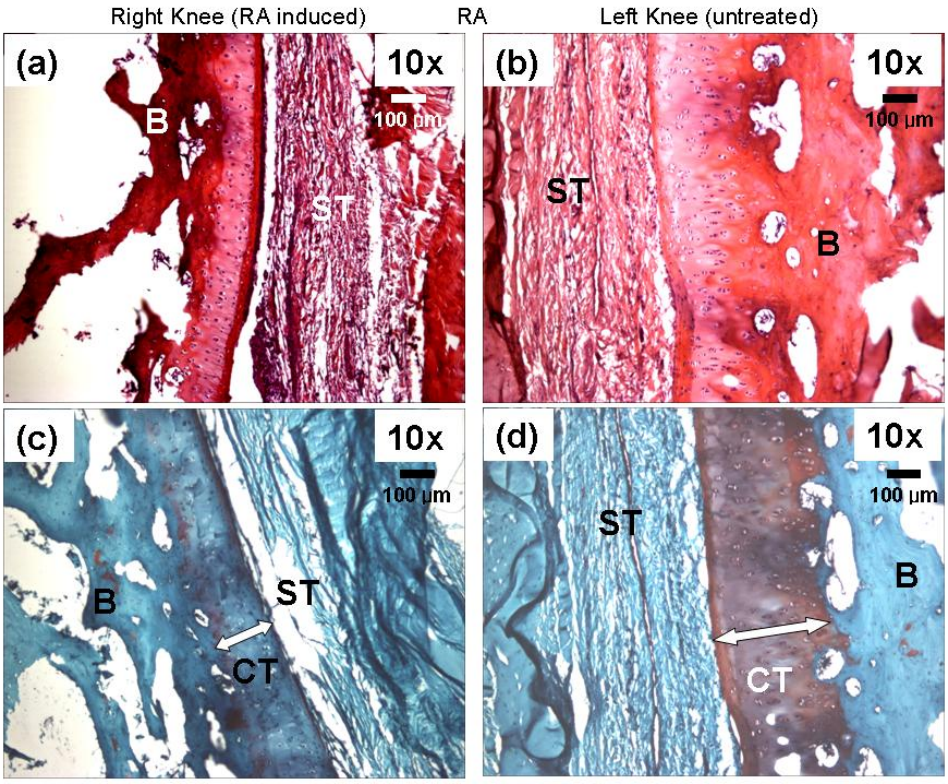

Figure 7-11: Representative images of histological analysis on rabbit knee joints in treatment or control group.

For the control group of RA, images (a-d) are shown with only cartilage and bone together with synovial tissue adjacent to the position corresponding to the biomaterial implantation or the osteochondral defect in other treatment group of rabbit: (a) and (b) are the right knee joint and the left knee joint, respectively, in H&E staining. (c) and (d) are the right knee joint and the left knee joint, respectively, in safranin-O/fast green staining. For the biomaterial-implanted or sham-operated groups, images are shown with biomaterial implantation site or the defect, in addition to the cartilage, bone, and synovial tissues adjacent to the biomaterial implantation or the defect. Red bracket indicates the original defect region. Higher magnification images are also shown together with the whole defect image. (e-p) images of agarose-implanted group of RAAG: (e) and (f) are adjacent tissue in the right knee joint and the left knee joint, respectively, in H&E staining. (g) and (h) are adjacent tissues in the right knee joint and the left knee joint, respectively, in safranin-O/fast green staining. (i) the whole agarose-implanted site/defect region in H&E staining. (j, k, l) images in H&E staining magnified from (i). (m) the whole agarose-implanted site/defect region in safranin-O/fast green staining. (n, o, p) images in safranin-O/fast green staining magnified from (m). (q-ab) images of PLGA-implanted group of RAPL: (q) and (r) are adjacent tissues in the right knee joint and the left knee joint, respectively, in H&E staining. (s) and (t) are adjacent tissues in the right knee joint and the left knee joint, respectively, in safranin-O/fast

green staining. (u) the whole PLGA-implanted site/defect region in H&E staining. (v, w, x) images in H&E staining magnified from (u). (y) the whole agarose-implanted site/defect region in safranin-O/fast green staining. (z, aa, ab) images in safranin-O/fast green staining magnifined from (y). (ac-an) images of sham-operated group of RASH: (ac) and (ad) are adjacent tissues in the right knee joint and the left knee joint, respectively, in H&E staining. (ae) and (af) are adjacent tissues in the right knee joint and the left knee joint, respectively, in safranin-O/fast green staining. (ag) the whole sham-operated defect region in H&E staining. (ah, ai, aj) images in H&E staining magnified from (ag). (ak) the whole sham-operated defect region in safranin-O/fast green staining. (al, am, an) images in safranin-O/fast green staining magnified from (ak). B: bone, ST: synovial tissue, CT: cartilage, SC: biomaterial scaffold. Both-sided arrow in white color indicates the cartilage thickness determined by the safranin-O staining.

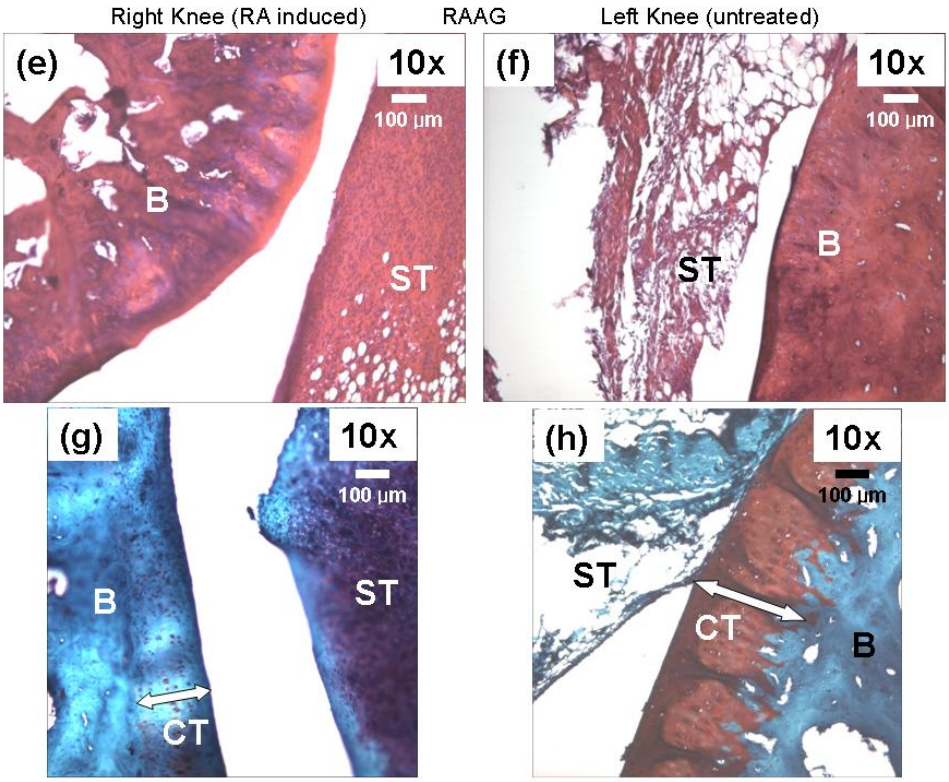

Figure 7-11: Representative images of histological analysis on rabbit knee joints in treatment or control group. (continued)

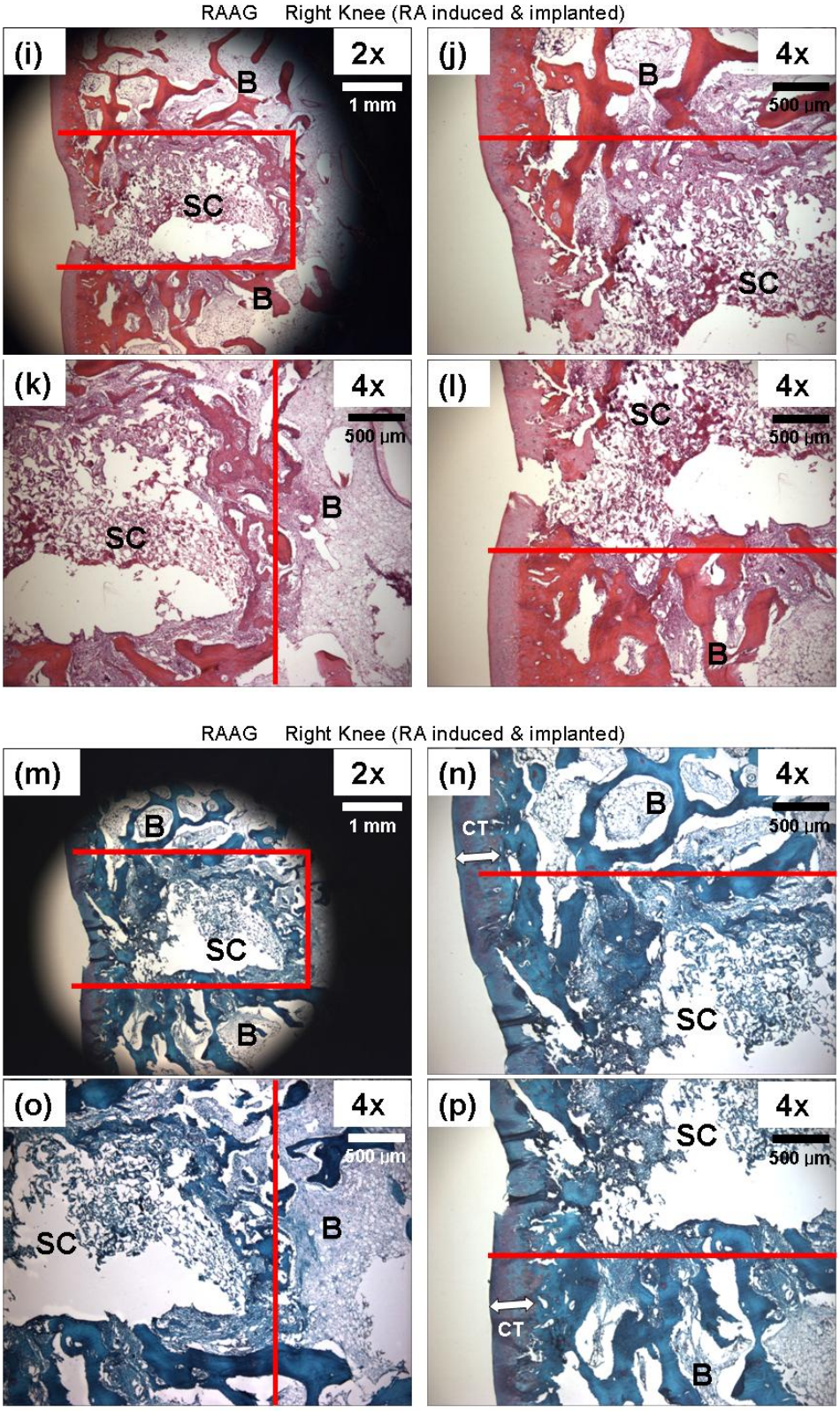

Figure 7-11: Representative images of histological analysis on rabbit knee joints in treatment or control group. (continued)

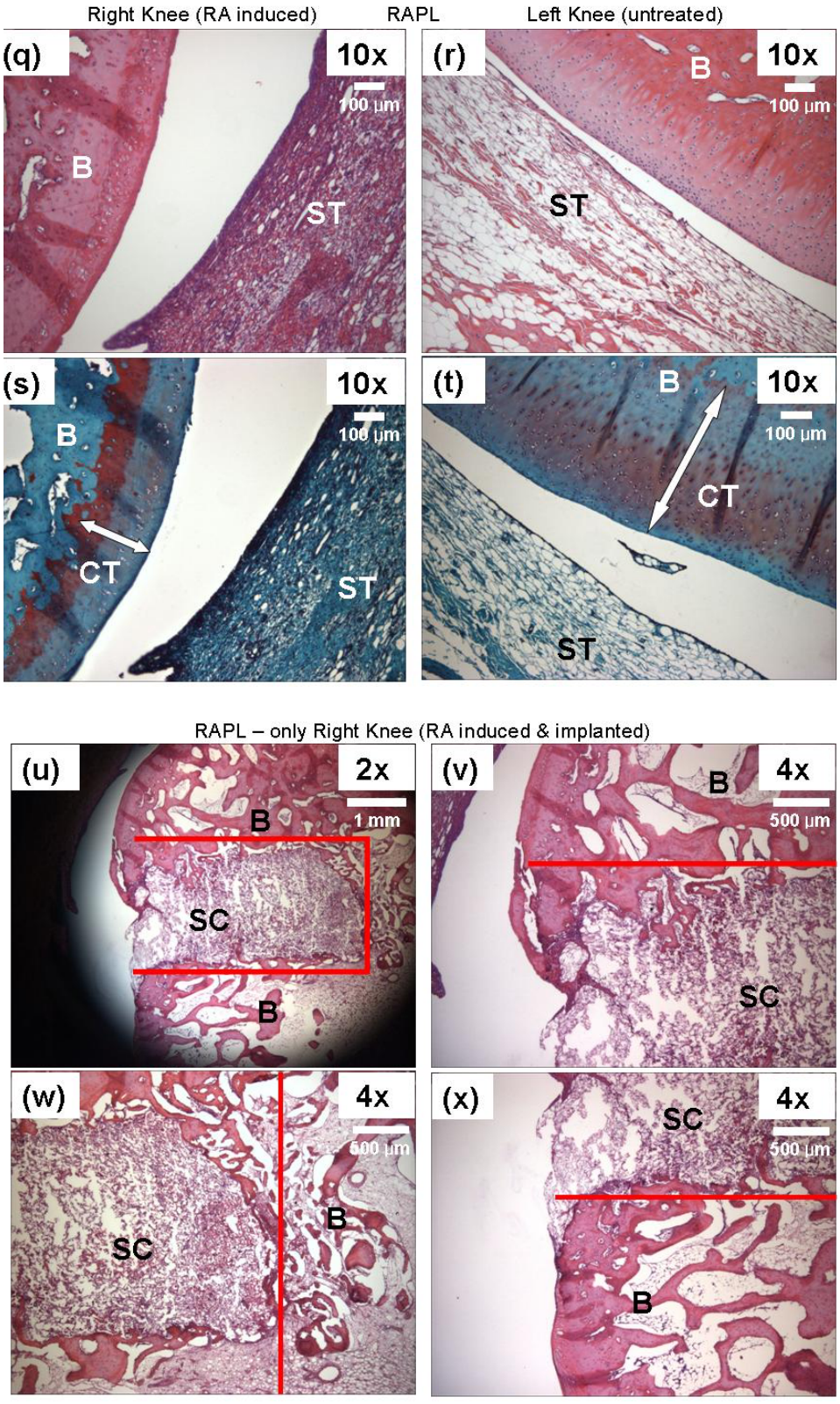

Figure 7-11: Representative images of histological analysis on rabbit knee joints in treatment or control group. (continued)

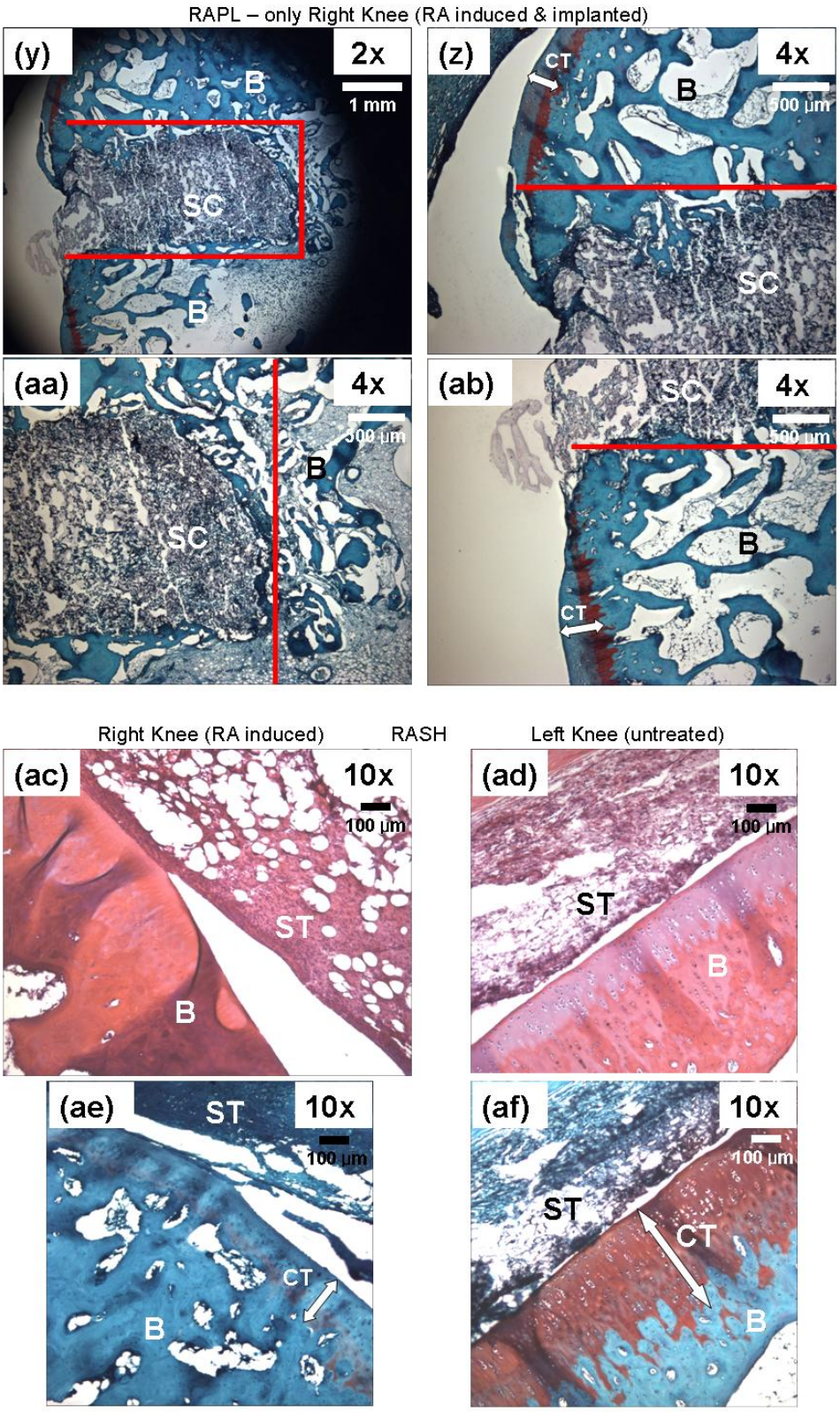

Figure 7-11: Representative images of histological analysis on rabbit knee joints in treatment or control group. (continued)

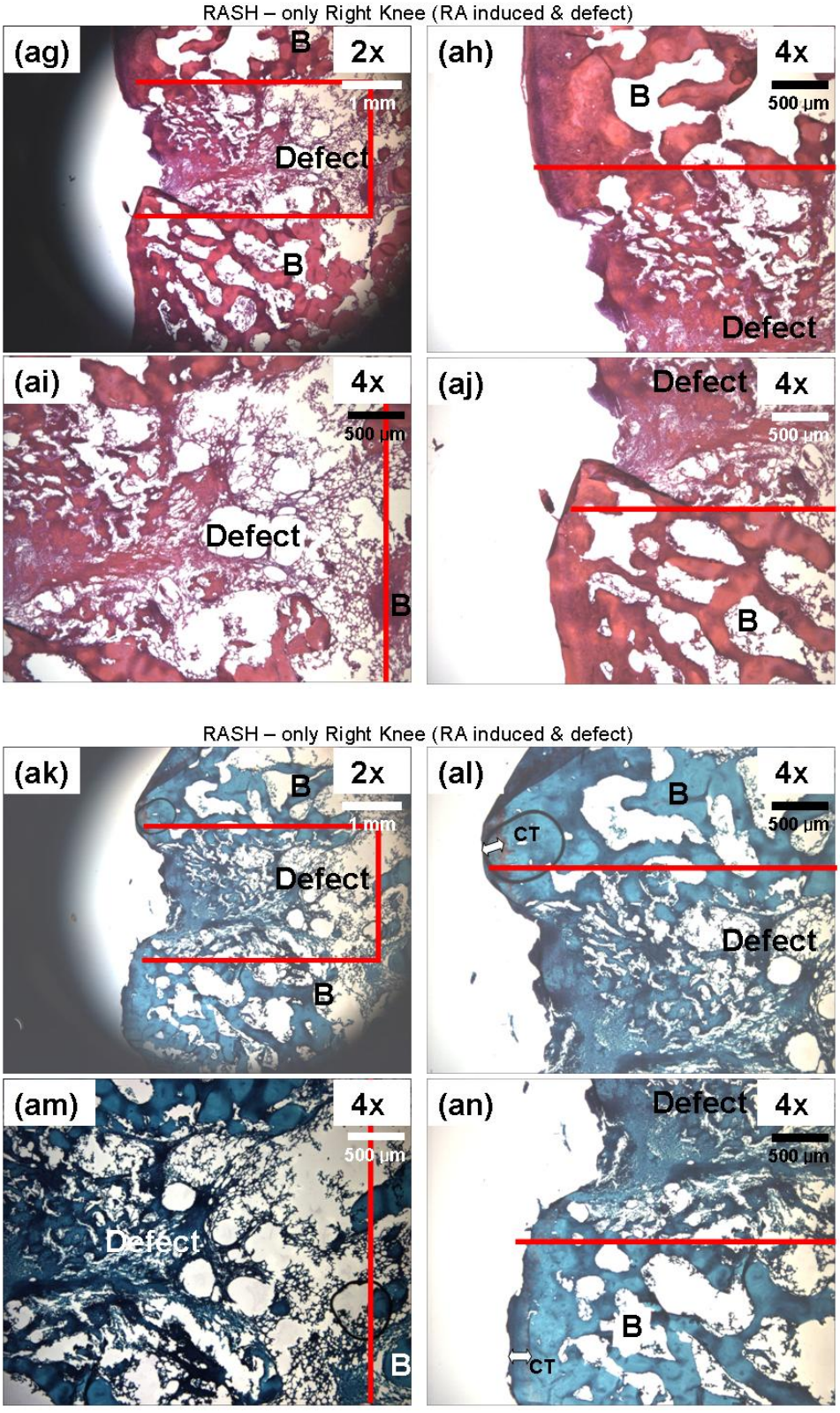

Figure 7-11: Representative images of histological analysis on rabbit knee joints in treatment or control group. (continued)

DISCUSSION:

The rabbit model developed herein combined together an AIA model for RA induction and biomaterial implantation into the knee joint that had not previously been studied. For this reason, the pilot study was necessary, above all things, to demonstrate feasibility of the model. First of all, the weight changes of all rabbits in the pilot study were observed within 15% of weight loss, which was the maximum loss for the decision to euthanize rabbits. In addition, expertise in rabbit handling, surgical procedure, biomaterial implantation, and sample collection by joint lavage were acquired through the pilot study. Collectively, findings of joint swelling, total leukocyte concentration (joint lavage), and differential leukocyte profile (joint lavage) in the pilot study confirmed that the model is acceptable and feasible for the experimental procedure to understand effects of biomaterial implantation into the RA knee joints.

The purpose of this research was to assess the effects of different biomaterials in 3-D scaffold porous form implanted into rabbit knee joints with induced RA. In this way, we assessed the integration of 3-D scaffold prepared from inherently different biomaterials scaffolds of PLGA or agarose, upon implantation into the knee joint of RA-induced rabbit. Clearly, different biomaterials implanted into the RA knee joint exerted effects to different levels especially in the contra-lateral untreated left knee joint or the systemic circulation of peripheral blood.

In the previous *in vitro* studies, the efforts of a large variety of immunobiological assays have been used to understand the mechanism behind DC phenotypical changes when DCs are treated with different biomaterial films or scaffolds. As a result, differential levels of DC maturation have been observed depending on the type of biomaterials used to treat the DCs, possibly associated with the inherently different chemistries of those biomaterials that are used. Based on these facts together with the previous results, taking into account that DCs play a

central role not only in the initiation and perpetuation of RA, but also in host response against biomaterials, associated with the adjuvant effect, it was hypothesized that different biomaterial scaffolds would exhibit an integration and acceptance to differential levels in the RA environment. These biomaterial implantation studies into rabbit joints with induced RA would hence provide a basis for biomaterial selection on which to build a biomaterial/tissue engineering strategy for treatment of diseased RA joints which may include incorporation of further immunomodulatory molecules and certainly the cells to form the new tissue.

Most noticeable observation in this study is that upon RA induction combined with biomaterial implantation or sham operation into the right knee joint, the knee swelling size and total leukocyte concentration in the right knee remarkably increased, compared to the untreated left knees, and these increased levels in the right knee consistently went throughout the study duration (Day 36). Unexpectedly, while the left knee of RA-induced rabbits with implanted PLGA scaffolds exhibited total leukocyte concentrations at levels that were significantly higher than all other treatments or control, this trend was not yet statistically significant with the number of animals tested to date. However, total leukocyte concentrations in the peripheral blood or in the joint lavage of the left knees were observed at differential levels depending on the biomaterial implant; PLGA scaffold implantation induced total leukocyte concentrations in the peripheral blood that were at a significantly higher level that for either agarose scaffold implanted or sham operated joints on Day 29. Furthermore, the left knee of RA-induced rabbits with implanted PLGA scaffolds exhibited significantly higher levels of total leukocyte concentration in the joint lavage as compared to those of rabbits with RA induction only, or sham operation through all time points.

Results of the differential leukocyte profiles in the joint lavages of the right knees of rabbits with induced RA with or without implanted biomaterial scaffolds as shown in Figure 7-8

are in line with the fact that synovial fluid of RA patients is heavily infiltrated with leukocytes that are predominantly composed of neutrophils (Pillinger and Abramson, 1995). Also, the percentages of granulocyte, lymphocyte, and monocyte composition observed in this study are very close to those reported in the literature wherein the rabbit AIA model was used (Kashiwagi et al., 2002). The granulocyte, which is combined together as neutrophils and eosinophils in this study, exhibited at least 80% in the total leukocytes counted for the right knees of all rabbits with induced RA, through this study duration.

In the previous *in vitro* studies in the Chapter 4 and 5, after 24 hours of DC treatment with different biomaterial 2-D films or 3-D scaffolds, CD44 expression on DCs and TNF-α release into supernatant from DCs were measured. For all cases, DC treatment with PLGA films or scaffolds induced CD44 expression or TNF-α release at levels significantly higher than DCs treated with agarose films or scaffolds, or for the negative control of iDCs. However, DCs treated with agarose films or scaffolds induced levels of these markers/cytokine release that were similar to the negative control of iDCs or significantly lower than observed for PLGA treated DCs. As an adhesion molecule facilitating the rolling of leukocytes by binding to the endothelium-expressed hyaluronan at sites of inflammation (Pure and Cuff, 2001), CD44 blocking procedure using specific anti-CD44 monoclonal antibody treatment induced *in vivo* anti-inflammatory effects in RA animal models (Mikecz et al., 1995; Mikecz et al., 1999). More recently, intravenous injection of anti-CD44 monoclonal antibody effectively suppressed leukocyte recruitment (rolling and adhesion) to the site of inflammation of murine RA model, also showing depletion of neutrophils in the peripheral blood (Hutas et al., 2008).

In the systemic circulation of peripheral blood, TNF-α has been accepted as the most important cytokine, among pro-inflammatory cytokines, involved in the RA pathophysiology and as a potent primer of neutrophils, the systemic effect of TNF-α on the neutrophil degradative

cascade observed from the bloodstream to the inflammatory site in RA disease pathogenesis has been significantly evaluated by highlighting various examples that blocking TNF-α activity down-regulating the neutrophil activation pathways (Edwards and Hallett, 1997) In addition, it has been reported that, upon induction of RA, rabbit model induced increase of leukocyte number in the peripheral blood and these leukocytes in the peripheral blood released higher levels of TNF-α compared to the level in the peripheral blood before RA induction (Kashiwagi et al., 2002). For human RA patients, Enbrel (a generic drug name of Etanercept) is one of the most popular drugs, which is a recombinant soluble form of human TNF-α receptor fusion protein. Enbrel is typically injected subcutaneously in a distance from the actual inflammatory site of the patient and then, it systemically inhibits the signaling pathway between TNF-α and TNF-α receptor by blocking TNF-α binding, thereby inducing suppression of inflammation at the RA site. Moreover, based on the clinical fact that symmetry is a remarkable feature of RA, the contra-lateral response to a unilateral inflammatory stimulus has been examined, and distal bilateral degeneration of articular cartilage was observed by a neurogenic mechanism (through nerve network) and/or a systemic circulation (Decaris et al., 1999). This indicates that untreated control knee might have been underestimated with its inflammation contra-laterally induced by intra-articular stimulus into the other knee within a single host (Shenker et al., 2003).

Thus, in association with the effect of non-biological materials on leukocyte activation within the systemic circulation (Hammerschmidt et al., 1980; Jacob et al., 1980) and our previous *in vitro* results for CD44 and TNF-α described above, it is conceivable that the systemic circulation of the peripheral blood possibly explains, at least partially, the mechanism behind which PLGA implantation into RA joint induced higher number of total leukocytes in the peripheral blood on Day 29 and in the left knee joints (untreated) throughout the study duration.

In the Chapter 6, autologous T cells were examined with their phenotype and polarization

upon co-culture of these T cells and DCs treated with different biomaterial films. Dendritic cells treated with agarose films (together with model antigen, OVA) induced CD4+CD25+FoxP3+ (T regulatory cells) expression on autologous T cells at level similar to iDCs and IL-10 release at higher levels whereas PLGA film treatment (together with model antigen, OVA) induced release of IFN-γ at higher levels, as compared to DC treatment with other biomaterial films, in the DC-T co-culture system. As a result of *in vivo* study using RA rabbit model wherein DCs also should be exposed to antigen and T cells, not all examinations shown here seem to be clearly correlated with the results observed in the previous *in vitro* T cell study. However, mechanism behind changes of blood total leukocyte concentration and total or differential leukocyte profile in the left knee joint lavage, which was possibly induced by contra-lateral effects associated with a systemic circulation, might be explained using the immunogenicity of PLGA observed from *in vitro* T cell study above.

To further understand the morphological changes of cells and tissues in cartilage and bone upon RA induction and biomaterial implantation/sham operation into the rabbit knee joint, micro-CT and histology analysis were also performed. Even though the cartilage thicknesses (a top layer in green color per each image) shown in the micro-CT images (Figure 7-10) seem similar between the right and left knees of only RA-induced rabbit, these rabbit knees exhibited higher value of x-ray attenuation in the right knee compared to the left knee. This indicates that the RA induction in the right knee might have proteoglycan content less than the untreated left knee, based on the fact that x-ray attenuation is a strong indicator of density of sulfated glycosaminoglycans (sGAGs) that are attached to the PG backbone (Palmer et al., 2006). In the histological analysis using safranin-O staining as shown in Figure 7-11, the RA-induced rabbits showed thinner cartilage layer which is weakly stained with safranin-O (red) in the RA-induced right knee compared to the untreated left knee. Collectively, these possibly indicate that RA

induction into the right knee might have cartilage destruction to a higher extent than the untreated left knee. The micro-CT images in coronal and sagittal view of the right knees showed that the agarose-implanted and sham-operated osteochondral defects are very similar to each other by showing red and yellow color pattern, whereas the PLGA-implanted defect did almost only green color. Interestingly, from the histological analysis, the agarose-implanted rabbit exhibited healing procedure of bone tissue into the defect much like the sham-operated rabbit, whereas the PLGA-implanted rabbit did not. So, this differential healing procedure between biomaterial scaffolds might partially explain the reason why the agarose-implanted and sham-operated defects showed those red and yellow color patterns similar to each other from the micro-CT images. However, it still needs to be clarified if these differential images in the micro-CT analysis are also ascribed to the differential interaction between the contrast agent (Hexabrix) and the hydrophilic (agarose) or hydrophobic (PLGA) biomaterials. As a result of histological examination, compared to the untreated left knee joints, thinner cartilages combined with poor safranin-O staining were found in the right knee joints from all rabbits (Figure 7-11). Old-age degenerated human cartilage (Bae et al., 2003) and healed cartilage layer of sham-operated osteochondral defect in normal rabbit joint (Frenkel et al., 2005) exhibited poor staining with safranin-O due to degeneration/degradation associated with fibrillation in the cartilage layer. Therefore, it is conceivable that degradation of cartilage might be induced in the biomaterial-implanted or sham-operated right knee joint in this study, possibly due to the combination of RA induction and biomaterial implantation or sham operation. Demineralized bone matrix (Gao et al., 2004) and collagen- or hyaluronan-based scaffold (Frenkel et al., 2005) has been employed to examine their effect on osteochondral defect repair upon implantation of these scaffold into the rabbit joints, and cartilage and bone were nicely healed in these studies. However, the studies in these literatures were performed using a normal rabbit without arthritis-induced circumstance into

the knee joint. Thus, it is not clear yet if the healing procedure observed for biomaterial-implanted knee joint in the present study is a typical healing process of cartilage and bone when a biomaterial scaffold is involved into the defect, due to the RA circumstance combined with biomaterial scaffold implantation. For this reason, an additional study using rabbits with biomaterial implantation or sham operation without RA induction should be performed as following step to further understand how RA circumstance affect cartilage repair and healing procedure into the biomaterial-implanted or sham-operated knee joint. Overall, biomaterial implantation into pre-existing severe disease situation accomplished a novel and challenging, clinically relevant model. However, effects of PLGA observed above, which were possibly induced by contra-lateral effects associated with a systemic circulation, motivated an additional follow-up study using increase number of rabbits to more clearly explain the immunogenicity of PLGA into *in vivo* condition.

Even though statistical significance was not reached with the limited number of rabbits used to date, the right knee of PLGA implanted rabbits showed a certain trend of higher levels of total leukocyte concentration compared to all other treatments or control through all time points. This indicates that an additional study with increase of rabbit number needs to be performed in order to get further information about statistical significance for this trend. In addition, for the differential leukocyte profile, while the right knee consistently exhibited predominant percentages of granulocytes for all treatments or control through all time points, the untreated left knee exhibited almost equal percentages between granulocyte and monocyte on Day 25, and then, on Day 29 and Day 36, the left knees with PLGA, agarose, or sham operation showed changes of percentages by increasing monocyte proportions. However, due to absence of naïve rabbit group in this study, it can not be clearly explained if these trends observed from the untreated left knees are correlated with the systemic circulation from the right knees. For this reason, the

naïve rabbit group should be added forthwith.

CHAPTER 8

CONCLUSIONS AND FUTURE WORK

Since tissue engineering has been recognized as a promising alternative for reconstruction and regeneration of diseased or damaged tissues, accompanied with a relatively simple procedure and long-term drug-free remission method, understanding host response to biomaterial which is combined with a tissue-engineered structure is central to design the tissue engineering with specific purpose. This thesis research contributed to the biomaterial development by demonstrating differential effects of different biomaterials frequently employed in tissue engineering field, focusing on phenotypical changes in DC maturation. In addition, the *in vitro* protocol for examination of biomaterial effects on T cell-mediated adaptive immunity was developed, demonstrating differential immunomodulatory impacts resulted upon co-culture of T cells and DCs treated with biomaterials. Following these *in vitro* steps, a new *in vivo* model with a specific disease of RA wherein DCs play a critical role in RA pathophysiology was developed to test immunomodulatory effects of biomaterials in the actual disease condition.

To obtain information essential to controlling of host response using biomaterials, five different biomaterials commonly used and relevant to combination products such as tissue engineered constructs or vaccine delivery systems were used to fully characterize DC and autologous T cell with immunological phenotypes upon DC treatment with these biomaterials. Furthermore, the framework of this thesis research was extended to an *in vivo* model to correlate all *in vitro* observations in the research.

However, to further understand mechanism behind the big picture of immunomodulatory strategies via control of DC phenotypes and ensuing T cell-mediated adaptive immunity in host response to biomaterials, several key areas may be investigated in future studies.

While the research procedures in this thesis were summarized by correlating *in vitro* biomaterial effects on DC and T cell phenotypes with *in vivo* biomaterial effects on RA circumstance, more detailed characterization of DC phenotypes and further developed method would be of benefit. For instance, hyaluronic acid (HA) film interestingly induced lower expression of CD44, as compared to iDCs, whereas HA overall inhibited DC maturation (Chapter 4). Surprisingly, even though CD44 has been well known as a potent receptor expressed on DCs to mediate DC clustering, migration, and maturation upon interaction with the hyaluronan components in the ECM (Weiss et al., 1997; Termeer et al., 2001), CD44 expression levels on DCs were induced by treatment with HA film even significantly lower than iDCs in this thesis research, possibly due to insolublized (cross-linked) film form and/or high molecular weight. (≥ 800,000 MW). Hyaluronic acid film also induced higher apoptosis level (Annexin V level) and lower endocytic ability than iDCs (Chapter 4). Furthermore, dendritic cells treated with HA films induced significantly lower levels of CD4 expression on co-cultured autologous T cells as compared to the negative control of untreated CD3+ T cells as well as significantly lower levels of CD25 expression compared to T cells in co-culture with DC treated with alginate or agarose films (Chapter 6). However, it can not be clearly answered only using these molecular weight and cross-linked condition of HA films tested in this thesis research.

From a view point of DC maturation associated with biomaterials other than HA film in this thesis research, patterns of CD44 expression were very similar to those of co-stimulatory molecule expression or MLR results as far as differential DC maturation upon DC treatment with different biomaterial films (Chapter 4). Dendritic cells showed upregulation in CD86 expression only when treated directly with biomaterials (Yoshida and Babensee, 2004) and PLGA or chitosan films induced CD44 expression on DCs in significantly higher levels than iDCs (Chapter 4). Moreover, PLGA was found, in the absence of carbohydrate unit recognizable by PRRs on DCs,

as the most potent stimulus (among all biomaterial examined herein) induced DC maturation in levels similar to the positive control of mDCs in the most examinations performed in this thesis (Chapter 4 and 5). These results indicate that, during 24 hour-treatment of DCs with these films, protein adsorption on these biomaterial films and consequent adhesion of cells to those protein adsorbed might be induced in higher levels compared to other biomaterial films or iDC control. In other words, CD44 might be deeply involved in DC maturation and consequent T cell activation in adaptive immunity.

Particularly, interaction of CD44 with intermediate-sized HA (MW ~ 200,000 Da) has been reported to induce apoptosis of DCs through nitric oxide (NO) production by DCs when tumor cells were involved (Yang et al., 2002b). High molecular weight HA fragments (6,000 kDa) induced a decreased level of TNF-α secretion, by specifically inhibiting TLR-2 signaling, from murine macrophages transfected with human TLR-2, as compared to the low molecular weight HA fragments (200 kDa) (Scheibner et al., 2006).

Therefore, understanding of the exact role of CD44 associated with relationship between CD44 and hyaluronic acid might be critical step forward to control of DC phenotypes and host response. These future procedures may be performed using a few specific methods. For instance, to understand how CD44 and HA film used in this thesis research interact each other, the hyaluronan component in ECM and HA film may be compared each other using physicochemical and immunobiological assessments. If the molecular weight and/or cross-linking density of HA films are differentially modulated and then, effects of these changes of HA films on DCs are compared to those of hyaluronan component in ECM, it would be of importance in better understanding effect of HA film on DC maturation or apoptosis. In addition, if CD44 and/or TLR2 pathway are blocked for DCs and then, these DCs are treated with HA film, it also would be of benefit for better understanding effect of HA film on DC maturation.

In the study using biomaterial scaffolds (Chapter 5 and 7), PLGA and agarose were selected for scaffolds used in the experimental procedures, because the cross-linked HA was too brittle to be formed in 3-D porous scaffold. However, through all *in vitro* investigations in this thesis research, HA film exhibited multifunctional impacts on controlling DC phenotypes by effectively suppressing DC maturation or T cell activation, as well as inducing of decreased endocytic ability or increased apoptosis of DCs. Therefore, if it is feasible, application of 3-D porous scaffold form of HA into the *in vitro* or *in vivo* experimental procedure would be of great to elucidate the mechanisms of HA-controlled DC and T cell phenotypes as well as further host response in tissue engineering. For instance, the chemically modified HA, Hyaff (Grigolo et al., 2002) may be utilized *in vitro* and *in vivo* study as long as it shows inherency identical to the cross-linked HA film used in this thesis research.

In this way, a more in-depth investigation of all HA-related features described above including CD44 behavior may be potential to understand key points in controlling DC phenotypes. In addition, from another viewpoint of immunotherapy for inducing secondary immune responses using artificial lymphoid organ, it would be of great interest to develop a strategy for localization or migration of immune cells (lymphocytes and DCs) using biocompatible scaffolds such as HA scaffold (Suematsu and Watanabe, 2004; Okamoto et al., 2007; Stachowiak and Irvine, 2008). Therefore, elucidating multifunctional effects of biomaterial scaffolds *in vitro* or *in vivo* on changes of DC phenotypes are expected to provide a guidance to design biomaterial scaffolds in applications of immunotherapy, various tissue engineering, or a combination of immunotherapy and tissue engineering.

Most noticeable observation in this entire thesis work was immunomodulating impacts of PLGA and agarose, which was shown in the range from DCs to T cell-mediated adaptive immunity. As shown in the Chapter 4, 5 and 6, PLGA induced immunogenicity whereas

agarose did tolerogenicity *in vitro*. Using *in vivo* animal model, various effects of different biomaterials on host immune response, especially on T cell-mediated adaptive immunity, have been extensively investigated upon implantation, injection, or administration of them into animal model. For instance, zinc-chitosan particles (adjuvant) combined with specific proteins (antigen) immunized by intraperitoneal injection were effective in sensitizing mice and guinea pig for antigen specific delayed type hypersensitivity (DTH), also resulting in stimulation of T and B lymphocytes (Seferian and Martinez, 2000). Upon subcutaneous injection, alginate hydrogel/DC constructs induced a large number of antigen-specific T cell trafficking towards the alginate matrix (Hori et al., 2008). Most recently, using a cage implant model of rat, three different biomaterials of Elasthane 80A, silicone rubber, and polyethylene terephthalate (PET) have been examined with their effects on differential activation of T cell subsets (Rodriguez et al., 2008). As a result, these different biomaterials induced T cell subsets (CD4+, CD8+, CD4+CD25+) in differential levels only upon the primary implantation. Similar to these examinations, another approach to studying the further multifunctional impacts of different biomaterials may be to transfer biomaterials into *in vivo* animal models to particularly understand their effects on T cell-mediated adaptive immunity.

In a view point of immunotherapy, a wide spectrum of immunobiological interactions between DCs and T cells has been extensively examined by adoptive transfer of DCs into *in vivo* animal models. For instance, ovalbumin peptide-pulsed DCs were transferred into mice and these DCs induced great expansion of antigen-specific T cells, as well as antigen-specific Th1 response, resulting in antitumor immunity (Lambert et al., 2001). Dendritic cells only capable of viral antigen presentation were expanded with their population in mice and upon adoptive transfer of these DCs into recipient mice, induced strong T cell responses, thereby accelerating viral clearance (Bedoui et al., 2009). Adoptive transfer of DCs previously treated with GM-CSF

into naïve mice demonstrated an expansion of FoxP3+ T cells and a significant delay in type-1 diabetes (Cheatem et al., 2009). Most recently, Hori et al. reported that when the alginate hydrogel (named as vaccination node) containing activated DCs was subcutaneously injected into mice, this combination of alginate and DCs attracted both host DCs and T cells to the site of injection more than a week *in vivo*, also showing that part of inoculated DCs trafficked to the draining lymph nodes (Hori et al., 2008).

In the conventional therapeutic methods in DC-based immunotherapy, various drugs (e.g., dexamethasone, glucocorticoid, retinoid) or mRNA transfection have been widely accepted to modulate differential DC phenotypes, thereby further mediating differential T cell response (Xia et al., 2005; Toebak et al., 2008; Noonan et al., 2008). However, anti-inflammatory drugs or mRNA transfection can lead to undesirable side effects or non-specific host response, frequently combined with complications in preparation of DC or host treatment (Arend and Dayer, 1995; Brennan et al., 1989; Elliott et al., 1993; Dayer and Fenner, 1992; Wooley et al., 1993; Nestle et al., 2005). However, DC treatment with biomaterials in this thesis research is extremely simple without any complication, showing how easily purified DC can be isolated from biomaterials after 24 hour treatment. In this way, it may be worthwhile to assess the ability of differentially biomaterial-treated DCs to non-pharmacologically drive T cell polarization.

Another potential of DC treatment with biomaterials was that even though DCs were isolated from biomaterial films and extracellular OVA antigen after the 24 hour-treatment, they continued to secrete the same cytokines in almost the same levels under the wholly changed culture conditions for 8 days (the Chapter 6 and Figure A6, APPENDIX). Therefore, based on results observed from immunomodulatory capacities of biomaterials (PLGA or agarose) in association with simple procedure of DC treatment with biomaterials, *in vivo* studies to understand ensuing adaptive immune response upon adoptive transfer of biomaterial-treated DCs

may be of great importance to further pursue this approach in the determination of role of biomaterials in non-pharmacological immunotherapy.

In the *in vivo* study using RA rabbit model (Chapter 7), the full study was performed using only 3 rabbits per treatment or control group. From the view point of typical statistics on fields of medicine or biomedical engineering, three rabbits are obviously not enough to substantiate effects of biomaterials implanted into the RA knee joints of rabbits. For this reason, another set of this full study has been always considered in the following step. However, a few interesting results were observed from the full study in the Chapter 7 and these results additionally motivate us to repeat another full study or increase treatment or control group. For instance, even though not statistically clear, the right knee of rabbits with implanted PLGA scaffolds with induced RA showed a certain trend of higher levels of total leukocyte concentration compared to all other treatments or control through all time points. This indicates that an additional study may be of importance to get statistical significance for this trend. In addition, we could find that additional studies using naïve rabbit group or biomaterial implantation or sham operation into the normal knee joint without RA needs to be performed to further understand effect of biomaterial implantation and/or RA induction on the knee joint of rabbit. In fact, TNF-α concentration in the joint lavage or peripheral blood collected from rabbits were measured using ELISA technique to understand effect of biomaterial implantation into the RA knee joint of rabbit on the pro-inflammatory cytokine concentration. However, joint lavage or blood samples from all rabbits in this study unexpectedly exhibited TNF-α concentration at levels below the detection limit of the ELISA assay for all time points of sample collection (Day 25, 29, and 36). So, joint lavage or blood sample might need to be collected earlier than the time point of Day 25 (e.g., Day 22 or Day 23 after Day 21 for RA induction or Day 22 for biomaterial implantation) to obtain the cytokine level enough to detect using ELISA

technique. Lastly, for RA induction into the rabbit knee joint, a different model of RA induction such as LPS-induced arthritis rabbit model might be of great interest to obtain variety of useful data to compare effects of different biomaterials.

The micro-CT analysis was very useful to understand effects of biomaterial implantation into the RA-induced knee joint on the cartilage degradation. However, the VOI of all defect femora scanned in this study was defined to include approximately 1 mm (wherever possible) of surrounding cartilage. For instance, the x-ray attenuation values obtained in this study were averaged for the entire circular region (approximately 5.2 mm of diameter) of the cartilage including the top area of biomaterial/defect (3.2 mm of diameter) at the center. So, these values of the attenuation might not provide accurate information of degradation of cartilage adjacent to the biomaterial/defect possibly due to differential interactions between the contrast agent and different biomaterials as well as the absence of cartilage layer at the top of biomaterial/defect as seen in the histology results of the PLGA-implanted or sham-operated knee joint. Therefore, in future work, the top area of the biomaterial/defect at the center of the entire circular region would be cut off and the remaining doughnut-shaped construct would be analyzed for the attenuation values. This analysis is of great interest to further understand how RA and the biomaterial implantation affect the real cartilage adjacent to the defect.

The ultimate goal of this thesis research is to suggest selection or design criteria of biomaterials for RA tissue engineering for human patients. However, in the Chapter 4, 5, and 6, all *in vitro* experimental procedures were performed using DCs derived from healthy donors. These DCs might not be enough to fully understand *in vitro* functional impacts of biomaterials in case the future application of biomaterials for RA disease is targeted, possibly due to pathophysiological complications of RA patient, which is not clearly explained yet (Waalen et al., 1986; Pettit and Thomas, 1999; Santiago-Schwarz et al., 2001). For this reason, if feasible, *in*

vitro use of DCs derived from RA patients for treatments with biomaterials would be essential to obtain information directly connected to *ex vivo* or *in vivo* tests in future.

The study presented herein begins to address differential levels of host response associated with different biomaterials with distinct, inherently different physicochemical features. The strength of the study in this thesis is the assessment and comparison of DC and T cell responses to biomaterials so widely and commonly used in combination products. An understanding of DC maturation as predictive of a biomaterial adjuvant effect can suggest selection or design criteria for biomaterials in applications of tissue engineering or vaccine/drug delivery with associated immune responses. Furthermore, elucidating the physicochemical properties of biomaterials and correlating these *in vitro* effects on DC and T cell phenotype changes with their *in vivo* adjuvant effects in animal studies are expected to provide guidelines for design and selection criteria for biomaterials in the combination products where immunological responses are of consequence, as well as immunotherapeutic intervention is accompanied by immunomodulatory impacts of biomaterials.

APPENDIX

A.1 Water content of biomaterial films

To assess effects of water content (hydrogelation) of the biomaterial films on *in vitro* phenotypical changes in DC maturation, water content of all biomaterial films were measured upon incubation of biomaterial films under the condition same as DC treatment with biomaterials. Briefly, all biomaterial films prepared with a size identical to those used in DC treatment as described in the Chapter 4, and then, biomaterial films were fully immersed in ddH_2O, followed by incubation of films at 37ºC for 24 hours. After this 24 hour incubation, excessive water on both surfaces of each biomaterial film was quickly absorbed by the filter paper and the weight of fully swollen biomaterial film was measured. After this weight measurement, biomaterial films were freeze-dried for 6 days and then, the weight of this freeze-dried film was measured. This weight of freeze-dried film was subtracted from the weight of fully swollen films and then, percentages of this difference (from the subtraction) out of the freeze-dried weight was considered as the water content (%) (Figure A1).

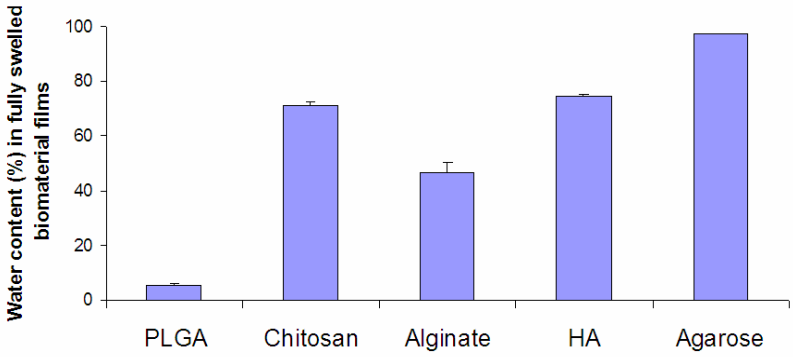

Figure A1: Water content (%) in fully swollen biomaterial films.
mean±SD, n=5

Based on the definition of the hydrogel which is at least 20% (w/w) water in its dried weight (Peppas and Mikos, 1986), except PLGA, all biomaterial films used in this thesis research can be considered as hydrogel. As mentioned in the Chapter 4, chitosan is another hydrophobic biomaterial of natural polysaccharides having carbohydrate units which are mainly composed of glucosamine with a high cationic charge density (Chandy and Sharma, 1990; Tangpasuthadol et al., 2003; Li and Tuan, 2005). In addition, the adhesion stability of protein adsorbed on different surface chemistries with different hydrophobicities has been shown with the highest level on the hydrophobic surface followed by the next highest one on the cationic surface (e.g., hydrophobic surface > cationic surface > neutral surface > anionic surface) under the physiological pH (Fraaye et al., 1986; Brash, 1983; Young et al., 1988). Accordingly, after 24 hour-treatment of DCs with biomaterial films, non-/loosely-adherent DC portion collected from PLGA film was observed with the least amount of 37±15% among all biomaterial films used in this study, followed by the next least one of 65±13% obtained from chitosan film (Chapter 4).

Considering the overall observations from *in vitro* experimental procedures in the Chapter 4, it seems that biomaterial with higher capacity of water uptake induces less DC maturation. However, the water content of chitosan film is observed in level higher than that of alginate film, similar to that of HA film. Collectively, it is conceivable that phenotypical changes in DC maturation are modulated by surface properties rather than other properties such as capability of water uptake.

A.2 Differential functional effects of clinical grade biomaterials on DC maturation

As described above in the Chapter 4, to test effects of biomaterial grade such as research or clinical grade, the clinical grade 2-D biomaterial films were also prepared, and examined with their effect on DC maturation, compared to the research grade which is mainly studied in the present study. In addition to the maturation marker expression result shown in the Chapter 4, MLR, Annexin V/PI, and DC morphologies in cytospins upon DC treatment with these clinical grade biomaterial have been performed (Figure A2, A3, and A4) as described in the method section in the Chapter 4. As same as the maturation marker expression, these additional examinations also resulted in levels or patterns very similar to those of the research grade biomaterials, thereby confirming that dendritic cell responses to clinical grade biomaterials were indistinguishable from their responses to the research grade biomaterials.

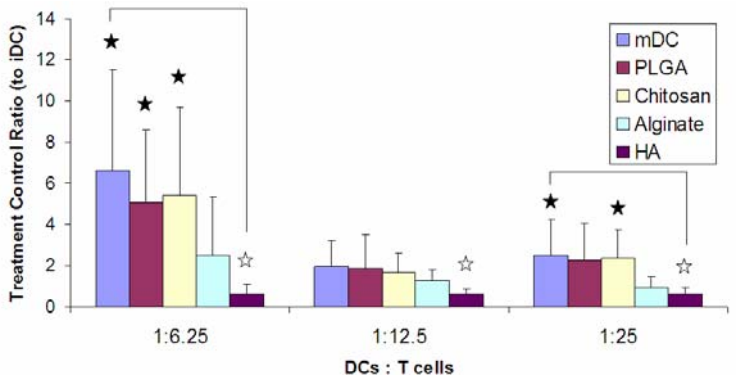

Figure A2: Allostimulatory capacities in Mixed Lymphocyte Reaction (MLR) in differential levels upon DCs treated with the clinical grade biomaterial films.

Similarly to the results obtained from DCs treated with the research grade biomaterial films in the Chapter 4, PLGA supported allogeneic T cell proliferation in levels significantly higher than iDCs, whereas HA suppressed those especially in the ratio of DCs : T cells in 1 : 6.25. Ratios to the iDCs are shown with mean±SD, n=6 donors (6 independent experiments with different donors). ★: $p \leq 0.05$, compared to iDCs and higher than iDC; ☆: $p \leq 0.05$, compared to iDCs and lower than iDC; Brackets: $p \leq 0.05$, statistically different between two biomaterial treatments.

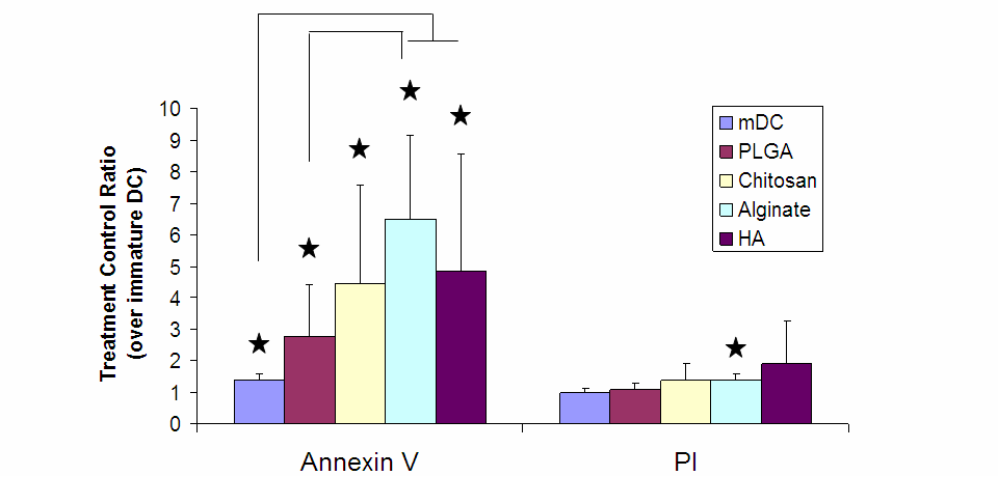

Figure A3: Geometric mean fluorescence intensity (gMFI) of flow cytometry analysis of Annexin V and propidium iodide (PI) expression in differential levels upon DCs treated with different biomaterial films in the clinical grade.

Dendritic cells treated with PLGA, chitosan, or alginate exhibited Annexin V expressions in higher levels than iDC. However, DCs treated with HA unexpectedly exhibited Annexin V expression in higher level than iDCs. Ratios to the iDCs are shown with mean±SD, n=6 donors (6 independent experiments with different donors). ★: $p \leq 0.05$, compared to iDCs and higher than iDC; ☆: $p \leq 0.05$, compared to iDCs and lower than iDC; Brackets: $p \leq 0.05$, statistically different between two biomaterial treatments.

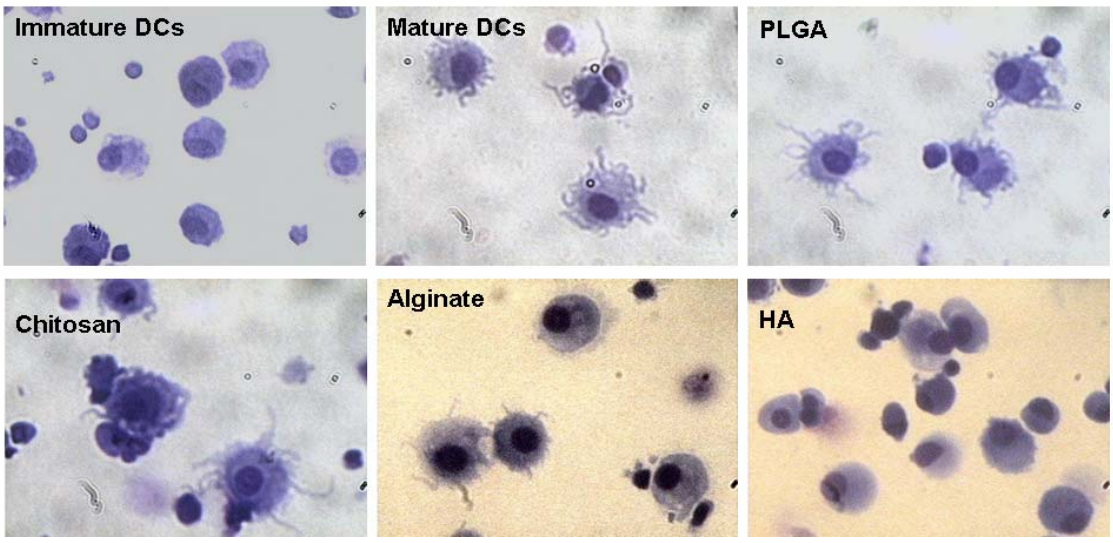

Figure A4: Dendritic cells treated with PLGA or chitosan films in the clinical grade possess cell morphologies similar to mDC induced with LPS treatment.

DCs derived from peripheral blood monocytes in the presence of GM-CSF and IL-4, treated with PLGA or chitosan films in the clinical grade showed similar morphology to that of mDCs, with the presence of dendritic processes, whereas the clinical grade alginate or HA exhibited morphologies similar to iDCs. Original magnification: 40×.

A.3 Differential functional effects of biomaterials on autologous T cell marker expressions when DCs are treated with biomaterials in the absence of model antigen, OVA.

As described above in the Chapter 6, to understand effects of biomaterials on autologous T cell marker expressions upon co-culture of T cells and DCs treated with different biomaterials, in the beginning of this investigation, DCs were treated with biomaterials in the absence of model antigen, OVA. Experimental procedure was identical to description in the method section of the Chapter 6, except use of model antigen, OVA when DCs were treated with biomaterials. As a result shown in Figure A5, expressions for each of all T cell markers (CD4, CD8, CD25, CD69) among DC treatments with biomaterial films were not induced at differential levels when DCs were treated with biomaterial films in the absence of OVA. These indicate that DCs treated only with biomaterial films, in the absence of co-delivered antigen, might be not sufficiently activated to induce differential T cell marker expression. Similar results have also been reported showing that DC exposure to an actual pathogen component is necessary to promote T helper responses (Sporri and Sousa, 2005).

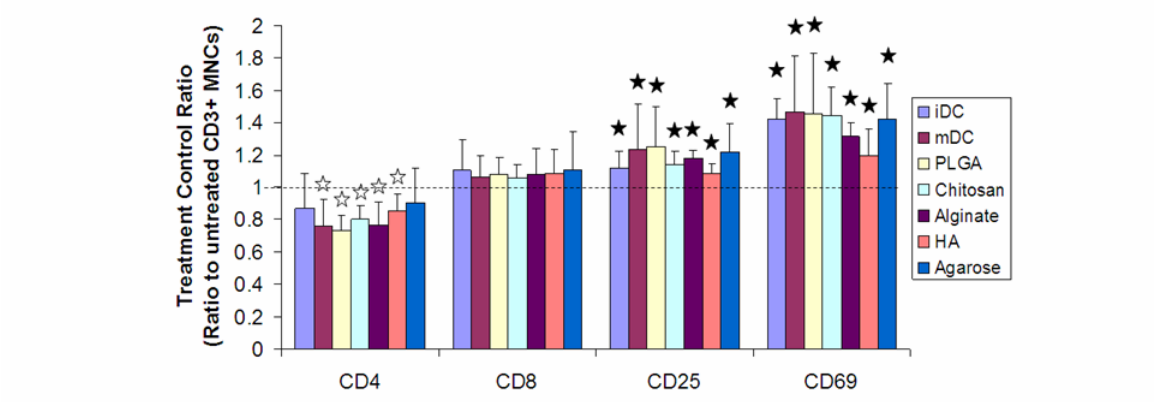

Figure A5: Geometric mean fluorescence intensity (gMFI) for each marker expression of CD4, CD8, CD25, & CD69 for autologous CD3+ T cells without differential levels between treatments upon co-culture with DCs treated with different biomaterial films in the absence of OVA antigen.

No marker was induced in differential levels compared between treatments. Ratios to the

untreated CD3+ MNCs are shown with mean±SD, n=6 donors (6 independent experiments with different donors). ★: $p \leq 0.05$, compared to control and higher than control; ☆: $p \leq 0.05$, compared to control and lower than control.

A.4 Differential functional effects of biomaterials on cytokine secretion from DCs in almost the same levels even after DCs were isolated from biomaterials.

As mentioned above in the Chapter 6, for the negative controls of the co-culture procedures from Day 6 to Day 14, a half of DCs from treatments with each biomaterial film, which were collected on Day 6 (supernatants from these DCs were discussed above for cytokine profiles as shown in Figure 6-6), were washed twice and then, kept cultured without T cells through Day 14 in the same condition with the DC-T co-culture system while the other half was used for the co-culture with autologous T cells. Interestingly, for the control culture of DCs without added autologous T cells, the cytokine profiles were the same at day 14 (Figure A6) as they were at Day 6 (Fig. 6-6) in the presence or absence of OVA antigen. These results indicate that, even though DCs were isolated from biomaterial films and extracellular OVA antigen after the 24 hour-culture, they continued to secrete the same cytokines in almost the same levels under the wholly changed culture conditions for 8 days.

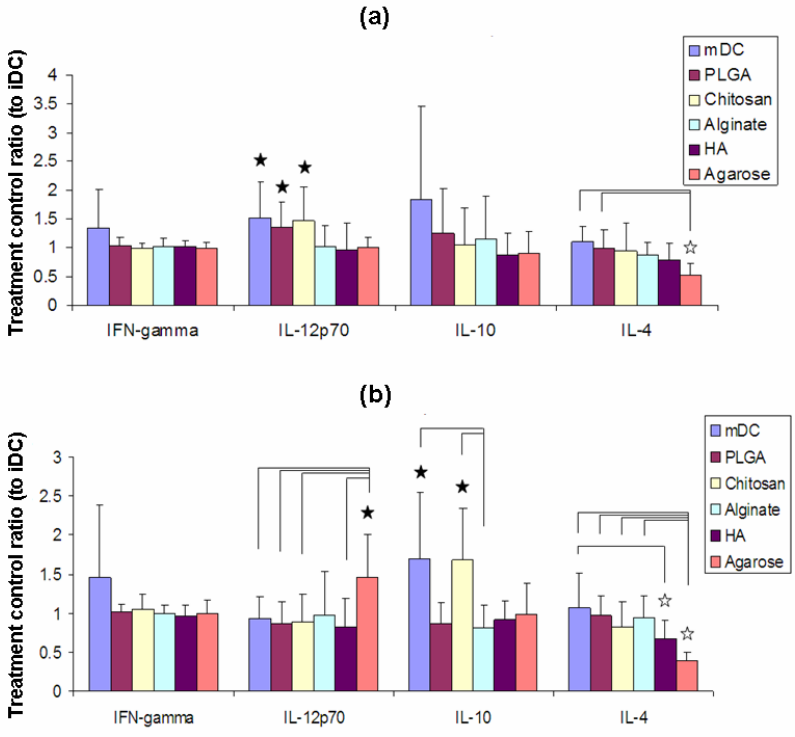

Figure A6: Geometric mean fluorescence intensity (gMFI) of cytometric bead array (CBA) for interferon (IFN)-gamma, IL-12p70, IL-10, IL-4 release for DCs treated with different biomaterial films without (Fig. A6a) or with (Fig. A6b) OVA antigen.

Cytokines were measured using the supernatant saved on Day 14 (after 8 days since DCs were treated with biomaterial films with or without antigen and then, isolated from biomaterials and extracellular antigen). As compared to the cytokine results shown in Figure 6-6, Th1 or Th2 cytokines were modulated in differential levels very similar to those released in Day 6.

Ratios to the iDCs are shown with mean±SD, n=6 donors (6 independent experiments with different donors). ★: $p \leq 0.05$, compared to iDCs and higher than iDC; ☆: $p \leq 0.05$, compared to iDCs and lower than iDC; Brackets: $p \leq 0.05$, statistically different between two T cells for DCs treated with different biomaterial films.

REFERENCES

Acharya, A.P., Dolgova, N.V., Clare-Salzler, M.J., and Keselowsky, B.G. (2008) Adhesive substrate-modulation of adaptive immune responses. Biomaterials 29,4736-4750.

Ademovic, Z., Holst, B., Kahn, R.A., Jorring, I., Brevig, T., Wei, J., Hou, X., Winter-Jensen, B., and Kingshott, P. (2006) The method of surface PEGylation influences leukocyte adhesion and activation. J Mater Sci Mater Med 17,203-211.

Aderem, A., and Ulevitch, R.J. (2000) Toll-like receptors in the induction of the innate immune response. Nature 406,782-787.

Agrawal, C.M., and Ray, R.B. (2001) Biodegradable polymeric scaffolds for musculoskeletal tissue engineering. J Biomed Mater Res 55,141-150.

Anderson, D.G., Levenberg, S., and Langer, R. (2004) Nanoliter-scale synthesis of arrayed biomaterials and application to human embryonic stem cells. Nat Biotechnol 22,863-866.

Anderson, J. (2001) Biological responses to materials. ANN REV MATER RES 31,81-110.

Anolik, J.H., Ravikumar, R., Barnard, J., Owen, T., Almudevar, A., Milner, E.C.B., Miller, C.H., Dutcher, P.O., Hadley, J.A., and Sanz, I. (2008) Cutting edge: Anti-tumor necrosis factor therapy in rheumatoid arthritis inhibits memory B lymphocytes via effects on lymphoid germinal centers and follicular dendritic cell networks. J Immunol 180,688-692.

Appel, H., Neure, L., Kuhne, M., Braun, J., Rudwaleit, M., and Sieper, J. (2004) An elevated level of IL-10- and TGF beta-secreting T cells, B cells and macrophages in the synovial membrane of patients with reactive arthritis compared to rheumatoid arthritis. Clinical Rheumatology 23,435-440.

Arend, W., and Dayer, J. (1995) Inhibition of the Production and Effects of Interleukin-1 and Tumor-Necrosis-Factor-alpha in Rheumatoid-Arthritis. Arthritis and Rheumatism 38,151-160.

Asquith, D.L., and McInnes, I.B. (2007) Emerging cytokine targets in rheumatoid

arthritis. Curr Opin Rheumatol 19,246-251.

Avice, M.N., Demeure, C.E., Delespesse, G., Rubio, M., Armant, M., and Sarfati, M. (1998) IL-15 promotes IL-12 production by human monocytes via T cell-dependent contact and may contribute to IL-12-mediated IFN-gamma secretion by CD4(+) T cells in the absence of TCR ligation. J Immunol 161,3408-3415.

Babensee, J., Anderson, J., McIntire, L., and Mikos, A. (1998) Host response to tissue engineered devices. Adv Drug Delivery Rev 33,111-139.

Babensee, J., and Paranjpe, A. (2005) Differential levels of dendritic cell maturation on different biomaterials used in combination products. J Biomed Mater Res 74A,503-510.

Bae, W.C., Temple, M.A., Amiel, D., Coutts, R.D., Niederauer, G.G., and Sah, R.L. (2003) Indentation testing of human cartilage - Sensitivity to articular surface degeneration. Arthritis and Rheumatism 48,3382-3394.

Banchereau, J., Briere, F., Caux, C., Davoust, J., Lebecque, S., Liu, Y.T., Pulendran, B., and Palucka, K. (2000) Immunobiology of dendritic cells. Annu Rev Immunol 18,767-+.

Banchereau, J., and Steinman, R. (1998) Dendritic cells and the control of immunity. Nature 392,245-252.

Banerjee, D.K., Dhodapkar, M.V., Matayeva, E., Steinman, R.M., and Dhodapkar, K.M. (2006) Expansion of FOXP3(high) regulatory T cells by human dendritic cells (DCs) in vitro and after injection of cytokine-matured DCs in myeloma patients. Blood 108,2655-2661.

Bansback, N., Regier, D., Ara, R., Brennan, A., Shojania, K., Esdaile, J., Anis, A., and Marra, C. (2005) An overview of economic evaluations for drugs used in rheumatoid arthritis - Focus on tumour necrosis factor-alpha antagonists. Drugs 65,473-496.

Baslund, B., Tvede, N., Danneskiold-Samsoe, B., Larsson, P., Panayi, G., Petersen, J., Petersen, L.J., Beurskens, F.J.M., Schuurman, J., van de Winkel, J.G.J., Parren, P.W.H.I., Gracie, J.A., Jongbloed, S., Liew, F.Y., and McInnes, I.B. (2005) Targeting interleukin-15 in patients with rheumatoid arthritis - A proof-of-concept

study. Arthritis and Rheumatism 52,2686-2692.

Bedoui, S., Prato, S., Mintern, J., Gebhardt, T., Zhan, Y., Lew, A.M., Heath, W.R., Villadangos, J.A., and Segura, E. (2009) Characterization of an Immediate Splenic Precursor of CD8(+) Dendritic Cells Capable of Inducing Antiviral T Cell Responses. J Immunol 182,4200-4207.

Bell, D., Young, J., and Banchereau, J. (1999) Dendritic cells. Adv Immunol 72,255-324.

Bennewitz, N., and Babensee, J. (2005) The effect of the physical form of poly(lactic-co-glycolic acid) carriers on the humoral immune response to co-delivered antigen. Biomaterials 26,2991-2999.

Benya, P.D., and Shaffer, J.D. (1982) Dedifferentiated Chondrocytes Reexpress the Differentiated Collagen Phenotype When Cultured in Agarose Gels. Cell 30,215-224.

Black, S.P., Constantinidis, I., Cui, H., Tucker-Burden, C., Weber, C.J., and Safley, S.A. (2006) Immune responses to an encapsulated allogeneic islet beta-cell line in diabetic NOD mice. Biochem Biophys Res Commun 340,236-243.

Brash, J.L. (1983) Protein Interactions at Solid-Surfaces. Abstr Pap Am Chem Soc 185,190-ORPL.

Brennan, F., Jackson, A., Chantry, D., Maini, R., and Feldmann, M. (1989) Inhibitory Effects of TNF-alpha Antibodies on Synovial Cell IL-1 Production in Rheumatoid-Arthritis. LANCET 2,244-247.

Bresnihan, B. (1999) Pathogenesis of joint damage in rheumatoid arthritis. J Rheumatol 26,717-719.

Bresnihan, B., and Tak, P. (1999) Synovial tissue analysis in rheumatoid arthritis. BEST PRACT RES CL RH 13,645-659.

Brodbeck, W., Nakayama, Y., Matsuda, T., Colton, E., Ziats, N., and Anderson, J. (2002) Biomaterial surface chemistry dictates adherent monocyte/macrophage cytokine expression in vitro. Cytokine 18,311-319.

Bu, W.F., Wu, L.X., Hou, X.L., Fan, H.L., Hu, C.W., and Zhang, X. (2002) Investigation

on solvent casting films of surfactant-encapsulated clusters. J Colloid Interface Sci 251,120-124.

Buckwalter, J., and Mankin, H. (1998) Articular cartilage repair and transplantation. Arthritis and Rheumatism 41,1331-1342.

Cancedda, R., Dozin, B., Giannoni, P., and Quarto, R. (2003) Tissue engineering and cell therapy of cartilage and bone. Matrix Biol 22,81-91.

Chan, G., and Mooney, D.J. (2008) New materials for tissue engineering: towards greater control over the biological response. Trends Biotechnol 26,382-392.

Chan, W.K., Law, H.K.W., Lin, Z.B., Lau, Y.L., and Chan, G.C.F. (2007) Response of human dendritic cells to different immunomodulatory polysaccharides derived from mushroom and barley. Int Immunol 19,891-899.

Chandy, T., and Sharma, C.P. (1990) Chitosan - as a Biomaterial. Biomater Artif Cells Artif Organs 18,1-24.

Chang, C., Kuo, T., Lin, C., Chou, C., Chen, K., Lin, F., and Liu, H. (2006) Tissue engineering-based cartilage repair with allogenous chondrocytes and gelatin-chondroitin-hyaluronan tri-copolymer scaffold: A porcine model assessed at 18, 24, and 36 weeks. Biomaterials 27,1876-1888.

Chang, D.T., Jones, J.A., Meyerson, H., Colton, E., Kwon, I.K., Matsuda, T., and Anderson, J.M. (2008) Lymphocyte/macrophage interactions: Biomaterial surface-dependent cytokine, chemokine, and matrix protein production. J Biomed Mater Res 87A,676-687.

Cheatem, D., Ganesh, B.B., Gangi, E., Vasu, C., and Prabhakar, B.S. (2009) Modulation of dendritic cells using granulocyte-macrophage colony-stimulating factor (GM-CSF) delays type 1 diabetes by enhancing CD4+CD25+regulatory T cell function. Clinical Immunology 131,260-270.

Chen, F., Frenkel, S., and DiCesare, P. (1999) Repair of Articular Cartilage Defects: Part II. Treatment Options. The American Journal of Orthopedics 28,88-96.

Cho, M.L., Ju, J.H., Kim, H.R., Oh, H.J., Kang, C.M., Jhun, J.Y., Lee, S.Y., Park, M.K., Min, J.K., Park, S.H., Lee, S.H., and Kim, H.Y. (2007) Toll-like receptor 2 ligand

mediates the upregulation of angiogenic factor, vascular endothelial growth factor and interleukin-8 CXCL8 in human rheumatoid synovial fibroblasts. Immunol Lett 108,121-128.

Cho, M.L., Jung, Y.O., Kim, K.W., Park, M.K., Oh, H.J., Ju, J.H., Cho, Y.G., Min, J.K., Kim, S.I., Park, S.H., and Kim, H.Y. (2008) IL-17 induces the production of IL-16 in rheumatoid arthritis. Experimental and Molecular Medicine 40,237-245.

Cieza, A., and Stucki, G. (2005) Understanding functioning, disability, and health in rheumatoid arthritis: the basis for rehabilitation care. Curr Opin Rheumatol 17,183-189.

Cinelli, M., Guiducci, S., Del Rosso, A., Pignone, A., Del Rosso, M., Fibbi, G., Serrati, S., Gabrielli, A., Giacomelli, R., Piccardi, N., and Cerinic, M.M. (2006) Piascledine modulates the production of VEGF and TIMP-1 and reduces the invasiveness of rheumatoid arthritis synoviocytes. Scand J Rheumatol 35,346-350.

Collier, T.O., and Anderson, J.M. (2002) Protein and surface effects on monocyte and macrophage adhesion, maturation, and survival. J Biomed Mater Res 60,487-496.

Concaro, S., Gustavson, F., and Gatenholm, P. (2009) Bioreactors for Tissue Engineering of Cartilage. Bioreactor Systems for Tissue Engineering 112,125-143.

Cox, J., and Coulter, A. (1997) Adjuvants - A classification and review of their modes of action. Vaccine 15,248-256.

Coyle, A.J., and Gutierrez-Ramos, J.C. (2001) The expanding B7 superfamily: Increasing complexity in costimulatory signals regulating T cell function. Nat Immunol 2,203-209.

Crompton, K.E., Tomas, D., Finkelstein, D.I., Marr, M., Forsythe, J.S., and Horne, M.K. (2006) Inflammatory response on injection of chitosan/GP to the brain. J Mater Sci Mater Med 17,633-639.

Cunningham, A.J., and Lafferty, K.J. (1977) Simple, Conservative Explanation of H-2 Restriction of Interactions between Lymphocytes. Scand J Immunol 6,1-6.

Dayer, J., and Fenner, H. (1992) The Role of Cytokines and Their Inhibitors in Arthritis. BAILLIERE CLIN RHEUM 6,485-516.

de Vos, P., Faas, M.M., Strand, B., and Calafiore, R. (2006) Alginate-based microcapsules for immunoisolation of pancreatic islets. Biomaterials 27,5603-5617.

de Vos, P., Hamel, A.F., and Tatarkiewicz, K. (2002) Considerations for successful transplantation of encapsulated pancreatic islets. Diabetologia 45,159-173.

Decaris, E., Guingamp, C., Chat, M., Philippe, L., Grillasca, J.P., Abid, A., Minn, A., Gillet, P., Netter, P., and Terlain, B. (1999) Evidence for neurogenic transmission inducing degenerative cartilage damage distant from local inflammation. Arthritis and Rheumatism 42,1951-1960.

Dhodapkar, M.V., and Steinman, R.M. (2002) Antigen-bearing immature dendritic cells induce peptide-specific CD8(+) regulatory T cells in vivo in humans. Blood 100,174-177.

Do, Y., Nagarkatti, P.S., and Nagarkatti, M. (2004) Role of CD44 and hyaluronic acid (HA) in activation of alloreactive and antigen-specific T cells by bone marrow-derived dendritic cells. J Immunother 27,1-12.

Edwards, S.W., and Hallett, M.B. (1997) Seeing the wood for the trees: The forgotten role of neutrophils in rheumatoid arthritis. Immunology Today 18,320-324.

Eldridge, J.H., Staas, J.K., Meulbroek, J.A., Mcghee, J.R., Tice, T.R., and Gilley, R.M. (1991) Biodegradable Microspheres as a Vaccine Delivery System. Mol Immunol 28,287-294.

Elliott, M., Maini, R., Feldmann, M., Longfox, A., Charles, P., Katsikis, P., Brennan, F., Walker, J., Bijl, H., Ghrayeb, J., and Woody, J. (1993) Treament of Rheumatoid-Arthritis with Chimeric Monoclonal-Antibodies to Tumor-Necrosis-Factor-alpha. ARTHRITIS RHEUM 36,1681-1690.

Ertl, H., Varga, I., Xiang, Z., Kaiser, K., Stephens, L., and Otvos, L. (1996) Poly(DL-lactide-co-glycolide) microspheres as carriers for peptide vaccines. Vaccine 14,879-885.

Espevik, T., Otterlei, M., Skjakbraek, G., Ryan, L., Wright, S.D., and Sundan, A. (1993) The Involvement of CD14 in Stimulation of Cytokine Production by Uronic-Acid Polymers. Eur J Immunol 23,255-261.

Feng, J., Zhao, L.H., and Yu, Q.Q. (2004) Receptor-mediated stimulatory effect of oligochitosan in macrophages. Biochem Biophys Res Commun 317,414-420.

Figdor, C.G., van Kooyk, Y., and Adema, G.J. (2002) C-type lectin receptors on dendritic cells and Langerhans cells. Nat Rev Immunol 2,77-84.

Flo, T.H., Ryan, L., Latz, E., Takeuchi, O., Monks, B.G., Lien, E., Halaas, O., Akira, S., Skjak-Braek, G., Golenbock, D.T., and Espevik, T. (2002) Involvement of Toll-like receptor (TLR) 2 and TLR4 in cell activation by mannuronic acid polymers. J Biol Chem 277,35489-35495.

Foti, M., Granucci, F., Pelizzola, M., Beretta, O., and Ricciardi-Castagnoli, P. (2006) Dendritic cells in pathogen recognition and induction of immune responses: a functional genomics approach. J Leukoc Biol 79,913-916.

Fraaye, J.G.E.M., Norde, W., and Lyklema, J. (1986) Charge-Potential Relation of Adsorbed Protein. Abstr Pap Am Chem Soc 192,27-Coll.

Fragonas, E., Valente, M., Pozzi-Mucelli, M., Toffanin, R., Rizzo, R., Silvestri, F., and Vittur, F. (2000) Articular cartilage repair in rabbits by using suspensions of allogenic chondrocytes in alginate. Biomaterials 21,795-801.

Freed, L.E., Marquis, J.C., Nohria, A., Emmanual, J., Mikos, A.G., and Langer, R. (1993) Neocartilage Formation Invitro and Invivo Using Cells Cultured on Synthetic Biodegradable Polymers. J Biomed Mater Res 27,11-23.

Freed, L.E., Martin, I., and Vunjak-Novakovic, G. (1999) Frontiers in tissue engineering - In vitro modulation of chondrogenesis. Clinical Orthopaedics and Related Research,S46-S58.

Frenkel, S.R., Bradica, G., Brekke, J.H., Goldman, S.M., Ieska, K., Issack, P., Bong, M.R., Tian, H., Gokhale, J., Coutts, R.D., and Kronengold, R.T. (2005) Regeneration of articular cartilage - Evaluation of osteochondral defect repair in the rabbit using multiphasic implants. Osteoarthritis Cartilage 13,798-807.

Fujii, S., Nishimura, M.I., and Lotze, M.T. (2005) Regulatory balance between the immune response of tumor antigen-specific T-cell receptor gene-transduced CD8(+) T cells and the suppressive effects of tolerogenic dendritic cells. Cancer Sci 96,897-902.

Fukumoto, T., Sperling, J.W., Sanyal, A., Fitzsimmons, J.S., Reinholz, G.G., Conover, C.A., and O'Driscoll, S.W. (2003) Combined effects of insulin-like growth factor-1 and transforming growth factor-beta 1 on periosteal mesenchymal cells during chondrogenesis in vitro. Osteoarthritis Cartilage 11,55-64.

Galois, L., Freyria, A., Herbage, D., and Mainard, D. (2005) Cartilage tissue engineering: state-of-the-art and future approaches. Pathol Biol 53,590-598.

Gao, J.X., Madrenas, J., Zeng, W., Cameron, M.J., Zhang, Z., Wang, J.J., Zhong, R., and Grant, D. (1999) CD40-deficient dendritic cells producing interleukin-10, but not interleukin-12, induce T-cell hyporesponsiveness in vitro and prevent acute allograft rejection. Immunology 98,159-170.

Gao, J.Z., Knaack, D., Goldberg, V.M., and Caplan, A.L. (2004) Osteochondral defect repair by demineralized cortical bone matrix. Clinical Orthopaedics and Related Research,S62-S66.

Gautier, G., Humbert, M., Deauvieau, F., Scuiller, M., Hiscott, J., Bates, E.E.M., Trinchieri, G., Caux, C., and Garrone, P. (2005) A type I interferon autocrine-paracrine loop is involved in Toll-like receptor-induced interleukin-12p70 secretion by dendritic cells. J Exp Med 201,1435-1446.

Geijtenbeek, T., Torensma, R., van Vliet, S., van Duijnhoven, G., Adema, G., van Kooyk, Y., and Figdor, C. (2000) Identification of DC-SIGN, a novel dendritic cell-specific ICAM-3 receptor that supports primary immune responses. Cell 100,575-585.

Ghosh, T.K., Mickelson, D.J., Fink, J., Solberg, J.C., Inglefield, J.R., Hook, D., Gupta, S.K., Gibson, S., and Alkan, S.S. (2006) Toll-like receptor (TLR) 2-9 agonists-induced cytokines and chemokines: I. Comparison with T cell receptor-induced responses. Cell Immunol 243,48-57.

Glicklis, R., Shapiro, L., Agbaria, R., Merchuk, J.C., and Cohen, S. (2000) Hepatocyte behavior within three-dimensional porous alginate scaffolds. Biotechnol Bioeng 67,344-353.

Grauer, O., Poschl, P., Lohmeier, A., Adema, G.J., and Bogdahn, U. (2007) Toll-like receptor triggered dendritic cell maturation and IL-12 secretion are necessary to

overcome T-cell inhibition by glioma-associated TGF-beta 2. J Neurooncol 82,151-161.

Grigolo, B., Lisignoli, G., Piacentini, A., Fiorini, M., Gobbi, P., Mazzotti, G., Duca, M., Pavesio, A., and Facchini, A. (2002) Evidence for redifferentiation of human chondrocytes grown on a hyaluronan-based biomaterial (HYAFF (R) 11): molecular, immunohistochemical and ultrastructural analysis. Biomaterials 23,1187-1195.

Hammerschmidt, D.E., Weaver, L.J., Hudson, L.D., Craddock, P.R., and Jacob, H.S. (1980) Association of Complement Activation and Elevated Plasma-C5a with Adult Respiratory-Distress Syndrome - Pathophysiological Relevance and Possible Prognostic Value. LANCET 1,947-949.

Hidaka, Y., Ito, M., Mori, K., Yagasaki, H., and Kafrawy, A.H. (1999) Histopathological and immunohistochemical studies of membranes of deacetylated chitin derivatives implanted over rat calvaria. J Biomed Mater Res 46,418-423.

Hitchen, P.G., Mullin, N.P., and Taylor, M.E. (1998) Orientation of sugars bound to the principal C-type carbohydrate-recognition domain of the macrophage mannose receptor. Biochem J 333,601-608.

Hori, Y., Winans, A.M., Huang, C.C., Horrigan, E.M., and Irvine, D.J. (2008) Injectable dendritic cell-carrying alginate gels for immunization and immunotherapy. Biomaterials 29,3671-3682.

Hou, Q.P., Grijpma, D.W., and Feijen, J. (2003) Porous polymeric structures for tissue engineering prepared by a coagulation, compression moulding and salt leaching technique. Biomaterials 24,1937-1947.

Hu, Y.H., Grainger, D.W., Winn, S.R., and Hollinger, J.O. (2002) Fabrication of poly(alpha-hydroxy acid) foam scaffolds using multiple solvent systems. J Biomed Mater Res 59,563-572.

Huang, C.Y.C., Reuben, P.M., D'Ippolito, G., Schiller, P.C., and Cheung, H.S. (2004) Chondrogenesis of human bone marrow-derived mesenchymal stem cells in agarose culture. Anat Rec A Discov Mol Cell Evol Biol 278A,428-436.

Hunter, R. (2002) Overview of vaccine adjuvants: present and future. Vaccine 20,S7-S12.

Hunter, T.B., Alsarraj, M., Gladue, R.P., Bedian, V., and Antonia, S.J. (2007) An agonist antibody specific for CD40 induces dendritic cell maturation and promotes autologous anti-tumour T-cell responses in an in vitro mixed autologous tumour cell/lymph node cell model. Scand J Immunol 65,479-486.

Hunziker, E. (2002) Articular cartilage repair: basic science and clinical progress. A review of the current status and prospects. Osteoarthritis Cartilage 10,432-463.

Hutas, G., Bajnok, E., Gal, I., Finnegan, A., Glant, T.T., and Mikecz, K. (2008) CD44-specific antibody treatment and CD44 deficiency exert distinct effects on leukocyte recruitment in experimental arthritis. Blood 112,4999-5006.

Hutchinson, F.G., and Furr, B.J.A. (1987) Biodegradable Carriers for the Sustained-Release of Polypeptides. Trends Biotechnol 5,102-106.

Hutmacher, D., Goh, J., and Teoh, S. (2001) An introduction to biodegradable materials for tissue engineering applications. Ann Acad Med Singap 30,183-191.

Hwang, S.M., Chen, C.Y., Chen, S.S., and Chen, J.C. (2000) Chitinous materials inhibit nitric oxide production by activated RAW 264.7 macrophages. Biochem Biophys Res Commun 271,229-233.

Ignatius, A.A., and Claes, L.E. (1996) In vitro biocompatibility of bioresorbable polymers: Poly(L,DL-lactide) and poly(L-lactide-co-glycolide). Biomaterials 17,831-839.

Indrawattana, N., Chen, G.P., Tadokoro, M., Shann, L.H., Ohgushi, H., Tateishi, T., Tanaka, J., and Bunyaratvej, A. (2004) Growth factor combination for chondrogenic induction from human mesenchymal stem cell. Biochem Biophys Res Commun 320,914-919.

Iwamoto, M., Kurachi, M., Nakashima, T., Kim, D., Yamaguchi, K., Oda, T., Iwamoto, Y., and Muramatsu, T. (2005) Structure-activity relationship of alginate oligosaccharides in the induction of cytokine production from RAW264.7 cells. FEBS Lett 579,4423-4429.

Jacob, H.S., Craddock, P.R., Hammerschmidt, D.E., Moldow, C.F., Davidson, C.S., Bunn, F., and Robinson, S. (1980) Complement-Induced Granulocyte Aggregation - Unsuspected Mechanism of Disease. N Engl J Med 302,789-794.

Jaganathan, K., Singh, P., Prabakaran, D., Mishra, V., and Vyas, S. (2004) Development of a single-dose stabilized poly(D,L-lactic-co-glycolic acid) microspheres-based vaccine against hepatitis B. J Pharm Pharmacol 56,1243-1250.

Janeway, C., and Medzhitov, R. (1998) Introduction: The role of innate immunity in the adaptive immune response. Semin Immunol 10,349-350.

Janeway, C., Travers, P., Walport, M., and Shlomchik, M. (2004) Immunobiology. Garland Publishing, New York.

Jeong, J.G., Kim, J.M., Cho, H., Hahn, W., Yu, S.S., and Kim, S. (2004) Effects of IL-1 beta on gene expression in human rheumatoid synovial fibroblasts. Biochem Biophys Res Commun 324,3-7.

Jones, J.A., Chang, D.T., Meyerson, H., Colton, E., Kwon, I.K., Matsuda, T., and Anderson, J.M. (2007) Proteomic analysis and quantification of cytokines and chemokines from biomaterial surface-adherent macrophages and foreign body giant cells. J Biomed Mater Res 83A,585-596.

Jonuleit, H., Schmitt, E., Schuler, G., Knop, J., and Enk, A.H. (2000) Induction of interleukin 10-producing, nonproliferating CD4(+) T cells with regulatory properties by repetitive stimulation with allogeneic immature human dendritic cells. J Exp Med 192,1213-1222.

Jorgensen, C., Gordeladze, J., and Noel, D. (2004) Tissue engineering through autologous mesenchymal stem cells. Curr Opin Biotechnol 15,406-410.

Jotwani, R., Pulendran, B., Agrawal, S., and Cutler, C.W. (2003) Human dendritic cells respond to Porphyromonas gingivalis LPS by promoting a Th2 effector response in vitro. Eur J Immunol 33,2980-2986.

Jung, Y.O., Min, S.Y., Cho, M.L., Park, M.J., Jeon, J.Y., Lee, J.S., Oh, H.J., Kang, C.M., Park, H.S., Park, K.S., Cho, S.G., Park, S.H., and Kim, H.Y. (2007) CD8alpha+dendritic cells enhance the antigen-specific CD4+T-cell response and accelerate development of collagen-induced arthritis. Immunol Lett 111,76-83.

Kalinski, P., Hilkens, C.M.U., Wierenga, E.A., and Kapsenberg, M.L. (1999) T-cell priming by type-1 and type-2 polarized dendritic cells: the concept of a third signal. Immunology Today 20,561-567.

Kang, H.J., Han, C.D., Kang, E.S., Kim, N.H., and Yang, W.I. (1991) An experimental intraarticular implantation of woven carbon fiber pad into osteochondral defect of the femoral condyle in rabbit. Yonsei Med J 32,108-116.

Kapsenberg, M.L. (2003) Dendritic-cell control of pathogen-driven T-cell polarization. Nat Rev Immunol 3,984-993.

Kashiwagi, N., Nakano, M., Saniabadi, A.R., Adachi, M., and Yoshikawa, T. (2002) Anti-inflammatory effect of granulocyte and monocyte adsorption apheresis in a rabbit model of immune arthritis. Inflammation 26,199-205.

Kato, M., Neil, T., Clark, G., Morris, C., Sorg, R., and Hart, D. (1998) cDNA cloning of human DEC-205, a putative antigen-uptake receptor on dendritic cells. Immunogenetics 47,442-450.

Kim, B., Baez, C., and Atala, A. (2000) Biomaterials for tissue engineering. World J Urol 18,2-9.

Klimiuk, P.A., Goronzy, J.J., and Weyand, C.M. (1999) IL-16 as an anti-inflammatory cytokine in rheumatoid synovitis. J Immunol 162,4293-4299.

Kohn, J., Welsh, W.J., and Knight, D. (2007) A new approach to the rationale discovery of polymeric biomaterials. Biomaterials 28,4171-4177.

Koike, E., Takano, H., Inoue, K., Yanagisawa, R., and Kobayashi, T. (2008) Carbon black nanoparticles promote the maturation and function of mouse bone marrow-derived dendritic cells. Chemosphere 73,371-376.

Kulseng, B., Skjak-Braek, G., Ryan, L., Andersson, A., King, A., Faxvaag, A., and Espevik, T. (1999) Transplantation of alginate microcapsules - Generation of antibodies against alginates and encapsulated porcine islet-like cell clusters. Transplantation 67,978-984.

Kuo, C., Li, W., Mauck, R., and Tuan, R. (2006) Cartilage tissue engineering: its potential and uses. Curr Opin Rheumatol 18,64-73.

Kustritz, M.V.R. (2000) The theriogenology question of the month - Agarose gel immunodiffusion (AGID) serologic testing for brucellosis. J Am Vet Med Assoc 216,181-182.

Kyriakides, T.R., Leach, K.J., Hoffman, A.S., Ratner, B.D., and Bornstein, P. (1999) Mice that lack the angiogenesis inhibitor, thrombospondin 2, mount an altered foreign body reaction characterized by increased vascularity. Proc Natl Acad Sci U S A 96,4449-4454.

Lahiji, A., Sohrabi, A., Hungerford, D.S., and Frondoza, C.G. (2000) Chitosan supports the expression of extracellular matrix proteins in human osteoblasts and chondrocytes. J Biomed Mater Res 51,586-595.

Lambert, L.A., Gibson, G.R., Maloney, M., Durell, B., Noelle, R.J., and Barth, R.J. (2001) Intranodal immunization with tumor lysate-pulsed dendritic cells enhances protective antitumor immunity. Cancer Res 61,641-646.

Lanzavecchia, A., and Sallusto, F. (2001) Regulation of T cell immunity by dendritic cells. Cell 106,263-266.

Lebre, M.C., Jongbloed, S.L., Tas, S.W., Smeets, T.J.M., Mclnnes, L.B., and Tak, P.P. (2008) Rheumatoid arthritis synovium contains two subsets of CD83(-)DC(-)LAMP(-) dendritic cells with distinct cytokine profiles. Am J Pathol 172,940-950.

Lebwohl, M., Gottlieb, A., Wallis, W., and Zitnik, R. (2005) Safety and efficacy of over 7 years of etanercept therapy in a global population of patients with rheumatoid arthritis. J AM ACAD DERMATOL 52,P195-P195.

Lee, C.T., and Lee, Y.D. (2006) Preparation of porous biodegradable poly(lactide-co-glycolide)/hyaluronic acid blend scaffolds: Characterization, in vitro cells culture and degradation behaviors. J Mater Sci Mater Med 17,1411-1420.

Lee, J., Shanbhag, S., and Kotov, N.A. (2006) Inverted colloidal crystals as three-dimensional microenvironments for cellular co-cultures. Journal of Materials Chemistry 16,3558-3564.

Lee, S.H., Kim, B.S., Kim, S.H., Kang, S.W., and Kim, Y.H. (2004) Thermally produced biodegradable scaffolds for cartilage tissue engineering. Macromolecular Bioscience 4,802-810.

Lenschow, D.J., Walunas, T.L., and Bluestone, J.A. (1996) CD28/B7 system of T cell costimulation. Annu Rev Immunol 14,233-258.

Li, W., and Tuan, R. (2005) Polymeric scaffolds for cartilage tissue engineering. Macromol Symp 227,65-75.

Little, S., Lynn, D., Ge, Q., Anderson, D., Puram, S., Chen, J., Eisen, H., and Langer, R. (2004) Poly-beta amino ester-containing microparticles enhance the activity of nonviral genetic vaccines. Proc Natl Acad Sci U S A 101,9534-9539.

Lutz, M.B., Kukutsch, N., Ogilvie, A.L.J., Rossner, S., Koch, F., Romani, N., and Schuler, G. (1999) An advanced culture method for generating large quantities of highly pure dendritic cells from mouse bone marrow. J Immunol Methods 223,77-92.

Mahnke, K., Qian, Y.J., Knop, J., and Enk, A.H. (2003) Induction of CD4(+)/CD25(+) regulatory T cells by targeting of antigens to immature dendritic cells. Blood 101,4862-4869.

Malemud, C.J. (2007) Growth hormone, VEGF and FGF: Involvement in rheumatoid arthritis. Clin Chim Acta 375,10-19.

Manning, P.J., Ringler, D.H., and Newcomer, C.E. (1994) The Biology of the Laboratory Rabbit. Academic Press, San Diego.

Marguti, I., Yamamoto, G.L., da Costa, T.B., Rizzo, L.V., and de Moraes, L.V. (2009) Expansion of CD4(+) CD25(+) Foxp3(+) T cells by bone marrow-derived dendritic cells. Immunology 127,50-61.

Martinon, F., Petrilli, V., Mayor, A., Tardivel, A., and Tschopp, J. (2006) Gout-associated uric acid crystals activate the NALP3 inflammasome. Nature 440,237-241.

Matzelle, M., and Babensee, J. (2004) Humoral immune responses to model antigen co-delivered with biomaterials used in tissue engineering. Biomaterials 25,295-304.

Matzinger, P. (1994) Tolerance, Danger, and the Extended family. Annu Rev Immunol 12,991-1045.

Mauck, R.L., Soltz, M.A., Wang, C.C.B., Wong, D.D., Chao, P.H.G., Valhmu, W.B., Hung, C.T., and Ateshian, G.A. (2000) Functional tissue engineering of articular cartilage through dynamic loading of chondrocyte-seeded agarose gels. J Biomech Eng-T ASME 122,252-260.

McInnes, I.B., and Liew, F.Y. (2005) Cytokine networks - towards new therapies for rheumatoid arthritis. Nature Clinical Practice Rheumatology 1,31-39.

Medzhitov, R. (2000) Toll-like receptors in innate and adaptive immunity. Mol Biol Cell 11,282A-282A.

Medzhitov, R., and Janeway, C. (1997) Innate immunity: Impact on the adaptive immune response.

Medzhitov, R., PrestonHurlburt, P., and Janeway, C. (1997) A human homologue of the Drosophila Toll protein signals activation of adaptive immunity. Nature 388,394-397.

Mellman, I., and Steinman, R. (2001) Dendritic cells: Specialized and regulated antigen processing machines. Cell 106,255-258.

Mikecz, K., Brennan, F.R., Kim, J.H., and Glant, T.T. (1995) Anti-Cd44 Treatment Abrogates Tissue Edema and Leukocyte Infiltration in Murine Arthritis. Nature Medicine 1,558-563.

Mikecz, K., Dennis, K., Shi, M., and Kim, J.H. (1999) Modulation of hyaluronan receptor (CD44) function in vivo in a murine model of rheumatoid arthritis. Arthritis and Rheumatism 42,659-668.

Mikos, A.G., Thorsen, A.J., Czerwonka, L.A., Bao, Y., Langer, R., Winslow, D.N., and Vacanti, J.P. (1994) Preparation and Characterization of Poly(L-Lactic Acid) Foams. Polymer 35,1068-1077.

Miossec, P. (1995) Proinflammatory and Antiinflammatory Cytokine Balance in Rheumatoid-Arthritis. CLIN EXP RHEUMATOL 13,13-16.

Mizuno, K., Okamoto, H., and Horio, T. (2004) Ultraviolet B radiation suppresses endocytosis, subsequent maturation, and migration activity of Langerhans cell-like dendritic cells. J Investig Dermatol 122,300-306.

Moldenhauer, A., Nociari, M.M., Dias, S., Lalezari, P., and Moore, M.A.S. (2003) Optimized culture conditions for the generation of dendritic cells from peripheral blood monocytes. Vox Sang 84,228-236.

Mori, T., Murakami, M., Okumura, M., Kadosawa, T., Uede, T., and Fujinaga, T. (2005) Mechanism of macrophage activation by chitin derivatives. J Vet Med Sci 67,51-56.

Moser, M., and Murphy, K.M. (2000) Dendritic cell regulation of T(H)1-T(H)2 development. Nat Immunol 1,199-205.

Mountziaris, P.M., and Mikos, A.G. (2008) Modulation of the inflammatory response for enhanced bone tissue regeneration. Tissue Engineering Part B-Reviews 14,179-186.

Murphy, W.L., Dennis, R.G., Kileny, J.L., and Mooney, D.J. (2002) Salt fusion: An approach to improve pore interconnectivity within tissue engineering scaffolds. Tissue Eng 8,43-52.

Nathan, C.F. (1987) Secretory Products of Macrophages. J Clin Investig 79,319-326.

Nelms, K., Keegan, A.D., Zamorano, J., Ryan, J.J., and Paul, W.E. (1999) The IL-4 receptor: Signaling mechanisms and biologic functions. Annu Rev Immunol 17,701-738.

Nestle, F.O., Farkas, A., and Conrad, C. (2005) Dendritic-cell-based therapeutic vaccination against cancer. Curr Opin Immunol 17,163-169.

Newman, K., Elamanchili, P., Kwon, G., and Samuel, J. (2002) Uptake of poly(D,L-lactic-co-glycolic acid) microspheres by antigen-presenting cells in vivo. J Biomed Mater Res 60,480-486.

Newman, K.D., Samuel, J., and Kwon, G. (1998a) Ovalbumin peptide encapsulated in poly(d,l lactic-co-glycolic acid) microspheres is capable of inducing a T helper type 1 immune response. J Control Release 54,49-59.

Newman, M., Balusubramanian, M., and Todd, C. (1998b) Development of adjuvant-active nonionic block copolymers. Adv Drug Delivery Rev 32,199-223.

Newtonnash, D.K., Tonellato, P., Swiersz, M., and Abramoff, P. (1990) Assessment of Chemokinetic Behavior of Inflammatory Lung Macrophages in a Linear under-Agarose Assay. J Leukoc Biol 48,297-305.

Noonan, D.M., Barbaro, A.D.L., Vannini, N., Mortara, L., and Albini, A. (2008) Inflammation, inflammatory cells and angiogenesis: decisions and indecisions. Cancer Metastasis Rev 27,31-40.

O'Driscoll, S.W. (1998) The healing and regeneration of articular cartilage. Journal of Bone and Joint Surgery-American Volume 80A,1795-1812.

Ohagan, D.T., Jeffery, H., and Davis, S.S. (1993) Long-Term Antibody-Responses in Mice Following Subcutaneous Immunization with Ovalbumin Entrapped in Biodegradable Microparticles. Vaccine 11,965-969.

Okamoto, N., Chihara, R., Shimizu, C., Nishimoto, S., and Watanabe, T. (2007) Artificial lymph nodes induce potent secondary immune responses in naive and immunodeficient mice. J Clin Investig 117,997-1007.

Orive, G., Carcaboso, A.M., Hernandez, R.M., Gascon, A.R., and Pedraz, J.L. (2005) Biocompatibility evaluation of different alginates and alginate-based microcapsules. Biomacromolecules 6,927-931.

Otterlei, M., Ostgaard, K., Skjakbraek, G., Smidsrod, O., Soonshiong, P., and Espevik, T. (1991) Induction of Cytokine Production from Human Monocytes Stimulated with Alginate. J Immunother 10,286-291.

Ouaaz, F., Arron, J., Zheng, Y., Choi, Y.W., and Beg, A.A. (2002) Dendritic cell development and survival require distinct NF-kappa B subunits. Immunity 16,257-270.

Palmer, A.W., Guldberg, R.E., and Levenston, M.E. (2006) Analysis of cartilage matrix fixed charge density and three-dimensional morphology via contrast-enhanced microcomputed tomography. Proc Natl Acad Sci U S A 103,19255-19260.

Papas, K.K., Long, R.C., Sambanis, A., and Constantinidis, I. (1999) Development of a bioartificial pancreas: II. Effects of oxygen on long-term entrapped beta TC3 cell cultures. Biotechnol Bioeng 66,231-237.

Park, J., and Babensee, J.E. (2009) Differential Functional Effects of Biomaterials on Dendritic Cell Maturation. (Submitted).

Pay, S., Erdem, H., Pekel, A., Simsek, I., Musabak, U., Sengul, A., and Dinc, A. (2006)

Synovial proinflammatory cytokines and their correlation with matrix metalloproteinase-3 expression in Behcet's disease. Does interleukin-1 beta play a major role in Behcet's synovitis? Rheumatol Int 26,608-613.

Peiser, L., Mukhopadhyay, S., and Gordon, S. (2002) Scavenger receptors in innate immunity. Curr Opin Immunol 14,123-128.

Peluso, G., Petillo, O., Ranieri, M., Santin, M., Ambrosio, L., Calabro, D., Avallone, B., and Balsamo, G. (1994) Chitosan-Mediated Stimulation of Macrophage Function. Biomaterials 15,1215-1220.

Peppas, N.A., and Mikos, A.G. (1986) Preparation Methods, and Structure of Hydrogels, in Hydrogels in Medicine and Pharmacy. CRC Press.

Pettit, A., and Thomas, R. (1999) Dendritic cells: The driving force behind autoimmunity in rheumatoid arthritis? Immunol Cell Biol 77,420-427.

Piemonti, L., Monti, P., Allavena, P., Leone, B.E., Caputo, A., and Di Carlo, V. (1999) Glucocorticoids increase the endocytic activity of human dendritic cells. Int Immunol 11,1519-1526.

Pillinger, M.H., and Abramson, S.B. (1995) The Neutrophil in Rheumatoid-Arthritis. Rheum Dis Clin N Am 21,691-714.

Pockaj, B.A., Basu, G.D., Pathangey, L.B., Gray, R.J., Hernandez, J.L., Gendler, S.J., and Mukherjee, P. (2004) Reduced T-cell and dendritic cell function is related to cyclooxygenase-2 overexpression and prostaglandin E-2 secretion in patients with breast cancer. Ann Surg Oncol 11,328-339.

Popa, C., van Lieshout, A.W.T., Roelofs, M.F., Geurts-Moespot, A., van Riel, P.L.C.M., Calandra, T., Sweep, F.C.G.J., and Radstake, T.R.D.J. (2006) MIF production by dendritic cells is differentially regulated by Toll-like receptors and increased during rheumatoid arthritis. Cytokine 36,51-56.

Pope, R.M. (2002) Apoptosis as a therapeutic tool in rheumatoid arthritis. Nat Rev Immunol 2,527-535.

Popov, I., Li, M., Zheng, X.F., San, H.T., Zhang, X.S., Ichim, T.E., Suzuki, M., Feng, B., Vladau, C., Zhong, R., Garcia, B., Strejan, G., Inman, R.D., and Min, W.P. (2006)

Preventing autoimmune arthritis using antigen-specific immature dendritic cells: a novel tolerogenic vaccine. Arthritis Res Ther 8,R141.

Potten, C., and Booth, C. (2002) Keratinocyte stem cells: a commentary. J Investig Dermatol 119,888-899.

Presicce, P., Taddeo, A., Conti, A., Villa, M.L., and Della Bella, S. (2008) Keyhole limpet hemocyanin induces the activation and maturation of human dendritic cells through the involvement of mannose receptor. Mol Immunol 45,1136-1145.

Pure, E., and Cuff, C.A. (2001) A crucial role for CD44 in inflammation. Trends Mol Med 7,213-221.

Radstake, T., van Lieshout, A., van Riel, P., van den Berg, W., and Adema, G. (2005) Dendritic cells, Fc gamma receptors, and Toll- like receptors: potential allies in the battle against rheumatoid arthritis. Annals of the Rheumatic Disease 64,1532-1538.

Rahfoth, B., Weisser, J., Sternkopf, F., Aigner, T., von der Mark, K., and Brauer, R. (1998) Transplantation of allograft chondrocytes embedded in agarose gel into cartilage defects of rabbits. Osteoarthritis Cartilage 6,50-65.

Ratner, B., and Bryant, S. (2004) Biomaterials: Where we have been and where we are going. Annu Rev Biomed Eng 6,41-75.

Ratner, B., Hoffman, A., Schoen, F., and Lemons, J. (2004) Biomaterials Science - An Introduction to Materials in Medicine. Elsevier Academic Press, San Diego.

Reddy, S., Swartz, M., and Hubbell, J. (2006) Targeting dendritic cells with biomaterials: developing the next generation of vaccines. Trends Immunol 27,573-579.

Reese, T.A., Liang, H.E., Tager, A.M., Luster, A.D., Van Rooijen, N., Voehringer, D., and Locksley, R.M. (2007) Chitin induces accumulation in tissue of innate immune cells associated with allergy. Nature 447,92-U97.

Reignier, J., and Huneault, M.A. (2006) Preparation of interconnected poly(epsilon-caprolactone) porous scaffolds by a combination of polymer and salt particulate leaching. Polymer 47,4703-4717.

Rescigno, M., Martino, M., Sutherland, C., Gold, M., and Ricciardi-Castagnoli, P. (1998) Dendritic cell survival and maturation are regulated by different signaling pathways. J Exp Med 188,2175-2180.

Robbins, P., Evans, C., and Chernajovsky, Y. (2003) Gene therapy for arthritis. GENE THER 10,902-911.

Rodriguez, A., Voskerician, G., Meyerson, H., MacEwan, S.R., and Anderson, J.M. (2008) T cell subset distributions following primary and secondary implantation at subcutaneous biomaterial implant sites. J Biomed Mater Res 85A,556-565.

Romani, N., Reider, D., Heuer, M., Ebner, S., Kampgen, E., Eibl, B., Niederwieser, D., and Schuler, G. (1996) Generation of mature dendritic cells from human blood - An improved method with special regard to clinical applicability. J Immunol Methods 196,137-151.

Rothoeft, T., Balkow, S., Krummen, M., Beissert, S., Varga, G., Loser, K., Oberbanscheidt, P., van den Boom, F., and Grabbe, S. (2006) Structure and duration of contact between dendritic cells and T cells are controlled by T cell activation state. Eur J Immunol 36,3105-3117.

Rudolph, E.H., and Woods, J.M. (2005) Chemokine expression and regulation of angiogenesis in rheumatoid arthritis. Curr Pharm Des 11,613-631.

Sacre, S.M., Andreakos, E., Kiriakidis, S., Amjadi, P., Lundberg, A., Giddins, G., Feldmann, M., Brennan, F., and Foxwell, B.M. (2007) The toll-like receptor adaptor proteins MyD88 and Mal/TIRAP contribute to the inflammatory and destructive processes in a human model of rheumatoid arthritis. Am J Pathol 170,518-525.

Sakaguchi, S. (2005) Naturally arising Foxp3-expressing CD25(+) CD4(+) regulatory T cells in immunological tolerance to self and non-self. Nat Immunol 6,345-352.

Sallusto, F., Cella, M., Danieli, C., and Lanzavecchia, A. (1995) Dendritic Cells Use Macropinocytosis and The Mannose Receptor to Concentrate Macromolecules in The Major Histocompatibility Complex Class-II Compartment - Down-Regulation by Cytokines and Bacteial Products. J Exp Med 182,389-400.

Sallusto, F., and Lanzavecchia, A. (1999) Mobilizing dendritic cells for tolerance,

priming, and chronic inflammation. J Exp Med 189,611-614.

Santiago-Schwarz, F., Anand, P., Liu, S., and Carsons, S. (2001) Dendritic cells (DCs) in rheumatoid arthritis (RA): Progenitor cells and soluble factors contained in RA synovial fluid yield a subset of myeloid DCs that preferentially activate Th1 inflammatory-type responses. J Immunol 167,1758-1768.

Scheibner, K.A., Lutz, M.A., Boodoo, S., Fenton, M.J., Powell, J.D., and Horton, M.R. (2006) Hyaluronan fragments act as an endogenous danger signal by engaging TLR2. J Immunol 177,1272-1281.

Schnurr, M., Galambos, P., Scholz, C., Then, F., Dauer, M., Endres, S., and Eigler, A. (2001) Tumor cell lysate-pulsed human dendritic cells induce a T-cell response against pancreatic carcinoma cells: an in vitro model for the assessment of tumor vaccines. Cancer Res 61,6445-6450.

Schutte, R.J., Parisi-Amon, A., and Reichert, W.M. (2009a) Cytokine profiling using monocytes/macrophages cultured on common biomaterials with a range of surface chemistries. J Biomed Mater Res 88A,128-139.

Schutte, R.J., Xie, L.L., Klitzman, B., and Reichert, W.M. (2009b) In vivo cytokine-associated responses to biomaterials. Biomaterials 30,160-168.

Seferian, P., and Martinez, M. (2000) Immune stimulating activity of two new chitosan containing adjuvant formulations. Vaccine 19,661-668.

Sharp, F.A., Ruane, D., Claass, B., Creagh, E., Harris, J., Malyala, P., Singh, M., O'Hagan, D.T., Petrilli, V., Tschopp, J., O'Neill, L.A.J., and Lavelle, E.C. (2009) Uptake of particulate vaccine adjuvants by dendritic cells activates the NALP3 inflammasome. Proc Natl Acad Sci U S A 106,870-875.

Shen, M.C., Garcia, I., Maier, R.V., and Horbett, T.A. (2004) Effects of adsorbed proteins and surface chemistry on foreign body giant cell formation, tumor necrosis factor alpha release and procoagulant activity of monocytes. J Biomed Mater Res 70A,533-541.

Shen, M.C., and Horbett, T.A. (2001) The effects of surface chemistry and adsorbed proteins on monocyte/macrophage adhesion to chemically modified polystyrene surfaces. J Biomed Mater Res 57,336-345.

Shenker, N., Haigh, R., Roberts, E., Mapp, P., Harris, N., and Blake, D. (2003) A review of contralateral responses to a unilateral inflammatory lesion. Rheumatology 42,1279-1286.

Sheriff, A., Gaipl, U.S., Voll, R.E., Kalden, J.R., and Herrmann, M. (2004) Apoptosis and systemic lupus erythematosus. Rheum Dis Clin N Am 30,505-+.

Shilyansky, J., Jacobs, P., Doffek, K., and Sugg, S.L. (2007) Induction of cytolytic T Lymphocytes against pediatric solid tumors in vitro using autologous dendritic cells pulsed with necrotic primary tumor. J Pediatr Surg 42,54-61.

Shoichet, M.S., Li, R.H., White, M.L., and Winn, S.R. (1996) Stability of hydrogels used in cell encapsulation: An in vitro comparison of alginate and agarose. Biotechnol Bioeng 50,374-381.

Singh, M., and O'Hagan, D. (1999) Advances in vaccine adjuvants. Nat Biotechnol 17,1075-1081.

Smith, G., Knutsen, G., and Richardson, J. (2005) A clinical review of cartilage repair techniques. J BONE JOINT SURG BR 87B,445-449.

Sokolovska, A., Hem, S.L., and HogenEsch, H. (2007) Activation of dendritic cells and induction of CD4(+) T cell differentiation by aluminum-containing adjuvants. Vaccine 25,4575-4585.

Sporri, R., and Sousa, C.R.E. (2005) Inflammatory mediators are insufficient for full dendritic cell activation and promote expansion of CD4(+) T cell populations lacking helper function. Nat Immunol 6,163-170.

Stachowiak, A.N., and Irvine, D.J. (2008) Inverse opal hydrogel-collagen composite scaffolds as a supportive microenvironment for immune cell migration. J Biomed Mater Res 85A,815-828.

Starke, J.R., Edwards, M.S., Langston, C., and Baker, C.J. (1987) A Mouse Model of Chronic Pulmonary Infection with Pseudomonas-Aeruginosa and Pseudomonas-Cepacia. Pediatr Res 22,698-702.

Stax, A.M., Crul, C., Kamerling, S.W.A., Schlagwein, N., van der Geest, R.N., Woltman, A.M., and van Kooten, C. (2008) CD40L stimulation of rat dendritic cells

specifically favors the IL-12/IL-10 ratio resulting in a strong T cell stimulatory capacity. Mol Immunol 45,2641-2650.

Stegel, V., Kopitar, A., Novakovic, B.J., Ihan, A., and Novakovic, S. (2006) Dendritic cells incubated with irradiated tumor cells effectively stimulate T lymphocyte activation and induce enhanced expression of CD69, CD25 as well as production of IFN gamma and IL4. Int Immunopharmacol 6,79-89.

Storgard, C., Stupack, D., Jonczyk, A., Goodman, S., Fox, R., and Cheresh, D. (1999) Decreased angiogenesis and arthritic disease in rabbits treated with an alpha v beta 3 antagonist. J Clin Investig 103,47-54.

Suematsu, S., and Watanabe, T. (2004) Generation of a synthetic lymphoid tissue-like organoid in mice. Nat Biotechnol 22,1539-1545.

Suh, J., and Matthew, H. (2000) Application of chitosan-based polysaccharide biomaterials in cartilage tissue engineering: a review. Biomaterials 21,2589-2598.

Sun, D.Q., Aydelotte, M.B., Maldonado, B., Kuettner, K.E., and Kimura, J.H. (1986) Clonal Analysis of the Population of Chondrocytes from the Swarm Rat Chondrosarcoma in Agarose Culture. J Orthop Res 4,427-436.

Sweeney, S.E., and Firestein, G.S. (2004) Rheumatoid arthritis: regulation of synovial inflammation. Int J Biochem Cell Biol 36,372-378.

Tabata, Y. (2009) Biomaterial technology for tissue engineering applications. Journal of the Royal Society Interface 6,S311-S324.

Tam, S., Dusseault, J., Polizu, S., Menard, M., Halle, J., and Yahia, L. (2005) Physicochemical model of alginate-poly-L-lysine microcapsules defined at the micrometric/nanometric scale using ATR-FTIR, XPS, and ToF-SIMS. Biomaterials 26,6950-6961.

Tan, H.P., Chu, C.R., Payne, K.A., and Marra, K.G. (2009) Injectable in situ forming biodegradable chitosan-hyaluronic acid based hydrogels for cartilage tissue engineering. Biomaterials 30,2499-2506.

Tangpasuthadol, V., Pongchaisirikul, N., and Hoven, V.P. (2003) Surface modification of chitosan films. Effects of hydrophobicity on protein adsorption. Carbohydr Res

338,937-942.

Temenoff, J.S., and Mikos, A.G. (2000) Review: tissue engineering for regeneration of articular cartilage. Biomaterials 21,431-440.

Termeer, C., Averbeck, M., Hara, H., Eibel, H., Herrlich, P., Sleeman, J., and Simon, J.C. (2003) Targeting dendritic cells with CD44 monoclonal antibodies selectively inhibits the proliferation of naive CD4(+) T-helper cells by induction of FAS-independent T-cell apoptosis. Immunology 109,32-40.

Termeer, C., Johannsen, H., Braun, T., Renkl, A., Ahrens, T., Denfeld, R.W., Lappin, M.B., Weiss, J.M., and Simon, J.C. (2001) The role of CD44 during CD40 ligand-induced dendritic cell clustering and maturation. J Leukoc Biol 70,715-722.

Termeer, C.C., Hennies, J., Voith, U., Ahrens, T., Weiss, J.M., Prehm, P., and Simon, J.C. (2000) Oligosaccharides of hyaluronan are potent activators of dendritic cells. J Immunol 165,1863-1870.

Tetik, O., Doral, M., Atay, A., and Leblebicioglu, G. (2004) Influence of irrigation solutions combined with colchicine and diclofenae sodium on articular cartilage in a rat model. KNEE SURG SPORT TR A 12,503-509.

Thomas, R. (1998) Antigen-presenting cells in rheumatoid arthritis. Springer Semin Immunopathol 20,53-72.

Thomas, R., MacDonald, K., Pettit, A., Cavanagh, L., Padmanabha, J., and Zehntner, S. (1999) Dendritic cells and the pathogenesis of rheumatoid arthritis. J Leukoc Biol 66,286-292.

Thomson, R.C., Yaszemski, M.J., Powers, J.M., and Mikos, A.G. (1995) Fabrication of Biodegradable Polymer Scaffolds to Engineer Trabecular Bone. J Biomater Sci Polym Ed 7,23-38.

Timmins, N.E., Scherberich, A., Fruh, J.A., Heberer, M., Martin, I., and Jakob, M. (2007) Three-dimensional cell culture and tissue engineering in a T-CUP (Tissue Culture Under Perfusion). Tissue Eng 13,2021-2028.

Toebak, M.J., Rooij, J., Moed, H., Stood, T.J., von Blomberg, B.M.E., Bruynzeel, D.P., Scheper, R.J., Gibbs, S., and Rustemeyer, T. (2008) Differential suppression of

dendritic cell cytokine production by anti-inflammatory drugs. Br J Dermatol 158,225-233.

Tomihata, K., and Ikada, Y. (1997) Crosslinking of hyaluronic acid with water-soluble carbodiimide. J Biomed Mater Res 37,243-251.

Tran, D.Q., Ramsey, H., and Shevach, E.M. (2007) Induction of FOXP3 expression in naive human CD4(+)FOXP3(-) T cells by T-cell receptor stimulation is transforming growth factor-beta-dependent but does not confer a regulatory phenotype. Blood 110,2983-2990.

Tran, K.K., and Shen, H. (2009) The role of phagosomal pH on the size-dependent efficiency of cross-presentation by dendritic cells. Biomaterials 30,1356-1362.

Tsiridis, E., Upadhyay, N., and Giannoudis, P. (2007) Molecular aspects of fracture healing: Which are the important molecules? Injury-International Journal of the Care of the Injured 38,S11-S25.

Tsokos, G., and Tsokos, M. (2003) The TRAIL to arthritis. J CLIN INVEST 112,1315-1317.

Tsuji, S., Matsumoto, M., Takeuchi, O., Akira, S., Azuma, I., Hayashi, A., Toyoshima, K., and Seya, T. (2000) Maturation of human dendritic cells by cell wall skeleton of Mycobacterium bovis bacillus Calmette-Guerin: Involvement of Toll-like receptors. Infect Immun 68,6883-6890.

Tun, T., Inoue, K., Hayashi, H., Aung, T., Gu, Y.J., Doi, R., Kaji, H., Echigo, Y., Wang, W.J., Setoyama, H., Imamura, M., Maetani, S., Morikawa, N., Iwata, H., and Ikada, Y. (1996) A newly developed three-layer agarose microcapsule for a promising biohybrid artificial pancreas: Rat to mouse xenotransplantation. Cell Transplant 5,S59-S63.

Valencia, X., Stephens, G., Goldbach-Mansky, R., Wilson, M., Shevach, E.M., and Lipsky, P.E. (2006) TNF downmodulates the function of human CD4(+)CD25(hi) T-regulatory cells. Blood 108,253-261.

Venkatesan, N., Barre, L., Benani, A., Netter, P., Magdalou, J., Fournel-Gigleux, S., and Ouzzine, M. (2004) Stimulation of proteoglycan synthesis by glucuronosyltransferase-1 gene delivery: A strategy to promote cartilage repair.

Proc Natl Acad Sci U S A 101,18087-18092.

Waalen, K., Thoen, J., Forre, O., Hovig, T., Teigland, J., and Natvig, J. (1986) Rheumatoid Synovial Dendritic Cells as Stimulators in Allogeneic and Autologous Mixed Leukocyte Reactions - Comparison with Autologous Monocytes as Stimulator Cells. Scand J Immunol 23,233-241.

Wang, M., and Yu, C. (2004) Silicone rubber: an alternative for repair of articular cartilage defects. KNEE SURG SPORT TR A 12,556-561.

Wang, Y., Rudym, D.D., Walsh, A., Abrahamsen, L., Kim, H.J., Kim, H.S., Kirker-Head, C., and Kaplan, D.L. (2008) In vivo degradation of three-dimensional silk fibroin scaffolds. Biomaterials 29,3415-3428.

Warr, G.A. (1980) A Macrophage Receptor for "(Mannose-Glucosamine)-Glycoproteins of Potential Importance in Phagocytic-Activity. Biochem Biophys Res Commun 93,737-745.

Weber, C.J., Safley, S., Hagler, M., and Kapp, J. (1999) Evaluation of graft-host response for various tissue sources and animal models. Ann NY Acad Sci 875,233-254.

Weiss, J.M., Sleeman, J., Renkl, A.C., Dittmar, H., Termeer, C.C., Taxis, S., Howells, N., Hofmann, M., Kohler, G., Schopf, E., Ponta, H., Herrlich, P., and Simon, J.C. (1997) An essential role for CD44 variant isoforms in epidermal Langerhans cell and blood dendritic cell function. J Cell Biol 137,1137-1147.

West, M.A., Wallin, R.P.A., Matthews, S.P., Svensson, H.G., Zaru, R., Ljunggren, H.G., Prescott, A.R., and Watts, C. (2004) Enhanced dendritic cell antigen capture via toll-like receptor-induced actin remodeling. Science 305,1153-1157.

Weyand, C., and Goronzy, J. (1997) Pathogenesis of rheumatoid arthritis. Med Clin N Am 81,29-&.

Whiteside, T.L., and Odoux, C. (2004) Dendritic cell biology and cancer therapy. Cancer Immunol Immunother 53,240-248.

Williams, D. (1987) Definitions in Biomaterials. Consensus Conference of the European Society for Biomaterials. Amsterdam, Elsevier, Chester, England, p. 72.

Winchester, R. (1981) Genetic-Aspects of Rheumatoid Arthritis. Springer Semin Immunopathol 4,89-102.

Wooley, P., Whalen, J., Chapman, D., Berger, A., Richard, K., Aspar, D., and Staite, N. (1993) The Effects of an Interleukin-1 receptor Antagonist Protein on Type-II Collagen-Induced Arthritis and Antigen-Induced Arthritis in Mice. ARTHRITIS RHEUM 36,1305-1314.

Xia, C.Q., Peng, R., Beato, F., and Clare-Salzler, M.J. (2005) Dexamethasone induces IL-10-producing monocyte-derived dendritic cells with durable immaturity. Scand J Immunol 62,45-54.

Yang, R., Yan, Z., Chen, F., Hansson, G.K., and Kiessling, R. (2002a) Hyaluronic acid and chondroitin sulphate A rapidly promote differentiation of immature DC with upregulation of costimulatory and antigen-presenting molecules, and enhancement of NF-kappa B and protein kinase activity. Scand J Immunol 55,2-13.

Yang, T.B., Witham, T.F., Villa, L., Erff, M., Attanucci, J., Watkins, S., Kondziolka, D., Okada, H., Pollack, I.F., and Chambers, W.H. (2002b) Glioma-associated hyaluronan induces apoptosis in dendritic cells via inducible nitric oxide synthase: Implications for the use of dendritic cells for therapy of gliomas. Cancer Res 62,2583-2591.

Yang, Y., Bolikal, D., Becker, M.L., Kohn, J., Zeiger, D.N., and Simon, C.G. (2008) Combinatorial polymer scaffold libraries for screening cell-biomaterial interactions in 3D. Adv Mater 20,2037-+.

Yao, Y.X., Li, W., Kaplan, M.H., and Chang, C.H. (2005) Interleukin (IL)-4 inhibits IL-10 to promote IL-12 production by dendritic cells. J Exp Med 201,1899-1903.

Yoshida, M., and Babensee, J. (2004) Poly(lactic-co-glycolic acid) enhances maturation of human monocyte-derived dendritic cells. J Biomed Mater Res 71A,45-54.

Yoshida, M., and Babensee, J. (2006) Differential effects of agarose and poly(lactic-co-glycolic acid) on dendritic cell maturation. J Biomed Mater Res 79A,393-408.

Yoshida, M., Mata, J., and Babensee, J.E. (2007) Effect of poly(lactic-co-glycolic acid) contact on maturation of murine bone marrow-derived dendritic cells. J Biomed

Mater Res 80A,7-12.

Yoshimura, S., Bondeson, J., Foxwell, B., Brennan, F., and Feldmann, M. (2001) Effective antigen presentation by dendritic cells is NF-kappa B dependent: coordinate regulation of MHC, co-stimulatory molecules and cytokines. Int Immunol 13,675-683.

You, R.I., Chang, Y.C., Chen, P.M., Wang, W.S., Hsu, T.L., Yang, C.Y., Lee, C.T., and Hsieh, S.L. (2008) Apoptosis of dendritic cells induced by decoy receptor 3 (DcR3). Blood 111,1480-1488.

Young, B.R., Pitt, W.G., and Cooper, S.L. (1988) Protein Adsorption on Polymeric Biomaterials .1. Adsorption-Isotherms. J Colloid Interface Sci 124,28-43.

Zeyda, M., Saemann, M.D., Stuhlmeier, K.M., Mascher, D.G., Nowotny, P.N., Zlabinger, G.J., Waldhausl, W., and Stulnig, T.M. (2005) Polyunsaturated fatty acids block dendritic cell activation and function independently of NF-kappa B activation. J Biol Chem 280,14293-14301.

Zhang, G., and Ghosh, S. (2001) Toll-like receptor-mediated NF-kappa B activation: a phylogenetically conserved paradigm in innate immunity. J Clin Investig 107,13-19.

Zhang, Z., McCaffery, J., Spencer, R., and Francomano, C. (2005) Growth and integration of neocartilage with native cartilage in vitro. J Orthop Res 23,433-439.

Zhao, Z., and Leong, K. (1996) Controlled delivery of antigens and adjuvants in vaccine development. J Pharm Sci 85,1261-1270.

Zwerina, J., Redlich, K., Schett, G., and Smolen, J. (2005) Pathogenesis of rheumatoid arthritis: Targeting cytokines. ANN NY ACAD SCI 1051,716-729.